Nitrous oxide and nitrate in the Grand River, Ontario: Sources, production pathways and predictability

by

Madeline S. Rosamond

A thesis
presented to the University of Waterloo
in fulfillment of the
thesis requirement for the degree of
Doctor of Philosophy
in
Earth Sciences

Waterloo, Ontario, Canada, 2013

AUTHOR'S DECLARATION

I hereby declare that I am the sole author of this thesis. This is a true copy of the thesis, including any required final revisions, as accepted by my examiners.

I understand that my thesis may be made electronically available to the public.

Abstract

The increased use of synthetic nitrogen fertilizers since the early 1900s has resulted in greater food production but also problems with nitrogen pollution in freshwaters. Nitrate (NO_3^-) is a common pollutant in rivers and groundwater in agricultural watersheds; the drinking water limit in Canada is 10 mg N/L. Microbial processing of NO_3^- and ammonium (NH_4^+) can produce nitrous oxide (N_2O), a potent greenhouse gas responsible for about 5% of the greenhouse effect. Rivers provide a complex environment, where a variety of redox conditions, available substrates and microbial populations can co-exist on small spatial and temporal scales. Therefore, many questions remain about N cycling in river environments.

N_2O is produced during anoxic microbial NO_3^- or NO_2^- reduction to N_2 (denitrification) and oxic microbial NH_4^+ oxidation to NO_3^- (nitrification). A significant portion (~25%) of global anthropogenic N_2O is produced in rivers and estuaries, but mechanisms are not clear and predictability is poor. The United Nations Intergovernmental Panel on Climate Change (IPCC) provides default equations for calculating N_2O emission estimates, in which annual NO_3^- loading to rivers is positively linearly related to N_2O emissions. However, it is unclear how sound these linear relationships are and if measured N_2O emissions are similar to IPCC estimates.

The Grand River watershed is the largest in southern Ontario. Nutrient discharge to the Grand River is high due to extensive agriculture and high urban populations. The river often has a hypoxic water column due to high community respiration in summer. However, although nitrogen pollution is significant, N cycling is not well understood in the river. This thesis shows that NO_3^- and NH_4^+ do not typically change on the diel scale, with the exception of two sites downstream of wastewater treatment plants (WWTPs). However, N_2O concentration changes dramatically. N_2O concentrations are higher at night and lower during the day for most sites, but are reversed at very low-nutrient sites. N_2O is therefore a sensitive indicator of changes in N cycling that may not be evident from NO_3^- and NH_4^+ concentrations or stable isotope ratios. Additionally, this work shows the importance of having a sampling design that captures diel variability in N_2O.

Previous work in rivers and streams worldwide focused on the appropriate N_2O:NO_3^- ratio used to predict N_2O emissions. In contrast, this thesis shows that there is a significant but very weak relationship between instantaneous N_2O emissions and NO_3^- concentrations. However, there is a much stronger negative exponential relationship between DO and N_2O. Annual N_2O emissions tripled between 2006 and 2007 but NO_3^- masses in the river were only 10% higher, likely because river

levels were lower and anoxia more prevalent in 2007. This research suggests that the IPCC needs a new conceptual model for N_2O-NO_3^- relationships in rivers.

N_2O is produced in rivers, partially due to microbial processing of NO_3^- and NH_4^+ from WWTP effluent. However, WWTP effluent may also include dissolved N_2O and CH_4 but this previously had not been directly quantified. It was also unclear if stable isotopic ratios of NH_4^+, NO_3^-, N_2O and CH_4 in WWTP effluent were distinct from river sources and could be used for effluent tracing. N_2O emissions from three WWTPs in the Grand River Watershed were measured over 24 hours in summer and winter. N_2O emissions were similar to direct emissions from WWTPs but CH_4 emissions were about an order of magnitude lower than direct WWTP emissions. This is a previously-ignored source of N_2O and CH_4 to the atmosphere. While stable isotopic ranges of NO_3^- and NH_4^+ were not always distinct from river sources, $\delta^{15}N$-N_2O, $\delta^{18}O$-N_2O and $\delta^{13}C$-CH_4 were distinct, making them potentially useful tracers of WWTP effluent in rivers.

N_2O isotopic signatures may help determine production and removal processes in rivers, but isotopic effects of the major production pathway, denitrification, have not been characterized for river sediments. This was addressed by preparing anoxic laboratory incubations of river sediment from two sites (non-urban and urban) in the Grand River and measuring stable isotopic effects of N_2O production via denitrification. Stable isotopic fractionations were similar to published values but, surprisingly, strongly negatively correlated to production rate, even though NO_3^- substrate was plentiful. This novel finding suggests that N_2O reduction resulting in isotopic effects is more prevalent in high-substrate systems than previously thought, and that N_2O reduction may be inhibited by high NO_3^- or NO_2^- or by lags in N_2O reductase activity in high N_2O-production incubations. This could explain why N_2O emissions from the Grand River are lower than predicted by IPCC equations, which assume that N_2O:(N_2O+N_2) ratios produced by denitrification are constant.

Concern about NO_3^- export to freshwater lakes and to oceans is growing, but the role of large, eutrophic rivers in removing watershed NO_3^- loading via denitrification and biotic assimilation is not clear. To understand how much NO_3^- the Grand River receives, and how much it removes annually, a NO_3^- isotope mass balance for the Grand River was created. The river denitrified between 0.5% and 17% of incoming NO_3^-, less than the 50% suggested by the IPCC. This is surprising, as the river is well mixed, has moderate to high NO_3^- concentrations, experiences hypoxia (promoting denitrification), and has extensive biomass (biofilm and macrophytes) that assimilate N. However, the river's short residence time (~3 days not counting reservoirs), organic carbon-poor sediment and

mineralization of organic matter could contribute to low denitrification rates. These findings suggest that denitrification rates in rivers worldwide could be lower than previously estimated.

Although error was high, most $\delta^{15}N\text{-}NO_3^-$ values for losses were in the expected range for denitrification and most $\delta^{15}N\text{-}NO_3^-$ values for gains were within ranges from tributaries, WWTP effluent and groundwater measured in the watershed. The model suggests that 68% to 83% of N loads to the watershed are lost before entering the Grand River, and 13% is exported to Lake Erie, leaving 5 to 19% lost in the Grand River from a combination of denitrification, assimilation and storage. These findings suggest that large rivers are much less efficient in denitrification than other locations in watersheds such as small streams, ponds, groundwater and riparian zones. They also indicate that agricultural NO_3^- loading is much higher than WWTP effluent, suggesting that N management strategies should focus on agricultural runoff and groundwater.

Given that $N_2O\text{:}NO_3^-$ relationships are weak and non-linear in the Grand River, a new conceptual model for $N_2O\text{:}NO_3^-$ relationships is presented. First, the Grand River dataset was supplemented with data from high-oxygen streams in southern Ontario. Regression tree analysis shows a weak relationship between NO_3^- and N_2O in these streams with no other factors (temperature, DO, NH_4^+, TP, DOC, etc.) improving fit. A conceptual model was then created, which posits that N_2O emission variability (between and within sites) increases with NO_3^- concentration when NO_3^- concentrations are above the threshold for NO_3^- limitation. The global dataset does not dispute this model, though a NO_3^- threshold was not clear. The lack of sites with both high NO_3^- and high N_2O may indicate a paucity of research on eutrophic sites. Alternatively, high NO_3^- may indicate oxic conditions (i.e. little to no denitrification to remove it) which are incompatible with very high N_2O emissions. In this case, the conceptual model can be modified such that N_2O variability decreases when $NO_3^- > \sim 4$ mg N/L. The work also shows that low DO consistently results in high N_2O emissions but high temperatures result in a very large range of N_2O emissions. This approach allows N_2O emissions, which have very high variability and are difficult to predict, to be constrained to likely ranges.

Acknowledgements

It really does take a village to raise a thesis. This research project would never have been designed, executed, analyzed, graphed, written up, edited or published without the hard work of the following:

Thanks first to Sherry Schiff, my patient supervisor for slightly over seven years. Her enthusiasm for science, keen mind and pointed but kind edits will not be forgotten. I hope I've absorbed a bit of her critical thinking skills and can bring some of her mindset to…whatever I end up doing.

Thanks to my committee – Bill Taylor, John Spoelstra and Ramon Aravena – and my external examiner, Robert Howarth. You were a great introduction to the scientific community: I've always felt that you were on my side, and wanted to improve my research and my research skills. Thanks for helpful committee meetings, great feedback and patience with this overdue and overly wordy thesis.

Richard Elgood has the largely underappreciated job of making a large research lab run smoothly. His help writing grants; ordering supplies; working out lab kinks; managing people with grace, tact and humour; securing nice offices with windows; putting up with my many mistakes and oversights; and lending an ear in times of stress cannot be overstressed. Rich, I'm going to miss your wit, organizational skills and endless patience.

Jason Venkiteswaran gets "honorary co-supervisor" status just like I promised, for all the science conversations, overly simple questions answered, free modeling and regression tree making with minimal complaint, and reading every single chapter and manuscript I wrote, when they were too rough for anyone else to see. I foresee a long and interesting scientific collaboration ahead of us, and many more Grad House beers/discussions. I'm sorry I accidentally called you Justin about 10 000 times.

Justin Harbin is not only a great friend, but has been helping me collect, prepare and analyze samples since 2007. Justin, your unendingly helpful attitude and sense of humour has helped me get through a lot of interesting times. I owe you a lot of C&D coffee. I'm sorry I accidentally called you Jason about 10 000 times.

Special thanks to Dr. Naohiro Yoshida, Dr. Sakae Toyoda and their large research group at the Tokyo Institute of Technology, my hosts during my Summer Fellowship in Japan in 2010. Thanks to Akiko Makabe for teaching me to use the N_2O isotopomer mass spectrometer.

The Schiff lab group is a large, fun and helpful rotating cast of characters. Thanks to grad students former and current: David Snider for science talks and great officemate times; Simon Thuss for being an example of a motivated, hardworking grad student (which of course I did not follow); Marlin Rempel for his great attitude and open invitation to Chile; Helen Baulch (my "big sister of science"); Ryan Hutchins; Pieter Aukes (SigmaPlot wizard extraordinaire); Eric Westberg and Natalie Senger (GIS gurus, both of them); Nick Flynn and Eduardo Cejudo. Thanks to all the lab workers we've had over seven years, especially Janessa Zheng, who's put up with me the longest (minus Justin). Many of these people were forced into unnatural sleep patterns just so I could get night-time N_2O samples and for that, I am very grateful. Thank you to the previous students who worked on the Grand River (and watershed) and paved the way for this research: Simon Thuss, Jennifer Hood, Ryan Hutchins, Eric Westberg, Marlin Rempel, Terra Jamieson, Heather Loomer, Sandra Timsic, Loreto Encalada and Eric Pastora.

I'll forever be grateful to the wonderful friends I made while in Waterloo. Thanks particularly to Jana Tondu, Marcelo Sousa, Mariano Arriaga and Heather Shrimpton for making 43 Young St E. so much fun. Jennifer Faubert, thanks for being an expert listener and adventurous spirit. Japan, Chicago and New York would have been much less fun without you. Thanks to Jessica Leung for being my exercise/CSA buddy and for your positive vibes. We all need to get together for dinner and Catan soon!

Thanks to my family. My mom has been cooking me Sunday dinner without fail for 7.5 years during my time in Waterloo, and has told me all about the Neanderthals. Without her, I'd never think to find out which mitochondrial DNA haplotype I am, or appreciate the outdoors as much as I do. My dad fixed my bike, told me terrible puns and pointed out when my published maps were incomplete. My sister Emily provided a lot of emotional support, whether she was in Vancouver, Montreal or London (the real one).

Financial support was provided by the Natural Sciences and Engineering Research Council of Canada (NSERC) Strategic and Discovery Grants to S. Schiff, as well as a Postgraduate Scholarship (Masters), Canada Graduate Scholarship (PhD) and Summer Fellowship in Japan to the author. Other funding to the author came from an Ontario Graduate Scholarship, the University of Waterloo, and the Japan Society for Promotion of Science.

Contents

List of Tables

List of Figures

Chapter 1: Introduction

1.1 Anthropogenic Nitrogen in the Environment

Nitrogen is an essential nutrient for all life. It is an important component of amino acids and other biochemicals. However, most nitrogen on the Earth's surface is in mineral form or in the atmosphere as N_2, both of which are generally biologically unavailable (Galloway 2003). Biologically reactive nitrogen (N_r) includes reduced ions (NH_4^+), oxidized ions (NO_3^-, NO_2^-), reduced and oxidized gases (NH_3, NO, N_2O, NO_x) and organic compounds (amino acids, uric acid, etc.). Before the early 20th century, almost all production of N_r occurred by biological fixation of N_2 to NH_4^+, performed by cyanobacteria, heterotrophic bacteria and fungi. This is an energy-intensive process in oxic conditions because of the triple bond between the N atoms (780 kJ/mol N_2) (Gutschick 1978) and seems to be favoured in anoxic environments (Vitousek et al. 2002). Additionally, N_r is created in the atmosphere via lightning.

Before the industrial revolution, farmers added N_r to N-limited crops, primarily as manure, human waste, guano and nitrate mineral extraction (Galloway 2003). Additionally, legumes with symbiotic N-fixing fungi were planted. In pre-industrial times, between 100 and 290 Tg N/yr N_r was added to the environment by terrestrial biological N fixation (Galloway 2003), though the true value is likely on the low end of this range (Galloway et al. 2004). In 1909, the Haber-Bosch process of industrial N fixation was invented. Today, anthropogenic N_r production – a combination of the Haber-Bosch process, NO_x production from fossil fuel burning, and cultivation of legumes – is around 165 Tg N/yr, approximately doubling natural N_r sources.

The Haber-Bosch process has dramatically helped increase agricultural yields and feed the growing human population worldwide, but has also increased N_r in the environment, as biological N_r removal (denitrification and anammox) rates have not kept up with N_r production rates (Galloway 2003). This is not without ecological costs. About 56 Tg total N/yr enters costal systems (Boyer and Howarth 2008), about 25 Tg N/yr of which is dissolved inorganic nitrogen (DIN) (Dumont et al. 2005). Leached N can over-fertilize aquatic ecosystems, resulting in eutrophication (Section 1.2).

Eutrophication, production of toxic gases (NOx) and greenhouse gases (N_2O) resulting from anthropogenic N_r are occurring today (Galloway 2003) but the problem will likely worsen in the future. Human population is projected to stabilize at around 9.6 billion people by 2070 (United

Nations Department of Economic and Social Affairs 2004, United Nations Department of Economic and Social Affairs 2013). Additionally, wealth increases are expected to reduce the number of people in absolute poverty from 1.4 billion to between 0.2 and 1.1 billion by 2050 (Hillebrand 2011). This will result in greater food consumption and greater meat consumption. Therefore, N_r export to coastal zones is expected to almost double to 47 Tg N/yr by 2050 (Seitzinger et al. 2002).

1.2 Biological Nitrogen Cycling in Rivers

The biological N cycle is complex, with many processes occurring in rivers and/or river sediments (Figure 1.1). The major processes significant to this thesis are briefly outlined here.

1.2.1 Autotrophic Nitrification

Nitrification, or oxidation of ammonia (NH_3) to nitrite (NO_2^-), is performed by chemolithotrophic bacteria and archaea, which couple this half-reaction to CO_2 fixation to organic carbon. The most well-studied nitrifying organisms are bacteria in the *Nitrosomonadaceae* family (e.g. *Nitrosomonas, Nitrosococcus*, etc.), but recent research has indicated that archaea of the *Thaumarchaeota* phylum perform most nitrification in many systems (Hatzenpichler 2012). It appears that bacteria are more competitive in high-NH_4^+ systems such as sewage plants and aquaria while archaea dominate nitrification in low-N systems such as the ocean (Sauder et al. 2011).

Bacterial nitrification occurs in two steps: NH_4^+ oxidation to hydroxylamine (NH_2OH) and oxidation of NH_2OH to NO_2^- (Equation 1.1, Equation 1.2). The first reaction is catalyzed by ammonia monooxygenase (Amo) and the second by hydroxylamine oxidoreductase (Hao).

$$\boldsymbol{NH_3 + O_2 + 2H^+ \rightarrow NH_2OH + H_2O} \qquad \textbf{Equation 1.1}$$

$$\boldsymbol{NH_2OH + H_2O \rightarrow NO_2^- + 5H^+ + 4e^-} \qquad \textbf{Equation 1.2}$$

Hydroxylamine oxidation can result in byproduct nitrous oxide (N_2O), by two mechanisms. First, Hao can catalyze the reaction between NH_2OH and NO_2^- to produce N_2O. Alternatively, NH_2OH can be converted to NO^- by Hao and subsequently converted to N_2O (Otte et al. 1999), which can then diffuse out of the cell.

The pathway for nitrification by ammonia oxidizing archaea (AOAs) is not well-understood (Hatzenpichler 2012). AOAs have a gene similar to the *amo* gene in nitrifying bacteria but the predicted protein structure is quite different and the protein may have a different function (Hatzenpichler 2012). They do not have a *hao* gene homologue. It has been proposed that archaeal

Amo oxidizes NH_3 to nitroxyl hydride (HNO), which is reduced to NO_2^- by an undescribed nitroxyl oxidoreductase (NxOR) but this has not been proven (Hatzenpichler 2012). AOAs produce N_2O in cultures and in oceans (Loscher et al. 2012, Santoro et al. 2011) but the mechanism is not known.

1.2.2 Heterotrophic Nitrification

Heterotrophic nitrifiers include bacteria and fungi that oxidize NH_3 to NO_2^- but do not fix CO_2. Many are also capable of reducing NO_2^- and/or NO_3^- to N_2 (see Section 1.2.4 below) in aerobic conditions (Stein and Yung 2003, Zhang et al. 2011). They have a similar Amo enzyme to autotrophic nitrifying bacteria but a different hydroxylamine reductase enzyme. This enzyme apparently is responsible for N_2O production in this pathway but is not inhibited by acetylene (C_2H_2), unlike the Hao used by autotrophic nitrifying bacteria. C_2H_2 is commonly used to block N_2O production by nitrification in soil and sediment incubations examining N_2O from denitrification but does not block N_2O production from heterotrophic nitrification.

1.2.3 Nitrite Oxidation

Nitrite oxidization is carried out by different bacteria than NH_3 oxidation, although both processes are often combined in the term "nitrification". Many nitrite oxidizing bacteria belong to the *Nitrobacter* and *Nitrococcus* genera. The reaction (Equation 1.3) is catalyzed by nitrite oxidoreductase (Noxr):

$$\boldsymbol{NO_2^- + H_2O \rightarrow NO_3^- + 2H^+ + 2e^-} \qquad \textbf{Equation 1.3}$$

This is an autotrophic process usually coupled to CO_2 fixation. N_2O is not produced during nitrite oxidation. There is no evidence that AOAs or any other archaea can perform nitrite oxidation.

1.2.4 Denitrification

Denitrification is the multi-step reduction of NO_3^- to N_2, via NO_2^-, nitric oxide (NO) and N_2O. Each step requires a unique enzyme. Denitrification is almost always a heterotrophic process usually coupled with organic carbon oxidation to CO_2 or other energy-yielding oxidation reactions. Denitrification occurs in hypoxic (low-oxygen) or anoxic (oxygen-free) environments. It is carried out by a large group of bacteria, fungi and archaea. All bacterial denitrifiers that have been isolated in laboratory are facultative anaerobes (i.e. will reduce O_2 if available and switch to NO_3^- reduction otherwise) (Cabello et al. 2004).

Heterotrophic denitrification is NO_3^- reduction coupled with reduction of organic carbon to CO_2. It yields ~452 kJ energy per mole organic carbon oxidized, depending on substrate type and

concentration (less than aerobic respiration: 476 kJ/mole), which is used to generate ATP. The sum of the four half reactions coupled with CH_2O oxidation is shown below:

$$4NO_3^- + 5CH_2O + 4H^+ \rightarrow 2H_2 + 7H_2O + 5CO_2 \qquad \textbf{Equation 1.4}$$

The half-reactions are catalyzed by nitrate reductase (Nar), nitrite reductase (Nir), nitric oxide reductase (Nor) and nitrous oxide reductase (Nos) (Figure 1.2). Denitrification enzymes are typically inhibited by high O_2 concentration, but each enzyme appears to have a unique O_2 threshold for activation, which changes with N substrate (Körner and Zumft 1989). Additionally, some denitrification enzymes appear to be continually present in cells even in oxic conditions (e.g. unspecified nitrate reductase (Patureau et al. 1996); Nar, Nir and Nor (Firestone and Tiedje 1979) and Nos (Körner and Zumft 1989)) and some are synthesized on the onset of denitrification (e.g. Nos (Firestone and Tiedje 1979). This appears to differ by microbial species.

Interestingly, up to one third of denitrifying bacteria in soils lack the *nos* gene, meaning that they cannot produce N_2 and therefore emit substantial N_2O (Philippot et al. 2011). Archaeal denitrification enzymes are not well understood but appear to be homologous to bacterial and fungal enzymes (Cabello et al. 2004). Some but not all denitrifying archaea are able to reduce N_2O to N_2 (Cabello et al. 2004).

Autotrophic denitrification is the coupling of NO_3^- reduction to oxidation of inorganic substrates. The resulting energy produced is used to fix CO_2 to organic carbon. This commonly occurs in areas with low organic carbon and available mineral substrates such as groundwater (Rivett et al. 2008). Typical inorganic substrates used in this reaction are thiosulphate ($S_2O_3^{2-}$), pyrite (FeS_2), hydrogen gas (H_2) and ferrous carbonate ($FeCO_3$). Autotrophic denitrification can occur in oxic environments (Zumft 1997), meaning that N_2O produced by this pathway can be confused with that from nitrification.

1.2.4.1 "Nitrifier denitrification"

The term "nitrifier denitrification" is typically used in the literature to refer to N_2O production via NO_2^- reduction by nitrifying bacteria, which occurs over a large range of oxygen concentrations. The term can also encompass any N_2O production occurring in oxic environments. Thus, several processes can be included, described briefly below.

First, many autotrophic nitrifying bacteria have functional denitrification enzymes and can reduce NO_2^- to N_2O or N_2, especially under low-O_2 conditions. This is thought to fill one or more of three

functions: remove toxic NO_2^- from cells, use NO_2^- as an electron acceptor when O_2 is low, and/or outcompete nitrite oxidizing bacteria for O_2 by removing their substrate NO_2^- (Hayatsu et al. 2008).

Additional pathways lumped in the term "nitrifier denitrification" include denitrification by heterotrophic nitrifiers in oxic environments (Section 1.2.2), which typically have low N_2O yields. In contrast, aerobic denitrification can also be performed by autotrophic denitrifiers which cannot oxidize NH_3 but can operate in oxic conditions. They typically have high N_2O yields (Zumft 1997).

Methanotrophic bacteria, which oxidize CH_4 to CO_2 for energy and also use CH_4 for cellular-C, simultaneously oxidize NH_3 to NH_2OH and then NO_2^- under oxic conditions. Instead of using Amo, they use methane monooxygenase for the first step and an Hao may be similar to that of autotrophic nitrifiers (Bedard and Knowles 1989). This reaction can produce N_2O but the reaction pathway is not well understood (Stein and Yung 2003).

"Nitrifier-denitrification" can also include the coupling of nitrification and denitrification by different organisms. For example, in aerobic sediments, nitrifiers and nitrite oxidizers produce NO_3^-, which is then taken up by denitrifying organisms living in anoxic microsites in the sediment. In low-NO_3^- systems, denitrification rates may be tightly coupled with NO_3^- production rates (Seitzinger et al. 2006).

The term "nitrifier-denitrification" will be avoided in this work because it encompasses many N_2O production pathways using different enzymes and it is unlikely that all pathways share common geochemical predictors and may result similar stable isotopic effects.

1.2.5 N_r Assimilation

N_r is taken up by almost all biota for use in cellular molecules such as proteins. N-fixing organisms can also form N_r by splitting N_2. This typically, but not always, occurs when N_r resources are low or unavailable. N-fixers include specialized cyanobacteria, heterotrophic bacteria, archaea and fungi.

In many rivers and streams, N_r uptake rates are around one order of magnitude higher than denitrification rates (Mulholland et al. 2004) and thus are a significant part of the biotic N cycle. Aquatic plants and algae make up a large part of the total biomass in many streams and rivers and therefore take up most N_r (Wetzel 1975). However, plant and algae N uptake is not as well understood as microbial and fungal N assimilation. NO_3^- uptake in plants and algae requires ATP-binding cassette enzymes, which use energy to draw NO_3^- into the cell (González-Ballester et al. 2004, Kraiser et al. 2011). In contrast, plants, alga and other organisms use ammonia transporters

(Amts) for NH_4^+ assimilation, but it is unclear if they passively channel NH_3 (which also passively diffuses into cells) or actively transport NH_4^+ across the cell membrane (Andrade et al. 2005). NH_4^+ uptake is more energetically efficient than NO_3^- uptake, but NH_4^+ is typically at least an order of magnitude lower in concentration than NO_3^- in well-oxygenated streams and rivers (Wetzel 1975). Multicellular, rooted plants (macrophytes) are also capable of "luxury uptake" of N_r that can be used later if N_r becomes scarce (James et al. 2006).

In gram-negative bacteria, NO_3^- is taken from outside the cell into the periplasm by an "unknown porin"; porins do not require energy for transport of small ions (Song and Niederweis 2012, Steen et al. 2013). However, NO_3^- transport from the periplasm to the cytoplasm requires two complexed proteins (NarK1 and NarK2) that require energy in the form of the proton motor force (i.e. H^+ must be pumped across the membrane to maintain an electromotive force) (Lin and Stewart 1998, Moir and Wood 2001, Wood et al. 2002). NO_3^- is then reduced in the cytoplasm using nitrate reductases (Nap and Nas) similar but not identical to those used in denitrification (Jepson et al. 2006). Cyanobacteria use Amts, which are presumed to be active transporters, to transport NH_4^+ into cells (Herrero et al. 2001). Assimilative nitrate reductase (NAS) in gram-negative bacteria is inhibited by NH_4^+ (Warnecke-Eberz and Friedrich 1993), indicating that bacteria preferentially assimilate NH_4^+ over NO_3^-.

1.2.6 Other N Cycling Processes

Several other biological N cycling processes occur in streams and rivers. Most are thought to play a small role in N cycling but some may be more important than previously realized. They are discussed briefly below.

Dissimilatory nitrate reduction to ammonia (DNRA) is an anaerobic heterotrophic process similar to denitrification but the end product is NH_4^+ (Rutting et al. 2011). It is performed by a variety of bacteria and fungi. DNRA theoretically produces less energy per mole CH_2O than does denitrification (299 kJ and 452 kJ, respectively) (Rutting et al. 2011) but laboratory studies indicate that actual energy yield is higher for DNRA (Strohm et al. 2007). Recent research has indicated that DNRA can be a major N cycling pathway in some aquatic ecosystems (Dong et al. 2011). The pathway uses Nir and cytochrome c nitrite reductase (Nrf) to produce NH_4^+ from NO_2^- (Simon 2002). Typically, about 1-2% NO_2^- reduced is converted to N_2O, probably as a detoxification byproduct (Rutting et al. 2011). N_2O production can be difficult to attribute to DNRA because many organisms may perform DNRA and denitrification simultaneously (Rutting et al. 2011).

Anammox (anaerobic ammonium oxidation) is a pathway performed by specialized bacteria in the phylum *Planctomycetes*. These bacteria react NO_2^- and NH_4^+ to produce N_2, H_2O and energy. The reaction occurs in a specialized organelle called an anammoxosome, which isolates a toxic intermediate produce, hydrazine (N_2H_4) (Thamdrup and Dalsgaard 2002). Anammox bacteria are slow-growing but exist in diverse environments such as the open ocean (Thamdrup and Dalsgaard 2002), groundwater (Robertson et al. 2012) and Arctic Ocean sediments (Rysgaard et al. 2004). Anammox bacteria are cultured commercially for use in wastewater treatment plants (WWTPs). N_2O is often produced in small quantities (~2% of total product) in WWTPs using anammox (Kampschreur et al. 2008) and in laboratory anammox cultures (Kartal et al. 2007); this may be due to N_2O production by anammox bacteria, possibly as a detoxification pathway, although the mechanisms is not understood (Kartal et al. 2007)

Denitrification was long thought to be the only biological sink for N_2O. However, it is now apparent that many bacteria have genes for a modified N_2O reductase (similar but not identical to Nos used in denitrification) but do not have genes for other enzymes needed for complete denitrification (Sanford et al. 2012). DNRA bacteria with a modified Nos gene were shown to reduce N_2O to N_2 (Sanford et al. 2012). Additionally, N_2O fixation to organic N using the enzyme for N_2 fixation (nitrogenase) was very recently demonstrated in marine cyanobacteria *in situ* and in laboratory experiments (Farías et al. 2013). The recent discovery of these two pathways indicates that biological N_2O removal could be more significant and complex than previously thought.

1.3 Stable Isotope Dynamics in N Cycling

1.3.1 Stable Isotope Theory

Stable isotopes are non-radioactive variants of elements with different numbers of neutrons but the same number of protons. Isotopes of the same element have near-identical chemical properties but the difference in nuclear mass results in changes in chemical, biological and physical reaction rates. Typically, in enzyme-mediated biological reactions, light isotopes are used preferentially because less energy is required to break bonds between light atoms.

Stable isotopic ratios are typically reported in delta (δ) notation relative to an international standard, in per mil (‰) units:

$$\delta = \frac{R_{sample}}{R_{standard}} - 1 \qquad \textbf{Equation 1.5}$$

where R_{sample} is the heavy-to-light isotopic ratio of the sample (e.g. $^{15}N/^{14}N$) and $R_{standard}$ is the same for the standard. The international standard for N is N_2 in air ($^{15}N/^{14}N = 0.003677$) and the international standard for O is Vienna Standard Mean Ocean Water (VSMOW, $^{18}O/^{16}O = 0.0020052$) (Kendall and Caldwell 1998).

There are two ways to report differences in isotopic ratios between substrates and products in biological reactions. The first is the isotope fractionation factor (α), defined as:

$$\alpha = \mathbf{R}_{product}/\mathbf{R}_{substrate} \qquad \textbf{Equation 1.6}$$

α is a unitless ratio. However, because isotopic fractionations can be small, resulting in α values near 1, sometimes the isotopic fractionation (ε) notation is used:

$$\varepsilon = \frac{R_{product}}{R_{substrate}} - 1 \qquad \textbf{Equation 1.7}$$

Like δ values, ε values are reported in permil (‰) units. To distinguish between N and O stable isotopic fractionations, the notations $\varepsilon^{15}N$ and $\varepsilon^{18}O$ will be used here.

The stable isotope ratios of N compounds (NH_4^+, NO_3^-, N_2O) can be used with other geochemical techniques to trace sources of N to rivers and streams, and to determine in-river N transformation processes. For NO_3^- and N_2O, both $^{15}N/^{14}N$ and $^{18}O/^{16}O$ can be measured. Much work has been conducted to understand how stable isotope ratios change between N species during biological N cycling processes. These are discussed briefly below.

1.3.2 How and Why Stable Isotopic Fractionations Occur

Differences in reaction rates between heavy and light stable isotopes result in changes in isotope ratios between substrates and products for biological reactions. Typically, lighter isotopes have faster reaction rates. However, the observed fractionation depends on substrate availability, substrate uptake rate, and the number of rate-limiting steps in the reaction.

For instance, in laboratory studies with no substrate limitation, maximum isotopic effects typically are observed. In natural systems, substrate may be limited, and organisms will take up and process all or most available substrate. If all substrate is used, the isotopic ratio of the product must equal that of the substrate to conserve mass. Natural systems and sediment incubation studies include many organisms which may have different inherent fractionation factors for the same pathway, and/or be

operating at different rates. In this case, the observed fractionation is an average of the relative fractionation factors and rates of all organisms contributing to the reaction.

There are three ways to measure the stable isotopic fractionation of a biological process. First, the substrate and products can both be measured outside cells. For example, in nitrification, NH_4^+ (substrate) and NO_3^- (product) can be measured. Alternatively, the substrate can be measured at multiple times as a single pool of substrate is used. This is useful in open systems where the end product disappears, or when the end product is difficult to measure isotopically: for instance, during denitrification, as N_2 may leave the system by degassing and is very difficult to measure without contamination with air. Lastly, in multi-step biological reactions, the substrate and an intermediate species can be measured. For instance, in denitrification, NO_3^- (substrate) and N_2O (intermediate) can be isotopically characterized, but this cannot produce an isotopic fractionation for full denitrification to N_2.

When only the substrate is measured, there are two possible ways that isotopic fractionation can be expressed. In scenario 1, the cell only uptakes the amount of substrate it requires for a reaction, and all substrate is used once it enters the cell. Isotopic fractionation therefore must occur upon substrate uptake. In scenario 2, isotopic fractionation occurs not during uptake but during enzyme-mediated reactions inside the cell. If fractionation in the remaining substrate is measurable, more substrate must be taken up than is used, and residual, unused substrate must leave the cell and mix with substrate in the environment (Figure 1.3). These scenarios may have different implications for controls on isotopic fractionation of N pathways in the environment and will be discussed below.

1.3.3 Nitrification and Nitrite Oxidation

Bacterial nitrification typically has a strongly negative $\varepsilon^{15}N$ between NH_4^+ and NO_2^-. An extensive literature review reports a range of -38‰ to -14‰, based on pure culture studies (Snider 2011). Bacterial nitrite oxidation has a positive $\varepsilon^{15}N$ (i.e. the product has more ^{15}N than the substrate), which is unusual in enzyme catalyzed reactions, ranging from 8‰ to 24‰ (Casciotti 2009).

As NH_4^+ does not contain oxygen, NO_3^- produced from nitrification and nitrite oxidation uses O atoms from water and oxygen. It was long thought that 2/3 of the O atoms came from water and 1/3 from O_2, with no isotopic fractionation (Kendall and Caldwell 1998). However, recent work suggests that this model is incorrect (Snider et al. 2010). Snider et al. (2010) found that between 37% and 88%

of O in nitrifier NO_3^- was from H_2O in temperate forest and agricultural soils. It also appears that isotopic fractionation occurs on incorporation of O into NO_3^-.

Isotopic fractionations between NH_4^+ and nitrifier-derived N_2O can also be measured. The literature range for $\varepsilon^{15}N$ is -112‰ to -12‰ (Snider 2011). Snider (2011) found $\varepsilon^{15}N$ values for NH_4^+ to N_2O ranging from -35‰ to -16‰ in soil incubations using temperature agricultural and forest soils. $\delta^{18}O$-N_2O from hydroxylamine oxidation commonly ranges from 13‰ to 31‰ but reason is not well understood (Snider 2011).

Interestingly, $\varepsilon^{15}N$ values between NH_4^+ and N_2O in cultured marine ammonia oxidizing archaea (AOAs) are higher than their bacterial counterparts (range: 3.8‰ to 7.6‰) (Santoro et al. 2011). $\delta^{18}O$-N_2O values had a very narrow range (33.0‰ to 34.9‰) and were slightly higher than bacterial nitrifier values (Santoro et al. 2011). These differences probably result from the unique but uncharacterized archaeal N_2O production enzyme.

1.3.4 Denitrification

Because contamination with air during N_2 isotopic analysis is difficult to avoid, only the NO_3^- to N_2O pathway will be addressed here. Typically, $\varepsilon^{15}N$ values for denitrification N_2O are lower than those for nitrification N_2O; values from the literature range from -55‰ to -10‰ (Snider 2011). Values of $\varepsilon^{18}O$ have a very large range, from -54‰ to 32‰ (Snider 2011). This is because $\varepsilon^{18}O$ is large and positive but can be overprinted by abiotic O exchange between H_2O (typically, $\delta^{18}O$-H_2O: -20‰ to 0‰ in temperate and tropical environments) and intermediates in the denitrification process, particularly NO_2^- (Snider et al. 2009). Lower net $\varepsilon^{18}O$ values in denitrification typically indicate high O exchange (Snider et al. 2009).

1.3.5 N_r Assimilation

The data on isotopic fractionation during N assimilation by plants, algae and microbes is scarce. The marine phytoplankton *Skeletonema costatum* was shown to isotopically fractionate upon assimilative uptake of NO_3^- at a concentration-independent value of -9‰ (Pennock et al. 1996). In contrast, fractionation during NH_4^+ uptake is concentration-dependent. At high NH_4^+ (> 0.28 mg N/L), fractionation ranged from -28.8‰ to -19.1‰. When NH_4^+> 0.28 mg N/L, fractionation is closer to zero (-7.3‰ ±3.0‰) (Pennock et al. 1996). A similar experiment with other marine alga showed concentration-dependency and a range of $\varepsilon^{15}N$ values from -20‰ to -5‰, suggesting that $\varepsilon^{15}N$ in algal NH_4^+ uptake may be species-dependent (Hoch et al. 1994).

Studies of isotopic fractionation during N uptake of submerged freshwater macrophytes are scarce. *Myriophyllum spicatum* did not exhibit any isotope fractionation when exposed to ^{15}N-labelled NO_3^- because it assimilated all available NO_3^- (Cohen and Bradham 2010). Several studies note that $\delta^{15}N$ of macrophyte tissue is very similar to WWTP effluent $\delta^{15}N$ values (Derse et al. 2007, Savage and Elmgren 2004). In contrast, in a survey of 30 UK lakes, macrophytes could be as much as 6‰ lower in $\delta^{15}N$ than total dissolved nitrogen (TDN) or sediment but could also be higher (Jones et al. 2004). This suggests that they may exhibit isotopic fractionation during N uptake. Isotopic fractionation (-7.9‰ to +7.5‰) during NH_4^+ uptake was noted in emergent rice plants in heavily-fertilized rice paddies, but not in NO_3^- uptake (Yoneyama et al. 1991). These contrasting data suggest that isotopic fractionation could be expressed in submerged macrophytes when N_r supplies are plentiful, but are not expressed when N_r is low.

1.4 Global Estimates of NO_3^- Leaching to and N_2O Emissions from Rivers and Streams

Rivers and streams are vulnerable to excess NH_4^+ and NO_3^- runoff and discharge from human activities of agricultural fertilization and human sewage outfalls. Excess N_r may result in eutrophication, though the role of N in limiting growth in rivers is variable and hotly debated (Conley et al. 2009, Schindler 2012, Elsaholi and Kelly-Quinn 2013). Eutrophication is the ecosystem response to excess nutrients, and has several undesirable effects. Typically, high nutrients promote high primary production. This leads to high community respiration, resulting in low oxygen conditions (hypoxia). Hypoxia is toxic to aerobic aquatic organisms such as invertebrates and fish (Wetzel 1975). Eutrophication also typically results in decreased biodiversity and ecosystem function (Wetzel 1975).

Additionally, both NH_4^+ and NO_3^- are toxic to wildlife. Environment Canada considers dissolved ammonia gas (NH_3) concentrations greater than 0.019 mg N/L toxic to aquatic life (Environment Canada 2003). This equals 0.30 mg N/L (NH_3 + NH_4^+) at pH 8, a typical pH value for the Grand River. NO_3^- concentrations greater than 2.9 mg N/L are considered toxic to aquatic life and the drinking water limit is 10 mg N/L (Environment Canada 2003). NH_4^+ and NO_3^- export to N-limited estuaries and oceanic coastal zones can cause eutrophication. The hypoxic zones in the Gulf of St. Lawrence are caused by high N_r inputs from the St. Lawrence River system, including the Grand River and the Laurentian Great Lakes (Ouellet et al. 2010).

Additionally, rivers, streams and estuaries produce around 25% of anthropogenic N_2O emissions to the atmosphere (Syakila and Kroeze 2011). N_2O is a greenhouse gas 298 times more powerful than CO_2 on a 100 year time scale (IPCC 2007). Additionally, N_2O breakdown in the stratosphere produces NO, the current primary cause of ozone depletion (Ravishankara et al. 2009). N_2O concentration in the atmosphere has been increasing since the industrial revolution, and now is ~320 ppb (European Environment Agency 2013), higher than pre-industrial concentrations of 270 ppb. The signatory countries to the United Nations Framework for Climate Change must report annual N_2O emissions from anthropogenic sources, including N_2O from rivers resulting from human NH_4^+ and NO_3^- additions. The IPCC encourages direct N_2O measurements but also provides "default equations" to estimate N_2O production in rivers. Canada currently uses these equations (Chang Liang, Environment Canada, personal communication) as do many other countries.

The conceptual model of the IPCC equations is as follows. N_r is applied to the landscape as synthetic fertilizer (F_{SN}), manure and sludge applied to crops (F_{ON}), urine and dung from grazing animals (F_{PRP}), N in crop residue (F_{CR}), and in soil organic matter (F_{SOM}). A fraction of the sum ($Frac_{LEACH}$) is expected to leach into surface waters (IPCC 2007):

$$N_{LEACH} = (F_{SN} + F_{ON} + F_{PRP} + F_{CR} + F_{SOM}) \times Frac_{LEACH} \qquad \textbf{Equation 1.8}$$

Where all values but $Frac_{LEACH}$ (unitless) are in kg N/year.

Once N_{LEACH} enters freshwater bodies, a fraction (EF_5) is expected to become N_2O via nitrification and denitrification. Therefore the equation for N_2O production from groundwater, rivers and estuaries is:

$$N_2O\ emission = EF_5 \times N_{LEACH} \qquad \textbf{Equation 1.9}$$

where N_2O emission is in kg N/year and EF_5 is a unitless ratio. EF_5 is further subdivided into portions that occur in groundwater and small agricultural streams ($EF_{5\text{-}g}$, default: 0.0025), rivers ($EF_{5\text{-}r}$, default: 0.0025) and estuaries ($EF_{5\text{-}e}$, default: 0.0025) (Ivens et al. 2011).

In the IPCC's Third Assessment Report (Intergovernmental Panel on Climate Change 1996), the default value for EF_5 (including groundwater, rivers and estuaries) was 0.025 (Table 1.1). The default $EF_{5\text{-}g}$ was 0.015, based on a review of six studies of N_2O and NO_3^- in agricultural groundwater (Nevison 2000). Nitrification and denitrification were assumed to have an equal emission factor of 0.005. Therefore, $EF_{5\text{-}r}$ was set to 0.0075, on the assumption that all N_{LEACH} would nitrify and half would denitrify (Nevison 2000). The remaining half of N_{LEACH} that was not denitrified entered

estuaries, where half of it was nitrified and half denitrified, resulting in an EF_{r-e} default value of 0.0025.

Since the Third Assessment Report, several studies suggested that EF_{5-g} and EF_{5-r} values were too high (Clough et al. 2006, Reay et al. 2003). Therefore both values were lowered to 0.0025 to match EF_{r-e} in the Fourth Assessment Report (IPCC 2007), resulting in a total EF_5 of 0.0075. Since then, other studies have suggested that the 1996 EF_{5-g} and EF_{5-r} values may be valid (Beaulieu et al. 2010, Beaulieu et al. 2011). The conceptual model the equations are based on is now unclear, but if the assumption that the fraction N_2O produced during nitrification and denitrification is the same is kept, one quarter of N_{LEACH} is nitrified and one-quarter is denitrified in each of the three locations (groundwater, river, estuary) with no permanent loss of N_{LEACH} through the system (Table 1.1, Figure 1.4).

1.5 The Grand River – Background

The 300 km-long Grand River is the largest Canadian river draining into Lake Erie. Its 7000 km^2 watershed has predominantly (80%) agricultural land use and 30 WWTPs discharging to the river and its tributaries. The Grand River is seventh-order at the mouth, with an annual average discharge of 56 m^3/s (Aquaresource 2009). The watershed is underlain by calcium carbonate-rich glacial tills and limestone and dolostone bedrock (Karrow and Morgan 2004).Because of high nutrient loading from wastewater and agricultural runoff and groundwater, the Grand River has several ecological and drinking problems. The central river, downstream of the large Kitchener-Waterloo-Cambridge area has very high macrophyte biomass (Hood 2012), high community respiration rates (Venkiteswaran et al, in submission), and periods of low dissolved oxygen in summer at night (Jamieson 2010, Thuss 2008). Biodiversity of benthic invertebrates and fish is also low in this region (Loomer 2009). There is concern that poor water quality and high water temperatures negatively impact the recreational fishery industry in the Grand River (Cooke 2006).

High nutrient concentrations also affect drinking water quality in the Grand River. Of the watershed's 900 000 residents, about half (~500 000) drink Grand River water (Grand River Conservation Authority 2008)Water quality problems often occur in Brantford, which is downstream of Kitchener-Waterloo and derives 100% of its drinking water from the river. NH_4^+ concentrations in winter at Brantford can be high enough to force the closure of drinking water intake pipes. NO_3^- concentrations are typically below the drinking water limit of 10 mg N/L. However, currently the

largest WWTP on the Grand River, in Kitchener, releases NH_4^+ in effluent. The plant is currently being upgraded to release NO_3^-. This may reduce NH_4^+ in Brantford's drinking water but drastically increase NO_3^- (Mark Anderson, personal communication). Nitrogen loading to the watershed, removal and storage on the landscape, and removal and transport in the river are not well understood, although this is crucial to managing the river for ecosystem health and drinking water quality.

1.6 Study Sites

The Grand River contains mesotrophic sites in the upper basin but is predominantly eutrophic, with high total phosphorus concentrations (range: 11.4 to 117.2 μg P/L, Table 1.2), and high epilithion and macrophyte biomass in summer. Dissolved oxygen (DO) has a strong diel cycle in summer, changing by >10 mg/L/day in some sites, with night-time DO concentrations at some sites < 2 mg/L. This raises concern about ecosystem stress and fish habitat. Additionally, the Grand River watershed population was 887 400 in 2006 (GSP Group 2010), about half of whom use river water for drinking. High NO_3^- and NH_4^+ concentrations, especially in winter, can force closure of municipal water intake pipes in the downstream communities of Brantford and Port Maitland (Cooke 2006). The river has significant seasonal changes in water chemistry; Figure 1.5 shows NO_3^- and N_2O concentrations from 2006 to 2012 at two sites: Bridgeport (Site 9), upstream of a large municipal area, and Blair (Site 11), downstream of the urban area.

This thesis utilizes 23 sampling sites on the Grand River, from ~6 km downstream of the source to the mouth. Sites are numbered 1 through 23 but Chapter 2 used a different naming system for four sites (Table 1.2). Sites were chosen to match Provincial Water Quality Monitoring Network sites and to capture the influence of upstream effects such as dams, WWTPs and major tributaries (Table 1.2).

These sites can be divided into four areas based on geomorphology and land use, described in more detail in Chapter 6. The Upper Agricultural area (Sites 1-9) is located in a glaciated till plain and moraine area. Most land use is agricultural, though effluent from small WWTPs from the towns of Dundalk, Arthur, Grand Valley, Elora, Fergus and Conestogo enters the river here. Many sites are mesotrophic (Table 1.2). The sixth-order Conestogo River joins the Grand River above Site 9. The Urban section (Sites 10 – 12) is dominated by the Kitchener-Waterloo-Cambridge municipal area (total population: 480 000). Sites here are heavily influenced by effluent from the Waterloo, Kitchener, Galt and Preston WWTPs. Site 11 (Blair) in particular routinely has DO < 2mg/L in summer at night-time. The Groundwater Recharge section (Sites 13 – 16) is in a predominantly

agricultural area with one town (Paris, population: 12 000). The Paris moraine, consisting largely of sand and gravel, contributes significant groundwater discharge into the river (Aquaresource 2009). This groundwater varies in NO_3^- and DO concentration but overall appears to dilute some of the nutrients and pollution from the Urban section (Westberg 2012). Lastly, the Lower Agricultural section (Sites 17 – 23) is again primarily agricultural. Here, the river flows over a low-gradient glaciolacustrine clay plain, and is deeper and slower than previous sites. The city of Brantford (population: 90 000) and smaller towns of Cayuga (population: 1500), York and Dunnville (population: 12 000) release treated WWTP effluent to the river.

1.7 Thesis Outline

Previous work on the Grand River has indicated that it had severe hypoxia problems in the Urban section (Jamieson 2010). Coupling of N and O cycles on the diel scale had been observed during night time hypoxic events at Site 11 (Thuss 2008) but where not reported elsewhere in the Grand River catchment. N_2O concentrations were known to be oversaturated with respect to the atmosphere at many sites in the river but N_2O emissions to the atmosphere were not quantified (Thuss 2008). Globally, N_2O emissions were thought to be linearly related to NO_3^- additions to rivers, after the IPCC equations (Section 1.4). WWTP effluent was known to contain NH_4^+ and NO_3^- but its N_2O and CH_4 content and stable isotopic composition was unknown. N_2O stable isotopic effects were well-characterized for soils but not for river sediments. The usefulness of N_2O stable isotopes in rivers to identify N cycling pathways was not clear. NH_4^+ and NO_3^- additions from runoff and WWTP effluent were known to be significant N_r sources to the Grand (Cooke 2006) but were not well quantified.

Thus, the overall goal of this thesis is to fill in the research gaps on N cycling described above in the Grand River, in order to better understand (a) N_2O production and emission, and (b) NO_3^- sources and processing in impacted rivers. I hope that this thesis will help make science-based management decisions for the Grand River Watershed and elsewhere. The thesis includes an introductory chapter (Chapter 1), six research chapters (2 through 7) and a conclusions chapter (8). The specific objectives of each chapter are discussed below.

Chapter 2 was previously published in the *Journal of Environmental Quality* (Rosamond et al. 2011) and addressed the coupling of N and O cycles on the diel scale in the Grand River and two of its tributaries (the Speed and Eramosa Rivers). Summer diel DO cycling exists at all sites where DO has been measured in the Grand River; even mesotrophic sites experience diel DO ranges of ~4

mg/L/day. Previous work had documented dramatic changes in N species (NO_3^-, NH_4^+ and N_2O) at Site 11 during hypoxic events at night (Thuss 2008). However, the presence or extent of N and O coupling on the diel scale when DO changes but conditions were always oxic was not known in the Grand River and little previous work had been published for other systems (Laursen and Seitzinger 2004, Harrison et al. 2005). DO, NO_3^-, NH_4^+ and N_2O were measured over ~28 hours in May, June, August and October at six river sites to determine the presence and extent of diel cycles in N species. Relationships between N_2O diel ranges and a variety of potential controls (NO_3^-, temperature, gas exchange coefficient, DO) were examined. Lastly, several sampling strategies were assessed on their ability to capture diel variability and to estimate the diel mean N_2O concentration.

Chapter 3 was previously published in *Nature Geoscience* (Rosamond et al. 2012). This chapter reports N_2O emissions from all 23 sites in the river, over a 2 year time span, with a special focus on the middle Grand River (Sites 8, 9, 11 and 13). It is the most complete dataset of riverine N_2O fluxes currently published. N_2O emissions were compared to temperature and concentrations of NO_3^-, NH_4^+ and DO to determine if IPCC equations held true. N_2O emissions and NO_3^- mass were also compared between a wet and dry year. The chapter discusses the usefulness of the IPCC paradigm and suggests alternate approaches based on this extensive dataset.

Chapter 4 is in review for publication in *Environmental Science and Technology* (manuscript number: es-2013-032776). WWTP effluent typically contains high concentrations of NH_4^+ and/or NO_3^-. Downstream N_2O production via these compounds is included in IPCC N_2O estimates but strangely, N_2O and CH_4 concentrations in effluent had never been measured and published. Some studies report $\delta^{15}N\text{-}N_2O$ and $\delta^{18}O\text{-}N_2O$ in wastewater within WWTPs (i.e. before they are emitted to water bodies) (e.g. (Townsend-Small et al. 2011, Toyoda et al. 2011)) but values varied by site and it was unclear if $\delta^{15}N\text{-}N_2O$, $\delta^{18}O\text{-}N_2O$ and $\delta^{13}C\text{-}CH_4$ could be predicted by WWTP type or if they were distinct from in-situ river sources and could be used as WWTP effluent tracers. Effluent was collected in summer and winter of a 24-hour cycle at a non-nitrifying WWTP, a partially nitrifying WWTP and a fully nitrifying WWTP in the Grand River watershed. DO, NO_3^-, NH_4^+, N_2O and CH_4 concentrations were measured, as well as $\delta^{15}N\text{-}NO_3^-$, $\delta^{15}N\text{-}NH_4^+$, $\delta^{15}N\text{-}N_2O$, $\delta^{18}O\text{-}N_2O$ and $\delta^{13}C\text{-}CH_4$. Dissolved N_2O and CH_4 concentrations were multiplied by effluent flow to estimate emissions and compared to direct emissions from WWTPs and to downstream emissions resulting from nitrification and denitrification of effluent NH_4^+ and NO_3^-. Stable isotopic values were compared to literature values for WWTP effluent (when available) and to river values to determine if effluent could be traced with stable isotopes.

Chapter 5 describes laboratory incubations measuring stable isotopic fractionation between NO_3^- and N_2O during denitrification in Grand River sediments. It is the first measurement of its kind using river sediment. The incubation set-up was modelled after denitrification incubations conducted using forest and agricultural soil (Snider et al. 2009) and quantified $\varepsilon^{15}N$ and $\varepsilon_{net}{}^{18}O$ for the production of N_2O from NO_3^-. Additionally, ^{18}O-labelled water was added so that the fraction O exchange (i.e. O in N_2O from H_2O, not from NO_3^-) could be quantified. $\varepsilon^{15}N$, $\varepsilon_{net}{}^{18}O$ and O exchange were compared to net N_2O production rate in order to determine if N_2O reduction to N_2 played a major role in isotopic fractionations.

Chapter 6 presents a NO_3^- mass balance for the Grand River in three seasons, using denitrification rates extrapolated from N_2O production rates and solving for NO_3^- loss or gain for 23 reaches in the river. A stable isotope mass balance is also presented, showing $\delta^{15}N$-NO_3^- values for incoming or outgoing NO_3^-. Lastly, an annual box model for the watershed is presented, including NO_3^- loads to the river from agriculture, WWTPs and septic beds. The objective is to quantify NO_3^- application to the watershed, leaching from the watershed and loss before the Grand River, NO_3^- loss within the Grand River and export to Lake Erie. It is hoped that this information is useful to managers in river systems where drinking water pollution by NO_3^- is a concern.

Chapter 7 examines N_2O-NO_3^- relationships in 24 oxic streams and rivers in Southern Ontario, to examine whether N_2O-NO_3^- relationships exist when DO is high. Regression tree analysis was used to determine if non-parametric relationships between N_2O and a variety of factors (temperature, DO, NH_4^+, TP, DOC, etc.) existed. These data are compared to the global published dataset, and a conceptual model was developed to explain changes in N_2O emission variability with NO_3^- concentration. The objective is to present a tool for scientists and managers for NO_3^- and N_2O management and measurement.

Chapter 8 summarizes the conclusions of the previous six chapters and puts them in context of greenhouse budgets, inventories, river management ecosystem health and drinking water quality. It outlines future directions that research can take to improve our understanding of N cycling and N_2O production and emission from rivers.

Table 1.1: IPCC emission factors for N_2O production in groundwater ($EF_{5\text{-}g}$), rivers ($EF_{5\text{-}r}$) and estuaries ($EF_{5\text{-}e}$), from the Third Assessment Report (Intergovernmental Panel on Climate Change 1996) and Fourth Assessment Report (IPCC 2007). Nitrification and denitrification were both assumed to produce 0.005 kg N_2O-N per kg NO_3^-N (Nevison 2000) in the Third Assessment Report.

	1999		2007	
	Value	Reasoning (Ivens et al. 2011, Nevison 2000)	Value	Reasoning (Ivens et al. 2011)
$EF_{5\text{-}g}$	0.015	Literature review	0.0025	Literature review
$EF_{5\text{-}r}$	0.0075	All nitrified, half denitrified	0.0025	Literature review
$EF_{5\text{-}e}$	0.0025	Remainder nitrified, half denitrified	0.0025	Literature review
EF_5 (total)	0.025		0.0075	

Table 1.2: Site descriptions, locations and codes in the Grand River discussed in this work. Some sites have different codes in Chapter 2. E = eutrophic (TP > 75 µg P/L), M = mesotrophic (TP: 25 to 75 µg P/L), O = oligotrophic (TP < 25 µg/L) (Dodds et al. 1998). Other points of interest (tributaries, WWTPs, dams etc.) are shown in grey shading where they enter the river. TP concentrations are means of three sampling events in June 2007, September 2007 and April 2009. See Chapter 6 for details on TP collection and analysis.

Sampling Site Number	Site code in Chapter 2	Site Name	Latitude	Longitude	Distance from source (km)	Altitude (masl)	Strahler number (Grand River)	Strahler number (smaller river)	Mean TP (µg P/L) (Trophic Status)
1		Dundalk	44° 8' 44.98"	-80° 20' 31.96"	2.93	517	3		23 (O)
2		Keldon	44° 2' 15.72"	-80° 22' 58.8"	21.43	481	4		29 (M)
		Black Creek (Luther Marsh) Confluence	43° 58' 26.26"	-80° 21' 36.23"	32.31	465	5	4	
3		Leggatt	43° 58' 2.7"	-80° 21' 17.84"	33.18	465	6		29 (M)
4		above Grand Valley	43° 55' 22.97"	-80° 19' 15.58"	40.45	458	6		25 (M)
		Grand Valley WWTP (1489)	43° 53' 35"	-80° 18' 55"	44.86	450	6		
5		Below Grand Valley	43° 51' 42.34"	-80° 16' 20.93"	53.11	444	6		27 (M)
6		Shands	43° 43' 29.9"	-80° 20' 38.3"	71.01	406	6		29 (M)
		Fergus WWTP (6050)	43° 42' 1.5"	-80° 22' 48.4"	75.38	390	6		
		Elora WWTP (3583)	43° 40' 49.0"	-80° 25' 53.2"	80.84	370	6		
7		Elora Gorge	43° 40' 35.77"	-80° 26' 45.38"	83.91	354	6		25 (M)
8	GR-1	West Montrose	43° 35' 8"	-80° 28' 53.6"	98.05	323	6		20 (O)
		Canagagigue Creek	43° 34' 25.42"	-80° 29' 25.63"	99.85	319	6	5	

		Confluence							
		Conestogo Golf Subdivision (101)	43° 32’ 37”	-80° 29’ 47”	105.71	311	6		
		Conestogo Confluence	43° 32’ 18.65”	-80° 29’ 10.98”	106.78	310	7	6	
		Laurel Creek Confluence	43° 28’ 57.83”	-80° 28’ 53.06”	119.12	299	7	4	
9	GR-2	Bridgeport	43° 28’ 54.7”	-80° 28’ 53.6”	119.24	298	7		24 (O)
		Waterloo WWTP (66627)	43° 28’ 46.1”	-80° 28’ 56.0”	119.47	295	7		
		Hopewell Confluence	43° 28’ 43.88”	-80° 25’ 18.58”	125.27	295	7	4	
10		Freeport	43° 25’ 18.5”	-80° 24” 39.3”	135	282	7		29 (M)
		Kitchener WWTP (164000)	43° 24’ 3.3”	-80° 25’ 12.1”	140.29	275	7		
11	GR-3	Blair	43° 23’ 9.8”	-80° 23’ 9.1”	145.82	274	7		82 (E)
		Speed River Confluence	43° 23’ 14.01”	-80° 22’ 1.00”	147.46	265	7	6	
		Preston WWTP (18727)	43° 23’ 10.22”	-80° 21’ 1.55”	148.91	265	7		
12		Parkhill Dam	43° 21’ 49.4	“-80° 19’ 1.2”	153.07	264	7		78 (E)
		Galt WWTP (60000)	43° 20’ 18.1”	-80° 19” 4.1”	155.93	255	7		
13	GR-4	Glen Morris	43° 16’ 38.02”	-80° 20’ 40.17”	164.13	244	7		54 (M)
14		Paris	43° 11’ 52.7”	-80° 22’ 55.1”	175.45	229	7		42 (M)
		Nith Confluence	43° 11’ 32.91”	-80° 22’ 56.94”	176.04	219	7	6	
		Paris WWTP (7700)	43° 10’ 42.6”	-80° 22’ 26.1”	179.3	215	7		

15	Power Line Road	43° 10 26.58	-80° 21' 11.06"	181.76	210	7		31 (M)
16	Brant CA footbridge	43° 9 8.34	-80° 19' 2.23"	187.89	208	7		25 (M)
	Brantford WWTP (73000)	43° 7 13.9	-80° 13' 45.8"	204.26	190	7		
17	Newport	43° 5 57.87	-80° 14' 25.39"	216.64	189	7		46 (M)
	Fairchild Creek Confluence	43° 6 37.47	-80° 7' 36.42"	228.28	188	7	6	
18	Six Nations	43° 5 50.50	-80° 5' 43.50"	232.29	187	7		44 (M)
	Caledonia WWTP (5655)	43° 4 8.1	-79° 56' 41.9"	246.34	185	7		
19	Sims Lock	43° 2 38.82	-79° 54' 32.28"	250.6	182	7		37 (M)
20	York	43° 1 14.40	-79° 53' 30.80"	253.6	181	7		41 (M)
21	Cayuga	42° 56 58.64	-79° 51' 38.04"	263.05	174	7		35 (M)
	Cayuga WWTP (1258)	42° 56 22.7	-79° 51' 16.0"	264.42	174	7		
22	Dunnville	42° 54 4.4	-79° 37' 8.5"	288.12	174	7		85 (E)
	Dunnville WWTP (5182)	42° 53 50.5	-79° 36' 29.0"	289.01	174	7		
23	Port Maitland	42° 51 35.74	-79° 34' 32.08"	295.66	173	7		62

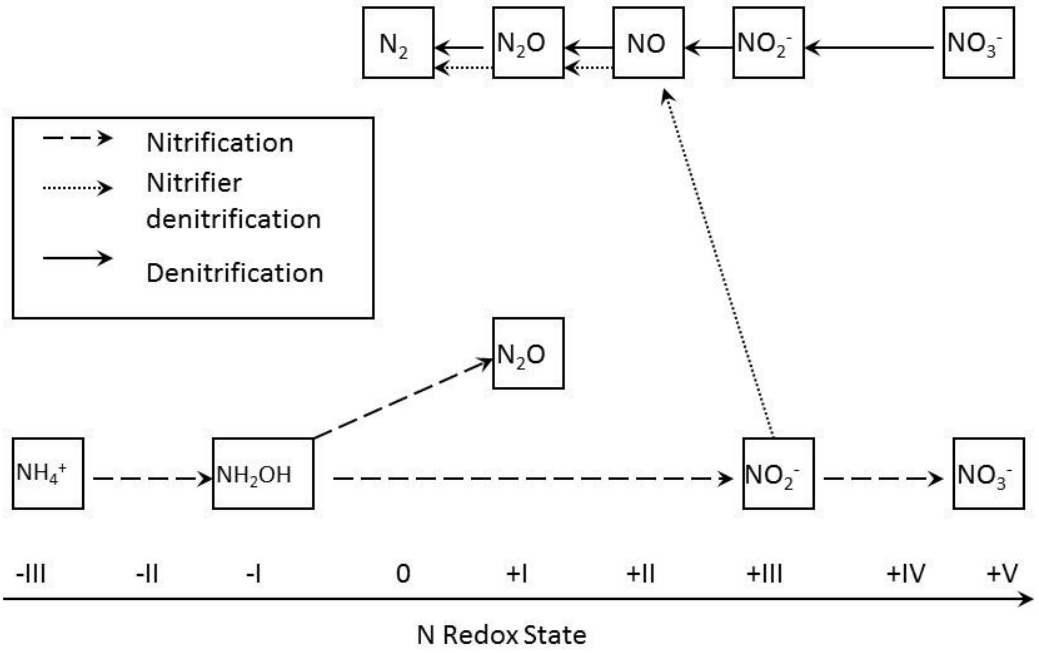

Figure 1.1: Selected biological N pathways found in rivers and streams.

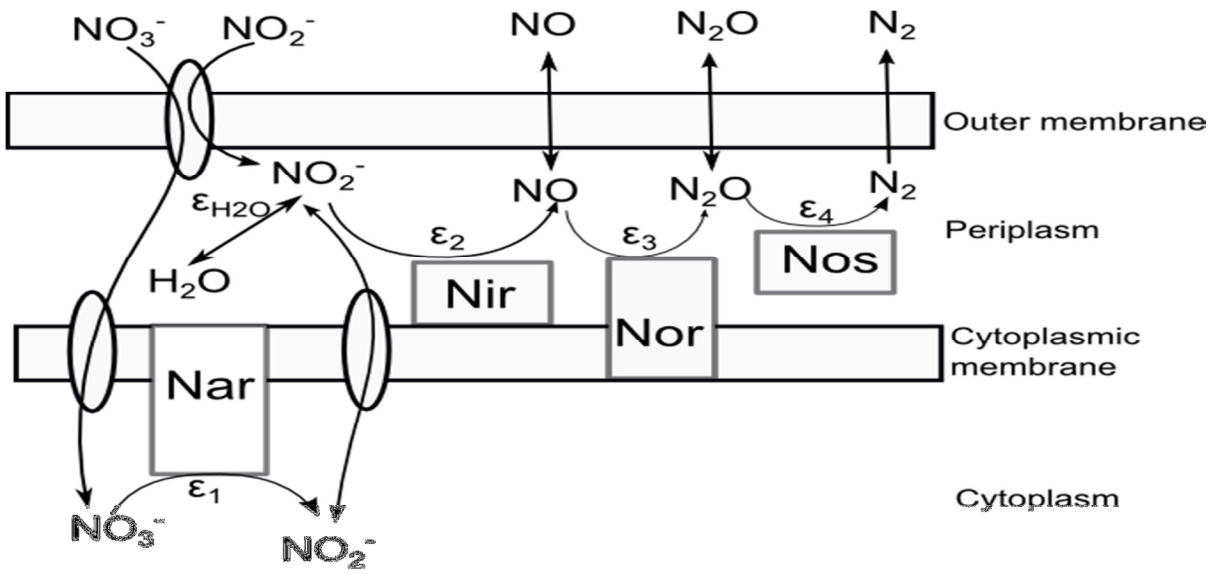

Figure 1.2: Heterotrophic denitrification in gram-negative bacteria. Transporters (active or passive) are represented by ovals and enzymes by rectangles. Non-charged gases NO, N_2O and N2 can freely diffusion through the cell's outer membrane but NO_3^- and NO_2^- must be transported across it. Nar: nitrate reductase; Nir: nitrite reductase; Nor: nitric oxide reductase; Nos: nitrous oxide reductase. Isotopic fractionations for ^{18}O only are shown for brevity. The net isotopic fractionation ($\varepsilon_{net}{}^{18}O$) is the sum of ε_1 through ε_4. O exchange with H_2O may occur with NO_2- or NO, inside or outside the cell, but is only shown with NO_2^- for brevity. The possible fractionation resulting from O exchange is shown as εH2O. Figure adapted from Figure 3 (Averill 1996) and Figure 1 (Steen et al. 2013).

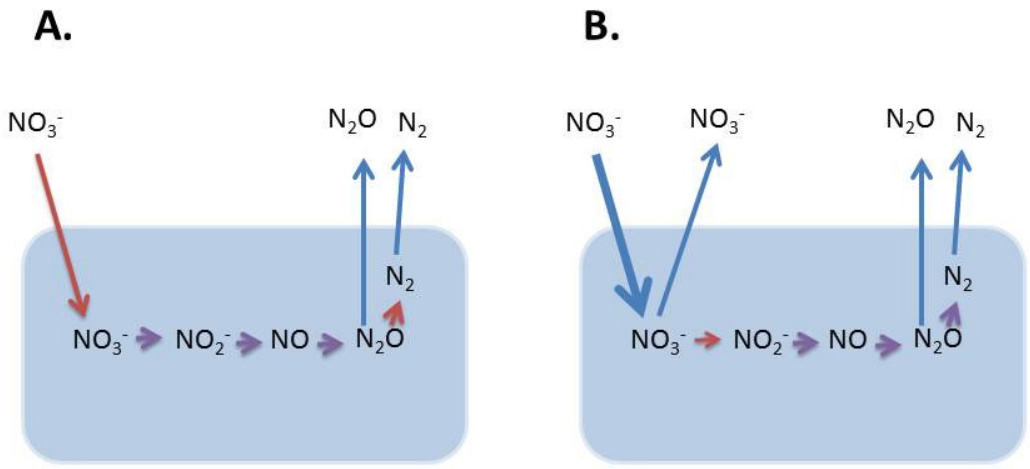

Figure 1.3: Conceptual model of stable isotopic effects measured during intracellular biological processes, using denitrification as an example. If a difference in isotopic ratios of the substrate (NO3-) outside the cell is measured, it is because (A) isotopic fractionation occurs on uptake into the cell, or (B) excess substrate is taken up with no fractionation and isotopic fractionation occurs during enzyme-mediated reactions in the cell and excess substrate leaves the cell. If products (N_2O, N_2) are isotopically distinct from substrate, at least one enzymatic reaction (in purple) must exhibit isotopic fractionation. Reactions and transports shown with blue arrows have no known isotopic fractionation.

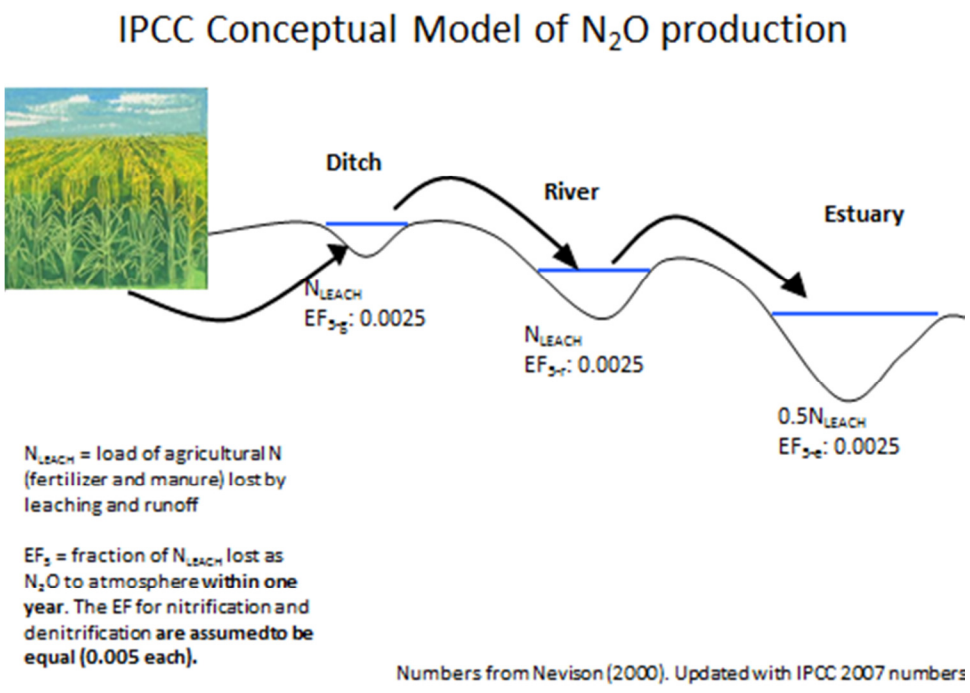

Figure 1.4: Conceptual model of the IPCC default equations for N_2O production and emissions from streams and rivers, using default values from the Fourth Assessment Report (IPCC 2007).

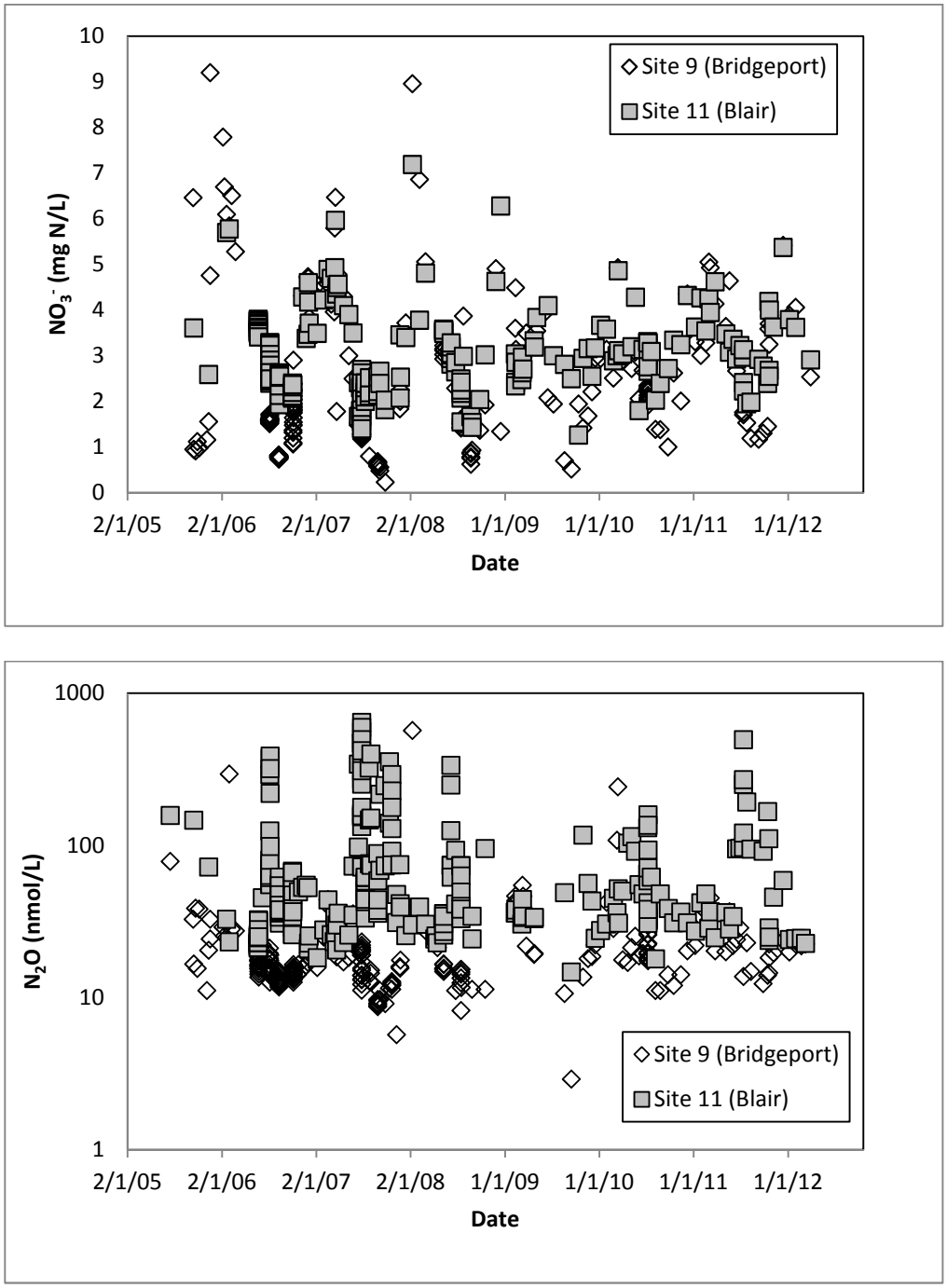

Figure 1.5: Seasonal changes in NO_3^- (top) and N_2O concentrations (bottom) at two sites in the Grand River over seven years. NO_3^- concentrations are higher at Site 9 and in winter. N_2O concentrations are higher at Site 11 and in summer.

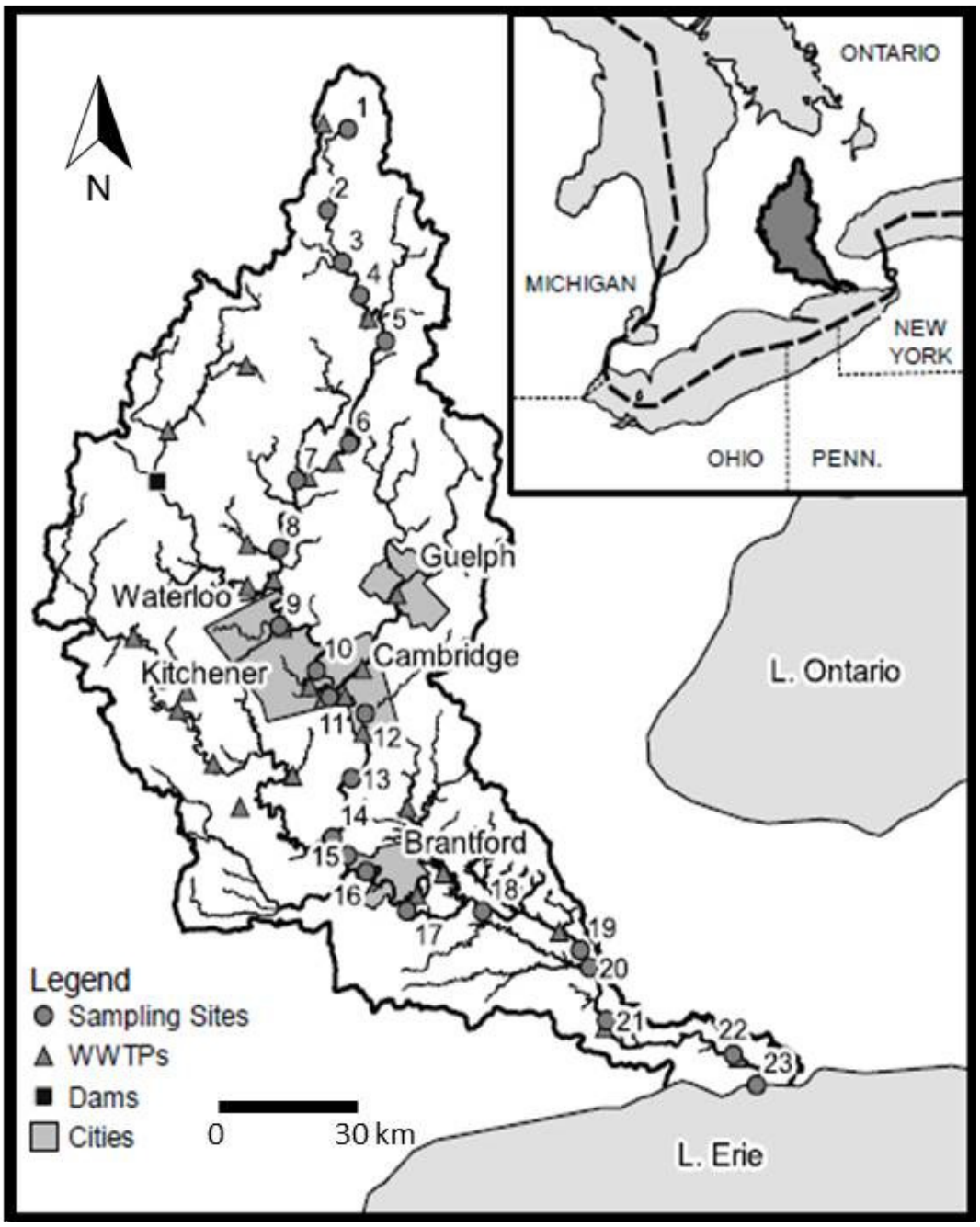

Figure 1.6: Map of the Grand River, Ontario and 23 sampling sites. WWTPs and dams are also shown. See Table 1.2 for site descriptions.

Chapter 2: Coupled Cycles of Dissolved Oxygen and Nitrous Oxide in Rivers along a Trophic Gradient in Southern Ontario, Canada

Abstract

Diel (24-h) cycling of dissolved O_2 (DO) in rivers is well documented, but evidence for coupled diel changes in DO and nitrogen cycling has only been demonstrated in hypereutrophic systems where DO approaches zero at night. Here, we show diel changes in N_2O and DO concentration at several sites across a trophic gradient. Nitrous oxide concentration increased at night at all but one site in spring and summer, even when gas exchange was rapid and minimum water column DO was well above hypoxic conditions. Diel N_2O curves were not mirror images of DO curves and were not symmetrical about the mean. Although inter- and intrasite variation was high, N_2O peaked around the time of lowest DO at most of the sites. These results suggest that N_2O must be measured several times per diel period to characterize curve shape and timing. Nitrous oxide concentration was not significantly correlated with NO_3^- concentration, contrary to studies in agricultural streams and to the current United Nations Intergovernmental Panel for Climate Change protocols for N_2O emission estimation. The strong negative correlation between N_2O concentration and daily minimum DO concentration suggested that N_2O production was limited by DO. This is consistent with N_2O produced by nitrite reduction. The ubiquity of diel N_2O cycling suggests that most DO and N_2O sampling strategies used in rivers are insufficient to capture natural variability. Ecosystem-level effects of microbial processes, such as denitrification, are sensitive to small changes in redox conditions in the water column even in low-nutrient oxic rivers, suggesting diel cycling of redox-sensitive compounds may exist in many aquatic systems.

2.1 Introduction

River and stream ecosystems are threatened by anthropogenic inputs of nutrients such as nitrogen and phosphorus. Excess nutrients can result in eutrophication, decreases in drinking water quality and aquatic habitat, and increased rates of production of greenhouse gases such as carbon dioxide (CO_2), methane (CH_4), and nitrous oxide (N_2O). Characterizing spatial and temporal variation in water chemistry is important for understanding biogeochemical cycling and for effective nutrient management.

Diel (24-h) cycles of many compounds have been noted in streams and rivers. Diel cycling may be caused by changes in temperature (e.g., (Gammons et al. 2005, Grimm and Petrone 1997)) and light (e.g., (Diez Ercilla et al. 2009, McKnight and Duren 2004)). Light-driven changes in net

photosynthesis and respiration can result in changes in dissolved inorganic carbon, which affects pH, and dissolved oxygen (DO) (e.g., (Odum 1956, Parker et al. 2009, Parker et al. 2010, Parkhill and Gulliver 1998, Poulson and Sullivan 2010). Nighttime DO lows are of particular concern because they can limit the habitat of aerobic organisms such as fish (Vanderploeg et al. 2009). Many microbial processes are sensitive to the redox state, which is affected by DO. Once-per-day sampling protocols for water quality can under-represent diel changes in water chemistry, skewing data and impinging on the ability to understand ecosystems processes and mitigate the impacts of eutrophication.

Diel cycling of nitrogen compounds is of particular interest because biologically reactive nitrogen compounds (i.e., nitrate [NO_3^-] and ammonium [NH_4^+]) are important nutrients, and sometimes pollutants, in aquatic ecosystems. The major microbial N cycling pathways of nitrification and denitrification are redox-sensitive. Nitrification is a term used for two oxic reactions performed by different groups of microbes: NH_4^+ oxidation to nitrite (NO_2^-) and oxidation of NO_2^- and NO_3^- through the stepwise reactions shown in Figure 2.1. The first reaction is performed by bacteria of the family *Nitrobacteriaceae*, methane-oxidizing bacteria, fungi, and crenoarchaea (Hayatsu et al. 2008). The second reaction is performed mostly by *Nitrobacter* spp. These reactions are often coupled with autotrophic CO_2 fixation to organic carbon (Hayatsu et al. 2008). Nitrous oxide, a powerful greenhouse gas, can be produced as a by-product of hydroxylamine oxidation in the first reaction or by nitrifier-denitrification, the reduction of NO_2^- to N_2 by nitrifiers. The latter reaction typically occurs in low-oxygen environments (Hayatsu et al. 2008). Denitrification, or anoxic NO_3^- reduction through NO, N_2O, and N_2 (Figure 2.1), is a respiratory pathway often coupled with oxidation of organic carbon or sulfide (Hayatsu et al. 2008). Denitrification is performed by a wide variety of microbes in aquatic communities. In very anoxic environments, N_2O can be taken up by cells and further reduced to N_2 (Zafiriou 1990)

Two types of diel patterns in denitrification rates in aquatic systems have been observed: daytime and nighttime increases. Daytime increases in N_2O concentration have been shown to occur when nitrification rates increase during the day due to higher temperature and pH, which then stimulates denitrification (e.g., (An and Joye 2001, Laursen and Seitzinger 2004, Lorenzen et al. 1998)). This may occur when sediment is NO_3^--limited or when there is minimal diel DO cycling at the sediment surface. Laursen and Seitzinger (2004) found higher rates of denitrification (and presumably nitrification) during the day in small agricultural streams but higher N_2O production at night, suggesting that the ratio of N_2O produced per mole of NO_3^-or N_2 produced by nitrification or denitrification, respectively, increased during the night.

Denitrification rates may decrease during the day due to DO dynamics. In environments with well-lit sediments colonized by photoautotrophs, benthic daytime oxygen production increases the depth to the sediment redox boundary, increasing the diffusion path length for NO_3^- from the overlying sediment surface and water column to the sediment anoxic zone (e.g., (Laursen and Carlton 1999, Lorenzen et al. 1998, Nielsen et al. 1990, Nielsen et al. 1990, Risgaard-Petersen et al. 1994). A similar diel pattern is observed in hypereutrophic systems with nighttime hypoxia (DO < 2 mg/L) driven by high community respiration. Diel cycling of compounds involved in anoxic metabolic processes (e.g., denitrification; iron, manganese, and sulfate reduction; and methanogenesis) suggest that rates of anoxic processes increase at night and are limited during the day by diffusion or higher DO (Gammons et al. 2009, Harrison et al. 2005). Harrison et al. (2005) associated daytime decreases in NH_4^+ and increases in NO_3^- with nitrification and associated nighttime NO_3^- disappearance and N_2O formation with denitrification.

In this study, we provide evidence of coupling of DO and N cycles in three temperate rivers (southern Ontario, Canada) with different trophic status. Dissolved oxygen and N cycling processes are linked because major N cycling processes are redox sensitive. We have chosen N_2O as an indicator of N cycling changes because it is produced by multiple N pathways (Figure 2.1); it is easily measured at the nmol/L level with good precision, allowing good quantification of small concentration changes; it degases to the atmosphere, making it less influenced by ground- or surface-water inputs than dissolved ions such as NO_3^-; and the extent of diel N_2O variability in rivers is not well understood. Although rivers and estuaries are thought to be significant sources of N_2O to the atmosphere (Kroeze et al. 2005), the diel variability of N_2O has been examined in only a few rivers and streams (Clough et al. 2006, Laursen and Seitzinger 2004). If diel cycling of N_2O is significant, once-per-day water chemistry sampling can misrepresent the mean diel concentration needed for calculating mean daily N_2O emissions to the atmosphere. In addition, the factors controlling N_2O production and N_2O diel cycling are not well understood. N_2O emissions from streams and rivers to the atmosphere are often estimated by assuming a linear correlation with NO_3^- concentration based on research in agricultural streams (IPCC 2007, Reay et al. 2003, Reay et al. 2005). However, this relationship does not consider the impact of redox state on N_2O dynamics in fluvial systems and has not been tested in larger or heavily affected rivers. Additionally, the effect of gas exchange on diel N_2O signals has not been examined in streams and rivers, even though high rates of gas exchange could remove diel signals in N_2O production. The expression of diel cycling of gaseous compounds depends on the rates of in-stream production and consumption and any diel changes to input (e.g., anthropogenic loading) and gas exchange with the atmosphere, which varies directly with the gas exchange coefficient (k) and the degree of saturation of the gas in question. The gas exchange

coefficient is dependent on water depth and velocity in turbulent systems such as rivers (Wilcock 1988). When flow conditions are constant over a diel period (e.g., in large rivers), only small, temperature-based diel changes in k occur. At constant hydraulic conditions, the gas flux is therefore dependent on the concentration of the dissolved gas relative to the atmosphere. If gas exchange rates are higher than diel changes in the net production of the gas of interest, then no diel change in concentration will be observed.

The purposes of this study were to determine (i) the presence and extent of diel variation in N_2O over the growing season (May to October) at several sites across the trophic gradient (oligotrophic to eutrophic); (ii) if N_2O diel curves are predictable (i.e., if they are consistent with DO curves, which are easier to measure and often better known); (iii) the potential factors influencing diel N_2O variability, such as diel DO amplitude and minimum, NO_3^- concentration, temperature, and gas exchange coefficient; (iv) the appropriate sampling methodology to capture diel variability and average daily N_2O concentrations and fluxes in lotic freshwaters; and (v) the implications for the sensitivity of in-stream N cycling processes to small diel changes in redox conditions in the water column.

2.2 Materials and Methods

2.2.1 Study Sites

The Grand River watershed (Figure 2.2), located in southern Ontario, Canada, is 6800 km^2 in area and has a population of approximately 1 million. About 80% of the land use is agricultural. Treated municipal wastewater, agricultural runoff/discharge, and septic tank releases are the main anthropogenic sources of nitrate (Cooke 2006). About half the population lives in the metropolitan area of the Region of Waterloo, in the middle of the watershed.

The Grand River is seventh-order and has an annual average discharge of 56 m^3/s to Lake Erie (Aquaresource 2009). Flows are heavily regulated by discharge from the Bellwood Reservoir above the Shand Dam (Figure 2.2). The catchment contains Paleozoic limestone and shale overlain by calcite-rich glacial drift. River water is typically well buffered by dissolved carbonate, and the pH ranged from 7.0 to 9.0 at all sites in this study. Anthropogenic eutrophication in the middle, urban reach of the river has been observed since at least the 1960s (Rott et al. 1998).

Four sites on the Grand River (GR) were sampled for diel variations in river water chemistry (Table 2.1and Table 2.2). Sites were numbered sequentially downstream. Unless otherwise noted below, no sites have significant regional groundwater loss or gain (Holysh et al. 2001) because the Grand River channel overlies a compacted, clayey till (Catfish Creek Till) (Barnett 1992), which is

considered an aquitard with low hydraulic conductivity (Martin and Frind 1998). Flow was very consistent over 28-h sampling events at all sites, except for a rise in flow due to a rain event at sites GR-1 and GR-2 in October 2006 (Mark Anderson, Grand River Conservation Authority, personal communication). Water depth was generally between 0.5 and 1 m during our sampling events. The substrate at all sites was similar, consisting primarily of coarse material (sand to cobble), with finer sediments in pool areas. Porosity was not measured. All sites had well lit substrates and significant epilithic biofilm on gravel cobbles at all sampling times, but biomass was not quantified for this study. Periphyton-coated macrophytes were present at all sites and times but were lower in abundance in May and October. Unpublished work on the Grand River indicates that epilithon drives community photosynthesis in early spring, but macrophytes dominate in summer (June through September), while the effect of sestonic photosynthesis is minor (Gao Chen, personal communication). A previous study at a site approximately 10 km upstream of site GR-1 indicated that epilithic biomass is often one order of magnitude higher than planktonic algal biomass (Barlow-Busch et al. 2006). Suspended chlorophyll *a* concentrations ranged from below detection to 10.7 mg/L over this study (sites Eramosa River [ER]-1 and SP-1 were not quantified).

Sites GR-1 and GR-2 are downstream of primarily agricultural areas and small towns with populations under 10,000. Based on total phosphorus (TP) concentrations (Table 2.2, after (Dodds et al. 1998)), site GR-1 was considered oligotrophic in May and July and mesotrophic in August and October. Site GR-2 was mesotrophic on all sampling dates. Patchy macrophyte growth was present at both sites in summer. Site GR-3 is downstream of two large municipal wastewater treatment plants (WWTPs) that release partially nitrified effluent to the Grand River. The effluent plume is generally fully mixed at this site, and there is no visible effluent "dead zone" of decreased algal and macrophyte growth. NH_4^+ is elevated at this site (typically > 0.1 mg N/L) (Table 2.2) compared with all other sites studied. Summer macrophyte growth is densest at site GR-3, where nightly hypoxic events are common (Cooke 2006). Site GR-3 was mesotrophic in May, July, and August 2006 and was eutrophic in October 2006 and June 2007. Diel variation in total P at site GR-3 (measured three to four times per diel cycle) was low (CV, 2.6–8.8%), suggesting that any diel changes in WWTP effluent flow did not affect the trophic status of the site. Site GR-4 is about 40 km downstream of the heavily urbanized area. There is significant groundwater recharge to the river starting about 3 km upstream of the site (Cooke 2006). The site was mesotrophic on all sampling dates, and macrophyte growth was sparse.

To increase the range of trophic levels and inorganic nitrogen concentrations in our study, we examined three sites on the Speed River (SP), a main tributary of the Grand River, and its tributary, the Eramosa River (ER). Sites ER-1 and SP-1 are located in agricultural areas, upstream of any

WWTPs. Both sites are oligotrophic in all seasons. Site SP-2 is artificially channelized and in a large urban area, about 200 m downstream of a top-draw reservoir and dam (Figure 2.2). Site SP-3 is about 2 km downstream of the Guelph WWTP, downstream of the "dead zone" of the effluent plume. Sites SP-2 and SP-3 were mesotrophic in July 2006 and oligotrophic in July 2007.

All sites were sampled 17 to 20 times over approximately 28 h on each sampling date. Cloudless days were chosen when possible. Grand River sites were sampled in May, July, August, and October 2006. Sites GR-1 and GR-2 were sampled simultaneously, and GR-3 and GR-4 were sampled 1 or 2 d later. Sites GR-2 and GR-3 were also sampled once in June 2007 to assess interannual variation in summer diel cycling. Sites SP-2 and SP-3 were sampled in July 2006, and all sites on the Speed and Eramosa Rivers were sampled in July 2007.

The average daily maximum temperature in July 2006 was 26.9°C, and total July precipitation was 152 mm. Temperatures in the summer of 2007 were similar (average July maximum: 25.2°C), but precipitation was much lower (total July precipitation: 50 mm) (Seglenieks 2011). Flows were regulated by reservoir discharge and were lower in 2007 than in 2006 (Table 2.2).

2.2.2 Sampling and Analysis

For consistency, sampling locations were marked with buoys in flowing water as near to the thalweg as was safe. At each sampling time, temperature, conductivity, and pH were measured with a YSI 556 MPS multiprobe (YSI, Yellow Springs, OH). The probe was calibrated with conductivity and pH standards before deployment at each sampling time. Dissolved oxygen (DO) samples were collected in 300-mL glass biological oxygen demand bottles with ground glass stoppers. Samples for NO_3^- and NH_4^+ were collected in 125-mL HDPE bottles, which had been washed in 1.2 mol/L HCl, rinsed, and soaked in deionized water to remove residual Cl^- before sampling. Dissolved N_2O samples were collected in two 50-mL glass serum bottles with prebaked red rubber stoppers (BD Vacutainer, Franklin Lakes, NJ) (a needle was used to remove bubbles during underwater capping). Nitrous oxide samples were preserved with 0.2 mL saturated $HgCl_2$ solution. Samples for stable isotopic analysis of DO (δ^{18}O-DO) were collected in pre-evacuated 125-mL serum bottles with prebaked butyl-rubber stoppers and metal crimps; 0.3 g of NaN_3 was added as a preservative before the bottles were evacuated. Total P samples were collected in 50-mL centrifuge tubes with plastic screw caps. All samples were kept at < 4°C in the dark until analyzed.

Samples of DO were analyzed within 24 h using the sodium azide modification of the Winkler titration technique ((American Public Health Association 1995)), with a precision of 0.2 mg/L. Samples of NO_3^- and NH_4^+ were filtered to 0.45 mm in the lab, and NH_4^+ samples were acidified to pH 4 with sulfuric acid. Concentration of NO_3^- was analyzed on an ion chromatograph (ICS-90; Dionex

Corp., Sunnyvale, CA) with 0.07 mg N/L precision (SD of 15 replicates of a standard solution) and a detection limit of 0.05 mg N/L. Samples of NH_4^+ were analyzed by the salicylate and nitroprusside colorimetric method (American Public Health Association 1995) on a Technicon AutoAnalyzer II (Technicon Instruments, Terrytown, NY) at 660 nm wavelength with a precision of 0.005 mg N/L and detection limit of 0.01 mg N/L. Samples with concentration >2 mg N/L were diluted.

Our instrumentation could detect the presence of nitrite (NO_2^-) but could not quantify it accurately. Nitrite (likely < 0.5 mg N/L) was noted at the GR-3 site in July 2006, August 2006, and June 2007. Nitrite here may have come directly from effluent from the Kitchener WWTP, in which it is sometimes observed (unpublished data).

Samples of N_2O were analyzed using a headspace method in which 5 mL of sample was removed while 10 mL of He was added. Bottles were shaken to equilibrate the headspace and dissolved phases. Approximately 3 mL of headspace was removed from the serum bottle and analyzed on a gas chromatograph (model CP3000; Varian, Santa Clara, CA) with an electron capture detector and 2 m × 3.2 mm SS column packed with Hayesep D 80/100 mesh (VICI Valco Instruments, Houston, TX). A P-5 mix (95% Ar and 5% CH_4) was used as the carrier gas. Dissolved N_2O concentration was calculated using Henry's Law after Lide and Fredrikse (1995). Precision (standard deviation of multiple air-equilibrated samples) was 6% or less at 8.5 nmol N_2O/L, and the detection limit was 3 nmol N_2O/L. Samples of δ^{18}O-DO were run with a helium headspace method on a modified Micromass VG IsoChrom gas chromatograph-isotope ratio mass spectrometer (Micromass HK, Manchester, UK) ((Venkiteswaran et al. 2008)). Total P samples were analyzed by the persulfate digestion and the ascorbic acid/molybdenum blue colorimetric method (APHA, 1995) on a Cary 100 US-VIS spectrophotometer (Varian) at 885 nm wavelength. The precision and minimum detection limits were both 0.05 mg P/L.

We used a non–steady-state model (PoRGy) to estimate gas exchange coefficient (k) values for dissolved oxygen (k_{DO}) by fitting diel DO and δ^{18}O-DO curves to equations containing the photosynthesis rate, the respiration rate, the δ^{18}O-H_2O value, the isotopic effect of community respiration, and k (Venkiteswaran et al. 2007). The value of k plays a large role in the concentration of dissolved gases in aqueous environments. However, k is difficult to measure directly in large rivers. Empirical equations can give a wide range of values for the same input parameters (Raymond and Cole 2001). Injected gas tracers such as SF_6 are impractical for large rivers and must be quantified multiple times in different flow conditions (Wilcock 1988). The PoRGy model avoids these problems but does not take into account flow changes or groundwater input, which influence modeled k values. These factors are probably negligible at our study sites except for site GR-4, which receives groundwater input from the Paris Moraine (Holysh et al. 2001). Best fit was obtained by

adjusting the input parameters to minimize the combined sum of squared error between the field data and model outputs. The model was run multiple times per dataset using random starting points, and the first five "good fits" ($r_2 > 0.8$ for DO and δ^{18}O-DO curves) were chosen and averaged. Standard deviations of *k* obtained by multiple runs of the same dataset were very low (< 0.0001–0.007; $n = 5$). Sites SP-3 and GR-4 (October) did not exhibit sufficient diel cycling in DO and $\delta^{18}O\text{-}O_2$, and the *k* values for these sites were thus unmodelable ($r^2 < 0.5$). The k values for N_2O (k_{N2O}) were calculated from k_{DO} using Schmidt numbers (Wanninkhof 1992).

An estimate of error on the modeled *k* values was obtained from the standard error (SE) of the slope of the regression between field and modeled DO and δ^{18}O-DO values, using the following equation:

$$\boldsymbol{SE\ of\ slope = slope\ \times (1 - r^2) \times 0.5/[r \times (n - 2)^{0.5}]} \qquad \textbf{Equation 2.1}$$

where *n* is the number of samples and *r* is the correlation coefficient (Zar 1996).

Standard errors of the slopes of the δ^{18}O-DO regression were larger than those for DO concentration and are therefore reported here. They ranged from 3.5% to 14.4%. Because these values incorporate error from all fitted parameters in the model (photosynthesis rate, the respiration rate, the isotopic effect of bulk respiration, and k), they are liberal estimates of the error on k. They are comparable to previously published error estimates on k (Moog and Jirka 1998).

Regression analysis of factors that may influence N_2O production rates (temperature, k_{N2O}, NO_3^-, minimum DO) and N_2O was completed in Systat SigmaPlot version 10.0 (Systat, Chicago, IL). *P* values < 0.05 were considered significant.

2.3 Results and Discussion

2.3.1 Presence and Extent of Diel Dissolved Oxygen, Nitrate, Ammonia, and Nitrous Oxide Cycling

River conditions varied substantially between diel sampling periods. Across all sites and seasons, average daily water temperature ranged from 10.6°C to 26.9°C. Flows ranged from summer low flows in July 2006 and June 2007 to storm flows in October 2006. Samplings from sites GR-1 and GR-2 were taken shortly after a storm on 4 October (10.8 mm rain) (Seglenieks 2011) (Table 2.1). Submerged macrophytes were present at all sites at all times but were less abundant in May and October than during summer sampling. Epilithon was present at all sites and times. Dissolved inorganic nitrogen concentrations were always three or four orders of magnitude higher than soluble reactive P concentrations, indicating that all systems were likely P limited (data not shown). Previous

research has also found evidence that periphyton (including diatoms) and seston are P limited in the Grand River (Barlow-Busch et al. 2006, Rott et al. 1998).

Diel DO curves were present at all sites and times, even with the large variation in river conditions. The presence of diel DO curves was determined by a diel concentration range (maximum – minimum) greater than twice the method precision and a minimum occurring before sunrise and a maximum occurring near solar noon. Dissolved oxygen increased during the day due to net in-stream autotrophy (i.e., photosynthesis > respiration) and decreased at night due to heterotrophy (Figure 2.3 to Figure 2.5). Diel DO curve amplitude was highest in July or August and was smallest in October at all Grand River sites. Site SP-2 (July 2007), immediately downstream of a dam, had the smallest diel range in DO (1.0 mg/L). Dissolved oxygen concentration was generally above 4 mg/L (~50% saturation) at all sites. The exception was site GR-3, where hypoxic conditions (DO < 2 mg/L) occurred during two sampling events. In July 2006 and June 2007, the nighttime DO minima were 1.1 and 0.8 mg/L (13.0 and 6.3% saturation), respectively.

Diel cycles of NO_3^- and NH_4^+ were only observed in midsummer at the few sites that were affected by WWTP effluent. NO_3^- decreased during the night at sites GR-3 and GR-4 in July 2006 and June 2007 and at site SP-3 at both sampling times. Diel NO_3^- concentration varied by 10% to 90% at these sites (Table 2.2). NH_4^+ increased during the night at site GR-3 in July and June by 1430% and 1640%, respectively (Table 2.2). Sites GR-3 and GR-4 are downstream of the Kitchener WWTP, which releases significant loads of NH_4^+ (Table 2.1) that are rapidly removed during the day by a combination of volatilization, biological uptake, and nitrification (Murray 2008). Site SP-3 is downstream of a WWTP releasing mostly NO_3^- (Table 2.1). Concentrations of NH_4^+ and NO_3^- at all WWTPs change little over 24 h or show little diel trend (Rosamond et al., unpublished). Decreases in NO_3^- concentration at night may have resulted from increased denitrification or decreased nitrification at night, but changes in biological uptake or effluent chemistry also could have occurred.

Diel cycling of N_2O occurred at every site and on most dates (Figure 2.3 to Figure 2.5). In general, there appeared to be two diel curve shapes: single peak and double peak. The majority of sampling events showed single peaks (e.g., sites GR-1, GR-2, and GR-4 on all dates but October 2006; site SP-1; and site SP-3), with N_2O increasing during the night and decreasing during the day. Some curves (site GR-3 in July, October, and June; site ER-1; and site SP-2 in July 2007) had a daytime and nighttime peak in N_2O. With the exception of site ER-1, nighttime N_2O peaks were higher than daytime peaks. Nitrous oxide was variable over 24 h at all GR sites in October but did not show consistent diel patterns except at site GR-3. Nitrous oxide patterns may have been affected by high storm-related flows at this sampling time.

The diel range of N_2O concentration (i.e., maximum N_2O concentration – minimum N_2O concentration) varied substantially within and between sites. Within a site, the diel N_2O range tended to increase with temperature, peaking in midsummer (July 2006 or June 2007) for all Grand River sites but site GR-1. This corresponded with low flow, high water temperature, and low nighttime minimum DO (Table 2.2). Photosynthetic biomass was also observed, but not quantified, to be highest at this time of year.

Intersite variation of the diel N_2O range was quite high, ranging from 2.3 nmol/L N_2O at site GR-4 (October) to 569.4 nmol/L N_2O at site GR-3 (July). Sites with the highest N_2O concentration and range (sites GR-3 and SP-3) were immediately downstream of WWTPs. Nutrients in the effluent increased productivity, resulting in larger diel DO ranges. Nitrous oxide concentrations were closest to saturation and had small diel ranges at less affected sites of lower trophic order with small diel DO cycles (e.g., sites ER-1 and SP-1). Nitrous oxide was always oversaturated, indicating that it was produced upstream of all sites, even those of lower trophic level and low NO_3^- concentration (Table 2.2). The k_{DO} values in rivers and streams are typically high (0.03–0.35 m/h, this study; 0.02–0.5 m/h, (Venkiteswaran et al. 2008) and references therein) compared with lentic systems with wind-driven gas exchange (0.005–0.11 m/h) ((Venkiteswaran et al. 2008) and references therein). The gas exchange coefficient in rivers is understood to be controlled by turbulent flow (i.e., water depth and velocity) and thus varies little in rivers over a diel period in the absence of hydraulic changes (McCutcheon 1989, Raymond and Cole 2001). Therefore, the presence of diel N_2O cycles at all sites indicates that gas exchange was not rapid enough to remove the diel signal, which must be related to changes in production, consumption, or the rate of N_2O diffusion from sediments, which are affected by depth of the sediment redox boundary.

There are few literature reports of diel N_2O variation in streams and rivers. Nitrous oxide concentration has been shown to increase during the day in a low-productivity river (Clough et al. 2007) and to increase at night in high-productivity rivers ((Harrison et al. 2005); this study: site GR-3 in July 2006 and August 2007). Laursen and Seitzinger (2004) measured N_2O twice over a diel cycle in low-productivity streams, showing higher nighttime N_2O concentration. Until now, however, complete diel N_2O curves peaking at night have not been demonstrated in oligotrophic and mesotrophic systems where diel cycling of NO_3^- and NH_4^+ does not occur and DO minima are well above hypoxic conditions.

2.3.2 Predictability of Shape and Timing of Diel Nitrous Oxide Curves

To examine the consistency of diel N_2O curve shape and timing across sites and dates, we compared diel N_2O and DO curves. This normalizes for the effects of gas exchange, which changes the timing

of the DO diel peak and trough relative to solar noon (Chapra and Di Toro 1991, Venkiteswaran et al. 2008). However, the differences in k_{DO} and k_{N2O} at the same temperature and the change in the k_{DO}/k_{N2O} ratio with temperature could affect the timing between the DO and N_2O peaks (Wanninkhof 1992). We used the largest and smallest values of k_{DO} modeled in this study (0.35 m/h at site GR-4 in May and 0.04 m/h at site SP-3 in July 2007) and calculated k_{N2O}. k_{N2O} values were then changed to reflect the temperature range over the study (10.6–26.9°C). Dissolved oxygen curves were modeled using k_{DO} and k_{N2O} with PoRGy. Differences between k_{DO} and k_{N2O} and differences with temperature affected the time of peak DO by one model time-step (5 min), which was much less than the sampling resolution in this study (~90 min). Thus, small, temperature-driven changes in k values do not significantly contribute to changes in peak timing for DO curves relative to N_2O curves.

Diel N_2O cycles were less smooth than DO curves, and the timing of N_2O peaks was less consistent (Figure 2.3 to Figure 2.5). Although N_2O curves typically peaked when DO concentrations were low, they were not mirror images of DO curves. Nitrous oxide curves were more asymmetrical about the mean than DO curves. Although the shape of N_2O curves was not consistent across sites or dates, N_2O peaks tended to be sharper than N_2O troughs, similar to DO curves. Ignoring October samples (except site GR-3), which do not show clear diel N_2O curves, the nighttime N_2O peak occurred on average 0.4 h after the DO minimum (SD, 2.1 h; n = 21; see Table 2.1). Daytime N_2O peaks (typically smaller than nighttime peaks) occurred on average 12.1 h after the DO minimum (SD, 1.9 h; n = 5). The resolution of these calculations is 60 to 90 min, or the time between samplings. Peak timing did not appear to have any relationship with season (i.e., the month of sampling) or with water temperature.

The high variability in diel N_2O curve shape and timing is likely because N_2O was typically farther from saturation than DO and because N_2O production processes are sensitive to changes in redox conditions and not to the more regular photoperiod. Like DO curves, N_2O curves are affected by physical factors (k value and temperature), production and consumption rates, microbial community composition, and variation in loading from an upstream point and nonpoint sources such as WWTP outfalls and areas of groundwater discharge. However, N_2O production by nitrification and denitrification is redox dependent. When the water column is oxic, denitrification can only occur in the anoxic lower sediment, whereas DO production is redox-independent and occurs in the water column and on the sediment surface (Muller and Weise 1987). Also, the ratio of N_2O to N_2 produced during denitrification has been shown to change with redox conditions, NO_3^- supply, and temperature, but these relationships are not fully understood (Silvennoinen et al. 2008). We therefore cannot predict when the maximum or average N_2O concentration will occur based on diel DO curves. Furthermore, diel N_2O curve shape is not consistent at one sampling site over multiple dates or on one

date over multiple sites. Therefore, N_2O must be sampled several times over a diel period to fully characterize the shape and timing of the diel curve.

2.3.3 Correlating Diel Nitrous Oxide Concentration Range to Potential Limiting Factors

To determine if the diel concentration range of N_2O can be predicted and to suggest factors limiting net N_2O production rates in these rivers, we compared diel N_2O concentration range (i.e., maximum concentration – minimum concentration per sampling event) with k_{N2O} and with factors that may influence nitrification or denitrification rates (average daily temperature, minimum DO concentration, diel DO concentration range, average daily NH_4^+, and NO_3^- concentration).

Diel N_2O range showed no significant correlation with k_{N2O} ($p = 0.602$) (Fig. 6), although k_{N2O} ranged by a factor of 10 between sites. The N_2O concentration is a balance between net N_2O production and loss to the atmosphere by gas exchange. Thus, similar N_2O production rates result in different N_2O concentrations if k_{N2O} is different between sites. However, the variation in diel N_2O range seen here must result from different net N_2O production rates because high k_{N2O} values did not correlate to low diel N_2O range. There was also no correlation with total P ($p = 0.2277$), indicating that trophic level cannot be used to predict the N_2O diel range at our sites. Small but significant correlations with temperature ($r^2 = 0.20$; $p < 0.0001$), NO_3^- ($r^2 = 0.46$; $p = 0.0003$), and NH_4^+ ($r^2 = 0.20$; $p = 0.0277$) were observed, but the correlations appear to be controlled by the two sampling events at site GR-3 with very high N_2O, midrange temperature, midrange NO_3^- concentrations, and high NH_4^+ concentrations (Figure 2.6). When these points are removed, the relationships are no longer strong ($r^2 < 0.05$ for all) or significant ($p > 0.2$ for NO_3^- and NH_4^+).

Thus, N_2O production was not limited by temperature, NO_3^- or NH_4^+ at our sites. This contrasts with previous work showing linear relationships between NO_3^- and N_2O in agricultural streams (Reay et al. 2003, Reay et al. 2005), which form the basis for the protocol for estimating N_2O fluxes from rivers and streams sanctioned by the Intergovernmental Panel on Climate Change (IPCC 2007). The assumption that increases in in-stream NO_3^- concentration (e.g., from intensification of agriculture) result directly in increases in N_2O is not true at our sites. This finding raises the possibility that NO_3^- and N_2O are not related in rivers affected by anthropogenic N sources, as is often assumed. A re-evaluation of this relationship at other field sites is necessary to determine if NO_3^- and N_2O are correlated across larger NO_3^- concentration ranges and on regional scales on which Intergovernmental Panel for Climate Change flux estimations are performed.

Diel N_2O range had a very strong inverse correlation with nighttime minimum DO concentration over a large range (0.8–8.8 mg/L) ($r^2 = 0.97$; $p = 0.0001$). When the GR-3 data with very high N_2O concentrations were removed, the linear relationship was weaker but still significant ($r^2 = 0.43$; $p =$

0.0010). This suggests that sites have sufficient NO_3^- or NH_4^+ to support N_2O production and are limited by high DO concentrations. Nitrous oxide production in the sediment likely follows DO concentrations at the sediment surface, which are affected by benthic photosynthesis and respiration and hyporrheic flow, as well as water column DO. However, all sites are shallow (0.5–1 m) and well mixed, indicating that benthic influences on DO should be expressed in the water column.

The relationship between minimum DO concentration and N_2O diel range suggests that one or more microbial processes favored by low DO are responsible for the bulk of N_2O production. Elevated nighttime N_2O production could result from increased rates of denitrification (as observed by (Harrison et al. 2005)) or from an increase in the N_2O/NO_3^- ratio produced by nitrification, which occurs in low-DO environments and likely results from the nitrifier-denitrification pathway (Campos et al. 2009, Goreau et al. 1980).

Further evidence for the importance of nighttime denitrification was provided at our most eutrophic sites (sites GR-3, GR-4, and SP-3), where NO_3^- sometimes decreased overnight. This trend has also been noted by Harrison et al. (2005) in a hypereutrophic stream. Nitrate removal at night is likely caused by denitrification (or by a decrease in nitrification at site GR-3, where NH_4^+ is high) because other NO_3^- removal mechanisms, such as biological uptake, would not be expected to be higher at night. Furthermore, the N_2O concentration peaked several hours before sunrise, while DO was still low, at site GR-3 in July 2006 and June 2007. This may be because very anoxic conditions resulted in a decrease in the N_2O/N_2 ratio produced by denitrification. Theoretically, the N_2O/N_2 ratio should decrease as anoxia develops because N_2O reduction to N_2 becomes more energetically favorable (Betlach and Tiedje 1981). However, a relationship between N_2O/N_2 and DO is not always observed in denitrification experiments (e.g., (Silvennoinen et al. 2008)).

Daytime N_2O production may have been low in our study because denitrification was diffusion-limited as DO production increased the depth to the sediment anoxic zone. This pattern in denitrification rates has previously been noted in sediment incubation experiments quantifying denitrification rate (Lorenzen et al. 1998, Rysgaard et al. 1994). Also, a longer N_2O travel path from the sediment anoxic zone to the surface could have allowed further reduction of N_2O to N_2. Two sites (site GR-3 in July, October, and June and site SP-2 in July 2007) showed double-peaked N_2O curves, with one peak occurring with high DO concentration. This pattern has not, to our knowledge, been observed before. However, small daytime single N_2O peaks have been observed in low-NO_3^- streams (An and Joye 2001, Clough et al. 2007, Lorenzen et al. 1998) and have been attributed to increased coupled nitrification and denitrification due to increased temperature, DO, and pH during the day. This mechanism may explain the daytime data at sites ER-1 (showing only a daytime peak) and SP-2, where the DO range was narrow (1.7 and 3.1 mg/L, respectively) and NO_3^- concentrations were low

(0.7 and 0.2 mg N/L, respectively); NO_3^- may have been a more important limiting factor than DO in these cases. The double peaks at site GR-3, however, occurred when nitrification of NH_4^+ from WWTP effluent was high and may include N_2O produced by nitrification or coupled nitrification–denitrification or may be affected by variation in WWTP effluent chemistry (Thuss 2008).

This study did not examine all potential influences on diel N_2O dynamics. Diel N_2O changes may have resulted from microbial cycling on or in sediment and attached to macrophytes. Alternatively, diel changes in sediment biogeochemistry may have modified hyporrheic water quality, resulting in water column cycles. Intersite differences in sediment and sediment pore water properties (e.g., the abundance of labile organic carbon substrate in sediment; pore water NO_3^-, NO_2^-, and NH_4^+ concentration; thickness of the sediment anoxic layer; and the diffusion coefficient across the sediment–water interface) could also have been important. Changes in N_2O production rates may also be related to changes in microbial community make-up, if different species cycle N at different rates or have different N_2O/N_2 or N_2O/NO_3^- ratios. Microbial ecology is understudied in aquatic systems, although Iribar et al. (Iribar et al. 2008) found that microbial communities in denitrification hotspots were not significantly genetically different from those in other areas in a river riparian zone. An examination of the relationship between NO_2^- and N_2O could be useful. We might expect nitrifier-denitrification or coupled nitrification–denitrification to become NO_2^- limited in anoxic environments (because oxic NH_4^+ oxidation to NO_2^- slows or stops) but not denitrification, which produces NO_2^- without DO. Stable isotopic analysis of NH_4^+, NO_3^-, and N_2O could also provide further insight into the production pathways of N_2O at our sites.

2.3.4 Implications for Sampling Strategies and N-Cycling Sensitivity to Redox Conditions

The wide extent of coupled DO and N_2O cycling demonstrated here suggests that (i) sampling programs must be designed to capture diel cycles when examining river biogeochemistry or greenhouse gas emissions and (ii) N_2O production processes are sensitive to relatively small changes in redox conditions.

To illustrate the effect of sampling protocol on calculated average N_2O concentration, several sampling strategies were examined (Figure 2.7). Because N_2O is typically lower in the day than at night, sampling once per diel in the daylight results in underestimation of the average diel N_2O concentration. Site GR-1 (July) was chosen to represent "typical" conditions because the diel N_2O range here is approximately the median of all samples collected. The diel N_2O curve with the greatest range (site GR-3, June) was used as the "worst case." We examined the variability of the calculated diel mean based on the number of points collected over the day (approximately equally spaced) and

the time of sampling. The following strategies were examined: (i) sampling eight times per diel cycle (i.e., every second diel point, about every 3 h); (ii) sampling four times per diel cycle (i.e., every third diel point, about every 6 h); (iii) sampling twice per diel cycle (approximately every 12 h); (iv) sampling once per 24 h; (v) sampling once per 24 h, but only during working hours (0830–1700 h local time), to replicate typical sampling protocols; and (vi) sampling twice per day at or around sunrise and solar noon (S+N). Each data point on the graph represents the calculated average N_2O concentration with a different sampling start time. For the first three scenarios, the simple mean of the samples collected over the diel cycle was calculated. Depending on the starting time chosen, there can be significant variation (i.e., greater than twice the analytical precision) in scenarios with one or few samplings per day. All calculated mean values are compared with the mean calculated using all diel points (Figure 2.7).

The ratio of $(C_{\text{once-per-day}} - C_{\text{sat}})/(C_{\text{daily-average}} - C_{\text{sat}})$ is equal to $F_{\text{once-per-day}}/F_{\text{daily-average}}$, where $C_{\text{once-per-day}}$ is the N_2O concentration measured once per day, C_{sat} is the saturation concentration, $C_{\text{daily-average}}$ is the average of samples collected over 24 h, and F is the flux of N_2O to the atmosphere. In the typical scenario, the mean N_2O value using all data points (average sampling resolution: 1.4 h) was 14.1 nmol/L. Calculated mean N_2O values were within 3 nmol/L when sampling resolution varied between 3 and 12 h (Figure 2.7). However, once-per-day sampling resulted in average N_2O concentration estimations ranging over 13 nmol/L, depending on the time of sampling chosen. The variation of samples collected during working hours was 5.3 nmol/L, but values were mostly below the diel average. The S+N method gave a value of 15.9 nmol/L, which is about 12% higher than the average N_2O concentration calculated with a 1.4-h resolution. Using the ratio above, emission calculations using N_2O concentration values collected once per day are 20 to 240% of those calculated using the 1.4-h time step. Using the sunrise and solar noon (S+N) method, emissions are 140% of those calculated with the 1.4-h time step.

In the "worst case," the diel mean N_2O concentration (average sampling resolution: 1.7 h) was 291 nmol/L. The range of the calculated mean N_2O was very high (194 nmol/L) with a 12-h time step and even higher with once-per-day sampling (569 nmol/L). Samples collected during working hours were lower than the diel mean. Averaging sunrise and solar noon values gives 271 nmol/L, which is about 10% lower than the diel average and within our analytical precision value for N_2O concentration. Using a concentration value collected once per day results in emissions 20% to 160% of those calculated with a 1.7-h time step. However, the S+N method gives an emission value 90% of that calculated with a 1.7-h time step.

The high variability in N_2O diel curve timing relative to the diel DO curve makes prediction of the maximum or average diel N_2O concentration difficult. To fully describe the timing and shape of the

diel N_2O curve and to accurately measure average and maximum diel values, several samples per 24-h period are recommended. At the least, sampling twice per day around sunrise and solar noon (i.e., approximately the highest and lowest N_2O concentration) produces an average within 15% of the diel mean concentration and emission calculations within 40% of diel mean emissions in our two examples. Once-per-day or occasional sampling methods are common in studies examining N_2O emissions from rivers (e.g., (Beaulieu et al. 2008, Clough et al. 2006, Cole and Caraco 1998, Garnier et al. 2006, McElroy et al. 1978, McMahon and Böhlke 1996, Nirmal Rajkumar et al. 2008, Richey et al. 1988, Robinson et al. 1998)), but this practice requires re-examination even when N_2O concentrations are not particularly high. The presence of N_2O diel cycling at all sites implies that rates of redox-sensitive microbial metabolic processes appear to respond to small diel changes in DO even when the system remains oxic. We have demonstrated that diel N_2O cycles can thus be produced at low- and high-productivity sites with a range of diel DO variability. Coupled diel cycles of DO, N_2O, and other redox-related compounds likely occur in many aquatic systems with diel DO cycles, even when hypoxic conditions do not occur.

2.4 Summary

Diel N_2O cycles coupled with diel DO cycles were present at all river sites studied across a trophic gradient in spring and summer. Some sites did not exhibit this pattern during an autumn sampling, possibly because of decreased in-stream productivity related to storm activity and macrophyte senescence.

The maximum N_2O concentration and the diel N_2O range were highest in summer at sites with low DO. Single and doubled-peaked diel N_2O curves were observed. Diel N_2O curves peaked, on average, 0.4 h before DO minima with a large standard deviation and were asymmetrical about the mean. In contrast to diel DO curves, the timing of N_2O peaks was inconsistent across sites and dates, indicating that diel N_2O curves cannot be predicted from diel DO curves.

The diel range in N_2O concentration did not correlate significantly with k_{N2O}, indicating that diel N_2O curves represent changing production rates. The diel N_2O range also did not correlate significantly with NO_3^-, indicating that N_2O production is not NO_3^- limited at these sites over a NO_3^- range typical for agriculturally affected systems. The assumption that N_2O concentration is a linear function of NO_3^-, commonly made when estimating N_2O emissions, did not hold at these sites and bears further investigation. Diel N_2O range showed a very strong negative correlation with minimum DO concentration, and N_2O maxima occurred at night when DO was low. This suggests that N_2O is produced by an anoxic metabolic process such as denitrification or nitrifier-denitrification and that this process was limited by high DO. Several samples per diel cycle are necessary to fully describe

the observed diel variation in N_2O concentration, especially when diel N_2O range is large, but reasonable estimates (±15%) can be made by averaging concentrations at sunrise and solar noon at our sites. The near-ubiquity of diel N_2O cycling observed here indicates that measurable biogeochemical responses to small changes in water column redox potential are likely overlooked in many oligotrophic and mesotrophic aquatic systems.

Table 2.1: Site locations and descriptions.

Site	Location	Stream Order	Distance Downstream of Major WWTP (km)	WWTP Name	NO_3^- load from WWTP (tonnes N/y)	NH_4^+ load from WWTP (tonnes N/y)	Other Notes
GR-1	43°35'7.43"N, 80°28'53.99"W	6	N/A	N/A	N/A	N/A	
GR-2	43°28'54.43"N, 80°28'53.06"W	7	N/A	N/A	N/A	N/A	c. 10 km downstream of Conestogo R. confluence
GR-3	43°23'9.94"N, 80°23'9.96"W	7	5	Kitchener	77	511	
			20	Waterloo	170	135	
GR-4	43°16'35.13"N, 80°20'49.95"W	7	9	Galt	228	9.4	c. 16 km downstream of Speed R. confluence
			15		61	0.8	
ER-1	43°41'15.48"N, 80° 7'8.32"W	4	N/A		N/A	N/A	
SP-1	43°41'21.26"N, 80°14'38.07"W	4	N/A		N/A	N/A	
SP-2	43°32'4.44"N, 80°15'4.07"W	6	N/A		N/A	N/A	c. 100 m downstream of top-draw dam
SP-3	43°29'3.25"N, 80°16'54.03"W	6	1.5	Guelph	1798	16	

N/A = not applicable (i.e. no upstream WWTP). WWTP effluent data from Environment Canada (2008).

Table 2.2: Physical and chemical data for diel sampling occasions, by site. Mean values are calculated over 24 hours. Trophic status after Dodds (1998).

Site	Sampling Date	Mean Flow (m^3/s)	Mean Temperature (°C)	Mean TP (µg/L)	Trophic Status	NH_4^+ range (mg N/L)	NO_3^- range (mg N/L)	Time of N_2O peak - Time of DO minimum (h)
GR-1	May-06	8.1	18.0	19.9	Oligotrophic	0.01 - 0.05	2.37 - 2.66	0.0
	Jul-06	4.8	19.5	19.2	Oligotrophic	0.02 - 0.08	0.96 - 1.28	1.4
	Aug-06	7.7	22.9	21.7	Oligotrophic	0.02 - 0.03	0.50 - 0.69	0.0
	Oct-06	8.4	12.9	33.0	Mesotrophic	0.02 - 0.52	0.87 - 1.55	
GR-2	May-06	14.7	15.6	23.4	Oligotrophic	0.01 - 0.02	3.41 - 3.65	-1.5
	Jul-06	9.4	21.9	28.2	Mesotrophic	0.02 - 0.05	1.52 - 1.72	-3.0
	Aug-06	11.0	24.1	39.6	Mesotrophic	0.02 - 0.05	0.74 - 0.82	1.7
	Oct-06	14.9	13.9	56.8	Mesotrophic	0.01 - 0.07	1.07 - 2.90	
	Jun-07	7.5	26.8	31.1	Mesotrophic	0.01 - 0.06	1.18 - 1.42	0.0
GR-3†	May-06	32.7	12.2	49.4	Mesotrophic	0.37 - 0.87	3.41 - 3.8	-4.7
	Jul-06	13.6	21.9	50.3	Mesotrophic	0.03 - 0.43	2.40 - 3.29	-1.3
	Aug-06	13.5	23.1	68.3	Mesotrophic	0.03 - 0.09	1.93 - 2.62	-1.5
	Oct-06	17.0	13.8	77.6	Eutrophic	0.33 - 1.05	2.07 - 2.40	
	Jun-07	9.6	26.9	86.9	Eutrophic	0.07 - 1.15	1.40 - 2.70	-3.3
GR-4‡	May-06	49.9	10.6	54.1	Mesotrophic	0.06 - 0.21	3.33 - 3.83	-1.6
	Jul-06	21.4	21.5	42.5	Mesotrophic	BD - 0.02	2.48 - 3.20	0.0

	Aug-06	15.9	23.3	58.7	Mesotrophic	0.02 - 0.04	2.25 - 3.22	0.0
	Oct-06	26.1	13.6	58.3	Mesotrophic	0.09 - 0.17	2.54 - 2.77	
ER-1	Jul-07	N/D	15.9	11.8	Oligotrophic	0.01 - 0.02	0.59 - 0.88	11.7
SP-1	Jul-07	N/D	18.2	8.6	Oligotrophic	0.01 - 0.02	0.14 - 0.25	0.0
SP-2	Jul-06	N/D	24.4	36.4	Mesotrophic	0.03 - 0.06	0.62 - 0.84	2.8
	Jul-07	2.1	21.2	13.4	Oligotrophic	0.02	0.49 - 0.56	3.0
SP-3	Jul-06	N/D	24.2	59.5	Mesotrophic	0.02 - 0.04	3.55 - 4.80	-3.0
	Jul-07	N/D	21.2	12.2	Oligotrophic	0.02	2.99 - 5.74	3.3

BD = Below Detection. N/D = no data.

† Flow data collected c. 5 km upstream

‡ Flow data collected c. 15 km upstream

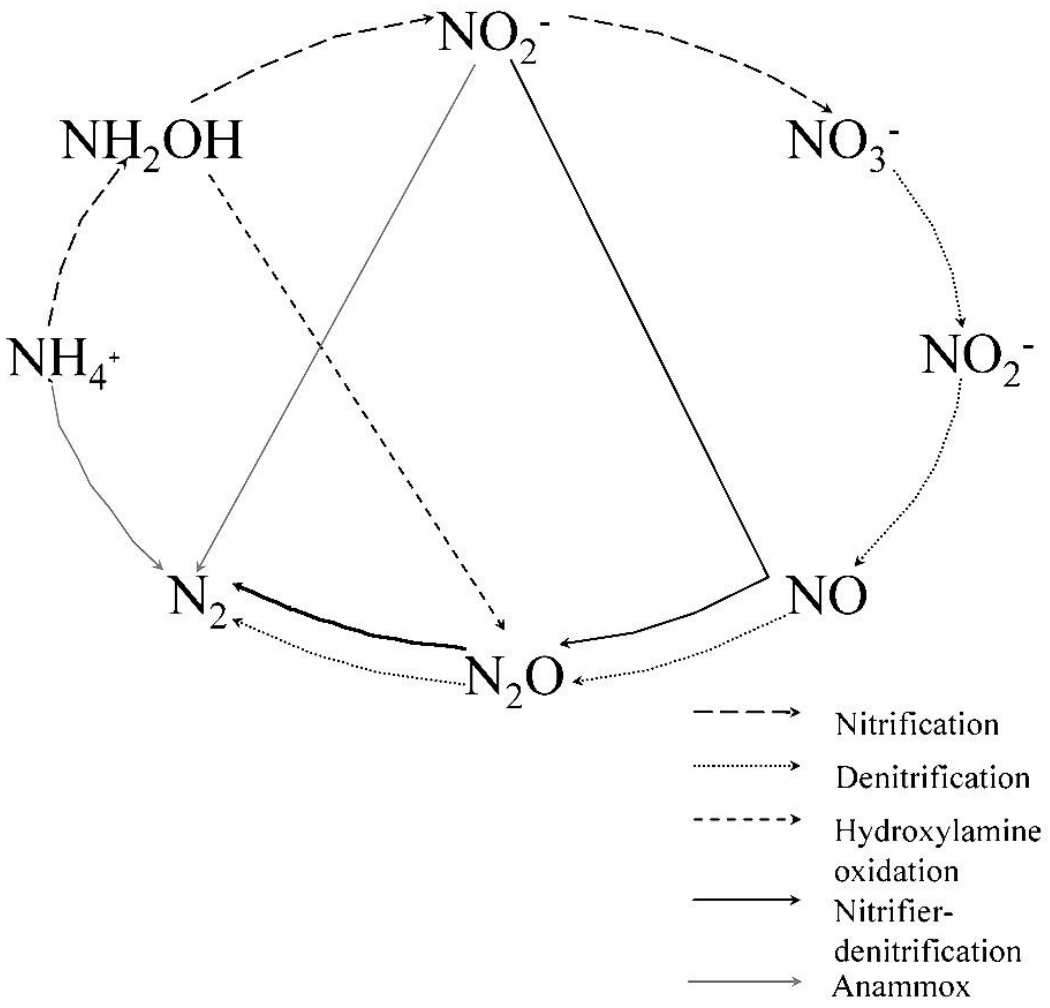

Figure 2.1: Common pathways of NO_3^-, N_2O, and N_2 production. Hydroxylamine oxidation is considered part of nitrification.

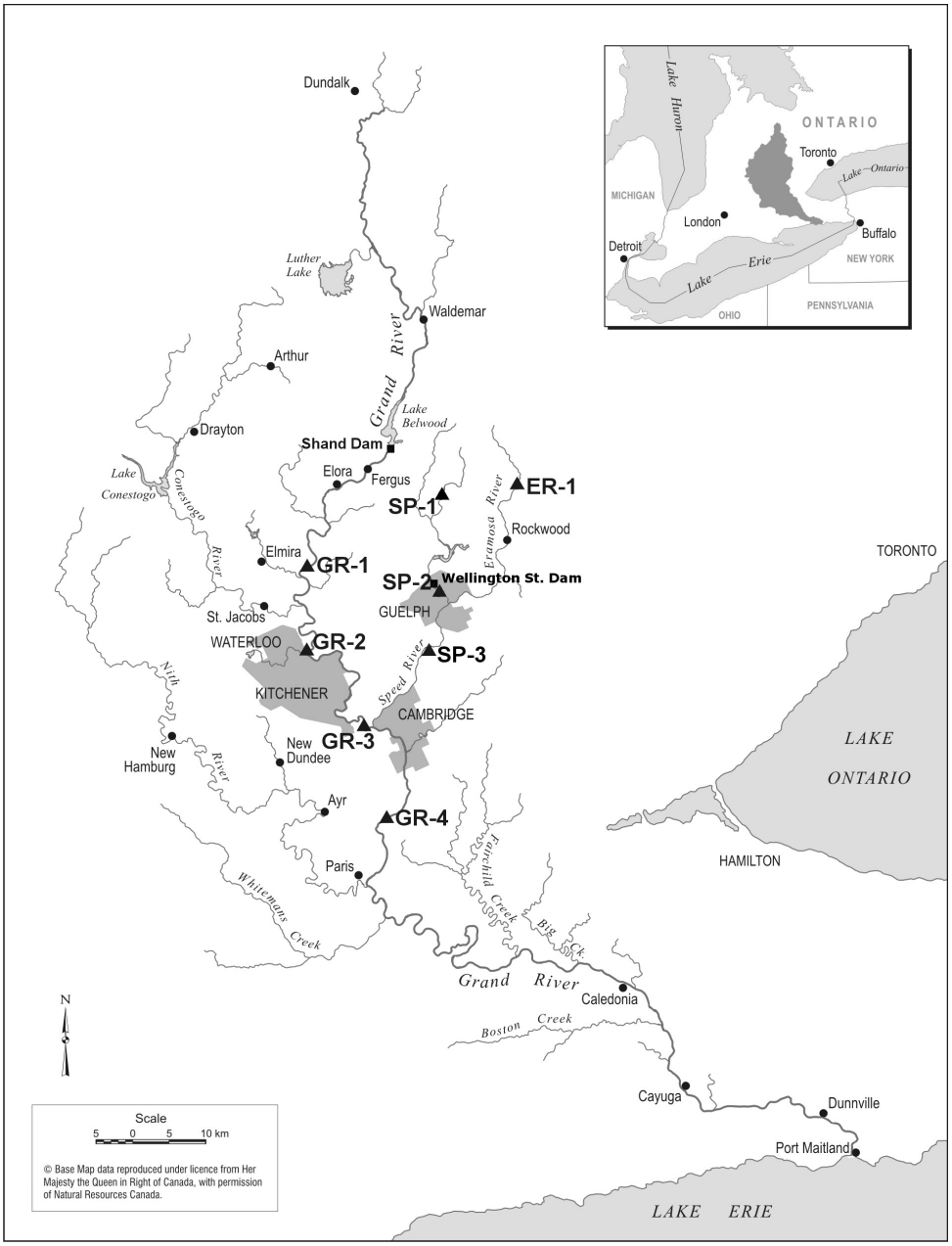

Figure 2.2: The Grand River Watershed, southern Ontario, Canada. Study sites on the Grand River, Eramosa R., and Speed R. are represented with triangles. Circles indicate towns and squares indicate dams. Note the large urban areas upstream of sites GR-3 and SP-3.

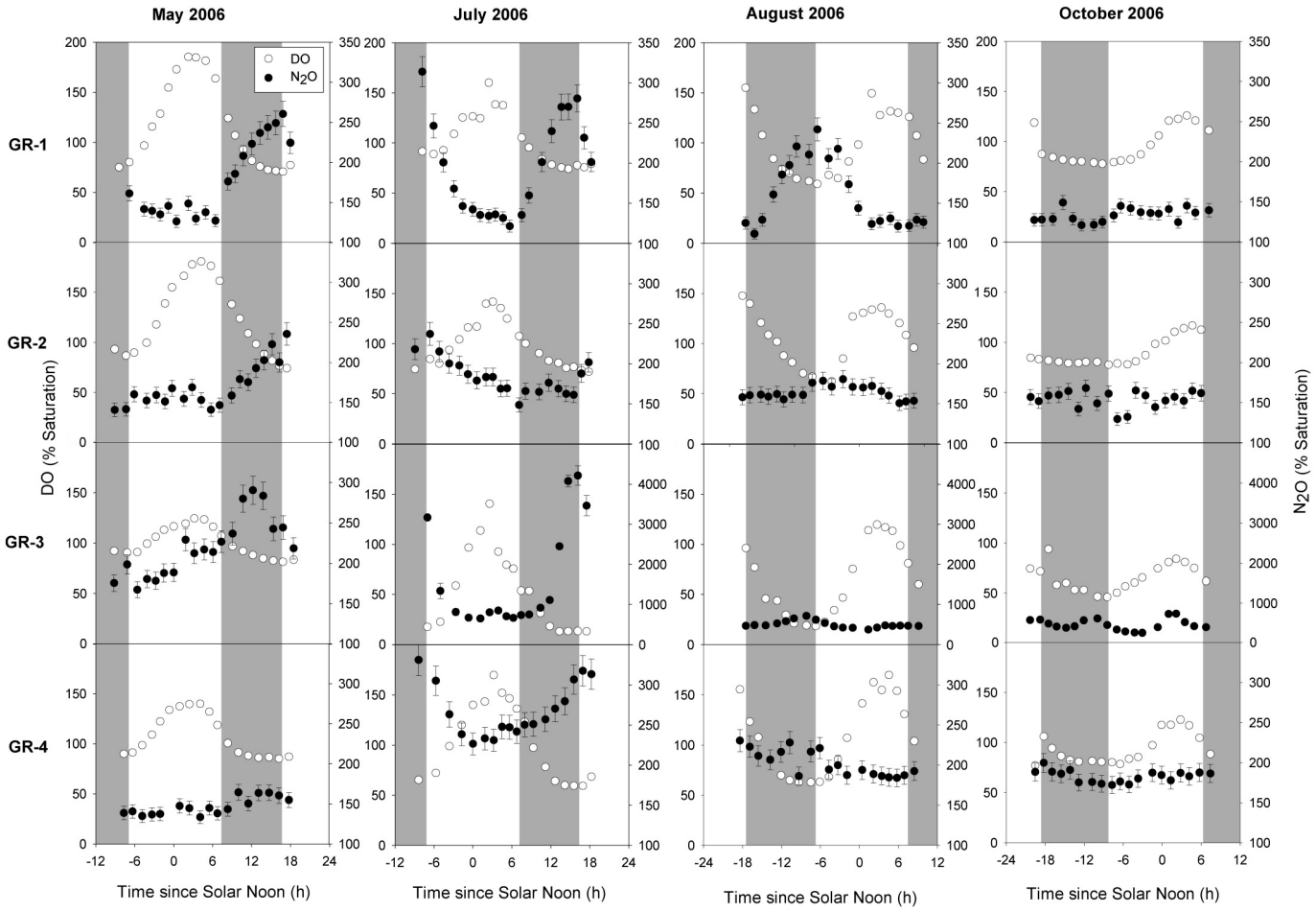
May 2006
July 2006
August 2006
October 2006
GR-1
GR-2
GR-3
GR-4
DO
N2O
DO (% Saturation)
N2O (% Saturation)
Time since Solar Noon (h)

Figure 2.3: Diel variability in DO and N_2O concentration at Grand River (GR) sites, 2006. Scale bars for DO are on the left, N_2O on the right. DO concentration at 100% saturation (20° C): 8.7 mg/L; N_2O concentration at 100% saturation (20° C): 8.9 nmol/L). Grey areas represent night-time concentrations. Error bars represent machine or technique precision (DO: 0.2 mg/L, N_2O: 6%). Note the different secondary y-axis scale for GR-3 on all dates but May 2006.

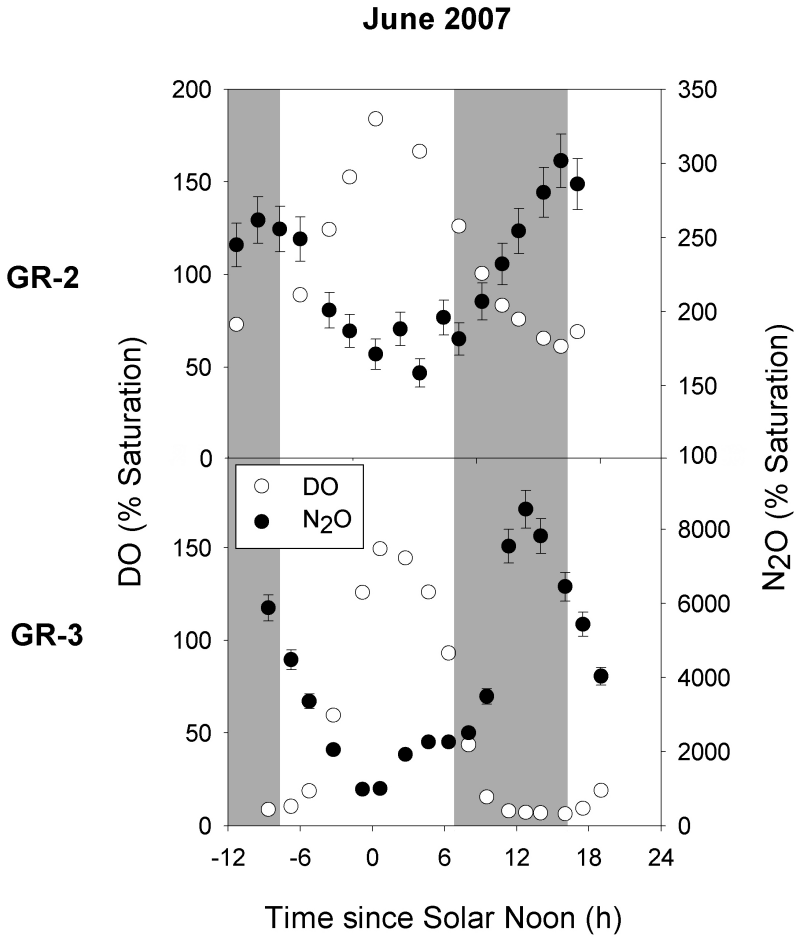

Figure 2.4: Diel variability in DO and N_2O concentration at Grand River (GR) sites, 2007. Scale bars for DO are on the left, N_2O on the right. DO concentration at 100% saturation (20° C): 8.7 mg/L; N_2O concentration at 100% saturation (20° C): 8.9 nmol/L). Grey areas represent night-time concentrations. Error bars represent machine or technique precision (DO: 0.2 mg/L, N_2O: 6%). Note the different secondary y-axis scale for GR-3 on both dates.

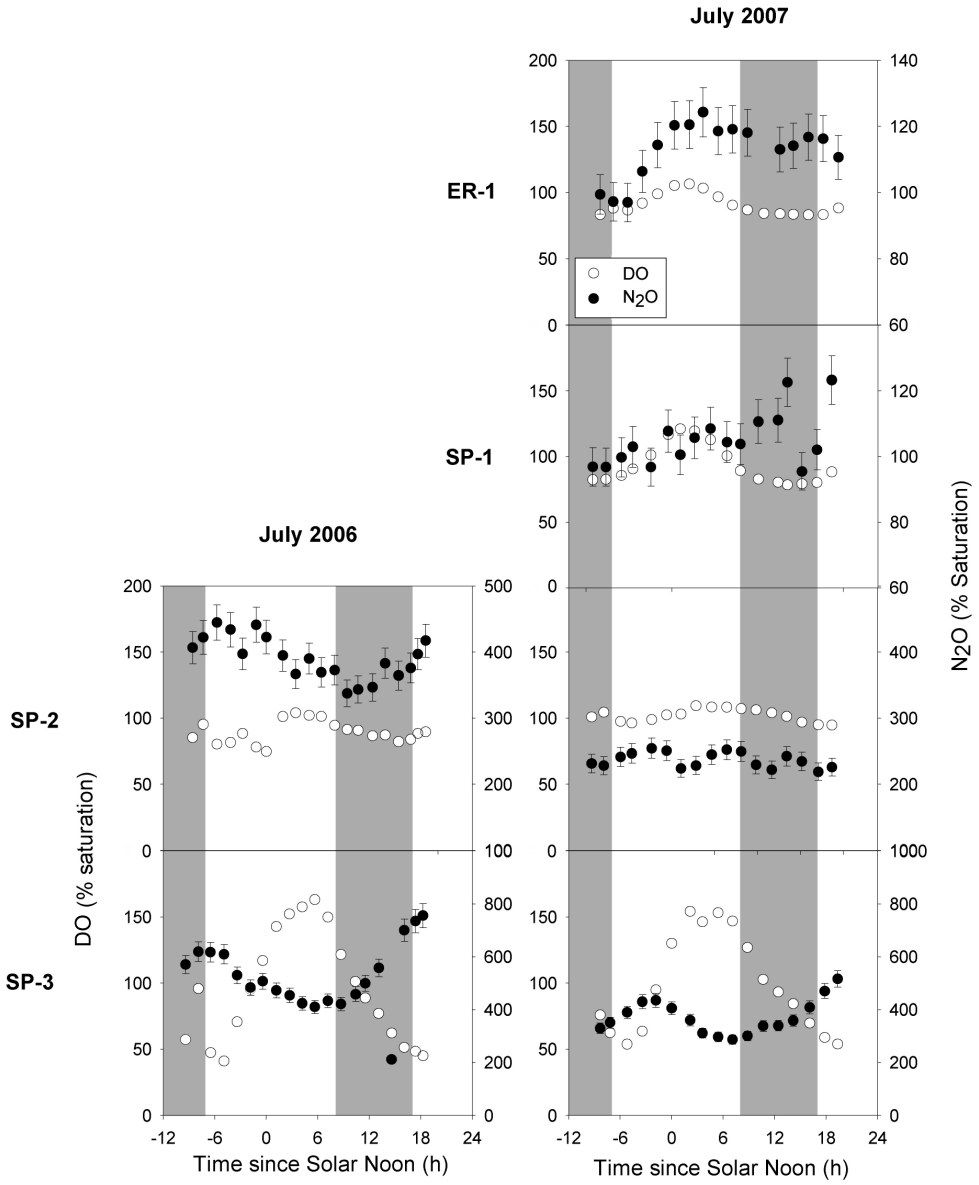

Figure 2.5: Diel variability in DO and N_2O concentration at Speed (SP) and Eramosa (ER) River sites. DO concentration at 100% saturation (20° C): 8.7 mg/L; N_2O concentration at 100% saturation (20° C): 8.9 nmol/L). Grey areas represent night-time concentrations. Error bars represent machine or technique precision (DO: 0.2 mg/L, N_2O: 6%). Note the unique secondary N_2O axis for each site.

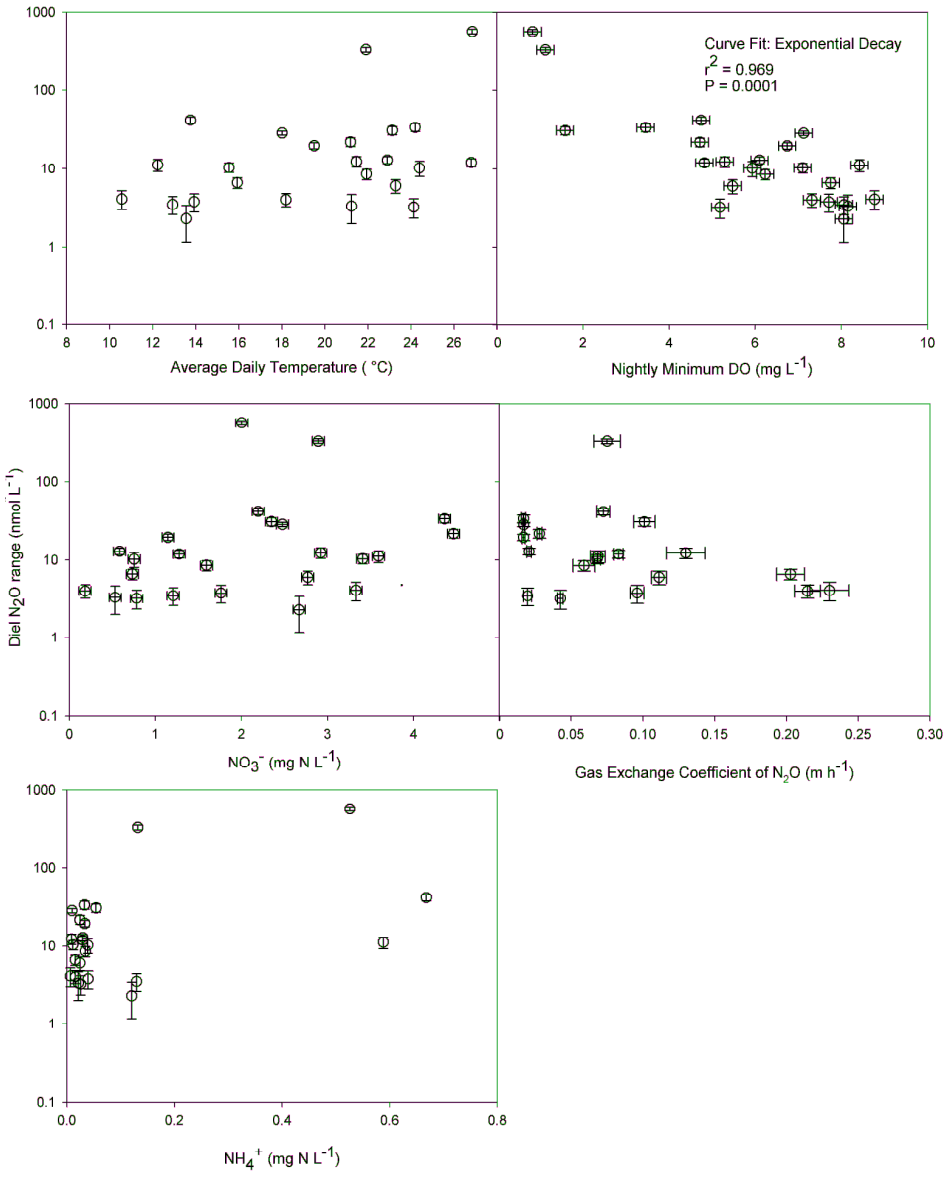

Figure 2.6: N_2O diel curve range versus temperature, minimum DO concentration, NO_3^- concentration and gas exchange coefficient (k_{N2O}). All correlations with diel N_2O range were insignificant ($p > 0.05$) except night-time minimum DO. Correlations of N_2O range and temperature, NO_3^- and NH_4^+ do not include the two points from GR-3 with very high N_2O. The

gas exchange coefficient could not be determined during the following sampling events: GM-3 (June 2007), GM-4 (August 2006, October 2006), SP-2 (July 2006, July 2007).

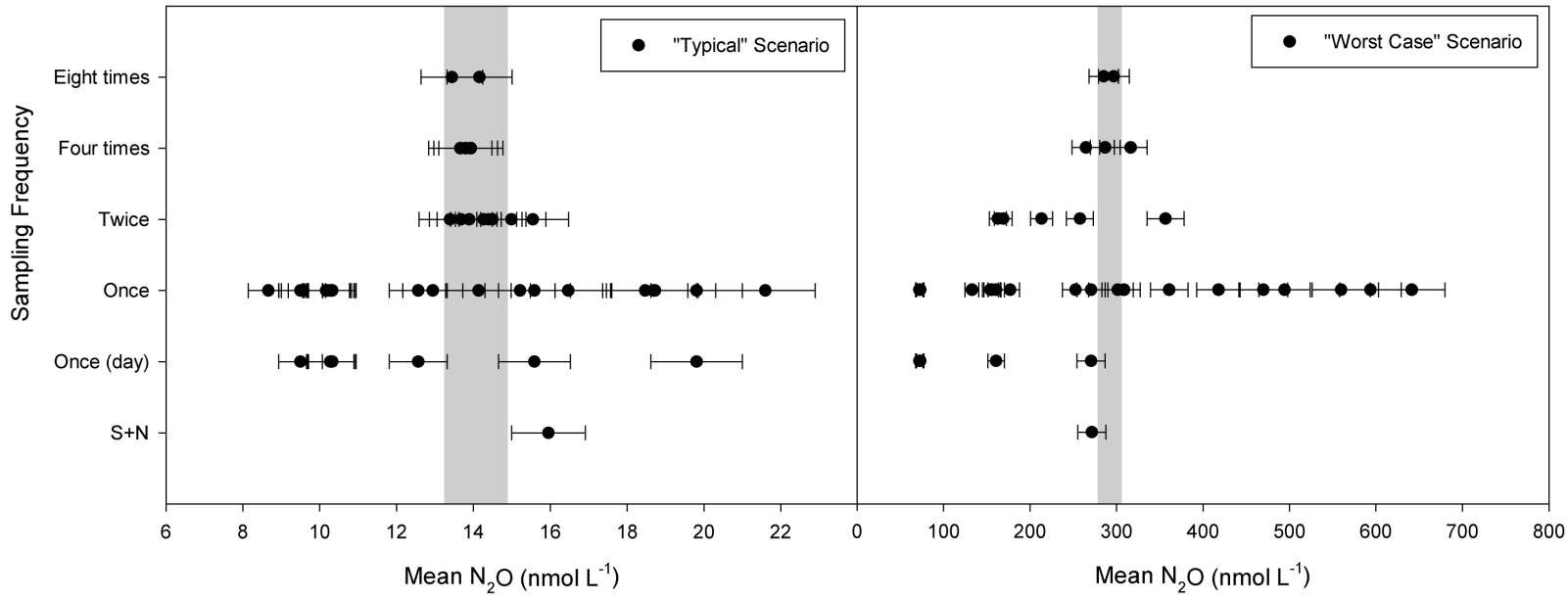

Figure 2.7: The range in estimates of the daily mean N_2O concentration using different sampling resolutions in a "typical" (average daily mean N_2O) and "worst case" (highest daily mean N_2O) conditions. Grey bars represent the diel average calculated with 14 to 17 samples per 24 h, plus or minus analytical precision (6%). Once = once per 24 hours, Twice = approximately every 12 hours, etc. Once (day) = once per diel period during typical working hours (8:30 AM to 5:00 PM, EDT). S+N = average of samples collected nearest to sunrise and solar noon. Note the difference in scales for the typical and worst case scenarios. Samples collected during working hours underestimate N_2O concentrations in the "worst case". The mean of the S+N sample is within 15% of the diel average for each site.

Chapter 3: Dependence of riverine nitrous oxide emissions on dissolved oxygen levels

Abstract

Nitrous oxide is a potent greenhouse gas, and it destroys stratospheric ozone (Ravishankara et al. 2009). Seventeen per cent of agricultural nitrous oxide emissions come from the production of nitrous oxide in streams, rivers and estuaries (Syakila and Kroeze 2011), in turn a result of inorganic nitrogen input through leaching, runoff and sewage. The Intergovernmental Panel on Climate Change and global nitrous oxide budgets assume that riverine nitrous oxide emissions increase linearly with dissolved inorganic nitrogen loads, but data are sparse and conflicting (Nevison 2000, Syakila and Kroeze 2011). Here we report measurements over two years of nitrous oxide emissions in the Grand River, Canada, a seventh-order temperate river that is affected by agricultural runoff and outflow from 30 waste-water treatment plants. Emissions were disproportionately high in urban areas and during nocturnal summer periods. Moreover, annual emission estimates that are based on dissolved inorganic nitrogen loads overestimated the measured emissions in a wet year and underestimated them in a dry year. We found no correlations of nitrous oxide emissions with nitrate or dissolved inorganic nitrogen, but detected negative correlations with dissolved oxygen, suggesting that nitrate concentrations did not limit emissions. We conclude that future increases in nitrate export to rivers will not necessarily lead to higher nitrous oxide emissions, but more widespread hypoxia most likely will.

3.1 Introduction

Nitrous oxide (N_2O) is responsible for about 9% of global climate forcing (IPCC 2007) but sources have been poorly quantified. Anthropogenic N_2O is largely produced by microbial metabolism of reactive N from agricultural fertilizers and/or human waste (IPCC 2007). The dominant pathways are nitrification of ammonium (NH_4^+) to nitrate (NO_3^-) and denitrification of NO_3^- to N_2O and finally N_2 (IPCC 2007). The global N_2O budget assumes a linear relationship between dissolved inorganic nitrogen (DIN) loads to rivers and riverine N_2O emissions, estimating global riverine N_2O emissions at 0.9 Tg/yr, or about 17% of anthropogenic agricultural N_2O emissions (Syakila and Kroeze 2011). However, the global budget indicates an N_2O increase of 5.4 Tg/yr (range: -7.5 to 18.7), whereas

atmospheric measurements indicate the value is 3.9 Tg/yr (range: 3.1 - 4.7; (IPCC 2007)). Uncertainty may be caused by paucity and poor quantification of spatial and temporal N_2O emission data from rivers (Table 3.1). Only one previous estimate of N_2O emissions includes diel data (Clough et al. 2007). To better capture spatial and temporal trends in riverine N_2O emissions and to examine the DIN/N_2O relationship, we measured dissolved N_2O concentrations and calculated emissions from the 300 km length of the seventh-order, highly nutrient-impacted Grand River.

The Grand River is the largest Canadian river draining into Lake Erie (watershed area: 6,800 km_2; river discharge at mouth: 56 m^3/s; (Aquaresource 2009) (Figure 3.1). Eighty per cent of the catchment is agricultural land (Cooke 2006) and 29 wastewater treatment plants (WWTPs) discharge DIN to the river and its tributaries (Figure 3.1, Table 3.2). We sampled every two to three weeks for two consecutive years, from May 2006 to April 2008. Average July temperature maxima were similar in 2006 and 2007 (26.9°C and 25.2°C respectively) but total July precipitation was lower in 2007 (50 mm versus 152 mm in 2006). Summer river flows were about 30% lower in 2007 than in 2006 at site 11 (Water Survey of Canada 2010). Twenty-three sites along the river were sampled, representing four major areas: agricultural land on a glacial till plain (sites 1-9), urban and downstream areas influenced by large WWTPs (sites 10-13), a reach with significant groundwater input (sites 14-16) and another predominantly agricultural area on a clay plain (sites 17-23; (Cooke 2006), Figure 3.1). Night-time hypoxia (DO < 2 m/L) has been observed at site 11, which is 5 km downstream of a WWTP releasing NH_4^+ to the river (Table 3.2).

3.2 Methods

Twenty-three sites along the length of the Grand River, Ontario, Canada (Figure 3.1) were sampled twice a day (before sunrise and in the early afternoon) on 14 June 2007, 5 September 2007 and 24 April 2009. Sites 1, 4, 8, 12, 16, 20 and 23 were also sampled at mid-morning. We sampled all sites once per day on 18 April 2008, 16 October 2008 and 24 March 2009. Sampling was conducted every two to three weeks at sites 8, 9, 11 and 13, from May 2006 to April 2008. Diel-intensive sampling (about every 1.5 h over 28 h) was conducted five times in spring, summer and fall in 2006 to 2008 at the same four sites. As the Grand River is shallow (mean depth < 1m at most sites) and well mixed, we filled sample bottles at wrist depth.

Duplicate samples for dissolved N_2O analyses were collected in 50 ml glass serum bottles, preserved with 0.2 ml saturated $HgCl_2$ solution in the field, and analysed using headspace gas

chromatography (Varian CP3000 gas chromatograph with an electron capture detector, 2m × 3.2mm stainless-steel column packed with Hayesep D 80/100 mesh) with a detection limit of 3 nmol/L N_2O and a precision (s.d. of multiple air-equilibrated samples) of 6% or less. DO was measured using the sodium azide modification of the Winkler titration (American Public Health Association 1995). The detection limit and precision were both 0.2 mg/l. The temperature was measured with a multiprobe (YSI 556 MPS). Flow data were provided by the Grand River Conservation Authority (D. Boyd, personal communication). Gas exchange coefficients (k) were calculated using the PoRGy model (Venkiteswaran et al. 2007, Wassenaar et al. 2010) for diel changes in DO and δ^{18}O-DO. Model runs with r^2 values of 0.8 or higher between observed and model-predicted values were used. During periods with no diel DO changes (that is, winter), mean k values for each site were used. No significant relationship between k and flow was found at sites 8, 9 and 13 ($p > 0{:}005$): The negative linear relationship between k and flow at site 11 ($r^2 = 0{:}35$, $p < 0.0001$) was considered too weak to adequately estimate winter k values based on flow measurements. Sites 6, 22 and 23 are lake-like reservoir sites, where the wind speed is expected to drive k. Here, k was calculated after (Crusius and Wanninkhof 2003) with wind speed data provided by the Grand River Conservation Authority (D. Boyd, personal communication).

N_2O emission rates were calculated using the thin boundary layer equation:

$$\boldsymbol{N_2O\ emission = k \times (C_{measured} - C_{sat})} \qquad \textbf{Equation 3.1}$$

where emissions are in micromoles per square metre per day, k is in metres per day, $C_{measured}$ is the measured N_2O concentration (mol/m^3) and C_{sat} is the equilibrium N_2O concentration, calculated after (Weiss 1970). Emissions were integrated linearly over time to obtain annual emissions. For areal integration, each sampling site represented a portion of the river, using the reaches of the Grand River Simulation Model (Anderson 2012). Reach boundaries were chosen to coincide with factors potentially changing water chemistry (for example, dams, tributaries, WWTPs and so on). To estimate annual N_2O emissions from the entire river, we assumed that the time-weighted average ratio of emissions from the middle Grand (sites 8-13) to emissions from the whole river during whole-river samplings (43%) was the same for annual emissions for the few months when there was insufficient data from the entire river.

Jackknifed Monte Carlo simulations were used to estimate the effects on modelled k values of using three data points per diel cycle. At four sites of diel-intensive sampling, data from four different

sampling dates were chosen for the simulations. The field data were randomly subsampled with decreasing numbers of points while ensuring that at least one sample was drawn from the three times of day (before sunrise, mid-morning and early afternoon) as in the less intensive diel sampling. Twenty-four combinations of data were modelled five times at each level of data. All acceptable model runs, those with r^2 values greater than 0.8 and providing a visually acceptable solution, were averaged. The k values at each level were compared with Welch's analysis of variance (R Core Development Team, 2011) to account for the unequal variances across levels. Across all field sites and dates, k values from 3-point modelling differed from those from 18-point modelling by 13-25% with a central tendency of 10%. Thus, we apply an error value of 10% to k values derived from three data points, and take the largest resulting propagated error (16%) as the error on emission measurements. Errors in reach area were not available from the Grand River Simulation Model but were much less than errors in k values.

Linear regressions were performed in Matlab, version R2011b (MathWorks). N_2O emission data were log-transformed ($\log_{10}$(emission+35)) to include negative numbers to pass normality tests. p values < 0.05 were considered significant. Goodness of fit was assessed with the Akaike Information Criterion.

3.3 Results and Discussion

The river was a source of N_2O to the atmosphere at almost all sites and times (flux rates: -35 to 4,200 μmol/m^2/d, n = 651). Annual whole-river N_2O emissions were 177 ± 5 kmol/yr and 490 ±14 kmol/yr (1.6±0.05 and 4.2±0.1 mol/km/d) in the 2006-2007 and 2007-2008 seasons, respectively. Spatial variation in emission rates was large; emissions were highest in the urban middle reach, especially downstream of the Kitchener WWTP (Figure 3.2). Although the river's urban-impacted reach (sites 10-13) represents only 5% of the total surface area, it accounted for 36%-38% of N_2O emissions (Table 3.3). Spikes in N_2O concentrations immediately downstream of WWTPs were similar to those in the Potomac River (McElroy et al. 1978) and Ohio River (Beaulieu et al. 2010). Summer emissions (June-August, 25% of the year) contributed disproportionately to annual N_2O emissions (42% in 2006-2007 and 56% in 2007-2008; Table 3.3).

Concentrations of N_2O varied on a diel basis at many sites in the watershed and were consistently highest at night when DO was low (Rosamond et al. 2011). This results in up to a 10-fold variability in diel N_2O emissions at the same site because the gas exchange coefficient (k) in rivers is controlled

by turbulent flow and diel changes in k are negligible (O'Connor and Dobbins 1958). Therefore, diel N_2O emissions can vary by over a factor of 10 at the same site. In the summer, night comprised 38% of the time but 50%-52% of the N_2O emissions from the river (Table 3.3). The largest measured instantaneous N_2O emission (4165 μmol/m^2/d) occurred at site 11 (downstream of the Kitchener WWTP) in July 2007 at night. These findings confirm previous suggestions (Rosamond et al. 2011) that other river studies have biased their N_2O emission estimates by omitting diel, seasonal and spatial variability in N_2O concentration (Table 3.1), although N_2O concentrations in a hypereutrophic drainage canal have also been shown to be highest at night (Harrison et al. 2005)

Despite the large impact of the urban zone on N_2O emissions, average N_2O emission rates from the entire Grand River were similar to those from rivers of similar catchment size (Table 3.1), although our sampling regime was much more intensive than previous studies. N_2O emissions in 2007-2008 were almost double those of 2006-2007. Several years' data may be required to characterize climate-driven inter-annual variation in N_2O emissions.

We compared measured N_2O emissions to estimations using Intergovernmental Panel on Climate Change (IPCC) equations, used by the signatory countries of the United Nations Framework Convention on Climate Change to report annual N_2O emissions. N_2O produced in rivers is assumed to relate linearly to DIN loads from agricultural fertilizers and manure and from sewage effluent. The former is estimated with the following equation:

$$\boldsymbol{N_2O\ emissions = N_{LEACH} \times EF_{5-r}} \qquad \textbf{Equation 3.2}$$

where N_2O emissions are in tonnes N/yr, N_{LEACH} is the annual flux of reactive N leached into the river from agricultural sources (tonnes N/yr) and $EF_{5\text{-}r}$ is the fraction of DIN nitrified and denitrified to N_2O over a year in rivers and streams, assuming constant N_2O production rates for each process and no groundwater N_2O input (Nevison 2000). The default value was formerly set at 0.0075 (Nevison 2000) in the 1996 IPCC protocol but was decreased to 0.0025 in 2006 because field studies suggested it was too high (Clough et al. 2006).

The second equation is for sewage effluent discharged directly to rivers:

$$\boldsymbol{N_2O\ emissions = N_{EFFLUENT} \times EF_{EFFLUENT}} \qquad \textbf{Equation 3.3}$$

where $N_{EFFLUENT}$ is the total annual mass of nitrogen in waste-water effluent (tonnes N/r) and $EF_{EFFLUENT}$ is an emission factor with a default value of 0.005 (IPCC 2007). We calculated IPCC estimates using annual WWTP DIN loadings (Table 3.2) and dissolved DIN loads in the upper,

agricultural watershed (upstream of site 8). This avoids including emissions from large tributaries but provides a conservative estimate of agricultural loading, as DIN is rapidly consumed and recycled in aquatic ecosystems (Ensign and Doyle 2006). Using default IPCC $EF_{5\text{-}r}$ and $EF_{EFFLUENT}$ values, N_2O emission estimates for the whole river were 233 and 254 kmol N_2O/yr in 2006-2007 and 2007-2008, respectively, or about 130% and 50% of the measured values, respectively (177 and 490 kmol/yr; Table 3.3). The discrepancies between measured N_2O emissions and IPCC estimates suggest that linear DIN models do not adequately predict N_2O emissions from rivers (Table 3.3). This has implications for the global N_2O budget, which is balanced using present IPCC $EF_{5\text{-}r}$ values (Syakila and Kroeze 2011).

Annual DIN loads and N_2O emissions do not have a simple linear relationship. DIN loads were 13% higher in 2007-2008 than in the previous year, but measured N_2O emissions were almost triple. The assumption made by the IPCC (IPCC 2007) and the global N_2O budget (Syakila and Kroeze 2011), that increases in DIN loads to rivers cause increases in N_2O emissions, should be carefully re-examined. Previous studies examining EF_5 values have suggested modifications (Clough et al. 2006, Reay et al. 2005) even when acknowledging no significant linear relationship between N_2O and DIN (Clough et al. 2006).

To understand potential controls on N_2O emissions, we compared instantaneous emissions with DIN, NO_3^-, temperature and DO (Figure 3.3). To our knowledge, no previous studies have made these comparisons. Contrary to IPCC assumptions, the highest N_2O emissions occurred at moderate NO_3^- concentrations. Temperature, NO_3^- and DIN all showed significant but small ($r < 0.20$) relationships with N_2O emission. However, DO showed a stronger, significant and negative relationship with N_2O emissions (Rosamond et al. 2011) (Figure 3.3). Multiple linear regressions combining DO, DIN and temperature did not increase goodness of fit. We suggest that EF values and simple or multiple linear regression analyses are not appropriate for N_2O dynamics in complex natural systems. Future work should consider approaches that include DO in N_2O predictive models.

DO seems to be a much stronger control than NO_3^- on N_2O emissions in impacted systems. The relationship is especially strong in the river's urban reach where NO_3^- production is high ($r = 0.61$, Table 3.4). Although NO_3^- concentrations are low to moderate, N_2O production does not seem to be NO_3^- limited. We suggest that N_2O is largely produced by denitrification in hypoxic or anoxic sediment. Summer low-flow conditions promote hypoxia through high community respiration and decreased DO solubility. Low DO in the water column is probably a proxy for poorly oxygenated

sediment. Many denitrifying microbes are facultative anaerobes, and switch from oxic respiration to denitrification in hypoxic environments[17]. During hypoxia, N_2O emissions dominate total annual emissions, whereas N_2O emissions from low-NO_3^- areas in the upper watershed are quite low (Table 3.3, Figure 3.2). The large increase in N_2O emission in the second year with almost no DIN increase was probably due to increased hypoxia at lower flows and higher temperatures. At present, IPCC methodology and the global N_2O budget (Syakila and Kroeze 2011) underestimate N_2O in 2007-2008, when more N_2O was produced during night-time hypoxia in the urban reach. This finding has implications for present and future N_2O budgets. N_2O emissions could be over- or underestimated worldwide, depending on the extent of hypoxia in rivers and the role of temperature in controlling microbial metabolic rates. The predicted doubling of DIN load to rivers by 2050 (Seitzinger et al. 2002) may not result in more N_2O. However, an increase in hypoxia due to eutrophication (from increased N and/or P input (Seitzinger et al. 2005)) would probably result in large increases in annual N_2O emissions from rivers and further decoupling of DIN and N_2O. Climate-change-related increase in water temperature causing decreased DO solubility and higher rates of microbial respiration and denitrification could have the same effect. This suggests that N_2O budget predictive modelling must take riverine DO dynamics into account. Many countries reporting to the IPCC do not have detailed DO data from rivers, but could perhaps estimate hypoxia using proxies such as water velocity and depth, summer air temperature and precipitation, and biological productivity or total phosphorus (Dodds et al. 1998).

3.4 Conclusions

This is the most complete multi-annual estimate of N_2O emissions from a single river and is the first study to compare N_2O emissions and DO. The highest N_2O emissions occurred in urban areas downstream of WWTPs, particularly during hypoxic summer nights. N_2O emissions are dynamic in rivers with large diel and/or spatial fluctuations in DO. Thus, previous studies of N_2O emissions from rivers probably missed crucial periods of high N_2O emissions (urban, night-time), skewing annual averages. Global N_2O budgets and sampling protocols in streams and rivers must recognize spatial and temporal variation in both DO and N_2O. Whole-river N_2O emissions can be either significantly lower or higher than DIN-based estimates, depending on the extent of hypoxia. This suggests that the global N_2O budget should be revised to consider DO-dependency of riverine N_2O emissions.

Table 3.1: NO_3^- concentrations, N_2O emissions and sampling frequency from streams and rivers, ordered by catchment size. Sites are divided into agricultural streams (top), mid-sized rivers (middle), and large rivers (bottom). Estuarine emissions are not included.

Ecosystem Name	Catchment area (km^2)	Average annual discharge ($m^3\ s^{-1}$)	Length of river segment studied/ Total river length ($km\ km^{-1}$)	NO_3^- range or average (mg N/L)	Average summer N_2O emission ($\mu mol/m^2/d$)	Average winter N_2O emission ($\mu mol/m^2/d$)	Average yearly N_2O emission ($\mu mol/m^2/d$)	Number of years sampled	Sampling sites per stream or river	Total samples collected per stream or river	Frequency of sampling
Toenepi Stream, NZ (Wilcock and Sorrell 2008)	15.5	ND	4.5/ND	0.070 to 3.44	0 to 27.5				3	20	Periodically in spring, summer, fall
Whangamaire Stream, NZ (Wilcock and Sorrell 2008)	23	ND	5.2/ND	8.17 to 16.0	0.11 to 96.9				3	18	Periodically in spring, summer, fall
Whakapipi Stream, NZ (Wilcock and Sorrell 2008)	48.9	ND	0.4/ND	1.42 to 4.47	0 to 5.21				3	5	Periodically in spring, summer, fall
Sitka Stream, Czech Republic (Hlavacova et al. 2006)	119	0.81	0.014/ND	ND			37	1	1	12	I

12 agri streams in Michigan (Beaulieu et al. 2008)	ND	ND	0.1/NA	0.003 to 27.4		30.2*	0.5 to 1		6 to 12	Once per month
10 streams, southern ON, Canada (Baulch et al. 2011)	ND	0.001 to 0.181	N/D	0.63	78		2	1 to 2	6 to 62	Summer diel sampling events (every 3-6 hours)
Drainage canals, Sonora, Mexico (Harrison and Matson 2003)	8 to 430	< 0.001 to 0.002	ND	BD to 14.4		140.6				Once per month year-round
LII River, New Zealand(Clough et al. 2006)	ND	ND	12/12	2.56 to 5.19	146.6		1	4	52	Once to twice per month in spring, fall and winter
Ouse R., UK (Dong et al. 2004)	3315	ND	ND	4.52 (0.56)		0.6	1	10 to 16 (including estuary)	4	Once per season
Grand R., ON, Canada (this study)	6800	56	298/298	BD to 9.0		35.7	2	23	370	Bi- or triweekly year-round
Grand R., ON, Canada (this	6800	56	298/298	BD to 9.0		16.5	2	23	281	Bi- or triweekly

study)										year-round
Temmesjoki R., Finland (Silvennoinen et al. 2008)	ND	ND	ND	1.18 (0.67)		46.4	1.75	6	78	~Once per month year-round at one site, spring to fall at 5 sites
Colne R., UK (Dong et al. 2004)	ND	ND	ND	5.91 (0.25)		0.3	1	10 to 16 (including estuary)	4	Once per season
Stour R., UK (Dong et al. 2004)	ND	ND	ND	5.64 (0.29)		0.3	1	10 to 16 (including estuary)	4	Once per season
Orwell R., UK (Dong et al. 2004)	ND	ND	ND	5.24 (0.27)		0.3	1	10 to 16 (including estuary)	4	Once per season
Deben R., UK (Dong et al. 2004)	ND	ND	ND	5.77 (0.46)		0.5	1	10 to 16 (including estuary)	4	Once per season
Trent R., UK (Dong et al. 2004)	ND	85	ND	8.33 (0.48)		0.5	1	10 to 16 (including estuary)	4	Once per season
Conwy R., UK (Dong et al. 2004)	ND	ND	ND	0.23 (0.04)	0.04			10 to 16 (including estuary)	3	Winter, spring, summer

Hudson River, NY (Cole and Caraco 2001)	33500	ND	240/507	0.84	5.5	1.5	19	121	Annual biweekly at one site; multiple site surveys in June, August, Sept.
South Platte River, CO (McMahon and Dennehy 1999)	63000	22.9	707/707	4.2 to 9.8	128.6	1	9	27	Fall, spring, summer
Ohio R., Ohio, USA (Beaulieu et al. 2010)	508202	2371	153/1579	0.82 +/- 0.05	10.3	1	29	61	Biweekly year-round at one site, one longitudinal study
Amazon River (Richey et al. 1988)	6000000	209000	2000/6400	N/D	9.8	3	11	99	~ Every four months

Numbers in brackets are standard error. ND = no data. BD = below detection.

*Annual emission includes streams sampled over 6 months and over 12 months.

Table 3.2: Nitrate and ammonium loads from the WWTPs on the Grand River in 2008 or 2009. Unless otherwise specified, data is from Environment Canada (Environment Canada 2010). N/D = no data. No effluent information for small WWTPs is collected by Environment Canada. The locations of the plants, relative to the sampling sites shown in Figure 3.1, are also given.

WWTP Name	Population Load	NO_3^- load from WWTP (tonnes N/yr)	NH_4^+ load from WWTP (tonnes N/yr)	Closest downstream site	Distance to closest downstream site (km)
Dundalk Lagoon	1400	N/D	0.9	2	~20
Grand Valley	1489	N/D	N/A	5	8.25
Fergus	6050	N/D	0.4	7	8.53
Elora	3583	N/D	5.6	7	3.07
Conestogo	101	N/D	N/A	9	13.53
Waterloo	66627	135	255	10	15.53
Kitchener	164000	47	583	11	5.53
Preston	18727	82	0.5	12	4.16
Galt	60000	279	4.5	13	8.2
Paris	7700	N/D	1.7	15	2.46
Brantford	73000	139	96	17	12.38
Caledonia	5655	N/D	N/D	19	4.26
Cayuga	1258	N/D	N/D	22	23.7
Dunnville	5182	N/D	N/D	23	6.65

Table 3.3: Summary of meteorological data, NO_3^- loads, and N_2O emissions by location and time over two years and the importance of urban, summer-time and night-time emissions to the total annual N_2O emission budget.

	Percentage of river area or time	2006-2007	2007-2008
Average July daytime high temperature (°C) (Seglenieks 2011)		26.9	25.2
Total July precipitation (mm) (Seglenieks 2011)		152	50
Average July discharge near site 11 (m^3/s) (Water Survey of Canada 2010)		12.5	9.6
Annual DIN load (tonnes N)		2160	2448
Total Annual N_2O Emission from River (kmol)		177	490
Annual N_2O Emission Predicted by IPCC Equations and global N_2O budget (Syakila and Kroeze 2011) (kmol)		233	254
N_2O Emission from Urban area (sites 10-13) (percentage of total annual)	5	36	38
Summer N_2O Emission from River (June - August) (percentage of total annual)	25	42	56
Nighttime N_2O Emission (percentage of total annual)	50	56	57
Summer Nighttime N_2O Emission (percentage of summer)	38	50	52

Table 3.4: r values for linear correlations of various factors versus N_2O emission by section of the Grand River. The multiple linear correlation includes all three variables and is calculated by comparing predicted and measured N_2O emission rates.

Section of River	Description	Number of Data Points	Temperature	NO_3^-	DO	Multiple Linear Correlation
1 (Sites 1 – 9)	Agricultural till plain	265	-0.13	0.33	-0.06	0.43
2 (Sites 10-12)	Urban	220	0.34	-0.41	-0.61	0.61
3 (Sites 13-	Groundwater recharge area	19	-0.14	0.41	-0.25	0.47
4 (Sites - 23)	Agricultural clay plain	39	0.34	-0.17	-0.04	0.23

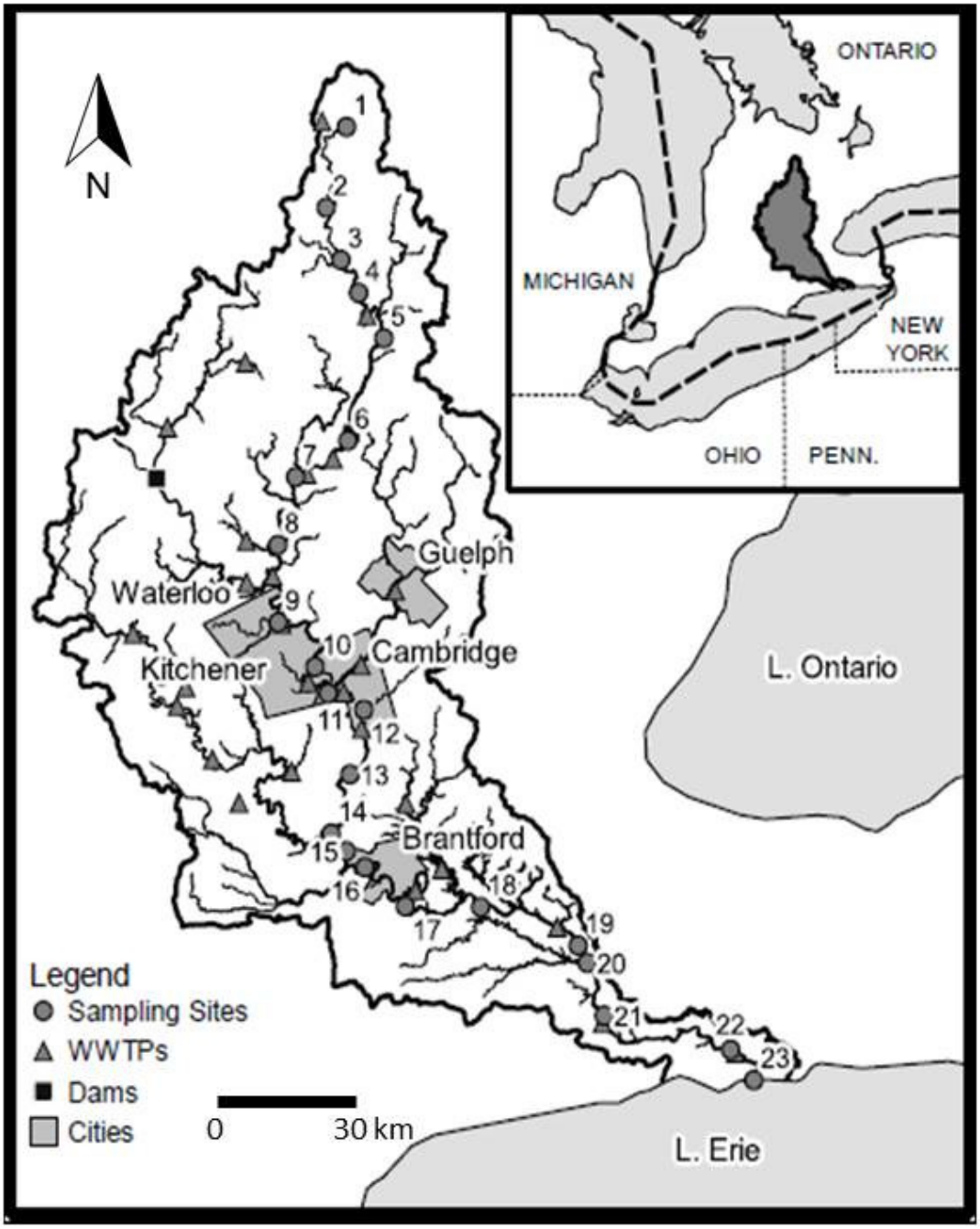

Figure 3.1: Map of the Grand River, Ontario, Canada. The 23 sampling sites (circles) used in this study and wastewater treatment plans (triangles) are shown.

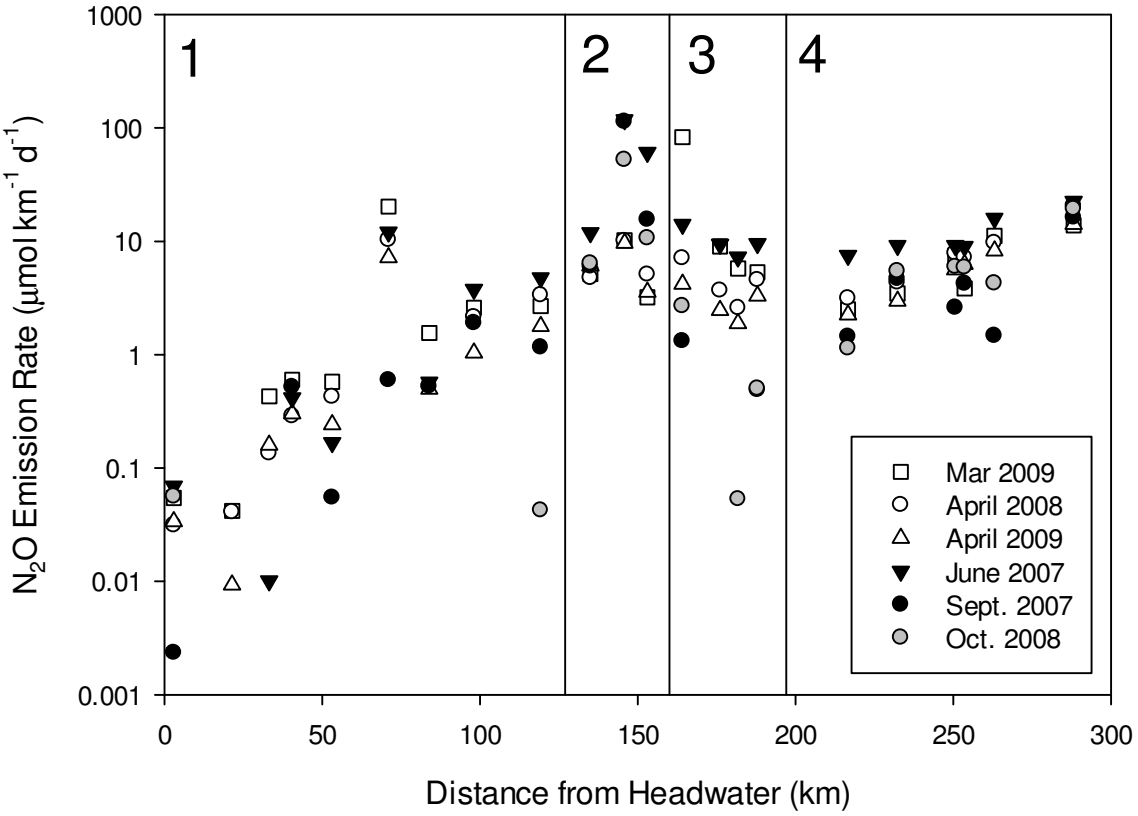

Figure 3.2: N_2O emissions at 23 sampling sites along the Grand River over six sampling events, showing elevated emissions in summer (black symbols) and in the urban reach (2). Black lines separate distinct reaches: Reach 1: Agricultural till-plain, Reach 2: Urban and Impacted, Reach 3: Groundwater Recharge, Reach 4: Agricultural clay plain. Symbols represent sampling events: Open squares: March 2009; open circles: April 2008; open triangles: April 2009; black triangles: June 2007; black circles: September 2007; grey circles: October 2008. Measurement error is smaller than symbols. Note the logarithmic y-axis.

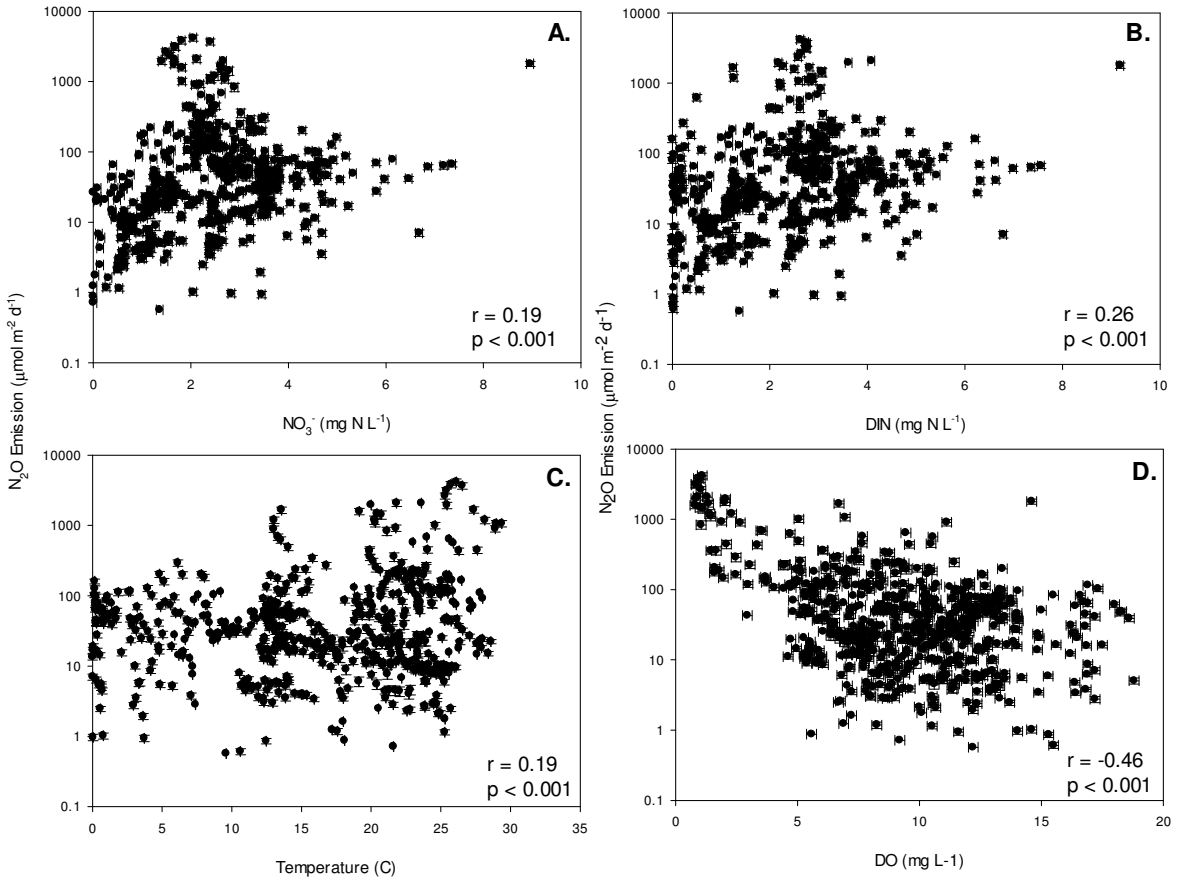

Figure 3.3: Instantaneous N_2O emissions versus NO_3^- (a), DIN (b), temperature (c) and DO (d). Linear correlation r and p values are shown. Error bars (standard deviation of multiple standard runs) are smaller than symbols. Note the log scale on the y-axis.

Chapter 4: Nitrous oxide and methane in wastewater effluent: Significance to global budgets and stable isotope tracing

4.1 Abstract

Few published data on N_2O and CH_4 concentration and stable isotope ratios from wastewater treatment plant (WWTP) effluents exist. It is therefore unclear if these are significant to atmospheric greenhouse gas budgets and if stable isotopic ratios are distinct from upstream sources. We present the first comparison of NH_4^+, NO_3^-, N_2O and CH_4 concentrations and stable isotopic ratios in summer and winter effluents from non-nitrifying, partially-nitrifying, and fully nitrifying WWTPs. Effluents were always supersaturated in N_2O and CH_4, even at WWTPs with extensive aeration. Dissolved N_2O loads in effluents were similar to direct emissions from WWTPs, and CH_4 emissions from effluents were < 5% of IPCC direct CH_4 emissions. NH_4^+ and NO_3^-, N_2O and CH_4 isotopic ratios had seasonal variability but low diel variability. N_2O isotopic ratios could not be predicted from NH_4^+ or NO_3^- values. NH_4^+ and NO_3^- stable isotopic ratios were not always different than upstream sources. However, N_2O and CH_4 stable isotopic ratios were consistently distinct from up-river sources, suggesting that isotopes could be used to trace effluent sources but must be characterized in stable isotopic mass balances of human-impacted systems.

4.2 Introduction

Nitrous oxide (N_2O) and methane (CH_4) are potent greenhouse gases (GHGs) responsible for about 6% and 18% of net anthropogenic climate forcing, respectively (IPCC 2007, Rodhe 1990). As of 2007, 190 countries have signed the United Nations Framework Convention on Climate Change, and are required to report yearly anthropogenic GHG emissions from various sources, using field measurements and/or empirical estimations determined by the Intergovernmental Panel on Climate Change (IPCC) (Intergovernmental Panel on Climate Change 1996).

N_2O is produced primarily by microbial metabolism of ammonia (NH_4^+) and nitrate (NO_3^-) in both terrestrial and aquatic ecosystems (Zafiriou 1990) (Figure 4.1). Some N_2O is also produced by fossil fuel combustion (Sahely et al. 2006). There are few studies on GHG production from WWTPs, although they contributed significant CH_4 and N_2O (690 Mt CO_2 equivalent) to the atmosphere in 2005 (IPCC 2007).

WWTPs release GHGs three ways: directly from the WWTP to the atmosphere; dissolved in effluent that is later degassed in downstream ecosystems such as rivers, estuaries, lakes or oceans; and indirectly via downstream processing of effluent NO_3^- and/or NH_4^+. Direct N_2O emissions from WWTPs in North America, Europe and Japan have been quantified (Czepiel et al. 1995) (Table 4.1). Dissolved N_2O loads in treated effluent released to aquatic environments have only been estimated, but not measured directly (Kimochi et al. 1998, Toyoda et al. 2011). The IPCC (IPCC 2007) assumes that WWTPs produce 3.2 g N_2O /capita/yr, based on one study of a small (population 6000 – 12000) secondary nitrifying WWTP in New Hampshire (Czepiel et al. 1995). Indirect N_2O emissions are predicted to be much larger than direct emissions from the WWTP itself. They are estimated with the following IPCC empirical equation (Intergovernmental Panel on Climate Change 1996):

$$\mathbf{N_2O\ (kg\ N_2O\ yr^{-1})} = \mathbf{N_{effluent}(kg\ N\ yr^{-1})} \times \mathbf{EF_{effluent}} \times \frac{\mathbf{44}}{\mathbf{28}} \left(\frac{\mathbf{kg\ N_2O}}{\mathbf{kg\ N}}\right) \qquad \textbf{Equation 4.1}$$

where $EF_{effluent}$ is an emission factor with a default value of 0.005 (IPCC 2007).

CH_4 is produced by microbial fermentation of organic carbon. CH_4 emissions from WWTPs are poorly studied (Czepiel et al. 1993, Toyoda et al. 2011), perhaps because many WWTPs in developed nations combust some CH_4 produced during treatment (Sahely et al. 2006). CH_4 emissions from centralized, aerobic WWTPs are estimated by the IPCC (IPCC 2007) as follows:

$$\mathbf{CH_4\ (kg\ CH_4\ yr^{-1})} = [\textstyle\sum_{i,j}(\mathbf{U_i} * \mathbf{T_i} * \mathbf{EF_j})] * (\mathbf{TOW - S}) - \mathbf{R} \qquad \textbf{Equation 4.2}$$

Where U_i is the fraction of the population in income group i, T_i is the degree of use of the treatment path by income group i, EF_j is the emission factor in kg CH_4/capita/yr, TOW is the total organics in wastewater per year in kg/yr, S is organic component removed as sludge in kg/yr, and R is CH_4 recovery per year in kg/yr. The default EF_j value is zero, resulting in no estimated fluxes to the atmosphere from aerobic WWTPs. Emissions occurring downstream of WWTP resulting from riverine metabolism of effluent organic carbon are not considered.

While some studies have measured N_2O fluxes released directly from WWTPs to the atmosphere (Czepiel et al. 1995, Townsend-Small et al. 2011), only two previous studies measured dissolved N_2O, $\delta^{15}N$-N_2O and $\delta^{18}O$-N_2O during wastewater treatment. Townsend-Small et al. (Townsend-Small et al. 2011) measured N_2O within a combined nitrification-denitrification water reclamation plant and in a partially nitrifying WWTP. Toyoda et al. (Toyoda et al. 2011) measured NO_3^-, N_2O and CH_4 concentration and stable isotopic values in a nitrifying plant in Tokyo. Neither directly measured

WWTP discharge. Fluxes and isotopic values are summarized in Table 4.1, Figure 4.4 and Figure 4.5. Both studies quantify GHG emissions to the atmosphere and attempt to determine gas production pathways (i.e. nitrification, denitrification, methane oxidation). However, they do not compare emissions to IPCC estimations, nor do they compare stable isotopic values of N_2O and CH_4 to upstream sources to determine if sewage GHGs can be traced isotopically in the environment.

Stable isotopic studies of NH_4^+, NO_3^-, N_2O and CH_4 in rivers can help elucidate sources and cycling processes (Rock and Mayer 2004, Sjodin et al. 1997). It is therefore important to know if point sources such as WWTP effluent are isotopically distinct from background river values. If so, they can be used as tracers of effluent downstream of discharge points. However, very few studies have isotopically characterized both effluent and upstream river sources (Table 4.1). In this study, we (a) compare dissolved loads of N_2O and CH_4 to estimates of direct emissions from WWTPs and from downstream processing of effluent NH_4^+ and NO_3^- to determine if WWTP effluent is an important, overlooked source of greenhouse gases to the atmosphere, (b) characterize both diel and seasonal variability in N_2O and CH_4 concentrations and isotopic values, as well as isotopic fractionations between substrates (NH_4^+ and NO_3^-) and N_2O, to determine the best sampling strategies to capture variability, and (c) determine if effluent N_2O and CH_4 are distinct isotopically from previous published data and from background sources and can therefore be used as tracers or indicators of anthropogenic impact.

4.3 Materials and Methods

In July 2007 and February 2008, 5-7 effluent samples over 24 hours were collected from three WWTPs in southern Ontario, Canada: WWTPs A and B on a seventh order river, and WWTP C on a sixth order river. WWTP A is approximately 20 km downstream of WWTP B. We also report data from a river site approximately 100 m upstream of WWTP A collected contemporaneously with effluent sampling. In July, this upstream site was sampled approximately every 1.5 hours over 28 hours. In February, it was sampled once, due to a lack of diel variability in winter river chemistry (Rosamond et al. 2011). River samples were collected at mid-arm depth in fast-flowing water. We have followed the Ontario Water Resources Act in considering the months of April to October "summer" and November to March "winter" (Ministry of the Environment of Ontario 2007).

Each WWTP treats wastewater differently. WWTPs A and B use secondary treatment and have a preliminary settler, a primary clarifier and aerator combination, and a secondary settling tank

(Vesilind 2003). WWTP C is a tertiary system, similar to the other two WWTPs, but with a longer aeration residence time and final sand filtration. Effluent is chlorinated at all three WWTPs before release, and subsequently chemically dechlorinated only at WWTP C. Little or no nitrification of sewage occurs in WWTP A, incomplete nitrification occurs at WWTP B, and complete nitrification occurs at WWTP C (Table 4.2).

Effluent was collected as close to its discharge point to the river as possible. It was collected directly from the discharge pipe before it entered the river at WWTPs B (pipe length: about 2 km) and C (pipe length: about 20 m). Longer pipe length between the WWTP and river may result in loss of GHGs by gas exchange. Effluent from WWTP A discharges effluent through a diffuser in the riverbed. Therefore, effluent was collected within the WWTP, immediately before it entered the discharge pipe. Effluent temperature; conductivity; concentration of dissolved oxygen (DO), chloride (Cl^-), NO_3^-, NH_4^+ , N_2O and CH_4; $^{15}N/^{14}N$ ratios of NH_4^+, NO_3^- and N_2O; $^{18}O/^{16}O$ of N_2O; and $^{13}C/^{12}C$ of CH_4 were measured. NO_3^- and NH_4^+ samples were filtered to 0.45 µm, and NH_4^+ samples were acidified to pH 4 with sulfuric acid. Dissolved N_2O and CH_4 concentration samples were collected in 50 mL serum bottles with no headspace and capped with pre-baked rubber Vacutainer™ stoppers. N_2O and CH_4 isotope samples were similarly collected in 100 mL serum bottles. N_2O and CH_4 concentration and isotope samples were preserved with 2 mL saturated aqueous mercuric chloride per L and kept refrigerated until analyzed within two weeks of collection. Temperature and conductivity were measured with a multiprobe (YSI 556 MPS).

NO_3^- and Cl^- concentrations were analyzed on a Dionex ICS-90 ion chromatograph. Precision and detection limit were 0.07 mg N/L and 0.05 mg N/L for NO_3^- and 1 mg/L and 0.2 mg/L for Cl^-. The chromatograph could detect but not quantify nitrite (NO_2^-), because Cl^- and NO_2^- peaks overlapped. Cl^- samples higher than 2 mg/L were diluted. NH_4^+ samples were analyzed by the salicylate and nitroprusside colorimetric method (American Public Health Association 1995) on a Technicon Auto analyzer at 660 nm wavelength with a precision of 0.005 mg N/L and detection limit of 0.01 mg N/L. Duplicate CH_4 and N_2O concentration samples were analyzed with a Varian CP-3800 gas chromatograph with a flame ionization detector and an electron capture detector, respectively, using a helium headspace equilibration technique. Concentrations were calculated using Henry's Law after Lide and Fredrikse (Lide and Frederikse 1995). Dissolved oxygen was titrated using the sodium azide modification of the Winkler technique with a precision and detection limit of 0.2 mg/ L (American Public Health Association 1995).

$\delta^{15}N\text{-}NH_4^+$ was analyzed using a modified acidified disk-PTFE trap method on a Micromass IsoChrom continuous flow mass spectrometer (Brooks et al. 1989, Spoelstra et al. 2011). $\delta^{15}N\text{ -}NO_3^-$ was analyzed using the modified silver nitrate method (Silva et al. 2000). This method may include nitrite (NO_2^-) present in the sample. Precision of $\delta^{15}N$ for both methods was 0.3‰.

Dissolved N_2O was stripped from samples using a novel technique (Thuss 2008) and stored in 10 mL borosilicate vials with butyl-blue rubber stoppers until analyzed. CH_4 isotopes were prepared with a helium headspace method (Venkiteswaran and Schiff 2005). CH_4 concentrations from WWTP C in winter were insufficient for $\delta^{13}C$ analysis. N_2O and CH_4 isotopic ratios were analyzed with a GV Isoprime mass spectrometer with a preconcentrator system. N_2O isotopic data were corrected after Kaiser et al. (Kaiser et al. 2003), using two internal N_2O standards. Precision was 0.2‰ for $\delta^{15}N$ and 0.5‰ for $\delta^{18}O$. Two N_2O isotope samples were rejected due to errors in sample processing. CH_4 isotope data were corrected to two internal standards according to Venkiteswaran and Schiff (Venkiteswaran and Schiff 2005) with a precision of 0.5‰. All isotope values are reported in permil (‰) notation: $\delta^{15}N$ versus air, $\delta^{18}O$ versus VSMOW, and $\delta^{13}C$ verses VPDB.

4.4 Results

Effluent temperatures varied little over any 24 period and were about 10° C to 15° C cooler in winter than in summer (Figure 4.2A-C), although daily high air temperature varied by over 30°C between summer (WWTPs A and B: 32.0°C; WWTP C: 26.5°C) and winter (WWTPs A and B: -1.8° C; WWTP C: -12.1°C) (Seglenieks 2011). All effluents were oxic, but DO concentrations were consistently lowest at WWTP A (mean: 4.8 mg/L), intermediate at WWTP B (7.7 mg/L) and highest at WWTP C (8.6 mg/L). DO concentrations varied little on the diel scale and were only slightly higher in winter than in summer at all sites (Figure 4.2A-C).

Total inorganic nitrogen (TIN = NO_3^-+NH_4^+), was similar at WWTPs A and C (about 25 mg N/L) but was often lower at WWTP B (about 13 mg N/L). Unless otherwise noted, values reported are means of both summer and winter samples, ± standard deviation. NH_4^+ concentrations were highest at WWTP A (24.2 ± 3.2 mg N/L) and lowest at WWTP C (0.10 ± 0.03 mg N/L), with the reverse trend in NO_3^- (Figure 4.2D-F). At all sites, mean NO_3^- concentrations were at least 0.5 mg N/L higher in winter than summer (Figure 4.2D-F). Data are not shown for summer NO_3^- values at WWTP A (range: 0.01 mg N/L to 0.22 mg N/L) and NH_4^+ concentrations at WWTP C year-round (range: 0.03 mg N/L to 0.12 mg N/L) due to insufficient sample size for isotopic analyses. NO_2^- was detected but

not quantified at WWTP B in summer. At other sampling times and locations, any NO_2^- present was not observed because of very high Cl^- peaks.

$\delta^{15}N\text{-}NH_4^+$ values were generally confined to a narrow range and were about 3‰ higher in summer than in winter at WWTPs A and B (Figure 4.2D-F). WWTP A had lower values (summer: 6.4±1.6 ‰, winter: 3.8±0.5‰) than WWTP B (summer mean: 15.2±1.4‰, winter mean: 11.5±1.0‰). $\delta^{15}N\text{-}NO_3^-$ also showed a narrow range over a 24 hour period but had a very large seasonal difference at WWTP B (summer: 25.3±1.2‰, winter: 8.9±1.5‰). WWTP C $\delta^{15}N\text{-}NO_3^-$ values were similar in summer (7.2± 1.1‰) and winter (8.2±0.4‰) (Figure 4.2D-F).

All samples collected were supersaturated in N_2O (210% to 14 100%). WWTP A had the highest concentration of N_2O in summer (837±475 nmol/L), but was lower in winter (280±77 nmol/L). WWTPs B and C showed smaller seasonal differences (Plant B: 389±177 nmol/L in summer and 484±73 in winter; Plant C: 179±90 nmol/L in summer and 322±61 nmol/L in winter).

$\delta^{15}N\text{-}N_2O$ values ranged widely between WWTPs but were generally well-constrained within individual WWTPs (Figure 4.3). $\delta^{15}N\text{-}N_2O$ values higher in summer than winter at all sites. $\delta^{15}N\text{-}N_2O$ values were lowest at WWTP B, moderate at WWTP C and highest at WWTP A (Figure 4.3). WWTP A. $\delta^{18}O\text{-}N_2O$ values were lower in summer than in winter at WWTP A (summer: 16.5±3.2‰, winter: 22.6±0.5‰) but otherwise were very similar between plants with no seasonal variation (WWTP B: 20.1±1.1‰; Plant C: 19.7±5.2‰) (Figure 4.2G-I, Figure 4.3).

Similar to the only previously published study of WWTP CH_4 (Toyoda et al. 2011), CH_4 was always extremely supersaturated (430% to 51 430%). Like N_2O, CH_4 was highest at WWTP A and lowest at WWTP C (Figure 4.2J-I). $\delta^{13}C\text{-}CH_4$ values showed little seasonal variation. Values were similar at WWTP A (-44.8±2.6‰) and WWTP B (-40.2±4.4‰) and were higher at WWTP C, where only winter values could be analysed due to insufficient sample sizes in summer (-32.7±1.8‰) (Figure 4.4).

4.5 Discussion and Conclusion

N_2O concentrations at WWTP C were similar to those reported for another nitrifying plant (132 nmol/L (Toyoda et al. 2009)); N_2O was higher at WWTPs A and B. Dissolved effluent N_2O load, calculated from data in Table 4.2 , is 2.0, 1.1, and 1.8 g-N_2O/capita/yr for WWTPs A, B, and C respectively. Since the rivers upstream of the WWTPs studied are consistently supersaturated in N_2O (Rosamond et al. 2011) and CH_4 (S. Timsic, unpublished data), we can therefore assume that all N_2O

dissolved in the released effluent will be released to the atmosphere from the river. In comparison, the median reported estimate of N_2O emissions directly from WWTPs is 11.4 g N_2O/capita/yr and the range is very large (range: 0.1 g N_2O/capita/yr to 1580 g N_2O/capita/yr) (Table 4.1). Emissions of dissolved N_2O in effluent discharged to rivers and other water bodies, a source ignored by the IPCC, can be similar in magnitude to direct N_2O emissions from WWTPs themselves. Additionally, N_2O emissions from WWTPs A and C are underestimated because any N_2O lost during travel within effluent pipes from the WWTP to the river was not measured.

Direct N_2O emissions from WWTP effluent can also be compared to indirect emissions produced by downstream microbial cycling of effluent N, calculated with Equation 4.1 (IPCC 2007). We compared mean measured N_2O and CH_4 emissions from effluent to calculated indirect emissions. Indirect emissions were calculated using both (a) total N (NO_3^- + NH_4^+ + organic N) loads in effluent, as reported in WWTP annual reports (Table 4.2), and to (b) our measured NO_3^- and NH_4^+. We did not quantify organic N. In both cases, direct effluent N_2O emissions are similar (range: 6% to 13% of indirect emissions (Table 4.2). Organic N in effluent (not quantified in our study) may mineralize downstream and contribute to higher indirect emission estimations. Thus, direct N_2O fluxes from WWTPs are small relative to estimated indirect fluxes. However, as IPCC estimates have been shown to both over- and underestimate indirect N_2O fluxes (Beaulieu et al. 2011, Rosamond et al. 2012), more research is needed to compare effluent loads with measured fluxes from rivers, to improve empirical emissions calculations.

Czepiel et al. (Czepiel et al. 1993) estimated direct CH_4 emissions to the atmosphere of 39 g CH_4/capita/yr from a WWTP in New Hampshire, while our estimates of direct CH_4 emissions from effluent were much smaller: 0.9 g CH_4/capita/yr, 0.8 g CH_4/capita/yr and 0.3 g CH_4/capita/yr for WWTPs A, B, and C respectively. These are similar to indirect estimates of CH_4 in-river (0.2 g CH_4/capita/yr) from a nitrifying plant in Japan (Toyoda et al. 2009) (Table 4.1). This source is currently unaccounted for in IPCC methodology (Intergovernmental Panel on Climate Change 1996, IPCC 2006).

TIN, N_2O and CH_4 concentrations varied over 24 hours at all three WWTPs (Figure 4.2). Effluent discharge from Plants A and B varies by about four-fold over a 24 hour period (Figure 4.5). If discharge changes resulted in dilution and not in changes to N cycling, TIN and/or N_2O should correlate to Cl^-, a conservative tracer. Alternatively, N_2O could be correlated to TIN if a constant fraction of TIN in the effluent is microbially processed to N_2O during treatment. To determine if Cl^-

or TIN could be used as a proxy measurement for N_2O, we compared N_2O concentration to Cl^- and TIN. All WWTPs showed high variability of TIN and N_2O over the diel period but little variation in Cl^- (Figure 4.5). Therefore, studies of WWTP effluent must be designed to take diel and seasonal variability N_2O and CH_4 concentration into account. Cl^- and TIN are not good proxies for N_2O concentration.

In contrast, the stable isotopic ratios of NH_4^+, NO_3^-, N_2O and CH_4 from all WWTPs had only a small diel range. However, $\delta^{15}N$ of NH_4^+, NO_3^-, and N_2O changed between summer and winter in most WWTPs (Figure 4.2). There was little (< 2‰) difference between mean summer and winter values of $\delta^{13}C$-CH_4 at WWTPs A and B (summer $\delta^{13}C$-CH_4 values for WWTP C were not measured) or $\delta^{18}O$-N_2O at WWTPs B and C. Thus, isotopic values of N_2O and CH_4 must include summer and winter data but need not be characterized on a diel scale.

There are few literature values of $\delta^{15}N$-NH_4^+ values in effluent and variation between and within WWTP types is large (Figure 4.1). (Secondary WWTPs, no nitrification: $\delta^{15}N$-NH_4^+: 2.9‰ to 14.7‰; secondary WWTPs, partial nitrification: 10.5‰ to 13‰). Our data show the same trend: Plant B (partial nitrification) has higher $\delta^{15}N$-NH_4^+ values than Plant A (no nitrification (Figure 4.2). Presumably the large variation in volatilization and nitrification result in the large range within plant types. There are also few published $\delta^{15}N$-NO_3^- values for effluent (Table 4.1). $\delta^{15}N$-NH_4^+ values from WWTP A and $\delta^{15}N$-NO_3^- values from WWTP C are generally similar to other WWTPs with similar processing methods (Table 4.1). Again, variation is large and denitrifying WWTPs seem to have higher $\delta^{15}N$-NO_3^- values than do non-nitrifying and nitrifying WWTPs (Table 4.1). The large ranges in $\delta^{15}N$-NH_4^+ and $\delta^{15}N$-NO_3^- values from the few published reports suggests that these values must be measured for each study site, not estimated from previous work.

Our measured $\delta^{15}N$ -N_2O and $\delta^{18}O$ -N_2O values in effluent were much lower than the tropospheric average ($\delta^{15}N$ -N_2O: 6.7‰, and $\delta^{18}O$ -N_2O: 44.6‰ (Kaiser et al. 2003)) (Figure 4.3). $\delta^{13}C$-CH_4 values in WWTP effluent were higher than the tropospheric value (-47.4‰, (Quay et al. 1999)), except for three samples from WWTPs A and B (Figure 4.4). Only two previous studies have published N_2O isotope data from WWTPs; $\delta^{15}N$-N_2O values from our effluents were similar (Townsend-Small et al. 2011, Toyoda et al. 2011) (Figure 4.3). However, N_2O from our WWTP effluents had lower $\delta^{18}O$-N_2O values than all previously published WWTP effluent, except for one nitrifying WWTP (Townsend-Small et al. 2011). Therefore, N_2O from our study sites plots in a unique area on a $\delta^{18}O$-N_2O - $\delta^{15}N$-N_2O isotope cross-plot (Figure 4.3). Most of our samples have higher $\delta^{13}C$-CH_4 values

than that of one previous study ((Townsend-Small et al. 2011, Toyoda et al. 2011). There is a large range of stable isotopic values of NH_4^+, NO_3^-, N_2O and CH_4 from WWTPs in the literature, even though the amount of published data is very small. This indicates that these values must be quantified for each study site, and using literature values is not sufficient.

Stable isotopic fractionations for N_2O production from nitrification and denitrification can be calculated with the following equation:

$$\boldsymbol{\varepsilon = (\alpha - 1)} \qquad \textbf{Equation 4.3}$$

where $\alpha = R_{N2O}/R_{NH4}$ for nitrification or R_{N2O}/R_{NO3-} for denitrification. Because we did not measure $\delta^{18}O\text{-}NO_3^-$ in effluent, we calculated ^{15}N isotopic fractionations only. ε values are shown in permil units.

It is unclear which process dominates N_2O production (if any) in the WWTPs, so ε values for both nitrification (ε_{NH4}) and denitrification (ε_{NO3}) were calculated where possible. However, this calculation does not take into account that as substrates (NH_4^+, NO_3^-) are consumed, (a) concentrations decrease, making isotopic analysis impossible, and (b) isotopic values of substrate increase (if ε is negative). Additionally, other processes such as NH_4^+ volatilization change the concentration and isotopic composition of substrates. Therefore, these isotopic fractionations are not meant to represent in-plant processing, but rather to determine if $\delta^{15}N\text{-}N_2O$ is predictable from $\delta^{15}N\text{-}NH_4^+$ and/or $\delta^{15}N\text{-}NO_3^-$.

Isotopic fractionations were always negative ($\delta^{15}N\text{-}N_2O < \delta^{15}N\text{-}NH_4^+$ or $\delta^{15}N\text{-}NO_3^-$, Table 4.3). Within each WWTP, isotopic fractionations vary by season by 8‰ to 12‰ with no consistent trend. The only exception is WWTP B (partial nitrification), where ε_{NH4} only varied by 2‰ between seasons. ε_{NH4} is closer to zero at WWTP A than at WWTP B and was not quantified at WWTP C. In contrast, there is significant overlap between WWTPs in ε_{NO3} values. The diel variability of isotopic fractionations was also relatively high (> 5‰) at WWTPs A and C, due to high variability in $\delta^{15}N\text{-}N_2O$. Thus, $\delta^{15}N\text{-}N_2O$ is not predictable from $\delta^{15}N\text{-}NH_4^+$ or $\delta^{15}N\text{-}NO_3^-$ values and must be characterized for individual WWTPs on the seasonal scale.

As in most rivers (Wetzel 1975), NH_4^+ concentrations upstream of the WWTPs were too low for isotopic analysis. However, $\delta^{15}N\text{-}NH_4^+$ values at WWTP B (10.5‰ to 16.0‰) were similar to or higher than the only previous published river $\delta^{15}N\text{-}NH_4^+$ value for a river upstream of a WWTP (11‰) (Sebilo et al. 2006). In contrast, $\delta^{15}N\text{-}NH_4^+$ values from Plant A, which experiences less NH_4^+ loss via volatilization and nitrification, were much lower (3.0‰ to 7.8‰). NH_4^+ concentration and

stable isotopic values can quickly change when added to rivers via effluent due to volatilization, nitrification and biotic uptake (Murray 2008), although it can also persist far downstream. Sebilo et al. (Sebilo et al. 2006) showed elevated NH_4^+ with no significant change in isotopic signature 120 km downstream of a WWTP on the Seine River, France. Thus, the use of NH_4^+ as a tracer of WWTP effluent is not advised.

In contrast, there is often sufficient NO_3^- in rivers upstream of WWTPs for isotopic analysis. River water collected immediately upstream of WWTP B concurrently with summer effluent sampling had a $\delta^{15}N\text{-}NO_3^-$ value of 6.5‰, much lower than WWTP B (24.2‰ to 26.6‰), but similar to values from WWTP C (6.0‰ to 11.5‰). Reported riverine dissolved $\delta^{15}N\text{- }NO_3^-$ values vary widely (-1.4‰ to 12.5‰, Table 4.1). Only summer $\delta^{15}N\text{-}NO_3^-$ values at WWTP B were outside this range (24.1‰ to 26.6‰). Stable isotopic analysis of NO_3^- does not appear to be a universal tracer of WWTP effluent in most rivers, perhaps because N sources and cycling processes are isotopically similar between rivers and effluents. However, stable isotopes of NO_3^- could be useful in some cases, depending on upstream NO_3^- sources and N cycling processes within the WWTP.

N_2O isotopic values can be distinct between river and effluent. Riverine N_2O upstream of WWTP B had higher $\delta^{18}O\text{-}N_2O$ values than effluent samples (Figure 4.3). River samples were also generally higher in $\delta^{15}N\text{- }N_2O$; the exception was WWTP A in summer. Two previous studies have characterized N_2O isotopic values in rivers. In both cases, $\delta^{18}O\text{-}N_2O$ was high (Bang Nara River, Thailand (Boontanon et al. 2000): $\delta^{18}O$: 36.6‰ to 63.8‰; Tama River, Japan (Toyoda et al. 2009): 17‰ to 53‰, with the low values found immediately downstream of a nitrifying WWTP). High $\delta^{18}O\text{-}N_2O$ values (> 30‰) in rivers are likely produced from denitrification and/or N_2O consumption (Snider et al. 2009), which is expected to dominate riverine N_2O production (Beaulieu et al. 2011, Rosamond et al. 2012). Townsend-Small et al. (Townsend-Small et al. 2011) have recently reported high $\delta^{18}O\text{-}N_2O$ values from a denitrifying WWTP (Figure 4.3). Therefore, $\delta^{15}N\text{-}N_2O$ and $\delta^{18}O\text{-}N_2O$ can be useful tracers of WWTP effluent, particularly from WWTPs that do not denitrify.

Riverine CH_4 collected upstream of WWTP B had lower $\delta^{13}C\text{-}CH_4$ values (-54.5‰ to -51.3‰) than effluent from all three WWTPs studied here, with the exception of one effluent sample (Figure 4.4). Our riverine samples are within the range (-58‰ to -36‰) reported in North American freshwater estuaries (Sansone et al. 1999). $\delta^{13}C\text{-}CH_4$ values generally increase as oxidation within WWTPs increases (Figure 4.4). Currently, there are no published $\delta^{13}C\text{-}CH_4$ values from denitrifying WWTPs, but they likely produce low $\delta^{13}C\text{-}CH_4$ values as oxidation potential is low. The small amount of data

available suggests that $\delta^{13}C\text{-}CH_4$ could be used as a tracer of effluent from non-denitrifying WWTPs. As with N_2O, CH_4 is a short-term effluent tracer, as it degasses downstream of effluent release, unless the receiving body is undersaturated. During degassing, N_2O and CH_4 approach isotopic equilibrium with the atmosphere. The distance downstream over which these gases retain isotopic values distinct from equilibrium depends on initial concentration and stable isotopic value, and the gas exchange coefficient.

Table 4.1: Concentrations, fluxes and stable isotopic values of NO_3^-, NH_4^+, N_2O and CH_4 from various WWTP types and from rivers. NN = no nitrification, PN = partial nitrification, FN = full nitrification, D = denitrification.

WWTP Type	N_2O emission from plant (g /capita/yr)	N_2O emissions from effluent (g /capita/yr)	CH_4 emission from plant (g /capita/yr)	CH_4 emissions from effluent (g /capita/yr)	$\delta^{15}N\text{-}NH_4^+$	$\delta^{15}N\text{-}NO_3^-$	$\delta^{15}N\text{-}N_2O$	$\delta^{18}O\text{-}N_2O$	$\delta^{13}C\text{-}CH_4$	Reference
2°, NN[1] (A)		2.0		1.1	2.9 to 7.8	4.2	-11.1 to 5.5	11.4 to 23.5	-52.8 to -42.1	This Study
2°, NN					6.5 to 14.7					(Sebilo et al. 2006)
2°, PN[2] (B)		1.1		0.7	10.5 to 16.0	7.6 to 26.6	-24.1 to -13.9	18.1 to 22.0	-47.4 to -35.8	This Study
2°, PN					13.6	5.6				(Kuuppo et al. 2006)
2°, PN	23 to 28									(Ahn et al. 2010) (Tallec et al. 2006)
2°, PN	5 to 26									(Ahn et al. 2010)
2°, processes not specified	3.2		39							(Czepiel et al. 1993, Czepiel et al. 1995)

3°, FN[3]					4 to 7				(Anisfeld et al. 2007)
3°, FN (C)		1.8		0.03	6.0 to 11.5	-27.3 to 0.0	9.8 to 28.7	-34.1 to -30.1	This Study
3°, FN (settling tank)	0.1	0.2	0.3	0.1	8.1	-4.4	49.8		(Toyoda et al. 2011)
3° , FN	13 to 97								(Ahn et al. 2010)
3° , FN	1.8								(Ahn et al. 2010)
2°, D[4]	0.43 to 1.89								(Kimochi et al. 1998)
2°, D	18.2								(Tallec et al. 2006)
3°, D					10 to 15				(Anisfeld et al. 2007)
3°, D	5.8 to 1580								(Itokawa et al. 1996)
3°, D					38				(Savage and Elmgren 2004)
3°, D					14 to 18				(Anisfeld et al. 2007)

3°, D	75.8		-42.1 to 7.9	19.9 to 51.0	(Townsend-Small et al. 2011)
3° , D	0.28 to 1.2				(Ahn et al. 2010)
3° , D	9.8 to 33				(Ahn et al. 2010)
3° , D	33 to 92				(Ahn et al. 2010)
3° , D	6.8				(Ahn et al. 2010)
3° , D	5.4				(Ahn et al. 2010)
3° , D	140				(Ahn et al. 2010)
3° , D	4.1				(Ahn et al. 2010)
Naugatuck and Quinnipiac R, Conn			4 to 12.5		(Anisfeld et al. 2007)
River Neva outflow, Russia			1 to 4		(Kuuppo et al. 2006)
Seine R. - upstream of WWTP		11	7 to 8		(Sebilo et al. 2006)

Seine R. - downstream of WWTP	15 to 30		(Sebilo et al. 2006)
Mississippi R., Missouri R., Ohio R., Yazoo R.		-1.4 to 12.3	(Chang et al. 2002)
Seventh order river, Ontario – upstream of WWTP B		6.5	This Study

[1]NN = no nitrification.

[2]PN = partial nitrification.

[3]FN = full nitrification.

[4]D = denitrification

Table 4.2: Properties of the three WWTPs studied and their influent and effluent quality. Top values are for summer months (April - October), bottom for winter (November - March). All data from WWTP annual reports (2006).

				Influent			Effluent			
	Population served	Average effluent flow ($m^3\ d^{-1}$)	Maximum effluent flow ($m^3\ d^{-1}$)	cBOD5[1] (mg/L)	NH_4^+-N (mg/L)	TKN[2] (mg/L)	cBOD5 (mg/L)	NH_4^+-N (mg/L)	NO_3^--N (mg/L)	TKN (mg/L)
WWTP A	284683	66181	103000	136	25.8	38.8	7	24.1	0.9	28.0
				(195)	(38.4)	(49.6)	(20)	(38.7)	(20.7)	(42.4)
				141	24.3	38.8	7	19.2	1.9	22.1
				(200)	(35.7)	(50.3)	(14)	(31.4)	(31.8)	(35.4)
WWTP B	167658	40782	61742	192	31.3	48.2	4	5.7	5.2	8.2
				(290)	(39.6)	(60)	(6)	(17)	(17.4)	(17.1)
				158	25.3	47.2	4	3.3	18.3	5.7
				(250)	(36.3)	(71.1)	(6)	(8.8)	(25.6)	(10.4)
WWTP C	118443	55928	81809	141	17.1	25.3	2	0.3	20.2	1.4
				(149)	(18.9)	(29.1)	(2)	(0.37)	(21.0)	(2.9)
				146	15.9	28.1	2	0.4	20.3	1.5
				(147)	(17.4)	(30.3)	(2)	(0.54)	(21.7)	(2.5)

[1]CBOD = Five-day carbonaceous biological oxygen demand (American Public Health Association 1995).

[2]TKN = Total Kjendahl Nitrogen ($NH_4^+ + NH_3$ + organic N)

Table 4.3: Calculated isotopic fractionation (ε) for nitrification and denitrification in summer and winter effluent at three WWTPs. Mean values per season are shown with standard deviation in brackets. N/d: no data.

			Nitrification ($NH_4^+ \rightarrow N_2O$)		Denitrification ($NO_3^- \rightarrow N_2O$)	
		$\delta^{15}N$-N_2O	$\delta^{15}N$-NH_4^+	$\varepsilon^{15}N$	$\delta^{15}N$-NO_3^-	$\varepsilon^{15}N$
WWTP A (non-nitrifying)	Summer	4.4 (1.1)	6.4 (1.6)	2.0 (0.7)	n/d[1]	n/d
	Winter	-6.8 (4.8)	3.8 (0.5)	10.6 (7.6)	4.2 (0.02)	10.9 (7.7)
WWTP B (partially nitrifying)	Summer	-16.0 (1.7)	15.2 (1.4)	30.8 (4.3)	25.3 (1.2)	40.3 (4.7)
	Winter	-21.6 (2.9)	11.5 (1.0)	32.7 (5.2)	8.9 (1.5)	30.2 (6.6)
WWTP C (fully nitrifying	Summer	-9.6 (5.9)	n/d	n/d	7.2 (1.1)	16.7 (10.5)
	Winter	-21.5 (4.0)	n/d	n/d	8.2 (0.4)	29.5 (5.7)

[1]No data.

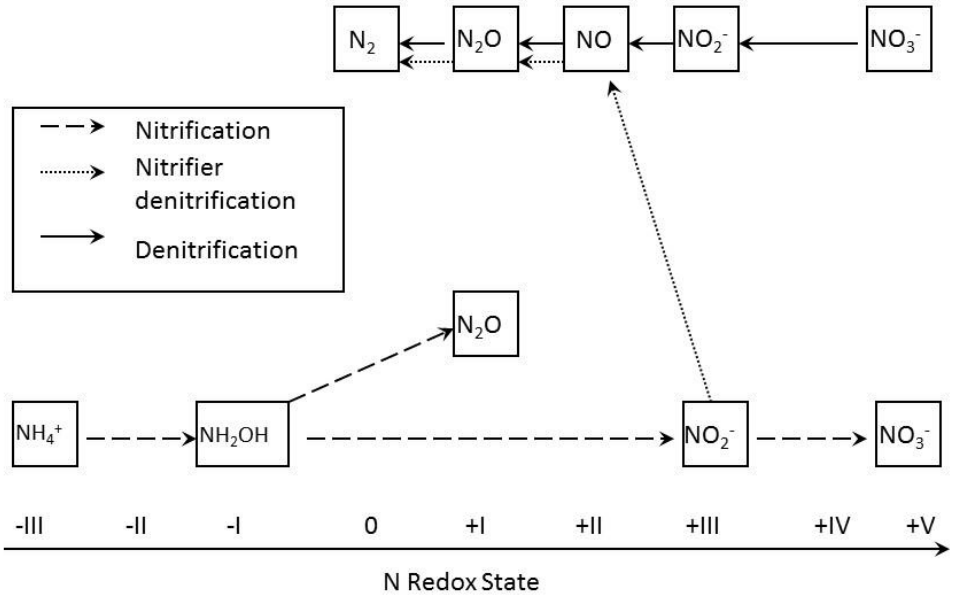

Figure 4.1: Pathways in the nitrogen cycle involving N_2O. Nitrification (NH_4^+ oxidation to NO_2^- and ultimately to NO_3^-), denitrification (NO_3^- reduction to N_2O and N_2), hydroxylamine oxidation and nitrifier-denitrification (reduction of NO_2^- by nitrifiers) are shown.

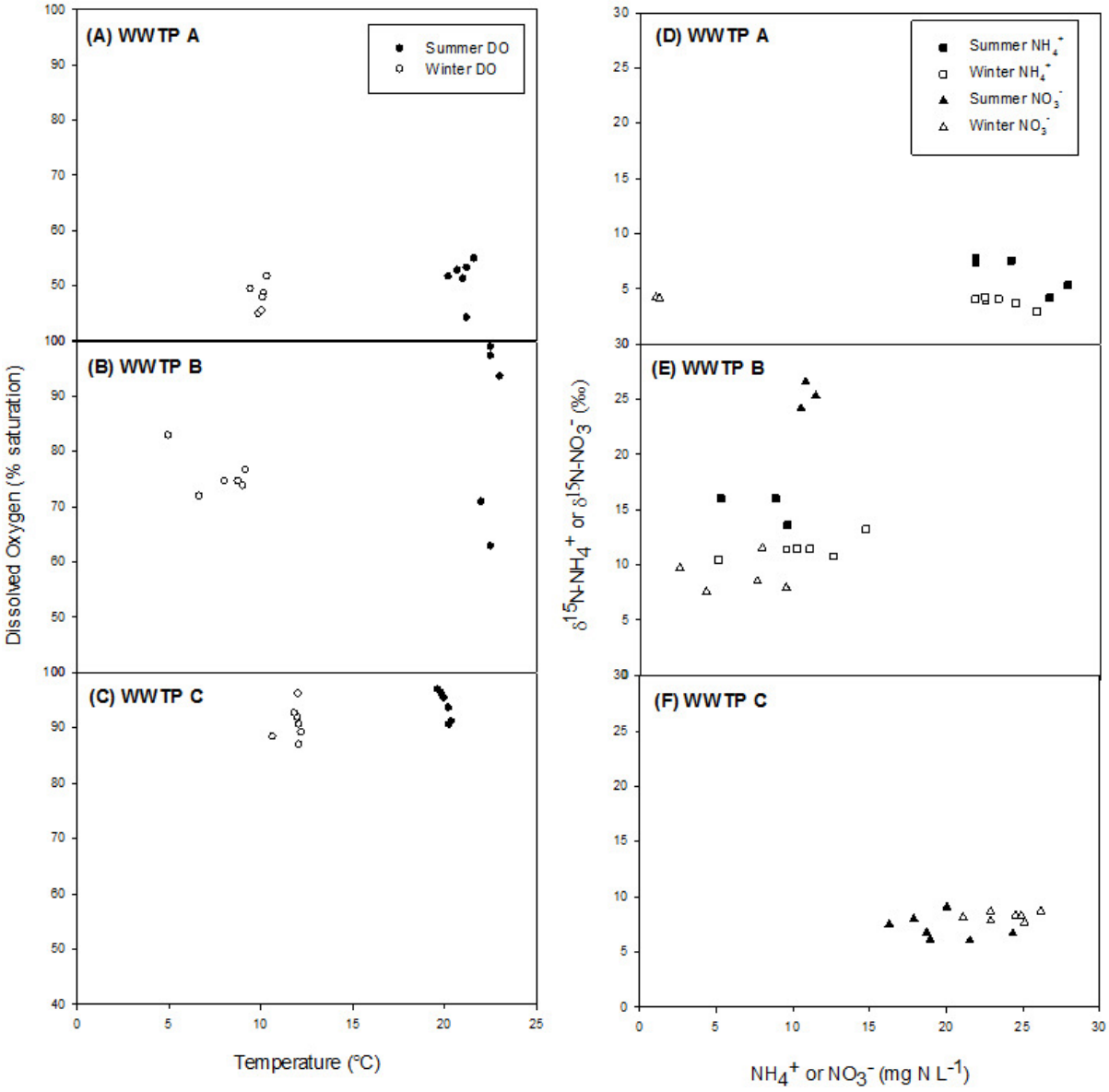
(A) WWTP A
Summer DO
Winter DO
(B) WWTP B
(C) WWTP C
Dissolved Oxygen (% saturation)
Temperature (°C)
(D) WWTP A
Summer NH4+
Winter NH4+
Summer NO3-
Winter NO3-
(E) WWTP B
(F) WWTP C
δ15N-NH4+ or δ15N-NO3- (‰)
NH4+ or NO3- (mg N L-1)

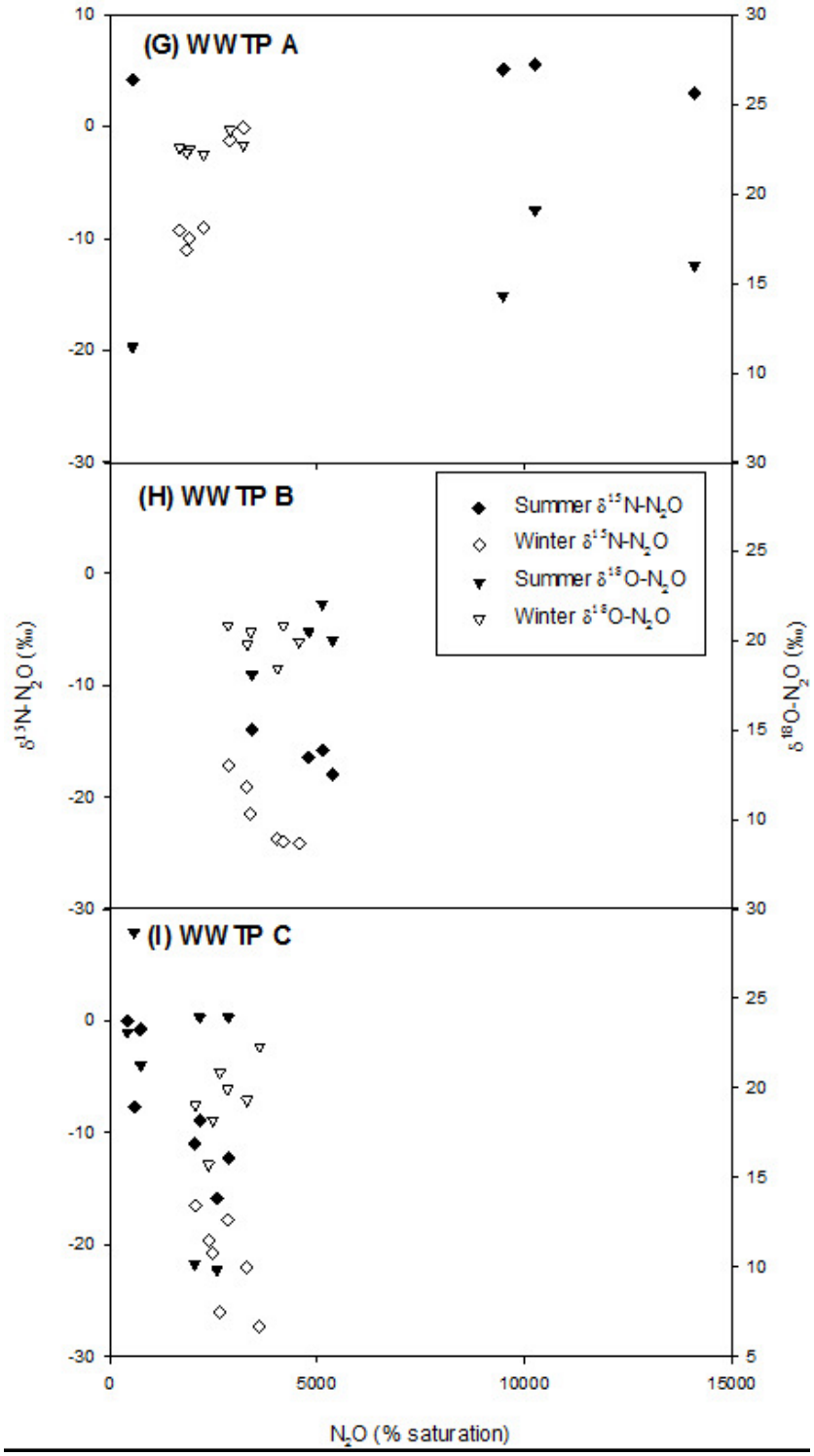

Figure 4.2: Chemistry of dissolved species at the three WWTPs. Temperature and DO are shown for WWTPs A (panel A), B (panel B) and C (panel C). WWTP A has high NH_4^+ and low

NO_3^- concentrations (panel D), WWTP B has both NH_4^+ and NO_3^- (panel E), and WWTP C has high NO_3^- and low NH_4^+ (panel F). Concentrations of NH_4^+ at WWTP C (0.03 mg N/L to 0.12 mg-N/L), and NO3- at WWTPs A (0.01 mg-N/L to 0.22 mg N/L) too low for isotopic analysis are not shown. Error is smaller than data point size. N_2O concentrations were highest at WWTP A (panel G), moderate at WWTP B (panel H) and lowest at WWTP C (panel I).

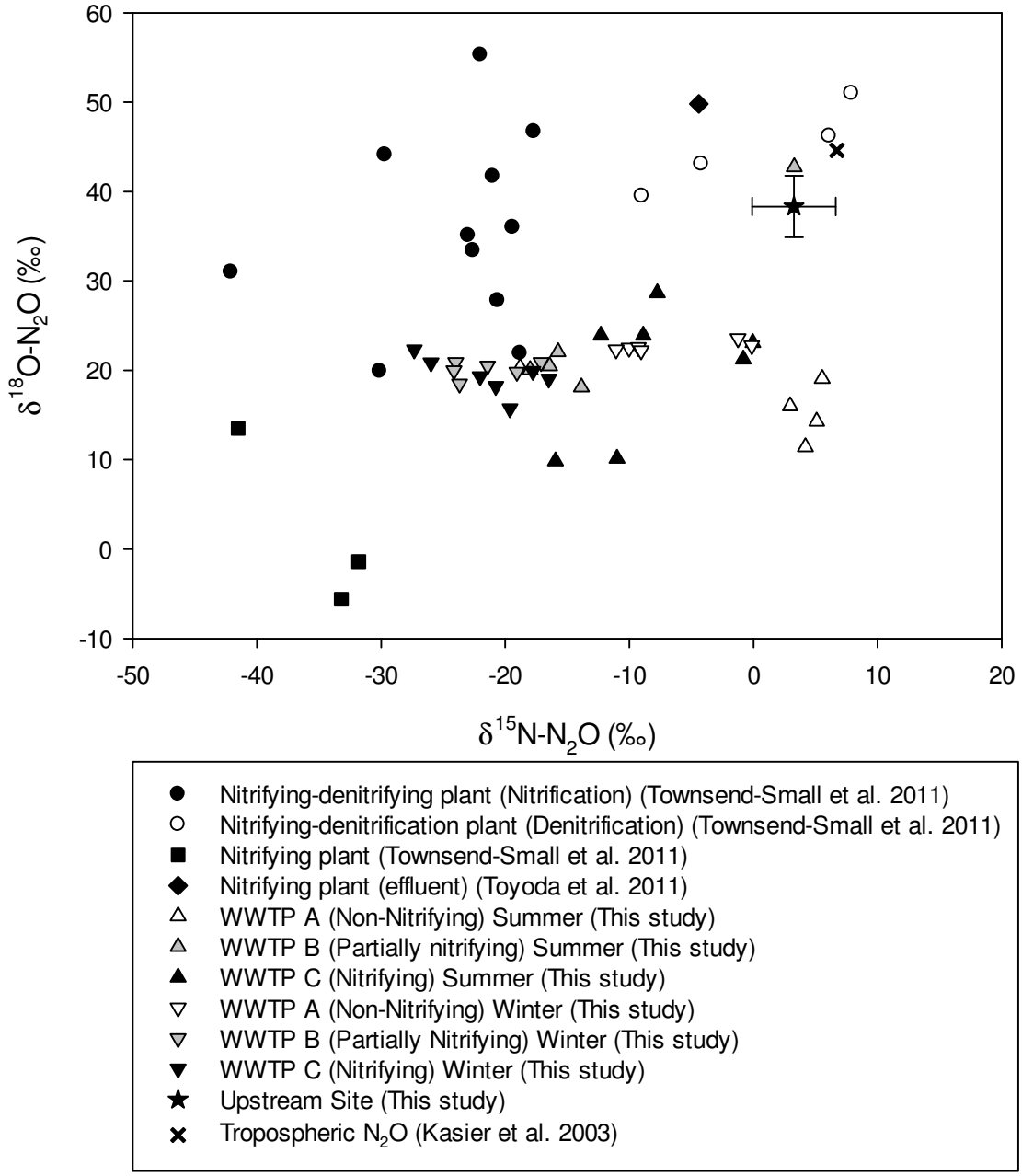

Figure 4.3: N_2O isotope cross plot showing N_2O from effluents and from WWTPs. Data from non-nitrifying WWTPs are in white, partially-nitrifying WWTPs in grey, nitrifying WWTPs in black and denitrifying WWTPs in white. The average value for tropospheric N_2O is shown with a black x (Kaiser et al. 2003). For this study, summer samples have upwards-pointing triangles and winter samples have downwards-pointing triangles. The average value for dissolved N_2O at a site upstream of WWTP B (Site 9) is shown with a star, plus or minus one standard deviation.

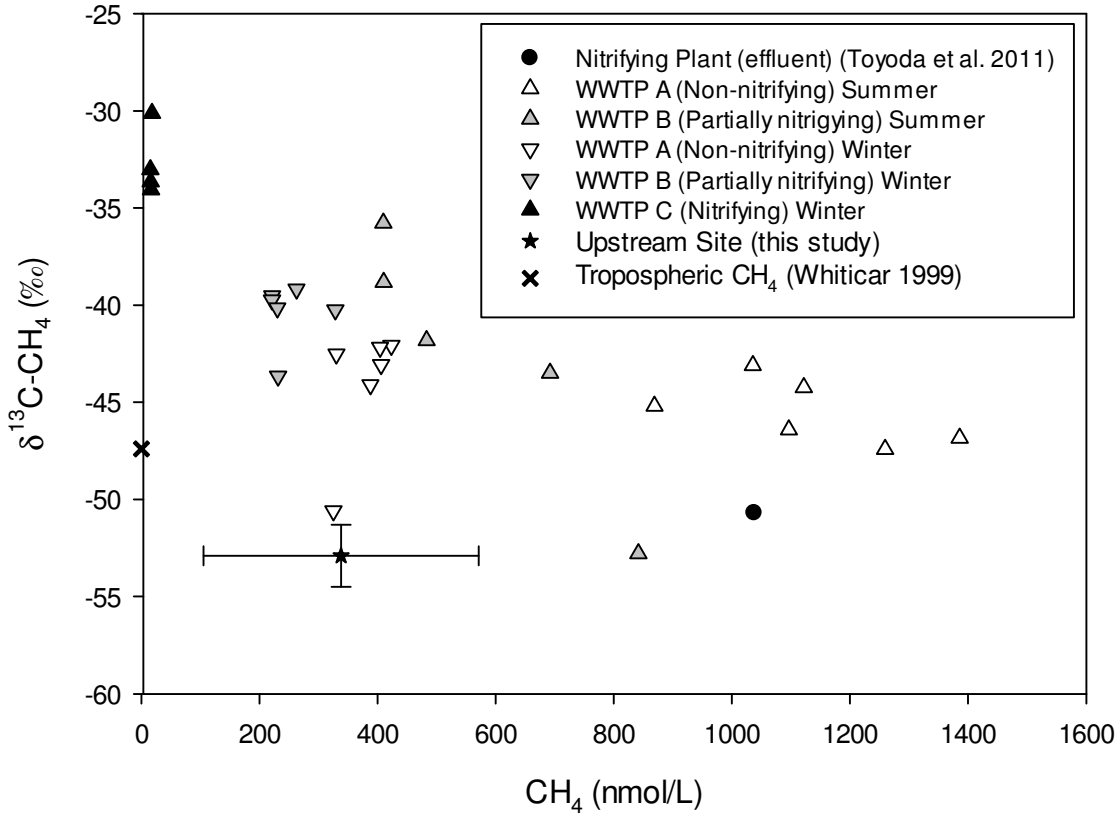

Figure 4.4: CH_4 concentration and isotopes in WWTPs and effluent. Upward pointing triangles represent summer samples and downward pointing triangles represent winter samples. N_2O from WWTP A (white triangles), WWTP B (grey triangles) and WWTP C (black triangles) are shown. The black star represents the average of 17 samples collected at a site upstream of WWTP A; error bars represent standard deviation. Tropospheric CH_4 is represented by the black x (Whiticar 1999).

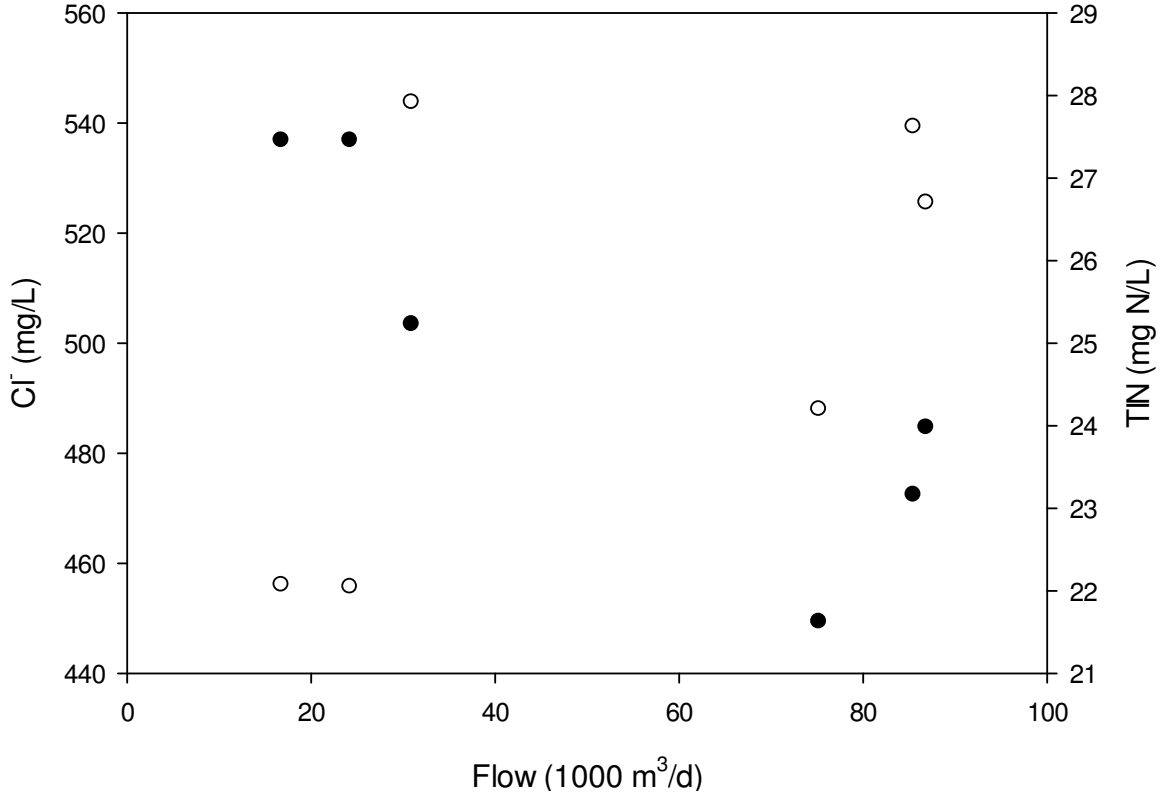

Figure 4.5: Discharge at WWTP B in summer versus Cl^- (black circles) and TIN (white circles). Discharge values are approximated from daily WWTP flow data (Grand River Conservation Authority, unpublished data).

Chapter 5: Stable isotopic fractionations of N_2O produced via denitrification in Grand River sediment

Abstract

Stable isotopic ratios of N_2O ($\delta^{15}N$, $\delta^{18}O$) may help determine microbial production pathways and/or the fraction N_2O produced per mole final product in complex natural systems. While N_2O from nitrification and denitrification typically have distinct stable isotopic values in soils and the ocean, overlap exists, particularly in $\delta^{18}O$. Variation and overlap can be caused by changes in microbial community, changing isotopic values of substrate (NH_4^+, NO_3^-), N_2O consumption, and exchange of O atoms between N species (NO_2^-, NO) and H_2O during denitrification. While the isotopic fractionation of N_2O produced during denitrification has been well studied in soils, no work has been published on river sediment, even though impacted rivers produce a significant portion of global anthropogenic N_2O and microbial communities could be quite distinct from soils. Therefore, laboratory incubations were conducted to measure the isotopic fractionation of N_2O production via denitrification on sediment from the Grand River, southern Ontario, Canada. Sediment was collected from two sites, upstream and downstream of urban wastewater treatment plant (WWTP) discharge, in spring, summer and fall 2009. Each sediment sample was subjected to a high NO_3^- addition (1300 mg N/L) and a lower NO_3^- addition (775 mg N/L). Water with high $\delta^{18}O$ values was also added to quantify O exchange with water. Isotopic fractionation values were similar to previous soil studies and had a large range. Surprisingly, N_2O production rates were 10 times higher when NO_3^- concentration less than doubled. No seasonal or site-based patterns in isotopic fractionation were significant. However, isotopic fractionations for ^{15}N and ^{18}O were positively correlated to each other and negatively correlated to N_2O production rate. Although N_2 concentration was not quantified, this suggests that low N_2O production rates were caused not by low total denitrification rate, but by N_2O consumption to N_2, resulting in isotopic enrichment of residual N_2O. Changes in N_2O production rate and isotopic fractionations over 4 hour incubations suggest that N_2O:(N_2O+N_2) ratios did not achieve steady state immediately, likely due to NO_2^- limitation of N_2O reductase and/or a lag in N_2O reductase activity relative to other enzymes in the denitrification pathway. O exchange with water did not show any trend with N_2O production rate, suggesting that O exchange does not occur during N_2O reduction to N_2 in these incubations. ^{15}N isotopic fractionation values in incubations were similar to those estimated from field data except for night-time samples from the sewage-impacted site. Isotopic fractionation estimated with field data may not be accurate due to differences between isotopic values of water column and sediment NO_3^-, upstream effects and differences between field and laboratory

microbial community and NO_3^- availability. These experiments show that quantifying stable isotopic ratios of N_2O in denitrification incubations is helpful in determining changes to the N_2O:N_2 ratio due to changes in N_2O reductase activity without quantifying N_2 concentrations.

5.1 Introduction

5.1.1 Use of Stable Isotopes for Determining N_2O Production Processes

Nitrous oxide (N_2O) is a greenhouse gas produced by two microbial pathways: nitrification (oxidation of ammonia to nitrate) and denitrification (reduction of nitrate to nitrous oxide and finally N_2). N_2O also appears to be produced in low quantities (< 2% of N_2 produced) as a detoxification pathway by anammox bacteria although the mechanism is not known (Kampschreur et al. 2008, Kartal et al. 2007). Anammox bacteria tend to be outcompeted by denitrifying bacteria when NO_3^- and organic C concentrations are high (Kartal 2008) and therefore will be ignored in this study.

Because N_2O is a greenhouse gas, there is significant interest in understanding production pathways of N_2O. This is aided by the different conditions necessary for the two main production pathways. Nitrification requires oxic to suboxic conditions and denitrification requires hypoxic or anoxic conditions. Previous work on pure microbial cultures and in soil microbial communities has shown that the stable isotopic fractionation (ε) of N_2O production ($\varepsilon\,^{15}N$, $\varepsilon\,^{18}O$) are quite different for nitrification ($\varepsilon\,^{15}N$: -55‰ to -15‰, $\delta^{18}O$: 20‰ to 30‰) and denitrification ($\varepsilon\,^{15}N$: -39‰ to -10‰, $\varepsilon\,^{18}O$: -42‰ to 43‰) (Snider 2011). This is a large range with overlap in ε values. ε values have not been quantified in river sediments, which could include much different microbial communities than soil. Pure culture studies have shown significant differences in ε within and between microbial species (Snider 2011).

N_2O from nitrification can be difficult to measure because (a) sufficient quantities for stable isotopic analysis can be difficult to capture because of low N_2O:NO_3^- production rates (Snider et al. 2012), and (b) it can be difficult to eliminate anoxic microsites in soils and sediments and therefore difficult to eliminate N_2O production by denitrification (including nitrifier-denitrification). The first problem can be circumvented by long incubation times in nitrification incubations (Snider et al. 2012) but O_2 can be depleted when respiration rates are high; flushing incubation bottles replenishes O_2 but also removes N_2O. The second problem is usually approached by running parallel incubations; in one, both nitrification and denitrification may occur. In the other, acetylene (C_2H_2) is added, which inhibits nitrifier N_2O production but not denitrifier N_2O production (Ryden et al. 1979). However, C_2H_2 addition does not block N_2O produced by heterotrophic nitrifiers (de Boer and Kowalchuk 2001) and

underestimates N_2O production from denitrification by promoting NO loss to NO_2 (which is not a denitrification product and not measured) (Bollman and Conrad 1997).

For these reasons, stable isotopic fractionations for denitrification only are examined in this study. In contrast to nitrification, denitrification typically produces higher N_2O:(N_2O:N_2) ratios than N_2O:NO_3^- ratios observed for nitrification (Klemedtsson et al. 1988) and incubations can easily be kept anoxic by adding a small amount of sediment, river water and nitrate substrate to a bottle with a large helium headspace.

Microbial community composition, and perhaps stable isotopic fractionation, could change with site and season because community composition depends on temperature, nutrient levels and other factors. N_2O production in the Grand River is low during the winter months (Chapter 6). Therefore, the stable isotopic signature of N_2O produced by denitrification was examined using river sediments from two sites collected in May, July and October 2009.

5.1.2 N_2O Production in Bacterial Cells and Stable Isotopic Fractionations

Stable isotopic fractionation of N_2O from the denitrification pathway is defined as:

$$\varepsilon = (R_{N2O}/R_{NO3^-} - 1) \qquad \textbf{Equation 5.1}$$

where R is the ratio of $^{15}N/^{14}N$ for $\varepsilon^{15}N$ or $^{18}O/^{16}O$ for $\varepsilon\,^{18}O$.

However, this equation simplifies the denitrification process, which occurs stepwise ($NO_3^- \rightarrow NO_2^- \rightarrow NO \rightarrow N_2O \rightarrow N_2$, Figure 5.1). Each step requires one enzyme, and is a potential site for stable isotope fractionation. Denitrification occurs in many types of organisms (bacteria, archaea and fungi) but the pathway is best understood in gram-negative bacteria. It is unclear if fractionation upon uptake of NO_3^- into cells occurs. NO_3^- uptake from the environment into the periplasm appears to require porins, which are passive transporters. Mutant bacteria with few or no porins take up NO_3^- slowly (Song and Niederweis 2012, Yoon et al. 2002) and have no Nir activity (Yoon et al. 2002) but the specific porins required and mechanism are not known. It is not known if porins impart any isotopic fractionation during transport. Once in the periplasm, NO_3^- is transported to the cytoplasm across the inner membrane (Figure 5.1), where NO_3^- reduction occurs. Transportation requires two proteins, NarK1 and NarK2; the first is a symporter using secondary active transport requiring an electrochemical gradient (i.e. an electrochemical gradient created by pumping H^+ across the membrane) (Wood et al. 2002). It is not known if the symporter imparts an isotopic fractionation. In the cytoplasm, NO_3^- is reduced to NO_2^- with a nitrate reductase (Nar) enzyme. NO_2^- is then transported back into the periplasm, and the rest of the denitrification chain occurs here (Figure 5.1).

Note that uncharged gases (NO, N_2O, N_2) can freely diffuse through either cell membrane. The isotopic effect of diffusion of gases through a membrane in water is likely less than through air (e.g. $\varepsilon^{15}N = 3.2‰$ and $\varepsilon^{18}O = 6.5‰$ for N_2O at steady state) due to interactions between polar water molecules and gases (Zeebe and Wolf-Gladrow 2001).

Alternatively, denitrifiers can take up NO_2^- from the environment. NO_2^- may not require active transport from the cytoplasm into the periplasm if HNO_2 diffuses passively through the membrane (Moir and Wood 2001). NO_2^- uptake is much more rapid than any of the enzyme-mediated denitrification steps within the cell, suggesting that observed ε values are a result of enzyme-catalyzed reactions, not uptake (Bryan et al. 1983).

Several enzymes used in the denitrification process are activated and inhibited by high concentration of substrates (Table 5.1). Transcription of genes for and production of all denitrification enzymes (Nar, Nir, Nor, Nos) is regulated by the dissimilatory nitrate respiration regulator (DNR), which is activated when O_2 is low and NO_3^- or NO_2^- is present (Arai 2011). Nitric oxide reductase (Nor) appears to be inhibited by high NO_3^- (Firestone, Firestone, & Tiedje, 1980). N_2O reductase (Nos) inhibitors are the best studied because of the potential to reduce N_2O production from denitrification by full N_2O reduction to N_2 (Weier, Doran, Power, & Walters, 1993). Nos is inhibited by NO_3^-, but this effect is not strong at circumneutral pH (Firestone, Smith, Firestone, & Tiedje, 1979). Nos is also inhibited by low pH (Geywitzhetz et al. 1993) and high concentrations of sulfide and metals (Manconi et al. 2006). The enzyme is much more strongly inhibited by NO_2^- (Firestone et al. 1979), which can accumulate at redox boundaries. Additionally, while all other denitrification enzymes appear to be continually present in denitrifier cells, Nos is synthesized only during anoxic conditions when NO_3^- substrate is present (Firestone and Tiedje 1979). Therefore Nos activation lags behind other denitrification enzymes, especially when conditions change rapidly to promote denitrification (e.g. the onset of anoxia, the addition of NO_3^- substrate to anoxic incubations) (Firestone et al., 1980).

Isotopic fractionations for both ^{18}O and ^{15}N may occur at each enzyme in the denitrification pathway (Figure 5.1). Previous laboratory incubations of pure microbial cultures and soil cultures have measured non-zero ε values for the $NO_3^- \rightarrow N_2O$ pathway (see above) indicating that isotopic fractionation occurs at Nar, Nir and/or Nor. Laboratory studies have also quantified ε values for $N_2O \rightarrow N_2$ ($\varepsilon\ ^{15}N$: -27‰ to -1‰; $\varepsilon\ ^{18}O$ including any O exchange: -42‰ to -5‰, $\varepsilon\ ^{18}O$: $\varepsilon\ ^{15}N \sim 3$) (Snider et al. 2009), meaning that isotopic fractionation occurs on the Nos enzyme.

Individual $\varepsilon\ ^{18}O$ values for each enzyme values are labeled in Figure 5.1 (ε_1, ε_2 etc.); each enzyme may also impart an isotopic fractionation for ^{15}N (not shown for clarity). The net isotopic

fractionation for ^{18}O ($\varepsilon_{net}{}^{18}O$) is the sum of ε_1 through ε_4. Measuring $\varepsilon^{18}O$ is somewhat complicated by the recent discovery of oxygen exchange between water and N intermediate species (most likely NO_2^- and NO) (Kool et al. 2007, Kool et al. 2009, Snider et al. 2013); O exchange can overprint $\varepsilon_{net}{}^{18}O$ values unless incubations are performed with water sources with distinct $\delta^{18}O$-H_2O values. It is unclear if oxygen exchange imparts any isotopic fractionation (Snider et al. 2013); this is labeled ε_{H2O} on Figure 5.1.

5.1.3 Effects of N_2O:N_2 on Isotopic fractionations

The amount of Nos activity relative to total denitrification can be quantified in the ratio of N_2O and N_2 produced by cells. If all NO_3^- denitrified is converted to N_2, N_2O:N_2 is zero and Nos activity is 100%. N_2O:N_2 has been measured in soil and culture incubations and ranges widely, from 0.02 to 5 (Senbayram et al. 2012, Silvennoinen et al. 2008, Silvennoinen et al. 2008, Weier et al. 1993). Higher ratios are typically seen with high NO_3^- addition (Senbayram et al. 2012) but the opposite has also been found (Weier et al. 1993). Boreal river and estuary sediments at ambient (low) NO_3^- concentrations had low N_2O:N_2 ratios (< 0.04) (Silvennoinen et al. 2008, Silvennoinen et al. 2008). Lower N_2O:N_2 ratios indicate more Nos activity. This should increase the $\delta^{15}N$-N_2O and $\delta^{18}O$-N_2O values as Nos imparts isotopic fractionation (resulting in lower $\delta^{15}N$ values in N_2). Since Nos can be inhibited by substrates (NO_3^-, NO_2^-), high-NO_3^- additions can be used in incubations to produce large amounts of N_2O (simplifying stable isotope analysis) and to assess isotopic fractionation when Nos activity is low.

5.1.4 O Isotope exchange between Water and Nitrite in Denitrification

Previous work has shown that measured net $\varepsilon^{18}O$ values can be significantly influenced by O exchange between water and intermediate N compounds during denitrification (Figure 5.1). This is because (a) O atoms in water exchange with O in some intermediate N compounds (likely NO_2^- and/or NO) either abiotically (inside or outside a cell) or during attachment to enzymes in the cell, and (b) O isotopes in natural water typically have much lower stable isotopic ratios (~ -10‰ in the Grand River) than N species in the denitrification chain. Rates of abiotic O exchange between NO_2^- and water are fast, especially at Cl^- concentration (Kool et al. 2007) and high NO_2^- concentration and low pH (Casciotti et al. 2007). Biological O exchange occurs during reduction of NO_2^- to NO because the reaction is reversible and O exchange has been noted in denitrifiers reducing NO to N_2O (Kool et al. 2007). Direct evidence of O exchange during NO_3^- reduction to NO_2^- is lacking, though O exchange has been observed at some point along the reduction path between NO_3^- and N_2O (Kool et al. 2007).

The fraction of O in N_2O coming from water (henceforth termed "fraction O exchange") must be quantified in order to understand the $\varepsilon_{net}{}^{18}O$ for any system. Snider et al. (2009) devised a method to determine the fraction O exchange in soil incubations by adding ^{18}O-enriched water. They found 65% to 91% O exchange in temperate upland and wetland soils. High values for fraction O exchange could artificially decrease the calculated value of $\varepsilon_{net}{}^{18}O$, especially if some O exchange occurs after some isotopic fractionation (e.g. ε_1, ε_2), erasing it partially or totally. For this reason, a negative linear relationship ($r^2 > 0.9$) was found between O exchange and $\varepsilon_{net}{}^{18}O$ (Snider et al. 2009).

5.2 Methods

5.2.1 Sediment Collection and Processing

Sediment was collected from two sites on the Grand River, southern Ontario, Canada (Figure 5.2) in spring, summer and autumn 2009. The Grand River watershed is the largest Canadian watershed draining into Lake Erie, has a high and rapidly growing population, and is heavily modified by human activities. Eighty percent of the watershed land is under agricultural use, and significant nutrient loads enter via wastewater treatment plants (WWTPs) from the cities of Waterloo, Kitchener and Cambridge, in the middle section of the river (Cooke 2006). The river has impaired water quality and ecological function because of its high population and nutrient discharge from agriculture and WWTPs. Water quality varies greatly longitudinally; thus, two sites with very different water quality were chosen for sediment collection. The river is well buffered by carbonate minerals, and pH ranges from 7.3 to 9.0 (n = 1538, data from 23 sites on the river in all seasons).

The first site, Bridgeport (Site 9), is located immediately upstream of the urban area and receives water from primarily agricultural areas. Here, NO_3^- is higher in winter (October to April: 3.5 ± 1.8 mg N/L (mean± standard deviation), n = 99) and lower in summer (May to September: 1.8 ± 1.0, n = 177). Because of in-river photosynthesis, dissolved oxygen (DO) in summer has a moderate diel cycle, but DO is always higher than 4 mg/L.

In contrast, Blair (Site 11) is located 5 km downstream of the largest WWTP in the watershed. It receives significant dissolved organic carbon, NH_4^+, NO_3^-, and phosphorus from effluent. Macrophyte biomass is very large in summer, resulting in very large diel DO cycles; DO can drop below 1 mg/L at night when photosynthesis ceases (Rosamond et al. 2011). N_2O in summer is always much above saturation but, when hypoxia occurs, can increase to more than 9000% saturation (Rosamond et al. 2011). NO_3^- concentrations are moderate year-round (3.0 ± 1.3 mg N/L, n = 247).

River sediments were collected from both sites to a depth of 10 centimeters, in order to capture the oxic and anoxic sediment zones. At the same time, river water was collected from each site, and kept refrigerated until needed. Water from each site was subsampled for NO_3^- and NH_4^+ analysis.

Sediments were returned to the laboratory and were sieved to 2 mm using a brass soil sieve to remove large pebbles.

5.2.2 Physical and Geochemical Characterization of Sediments and River Water

Sediment sub-samples were weighed wet and oven-dried to measure sediment saturation capacity. Sediment organic matter was quantified by loss on ignition (LOI) at 550º C for four hours.

NH_4^+ and NO_3^- concentrations were analysed in (a) river water collected at the same time as sediment, (b) water stored with saturated sediment (a mix of pore water and river water) and (c) sorbed to sediment. NO_3^- was extracted from sediments with deionized (DI) water and NH_4^+ was extracted with 2M potassium chloride (KCl). NH_4^+ was analyzed by UV colorimetry and NO_3^- by ion chromatography in all instances. All water samples were filtered before analysis. Precision was 0.005 mg N/L for NH_4^+ and 0.07 mg N/L for NO_3^- analysis.

At the completion of each experiment, incubation water was filtered for $\delta^{18}O\text{-}H_2O$. $\delta^{18}O\text{–}H_2O$ was analyzed as described in section 5.4.3.

5.2.3 Preparation and Measurement of $\delta^{18}O\text{-}H_2O$ in Incubations

In each experiment, DI water was added to saturated sediment to (a) prevent desiccation, (b) facilitate full mixing of sediment on the orbital shaker by decreasing viscosity, and (c) allow for the addition of ^{18}O-enriched water to quantify O exchange between H_2O and N compounds during denitrification.

^{18}O-enriched water was prepared by diluting 1.6 atom% water (Bio-Rad Laboratories, Hercules, CA) with Nanopure DI water ($\delta^{18}O$: ~ -10.8‰) to between ~20‰ and ~120‰. Due to limited supply, later incubations were less ^{18}O-enriched.

Because sediments were already saturated with river water, $\delta^{18}O\text{-}H_2O$ from each incubation was analyzed via a modified CO_2 equilibrium method on a GV Instruments isotope ratio mass spectrometer. Precision was 0.2‰.

5.2.4 Incubation Set-Up and Design

Laboratory incubations were designed to test the effects of site (Bridgeport and Blair), season (spring, summer and fall) and NO_3^- level (high and lower) on isotopic fractionations of N_2O production via denitrification in sediments. This resulted in 6 incubations per site, labeled BR-A

through BR-F for Bridgeport and BL-A through BL-F for Blair (Table 5.2). Each incubation included six jars per site: duplicates of three $\delta^{18}O$-H_2O values (ambient, medium and high). High- and low-NO_3^- additions from the same season were conducted on the same batch of sediment, within a period of one or two days to prevent drastic changes in microbial community structure. Sediment was refrigerated wet between incubations.

Incubation chambers consisted of 500 mL borosilicate jars (Wheaton GL 45, Wheaton Science Products Inc., Millville, N.J.). Jars were capped with halo-butyl rubber, 43 mm, 2-leg lycophilization stoppers (Wheaton Science Products Inc., Millville, N.J.). A 43 mm silicon septum (Chromatographic Specialties, Brockville, ON) was added on top, and both were secured using an open-topped screw cap (Wheaton Science Products Inc., Millville, N.J.). Snider et al. (Snider et al. 2009) previously determined that this set-up is gas-tight and that none of the materials produced N_2O. 50 g wet sediment was added to the chambers, with 20 mL of water, then stoppered and flushed with ultra-high purity helium (UHP He) for 10 minutes at ~600 mL/minute to establish anoxia. Jars were placed on an orbital shaker (200 rpm) in the dark for 10 to 12 hours before the start of the incubation such that sediments were continually suspended. The preincubation was designed to remove background NO_3^- and N_2O Present in the sediment. It also encouraged development of an anaerobic microbial community.

After preincubation, potassium nitrate (KNO_3) was added to each jar at 1.3 mg N/g-sed_{dw} (~1300 mg N/L pore water) and 0.8 mg N/g-sed_{dw} (~775 mg N/L pore water) levels. High concentrations were chosen in order to produce sufficient N_2O for isotopic analyses, after Snider (2011). The KNO_3 used has a $\delta^{15}N$ value of 13.8 ± 0.3‰ and a $\delta^{18}O$ value of 28.0 ± 0.8‰. Jars were recapped, purged with He and left on the orbital shaker for ~1 hour before analysis. To sample the jars, 60 mL UHP He was added to the headspace of each jar and 60 mL headspace removed and stored in evacuated (10^{-1} torr) 50 mL glass serum bottles (Wheaton Science Products Inc., Millville, N.J.) with pre-baked 20 mm butyl-blue rubber stoppers (Bellco Glass, Inc., Vineland, N.J.) and aluminum crimp seals (Chromatographic Specialties, Brockville, ON). This gas was later analyzed for N_2O concentration and isotopic ratios ($\delta^{15}N$ and $\delta^{18}O$). After each sampling event, jars were purged with UHP He for 10 minutes and returned to the shaker. This promoted mixing of NO_3^- and gases through the sediment and reduced the likelihood of significant N_2O consumption caused by local NO_3^- loss.

Denitrification incubations were sampled four times over 4 -5 hours to minimize NO_3^- pool reduction (and isotopic enrichment) and to avoid N_2O reduction. Flushing between sampling also avoided N_2O build-up and possible N_2O reduction.

5.2.5 N_2O Concentration and Isotopic Analysis

N_2O concentration was analyzed with an electron capture detector (ECD) on a Varian CP 3800 gas chromatograph (Varian Canada, Inc.) designed for greenhouse gas analysis. A calibration curve was created daily using commercial certified standards (0.1, 1.0, 10.0 and 100.0 ppm N_2O v/v; Matheson Tri-Gas, Inc.; Praxair Canada, Inc.) Detection limit (0.1 ppm) was much lower than any incubation samples. Precision (standard deviation of multiple standards) was 6% or less.

Stable isotopic ratios of N_2O ($\delta^{15}N$ and $\delta^{18}O$) were analyzed on a continuous flow-isotope mass spectrometer (CF-IRMS) in line with a TraceGas gas chromatograph pre-concentrator system (GV instruments, Thermo Electron Corp., Manchester, UK). Samples and working standards were injected through a septum port and CO_2 and H_2O were removed with chemical traps (magnesium perchlorate and Ascarite) and a Nafion membrane (Perma Pure LLC, Toms River, NJ). N_2O was concentrated by cyrofocusing in liquid N_2. It was then passed through a 30 m GC column to separate any remaining CO_2 and N_2O. N_2O was then introduced to the IRMS, where mass/charge ratios of 44 ($^{14}N^{14}N^{16}O$), 45 ($^{15}N^{14}N^{16}O$) and 46 ($^{14}N^{14}N^{18}O$) were compared to reference tanks of commercial N_2O (99.5 – 99.9% purity, Praxair Canada, Inc.).

$^{15}N/^{14}N$ and $^{18}O/^{16}O$ ratios in N_2O samples were reported in delta (δ) notation in parts per thousand (permil, ‰):

$$\delta = (R_{sample}/R_{standard} - 1) \qquad \textbf{Equation 5.2}$$

where R is the ratio of the heavy to light isotope (e.g. $^{15}N/^{14}N$). All data are reported relative to international standards AIR for ^{15}N and VSMOW for ^{18}O, unless otherwise stated.

Monitoring tanks and working standards ($\delta^{15}N$: 2.78‰; $\delta^{18}O$: 39.96‰) were calibrated against local tropospheric N_2O because there is no internationally recognized reference material for N_2O isotopic analysis. Tropospheric N_2O was assigned a value of $\delta^{15}N$ = 6.72‰ and $\delta^{18}O$ = 44.62‰ (Kaiser et al. 2003). Kaiser et al. (2003) found that tropospheric N_2O isotopic composition varied little in the northern hemisphere. Precisions (standard deviation of working standards) for $\delta^{15}N$-N_2O and $\delta^{18}O$-N_2O were typically 0.2‰ and 0.4‰ respectively. N and O isotopic ratios were corrected for rare isotopologues that contribute to mass 45 ($^{14}N^{14}N^{17}O$) and mass 46 ($^{15}N^{14}N^{17}O$ and $^{15}N^{15}N^{16}O$). Corrections were also applied for machine drift and the relationship between peak size and apparent isotope ratios.

5.2.6 Comparison to Field Data

Stable isotopic fractionation during N_2O production from denitrification in the field was estimated by analyzing dissolved NO_3^- and N_2O from the river for concentration and stable isotopic ratios of N and O.

Water samples were collected approximately every 1.5 hours over a 28-hour period in June 2007 at Bridgeport and Blair (Figure 5.2). Water was collected for NO_3^- concentration and stable isotopic analysis in 125 mL and 1 HDPE bottles respectively. Samples were kept cold and filtered to 0.45 µm upon returning to the laboratory. Water for N_2O concentration analysis was collected in 50 mL glass serum bottles, capped with pre-baked red rubber stoppers (BD Vacutainer, Franklin Lakes, NJ). N_2O isotope samples were collected in 500 mL borosilicate jars capped with black rubber lycophilization stoppers, described above. Both bottle types were capped underwater with a needle to eliminate gas bubbles. N_2O samples were preserved with 2 mL saturated mercuric chloride ($HgCl_2$) solution per litre water.

NO_3^- and N_2O concentrations and N_2O isotopic ratios were measured as above. NO_3^- isotopic ratios were measured via the silver nitrate method (Silva et al. 2000). $AgNO_3$ was analysed with a breakseal method (Spoelstra et al. 2001). An elemental analyzer IRMS was used for $\delta^{15}N\text{-}NO_3^-$ analysis and a VG PRISM mass spectrometer was used for $\delta^{18}O\text{-}NO_3^-$. Precision was 0.5‰ and 0.6‰ and $\delta^{15}N$ and $\delta^{18}O$ values, respectively.

Samples for N_2O concentration were prepared by removing 5 mL of sample while injecting 10 mL of He, and equilibrating the headspace using a rotary shaker. A 5 mL subsample of headspace was analyzed on the Varian 3800 CP GC, as above. Concentrations were calculated using Henry's Law after Lide and Frederikse (Lide and Frederikse 1995). Gas for dissolved N_2O isotope analyses were pre-concentrated using a purge and trap method (Thuss 2008) and analyzed on the CF-ICMS, as above.

In a previous study, the SIDNO model was used to calculate N_2O isotopic ratios of N_2O production from dissolved N_2O isotope ratios, taking into account gas exchange (Thuss 2008). The model assumes steady state N_2O production. Additionally, an isotope mass balance was used to remove effluent N_2O (which has a different isotopic ratio than that produced in the river, Chapter 4) using effluent N_2O concentrations and stable isotope values in order to estimate the $\varepsilon^{15}N$ and $\varepsilon^{18}O$ of in-situ N_2O production (Thuss 2008) for night (sunset to sunrise) and day (sunrise to sunset). These $\varepsilon^{15}N$ and $\varepsilon^{18}O$ values are used in this study.

5.3 Results

5.3.1 Sediment Parameters

Sediment collected at Bridgeport and Blair had low organic carbon content (1.7 to 5.6%). Organic carbon did not vary with season and was not significantly different by site (t-test: $p = 0.680$; SigmaPlot 12.0, Systat Software Inc., Chicago IL) (Table 5.3). NO_3^- and NH_4^+ in sediment were below detection.

5.3.2 Net N_2O Production Rates

There was net N_2O production in all incubations (range: 0.8 nmol/h/g dry-weight sediment (g-sed_{dw}) to 90.8 nmol/h/g-sed_{dw}), Table 5.4, Figure 5.3. Net N_2O production rates from high-NO_3^- treatments were always higher than from low-NO_3^- treatments. N_2O production was typically higher from Blair sediments than from Bridgeport sediments, although this difference was small in spring with high NO_3^- addition (Treatment A). Seasonal trends were different between the two field sites. At Bridgeport under high NO_3^- addition, there were no seasonal trends. However, under low NO_3^- addition, N_2O was highest in summer and indistinguishable in spring and autumn (Table 5.4). At Blair, there were no seasonal differences in N_2O production under low NO_3^- additions but summer N_2O production was higher than spring and autumn in high NO_3^- incubations (Table 5.4).

5.3.3 Stable Isotopic Abundances of N_2O Produced in Incubations

$\delta^{15}N$-N_2O values ranged widely in experiments from -16.1‰ to 4.7‰ (Figure 5.3).However, values were slightly more constrained by site (BR: -13.1‰ to 4.7‰, BL: -16.1‰ to 0.9‰). This wide range is partially due to changes in $\delta^{15}N$-N_2O over the course of the incubations. In high-NO_3^- incubations (A, C and E), the first sampling had high $\delta^{15}N$-N_2O values. Thereafter $\delta^{15}N$-N_2O values were consistently low and stable in most bottles. In contrast, in low-NO_3^- incubations (B, D and F), $\delta^{15}N$-N_2O increased over the course of the incubation. All $\delta^{15}N$-N_2O values were much lower than that of the NO_3^- substrate (13.8‰).

$\delta^{18}O$-N_2O values varied widely (41.5‰ to 129.5‰) depending on the $\delta^{18}O$-H_2O value in each incubation jar. All incubations, except BL-D, had no change in $\delta^{18}O$-N_2O after sampling time 1, even when $\delta^{15}N$-N_2O increased over time.

5.4 Discussion

5.4.1 N_2O Production Rates

N_2O production rates were higher than in similar denitrification incubations conducted with forest and agricultural soil by Snider et al. (2009) (mean production rate: 1.5 nmol N_2O/h/g-sed_{dw} to 38.6 nmol N_2O/h/g-sed_{dw}). The high production rates, high NO_3^- and low NH_4^+ in the jars, and anoxic conditions indicate that N_2O was likely produced by denitrification.

The first sampling (at ~1 hour) of three spring incubations (BR-A, BL-A, BL-B) showed lower production rates than subsequent samplings. Production rates did not change in any incubation over the last 3 samplings. This suggests that a quasi-steady state was achieved after 2 hours or less.

N_2O production rates were almost always higher in Blair sediments than Bridgeport when season and NO_3^- addition were the same. The exceptions were Incubation D (summer, low NO_3^- addition), and Incubation E (autumn, high NO_3^- addition) in which similar rates were observed between the two sites. Higher production rates with Blair sediment may indicate that more NO_3^- was reduced because the denitrifier biomass is larger than at Bridgeport and/or because organic carbon was more labile. Additionally, the Blair community may have produced more N_2O per unit NO_3^- reduced than that at Bridgeport. This could be due to Nos inhibition or a lower proportion of Nos genes in this community. About one-third of denitrifying bacteria that have been DNA-sequenced lack genes for N_2O reductase (Nos) and therefore cannot reduce N_2O to N_2 (Philippot et al. 2011). Incubation experiments show that some, not all, soil communities reduced excess N_2O produced by these bacteria (Philippot et al. 2011). It is currently unknown how these organisms are distributed in the environment, and how prevalent Nos-deficient microbes are in river sediments.

A 60% increase in NO_3^- addition between low and high-NO_3^- incubations resulted in an order of magnitude increase in N_2O production, at both sites and all seasons. The only exception was in incubations BR-C and BR-D (summer), in which N_2O production only tripled between low and high NO_3^- additions. N_2O production was not limited by NO_3^- substrate ability and differences between incubations were likely due to N_2O consumption. However, this may not apply directly to field studies because NO_3^- concentrations were very high in order to produce measureable quantities of N_2O. See Section 5.4.4 for further discussion.

5.4.2 $\varepsilon^{15}N$: comparisons to literature values

In most incubations, $\delta^{15}N$-N_2O values were consistent within error over the whole incubation or after the first sampling (~1 hour), suggesting that a quasi-steady state had been reached. However, BR-E

(Bridgeport, Autumn, high NO_3^-) did not achieve steady $\delta^{15}N\text{-}N_2O$ values until the last two samplings. Conversely, at Bridgeport and Blair in Incubations D and F (Summer and Autumn, low NO_3^-), $\delta^{15}N\text{-}N_2O$ values increased over the incubation period, by between 1 and 6‰. Thus, when calculating average $\delta^{15}N\text{-}N_2O$ and isotopic fractionations, the first sampling was removed from low-NO_3^- BR incubations (BR-B, BR-D and BR-F). The second sample was also removed from BR-E and one very high $\delta^{15}N\text{-}N_2O$ value was removed from BR-F.

Isotopic fractionations for ^{15}N for high-NO_3^- incubations (A, C and E) (-27.1‰ to -21.3‰, Table 5.4) and were similar to those found by Snider et al. (Snider et al. 2009) (-29‰ to -20‰), and were confined to a smaller range than previous literature values (-39‰ to -10‰ (Snider et al. 2009)). This is a narrow range of $\varepsilon^{15}N$ values, considering that differences in temperature, NO_3^- and organic C between sites and seasons may drive changes in microbial community.

However, $\varepsilon^{15}N$ values were more positive and had a larger range in low-NO_3^- incubations (-23.8‰ to -12.4‰) than in high-NO_3^- incubations (-27.1‰ to -21.3‰), indicating less fractionation and/or the occurrence of one or more N_2O isotopic enrichment process.

5.4.3 $\varepsilon_{net}{}^{18}O$ and Oxygen Exchange: Comparison to Literature Values

In all incubations, $\delta^{18}O\text{-}N_2O$ increased as $\delta^{18}O\text{-}H_2O$ increased (Figure 5.3). This indicates that some O in N_2O was contributed by water molecules, not NO_3^-. The percentage oxygen exchange was quantified using methods from Snider et al. (2009). First, $\delta^{18}O\text{-}N_2O$ and $\delta^{18}O\text{-}H_2O$ were both made relative to the $^{18}O/^{16}O$ ratio of the NO_3^- substrate (not the international standard) using equation 5.3. This eliminates an independent variable and allows separation of the influence of NO_3^- and H_2O on $O\text{-}N_2O$.

$$\delta^{18}O_x \text{ (rel. } NO_3^-) = R_x/R_{NO3} - 1 \qquad \textbf{Equation 5.3}$$

Where x is N_2O or H_2O, and $R = {}^{18}O/{}^{16}O$

When $\delta^{18}O\text{-}H_2O$ (rel. NO_3^-) is plotted on the x-axis versus $\delta^{18}O\text{-}N_2O$ (rel. NO_3^-), a positive linear trend is evident (Figure 5.4, range in r^2: 0.91 to 1.00). In all incubations, the regression line slope was between, but not equal to, zero and 1. This indicates that all $\delta^{18}O\text{-}N_2O$ values were derived from a mix of oxygen from NO_3^- and from water, i.e. that O exchange between N species and H_2O occurs. The slope of the regression is the mean fraction O exchange and the y-intercept is the net $\varepsilon^{18}O$ value ($\varepsilon_{net}{}^{18}O$), or $\varepsilon^{18}O$ value that would be expressed if oxygen exchange were zero. This method of calculating O-exchange gives a minimum value because ε_{H2O} (Figure 5.1) is assumed to be zero (Snider et al. 2013).

If no O-exchange occurs, $\varepsilon_{net}{}^{18}O$ is equal to $\varepsilon^{18}O$, and the slope of the regression lines shown in Figure 5.4 is zero. In this case, $\delta^{18}O\text{-}N_2O$ will be higher than $\delta^{18}O\text{-}NO_3^-$ because all isotopic fractionations shown Figure 5.1 are positive (Snider et al. 2013). Using this method, $\varepsilon_{net}{}^{18}O$ is "corrected" to remove the effects of O exchange. However, the two are not entirely independent because of the interaction between the multiple steps of denitrification. As O exchange increases, $\varepsilon_{net}{}^{18}O$ should decrease because O from N species are replaced by O from H_2O (Snider et al. 2009), unless fractionations occurring after O-exchange (e.g. ε_4) are large contributors to $\varepsilon_{net}{}^{18}O$.

O-exchange varied between incubations (range: 60% to 83%, Table 5.4) but no differences between sites, seasons or NO_3^- additions were observed. The range observed was similar to that in forest, wetland and agricultural soils (range: 64% to 94%) (Snider et al. 2009, Snider 2011). Interestingly, Snider et al. (2009) found a low but narrow range of high O-exchange (64% to 70%) in wetland soils, which could have microbial communities more similar to river sediment than upland forest soils because they are more frequently saturated. This might suggest that there is greater variability in microbial community in fresh sediment from the Grand River than there is in wetland sediments that have been dried and used in incubations after room temperature storage (Snider et al. 2009).

The $\varepsilon_{net}{}^{18}O$ in incubations ranged from 48.6‰ to 67.0‰ (Table 5.4). These values are higher than most reported by Snider et al. (Snider et al., 2009) (range: 17‰ to 43‰) and higher than those reported for *Pseudomonas aureofaciens*, which exhibits little O-exchange ($\varepsilon^{18}O$ = 40‰, (Casciotti et al. 2002)). There were no trends with site or season, but $\varepsilon_{net}{}^{18}O$ was larger at each site at the low NO_3^- treatment. This suggests that ε_4 ($N_2O \rightarrow N_2$), which occurs after O exchange may be a significant portion of $\varepsilon_{net}{}^{18}O$.

Controls on O exchange and $\varepsilon_{net}{}^{18}O$ are still largely unknown. O exchange is known to differ greatly between microbial species (Kool et al. 2007) but environmental controls are not understood. Snider et al. (Snider et al. 2009) showed that O-exchange and $\varepsilon_{net}{}^{18}O$ can vary between soils, but this study shows that N_2O reduction may also have a large effect on $\varepsilon_{net}{}^{18}O$ values.

5.4.4 Relationship between Isotopic Effects and N_2O Reductase Inhibition

Little difference is seen in $\varepsilon^{15}N$ and $\varepsilon_{net}{}^{18}O$ between the Bridgeport and Blair sites and between seasons. However, $\varepsilon^{15}N$ and $\varepsilon_{net}{}^{18}O$ both show negative relationships with N_2O production rate (Figure 5.5). $\varepsilon^{15}N$ and $\varepsilon_{net}{}^{18}O$ show a positive linear relationship a slope of 1.1 (r^2 = 0.5, $p < 0.0001$) (Figure 5.6). In contrast, O exchange did not show any relationship with production rate, $\varepsilon^{15}N$ or $\varepsilon_{net}{}^{18}O$.

There are several possible explanations for the low N_2O production rates and high ε values at the end of some incubations, particularly in low-NO_3^- treatments. First, $\delta^{15}N\text{-}NO_3^-$ and $\delta^{18}O\text{-}NO_3^-$ values could have increased over the course of the incubation due to preferential use of isotopically lighter NO_3^- during denitrification. If $\varepsilon^{15}N$ and $\varepsilon_{net}{}^{18}O$ were constant, this would have result in higher isotopic ratios in N_2O. However, about 30% of the NO_3^- pool must have been consumed in order for NO_3^- isotopes to change measurably (based on a typical $\varepsilon^{15}N$ of -15‰, Table 5.4). N_2 was not quantified in these experiments, but liberal losses to N_2 can be estimated with an $N_2O:(N_2O+N_2)$ ratio of 1:100. This yields an estimated 2% to 8% total loss in NO_3^- over the course of the experiments, which would not result in any measurable change in the isotopic ratios of the NO_3^- pool.

Secondly, gross N_2O production rates could be higher in higher-NO_3^- incubations and $N_2O:(N_2O+N_2)$ ratios could be consistent between NO_3^- treatment types. To account for different $\varepsilon^{15}N$ and $\varepsilon^{18}O$ between high and low NO_3^- incubations, isotopic fractionation would have to be rate dependent. While the isotopic fractionation factor of N_2O reduction can change with reaction rate (Vieten et al. 2007), this has not been observed in N_2O production by denitrification, possibly because it is difficult to measure. It also seems unlikely that denitrification would be NO_3^- limited at 0.8 mg $N/g\text{-}sed_{dw}$ NO_3^- addition but not at 1.3 mg $N/g\text{-}sed_{dw}$ NO_3^- addition, especially as laboratory incubations have observed maximum denitrification rates at 25 μg N/g soil (Limmer and Steele 1982). If NO_3^- were limiting denitrification, ten-fold increase in N_2O production is difficult to explain, as NO_3^- concentrations varied by less than a factor of two. For these reasons, simple changes in denitrification rate are unlikely to explain all the differences between high and low NO_3^- additions and, as a result, the $N_2O:(N_2O+N_2)$ ratio must have been different between the two treatments.

One way the $N_2O:(N_2O+N_2)$ ratio can change is by the inhibition of N_2O reductase (Nos) in some jars, resulting in higher net N_2O production and lower $\varepsilon^{15}N$ and $\varepsilon_{net}{}^{18}O$ values in high-NO_3^- incubations. In lower- NO_3^- treatments, Nos may not have been inhibited, and thus some N_2O would be consumed. When N_2O is reduced, an isotopic fractionation (ε_4) discriminates against both ^{15}N and ^{18}O, explaining the higher $\varepsilon^{15}N$ and $\varepsilon_{net}{}^{18}O$ measured at lower NO_3^- concentration. However, NO_3^- concentrations of 0.02 mg N/g-soil have been shown to inhibit Nos at circumneutral pH (Firestone and Tiedje 1979). Our incubations had higher NO_3^- (0.8 mg $N/g\text{-}sed_{dw}$ to 1.3 mg $N/g\text{-}sed_{dw}$), making it unlikely that either treatment would exhibit Nos inhibition. However, Firestone et al. (1979) found much lower NO_2^- concentrations (0.004 mg N/g-soil) effectively inhibited N_2O reductase in the same soils. NO_2^- was not measured in this study, but is it possible that NO_2^- accumulated in incubation jars if nitrate reduction occurred faster than nitrite reduction. NO_2^- accumulation could have occurred faster in higher-NO_3^- treatments because of high availability of NO_3^-. Previous work has shown that in

batch reactors, NO_2^- can accumulate on the onset of denitrification, and higher initial NO_3^- concentrations result in bigger NO_2^- peaks (Sun et al. 2009); however, this was tested on lower NO_3^- concentrations (30 to 65 mg N/L) than this study (775 to 1300 mg N/L). Presumably, NO_2^- produced in some cells must enter the environment to inhibit Nos in more cells but the mechanism for this is not known.

Lastly, lower N_2O production rates and high ε values may be explained by the well-documented lag in N_2O reductase (Nos) activation after production of other enzymes used in denitrification (Figure 5.7). Several studies have reported decreased N_2O production over time during denitrification in soils and microbial cultures. Firestone and Tiedje (1979) were the first to describe and explain the pattern in anoxic denitrification incubations on agricultural soils. They added $^{13}NO_3^-$ and monitored N_2O and N_2 over 48 hours, using C_2H_2 to block N_2O reduction in some replicates. They found that the N_2O:(N_2O+N_2) ratio produced during denitrification was low, between 25% and 66% for the first 1-3 hours of incubations, which was attributed to "pre-existing conditions of soil" (Firestone and Tiedje 1979). Between 16 to 33 hours, N_2O production was steady, with N_2O:(N_2O+N_2) ratios between 0.46 and 0.48. In the last stage, after 33 hours, N_2O:N_2 dropped again to 0% (i.e. entirely N_2) to 20%. When chloramphenicol (which inhibits the production of new proteins) was added, N_2O:(N_2O+N_2) ratios remained high (0.83) throughout the experiment (33 hours). This suggests that little to no Nos was present in cells on the onset of the experiment, but was synthesized during denitrification, with a large increase in activation around 33 hours. NO_3^- concentrations remained consistent (0.02 mg N/g-soil) throughout the entire incubation process. If this model explains the differences between low and high-NO_3^- incubations in this study, Nos lag time must increase with NO_3^- (or possibly NO_2^-) substrate concentration. This was not observed over the 5 hour incubation run time; N_2O production rate did not change significantly after the first time step in any incubation. To our knowledge, a positive relationship between Nos lag time and NO_3^- concentration has not been reported in the literature; incubation experiments with longer run times are needed to determine if this relationship exists.

To test if it is possible that N_2O reduction is the only mechanism responsible for the differences in N_2O concentration, $\varepsilon^{15}N$ and $\varepsilon^{18}O$ between NO_3^- treatments, the isotopic fractionation for N_2O reduction (ε_4 in Figure 5.1) was calculated using the Rayleigh distillation equation, assuming initial N_2O production and N_2O isotopic values are identical between high- and low-NO_3^- incubations. For each site and season, the N_2O concentration and stable isotopic values from the high-NO_3^- incubation were used as the "initial" values (no N_2O reduction) and the values from the low-NO_3^- incubation were used as the "final" values (some N_2O reduction). The Rayleigh equation was designed for a closed system with a finite pool of reactant (here, N_2O) that is not replenished during the reaction.

Thus, it is an oversimplification of the incubation experiments, where N_2O production and consumption occur simultaneously. However, if the calculated ε4 values are very different than published values from pure cultures and soil experiments, the hypothesis can be discounted, and differences between incubations cannot be attributed only to N_2O consumption. The Rayleigh equation, rearranged to solve for ε, is:

$$\boldsymbol{\varepsilon = \frac{\ln\left(\frac{R}{R_0}\right)}{\ln\left(\frac{P}{P_0}\right)}} \qquad \textbf{Equation 5.4}$$

were ε is shown in permil, R is the $^{15}N/^{14}N$ or $^{18}O/^{16}O$ ratio of N_2O in the low-NO_3^- incubation, R_0 is the $^{15}N/^{14}N$ or $^{18}O/^{16}O$ ratio in the high-NO_3^- incubation, P is the N_2O production rate in the low-NO_3^- incubation, and P_0 is the N_2O production rate in the high-NO_3^- incubation. $^{18}O/^{16}O$ ratios were calculated using $\varepsilon_{net}{}^{18}O$ to remove the effect of O exchange. Calculated values for $\varepsilon_4{}^{15}N$ ranged from -8.1‰ to -2.5‰, on the high end of values reported in the literature for N_2O reduction (-27‰ to -1‰ (Snider et al. 2009). Estimated $\varepsilon_4{}^{18}O$ values ranged from -6.7‰ to -4.0‰, which is on the high end of the range of literature values (-42‰ to -5‰) but these values may be low due to O exchange (Snider et al. 2009). The $\varepsilon_4{}^{18}O$:$\varepsilon_4{}^{15}N$ ratio is well-constrained in literature to 2.4‰ to 3‰ (Snider et al. 2009, Vieten et al. 2007) while values calculated here are lower (0.1‰ to 2.2‰). This may be because the effect of O exchange (which brings $\varepsilon^{18}O$ values closer to that of H_2O, in this case more negative) has been removed in this study, but not in previous studies. Thus, there is no isotopic evidence to discount the theory that differences in N_2O production and isotopic values between high and low NO_3^- incubations can be attributed only to N_2O reduction. However, other possibilities are discussed below.

Of the four possible explanations for the changes in N_2O production rate, $\varepsilon^{15}N$ and $\varepsilon^{18}O$ between high- and low-NO_3^- incubations, it appears that two can be discounted. Changes could not be caused by NO_3^- enrichment due to the very large NO_3^- pool and relatively low N_2O production. It is unlikely that the differences are solely due to increased denitrification rates (with constant N_2O:(N_2O+N_2) ratio) due to very high NO_3^- concentrations and the 3 to 10-fold increase in N_2O production when NO_3^- is only doubled. Thus, it appears that the N_2O:(N_2O+N_2) ratio must change between incubations. This may be because high NO_3^- or NO_2^- inhibits N_2O reductase in the high-NO_3^- incubations and less so in the low-NO_3^- incubations. Alternatively or concurrently, Nos lag time may be longer in the high-NO_3^- incubations, allowing more N_2O accumulation over the 5-hour experiment run time. In either case, the isotopic fractionation associated with Nos is likely responsible for the increase in $\varepsilon_{net}{}^{15}N$ and $\varepsilon_{net}{}^{18}O$ in the low-NO_3^- incubations.

Given that complete inhibition of Nos has been shown to occur in soil incubations with much lower NO_3^- additions than used here (0.02 mg N/g moist soil, (Firestone and Tiedje 1979) compared to 0.8 to 1.3 mg N/g-sed_{dw} used here), it is surprising that Nos is not deactivated in both incubation types. Differences in the N_2O:(N_2O+N_2) ratio between incubations may call into question the usefulness of laboratory sediment incubations in mimicking river conditions. The high NO_3^- concentration in incubations is necessary to prevent increased $\delta^{15}N$-NO_3^- and $\delta^{18}O$-NO_3^- values caused by NO_3^- consumption (in order to easily measure $\varepsilon^{15}N$ and $\varepsilon^{18}O$) but this likely results in a very different N_2O:(N_2O+N_2) and therefore net $\varepsilon^{15}N$ and $\varepsilon^{18}O$ than in river sediments.

Interestingly, the fraction of O exchange did not change with net N_2O production. This is probably because the $\varepsilon^{15}N$ and $\varepsilon^{18}O$ changes observed with net N_2O production are related to N_2O reduction but O exchange occurs earlier in the denitrification chain, on NO_2^- (Casciotti et al. 2007) and/or NO (Kool et al. 2007).

5.4.5 Comparison between Field Estimations and Incubation Isotopic Fractionations

Isotopic fractionations within the Grand River at Bridgeport and Blair were estimated using isotopic ratios of NO_3^- and N_2O collected in the water column. Isotopic ratios of N_2O production were calculated using SIDNO, assuming steady state (Thuss 2008). Because N_2O and NO_3^- isotopic ratios change on a diel scale, particularly at Blair (Thuss 2008) average night-time (sunrise to sunset) and day-time NO_3- and N_2O isotopic values were used for calculating $\varepsilon^{15}N$ and $\varepsilon^{18}O$ using Equation 5.1. These estimates are not ideal for several reasons. First, it was not possible to quantify the isotope ratios of NO_3^- in sediment, which might be significantly different than in the water column, due to NO_3^- diffusion, production and consumption. Second, instantaneous N_2O and NO_3^- measurements represent a combination of upstream sources, not the N_2O produced at one discrete spot in the river. Lastly, it was also not possible to quantify oxygen exchange in river samples because river water has a consistent $\delta^{18}O$-H_2O value. Therefore, $\varepsilon_{net}{}^{18}O$ was estimated using the average O exchange fraction for each site, as determined by incubations, and an average $\delta^{18}O$-H_2O value for the Grand River (-10‰). $\delta^{18}O$-H_2O changes between sites and seasonal changes were small (< 1‰) and were ignored.

Field isotopic fractionations for N_2O production are shown in Figure 5.6. Because of the large diel range in $\delta^{15}N$-N_2O and $\delta^{18}O$-N_2O at Blair but only a small change in NO_3^- stable isotopic ratios (Thuss 2008), day and night estimations are very different at that site. At both sites, estimated $\varepsilon_{net}{}^{18}O$ are within the large range determined by incubations. Bridgeport has relatively high $\varepsilon^{15}N$ values but moderate $\varepsilon^{18}O$ values (Figure 5.6), suggesting that differences in N_2O reduction alone cannot explain

the differences in N_2O isotopic ratios between Bridgeport and Blair. One possibility is that $\varepsilon_{net}{}^{18}O$ is poorly estimated because in-river O exchange rates are not known. Alternatively, differences in the microbial community between Bridgeport and Blair may explain why field $\varepsilon^{15}N$ values are so different but $\varepsilon_{net}{}^{18}$ values are similar between the sites. Microbial communities in sediment incubations may also be very different than those contributing to N_2O in the river. Denitrification in biofilms can be significant sources of N_2O (Nielsen et al. 1990, Schreiber et al. 2009) but biofilms were not included in this study. Lower N_2O production rates at Bridgeport might be explained by (a) lower net denitrification rates than Blair, due to lack of water column hypoxia, lower NO_3^- during the growing seasons, and/or differences in organic C concentration and lability (not measured), and/or (b) lower N_2O:(N_2O+N_2). Because the river never approaches hypoxia at Bridgeport, denitrification rates are likely relatively constant (as seen in the modest diel N_2O concentration cycle) and N_2O reductase (Nos) is not expected to be in disequilibrium with other denitrification enzymes. Nos may not be inhibited by the presence of NO_2^-, which has not been observed in the water column at this site. However, NO_2^- in sediment pore water has not been quantified.

At Blair, estimated field $\varepsilon^{15}N$ values are slightly lower than those from low-NO_3^- incubations during the day (Figure 5.6). However, at night, estimated $\varepsilon^{15}N$ values are about 15‰ lower than any incubation conducted. $\varepsilon^{18}O$ values are also low. Water column hypoxia occurs at Blair in summer at night, and occurred during this sampling event (minimum: 0.7 mg/L). Hypoxia likely acts similarly to a large addition of NO_3^- to an anoxic incubation bottle by promoting the onset of denitrification at high rates, and N_2O reductase activity lags behind NO_3^-, NO_2^- and NO reductases (Figure 5.7). This would help explain the increase in concentration of N_2O and decrease in $\delta^{15}N$-N_2O and $\delta^{18}O$-N_2O observed between day and night at Blair (Thuss 2008). The diel N_2O curve at Blair on June 26-27, 2007 was unusual compared to other locations in the Grand River because N_2O concentration peaked ~4 hours before dawn (Figure 5.8). As N_2O concentrations dropped between 2:00 AM and dawn, $\delta^{15}N$-N_2O declined but $\delta^{18}O$-N_2O increased. Denitrification rates likely did not decrease in this period, as substrate (NO_3^-, DOC) was still plentiful and the inhibitor (DO) was low. If the N_2O:(N_2O+N_2) ratio decreased due to an Nos activity increase, $\delta^{15}N$-N_2O and $\delta^{18}O$-N_2O should both have increased, which was not observed. Other possible explanations could be changes in the substrate ($\delta^{18}O$-NO_3^-), upstream effects and/or differences between water column pore water NO_3^- isotopic ratios.

5.4.6 Usefulness of Stable Isotope Analysis in Denitrification Incubations

Seminal work conducted by Mary Firestone and others in the 1970s and 1980s showed that N_2O production and N_2O:N_2 ratios in soils by denitrification was influenced by time and concentrations of NO_2^-, NO_3^- and O_2 (Firestone and Tiedje 1979, Firestone et al. 1979, Firestone et al. 1980). They

hypothesized that a lag in the production of N_2O reductase results in a peak and then decrease of N_2O, even when NO_3^- is plentiful (Firestone et al. 1980). However, accurately measuring N_2 in these incubations was necessary, and only indirect evidence could be provided for N_2O production pathways. Stable isotopic analysis of N_2O in denitrification incubations gives insight into N_2O production pathways instead of net N_2O rates only. For instance, Snider (Snider 2011) shows a large difference in $\delta^{15}N$-N_2O produced by nitrification versus denitrification and ascribes values to the intermediate denitrification $\varepsilon^{18}O$ values (ε_1, ε_2, ε_3 etc.) and to oxygen exchange. In this study, high $\varepsilon^{15}N$ and $\varepsilon_{net}{}^{18}O$ values at low N_2O production rates indicate that more N_2O consumption must be occurring in low-NO_3^- incubations than in high-NO_3^- incubations. N_2O reductase may be inhibited by NO_3^- or NO_2^- or may have a longer activation time when substrate is more plentiful. Thus, stable isotopic analysis of N_2O can indicate changes to the N_2O:(N_2O+N_2) ratio caused by N_2O reduction, which results in net N_2O production decreases, and $\varepsilon^{15}N$ and $\varepsilon_{net}{}^{18}O$ increases. Advances in laser spectrometry likely will make N_2O stable isotopic analysis cheaper and easier than N_2 concentration measurement, which is easily contaminated with air (Groffman et al. 2006). Thus, stable isotopic analysis of N_2O can provide important information about N_2O production pathways in incubations, and can suggest information about the N_2O:(N_2O+N_2) ratio, while making N_2 analysis unnecessary.

5.5 Conclusions

Denitrification incubations with Grand River sediment always produced N_2O. Overall, more N_2O was produced in sediment from Blair (urbanized, downstream of a large WWTP) than at Bridgeport (upstream of urban sources of N pollution). Surprisingly, increasing NO_3^- addition from 0.8 to 1.3 g N/g-sed_{dw} resulted in an order of magnitude increase in N_2O production, except in summer at Bridgeport. Lower N_2O production resulted in higher $\varepsilon^{15}N$ and $\varepsilon_{net}{}^{18}O$ values but the fraction of O exchange did not change. High net N_2O production and low, steady ε values likely indicate that little N_2O consumption occurs because N_2O reductase (Nos) was inhibited, possibly by high NO_3^- or NO_2^- and/or by a lag in activity relative to other reductases in the denitrification pathway. To separate the effects of NO_3^-, NO_2^-, and incubation time on Nos, further experiments quantifying NO_2^- and using longer run times must be conducted.

Stable isotope fractionation (ε) values measured in incubations were within the range of previous literature results. They were also similar to those estimated from field data, except for low $\varepsilon^{15}N$ and $\varepsilon^{18}O$ field estimates at night at Blair, where N_2O production is very high. This could indicate that the N_2O:(N_2O+N_2) ratio is higher at night than in the day at Blair. This suggests that researchers should expect that $\varepsilon^{15}N$ and $\varepsilon^{18}O$ are not consistent throughout large, complex rivers due to changes in redox

conditions and substrate that control Nos activity. $\varepsilon^{15}N$ and $\varepsilon^{18}O$ from rivers are difficult to predict and must be measured if N_2O isotopic values are studied.

Additionally, the in-river microbial community may isotopically fractionate more than the captured community in incubations. Other possibilities are that instantaneous river water column sampling does not accurately reflect isotopic values of NO_3^- and N_2O in sediment, due to upstream effects, sediment NO_3^- sources that are not well represented in the water column, etc. While denitrification incubations may represent disequilibrated systems with no diffusion and therefore may not be ideal models of river sediment behavior, isotopic analysis of incubations yields valuable insight into the balance of N_2O production consumption (i.e. the N_2O:(N_2O+N_2) ratio) that may not be obvious by examining N_2O concentration only.

Table 5.1: Controls on the enzyme activation and inhibition used in each step of denitrification. See Figure 5.1 for the location of enzymes in gram-negative denitrifying bacteria. Transporter proteins are also shown, which do not have activating or inhibiting conditions.

Step	Protein used	Conditions for activation	Conditions for inhibition
NO_3^- uptake (outside cell to periplasm)	Unknown porin (Song and Niederweis 2012, Steen et al. 2013)	NA	NA
NO_3^- transport (periplasm to cytoplasm)	NarK1 and NarK2 (Wood et al. 2002)	NA	NA
$NO_3^- \rightarrow NO_2^-$	Dissimilatory nitrate reductase (Nar)	Low O_2 (Arai 2011, Moir and Wood 2001)	Oxic conditions; N_2O (Moir and Wood 2001)
$NO_2^- \rightarrow NO$	Nitrite reductase (Nir)	Low O_2 (Arai 2011)	Oxic conditions (Moir and Wood 2001)
$NO \rightarrow N_2O$	Nitric oxide reductase (Nor)	Low O_2 (Arai 2011)	Oxic conditions (Moir and Wood 2001); high NO_3^- (Firestone et al. 1979)
$N_2O \rightarrow N_2$	Nitrous oxide reductase (Nos)	Low O_2 (Arai 2011), onset of denitrification	Oxic conditions (Moir and Wood 2001); moderate NO_3^-; low NO_2^- (Firestone and Tiedje 1979)

Table 5.2: Experimental set-up of denitrification experiments.

Season	Site	NO_3^- Addition	Treatment Name	$\delta^{18}O$-H_2O (number of replicates)
Spring	Bridgeport	High	BR-A	Low (2)
				Medium (2)
				High (2)
		Low	BR-B	Low (2)
				Medium (2)
				High (2)
	Blair	High	BL-A	Low (2)
				Medium (2)
				High (2)
		Low	BL-B	Low (2)
				Medium (2)
				High (2)
Summer	Bridgeport	High	BR-C	Low (2)
				Medium (2)
				High (2)
		Low	BR-D	Low (2)
				Medium (2)
				High (2)
	Blair	High	BL-C	Low (2)
				Medium (2)
				High (2)
		Low	BL-D	Low (2)
				Medium (2)
				High (2)
Autumn	Bridgeport	High	BR-E	Low (2)
				Medium (2)
				High (2)
		Low	BR-F	Low (2)
				Medium (2)
				High (2)
	Blair	High	BL-E	Low (2)
				Medium (2)
				High (2)
		Low	BL-F	Low (2)
				Medium (2)
				High (2)

Table 5.3: Physical and chemical properties of sediments used in denitrification experiments. BD = below detection.

	Bridgeport			Blair		
	Spring	Summer	Autumn	Spring	Summer	Autumn
Sediment Saturation Capacity (g H_2O/g-sed_{dw})	0.46	0.41	1.00	0.43	0.57	0.74
Sediment Organic Content (%)	2.2	1.7	5.4	2.1	2.6	3.9
NH_4^+ (µg N/g-sed_{dw})	BD	BD	BD	BD	BD	BD
NO_3^- (µg N/g/sed_{dw})	BD	BD	BD	BD	BD	BD

Table 5.4: Summary of N_2O production rates, N_2O isotopic values, isotopic effects and percentage oxygen exchange in denitrification incubations.

Treatment	Mean N_2O Production Rate (nmol N_2O/h/g-sed_{dw}) [1σ, n]	Mean $\delta^{15}N$-N_2O (‰) [1σ, n]	Mean N isotopic fractionation (ε) (‰) [1σ, n]	Percent $H_2{}^{18}O$ incorporation into $N_2{}^{18}O$ (%) [1σ, n]	Mean net O isotopic fractionation (ε_{net}) (‰) [1σ, n]
BR-A Spring, high NO_3^-	32 [8.2, 24]	-10.4 [1.0, 24]	-23.8 [1.0, 24]	74 [4, 24]	56.3 [1.3, 20]
BR-B Spring, low NO_3^-	2.8 [1.1, 24]	-2.9 [1.9, 12]	-16.5 [1.9, 12]	74 [5, 12]	67.0 [1.6, 12]
BR-C Summer, high NO_3^-	32 [3.4, 24]	-12.4 [0.6, 24]	-25.9 [0.6, 24]	80 [9, 24]	44.2 [2.3, 24]
BR-D Summer, low NO_3^-	10 [2.3, 24]	-3.1 [2.7, 24]	-21.5 [1.0, 18]	71 [15, 18]	52.4 [4.0, 18]
BR-E Autumn, high NO_3^-	43 [32, 24]	-6.9 [1.9, 10]	-21.3 [1.4, 7]	77 [28, 7]	48.6 [8.0, 7]
BR-F Autumn, low NO_3^-	2.9 [1.1, 24]	1.2 [2.9, 13]	-12.4 [2.9, 13]	79 [7, 12]	60.0 [2.1, 12]
BL-A Spring, high NO_3^-	31 [12, 24]	-13.6 [1.3, 24]	-27.1 [1.3, 24]	74 [3, 24]	51.1 [1.1, 24]
BL-B Spring, low NO_3^-	9.1 [4.7, 24]	-10.6 [1.7, 24]	-23.8 [1.3, 18]	83 [5, 18]	58.1 [1.5, 19]
BL-C Summer, high NO_3^-	65 [5.3, 24]	-10.9 [1.0, 24]	-24.3 [1.0, 24]	60 [9, 24]	50.0 [2.2, 24]
BL-D Summer, low NO_3^-	9.0 [1.6, 26]	-3.1 [2.7, 24]	-16.6 [2.6, 23]	67 [15, 23]	63.1 [3.8, 23]
BL-E Autumn, high NO_3^-	45 [15, 24]	-11.6 [1.9, 23]	-25.7 [1.6, 20]	71 [17, 20]	54.2 [4.3, 20]
BL-F Autumn, low NO_3^-	7.8 [0.9, 24]	-4.5 [1.6, 23]	-18.1 [1.6, 2.0]	75 [8, 20]	66.4 [2.3, 20]

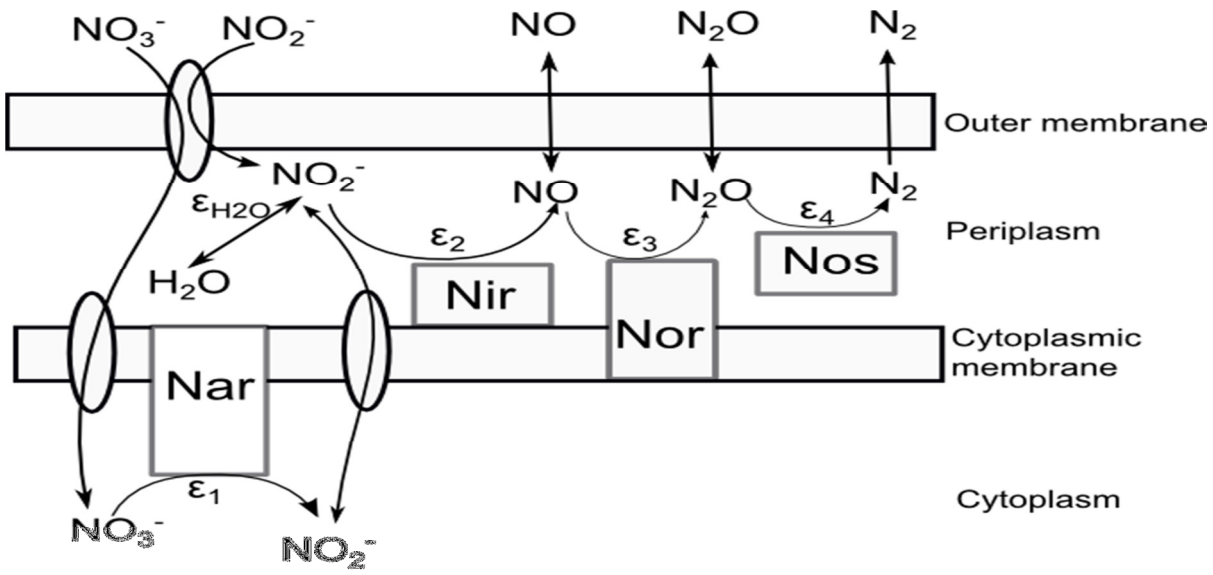

Figure 5.1: Denitrification in gram-negative bacteria. Transporters (active or passive) are represented by ovals, and enzymes by grey boxes. Non-charged gases NO, N_2O and N_2 can freely diffuse through the cell's outer membrane by NO_3^- and NO_2^- must be transported across it. Nar: nitrate reductase; Nir: nitrite reductase; Nor: nitric oxide reductase; Nos: nitrous oxide reductase. Isotopic fractionations for ^{18}O only are shown for brevity. The net isotopic fractionation ($\varepsilon_{net}{}^{18}O$) is the sum of ε_1 through ε_4. O exchange with H_2O may occur with NO_2^- or NO, inside or outside the cell, but is only shown with NO_2^- for brevity. The possible fractionation resulting from O exchange is shown as ε_{H2O}. Figure adapted from Figure 3 (Averill 1996) and Figure 1 (Steen et al. 2013).

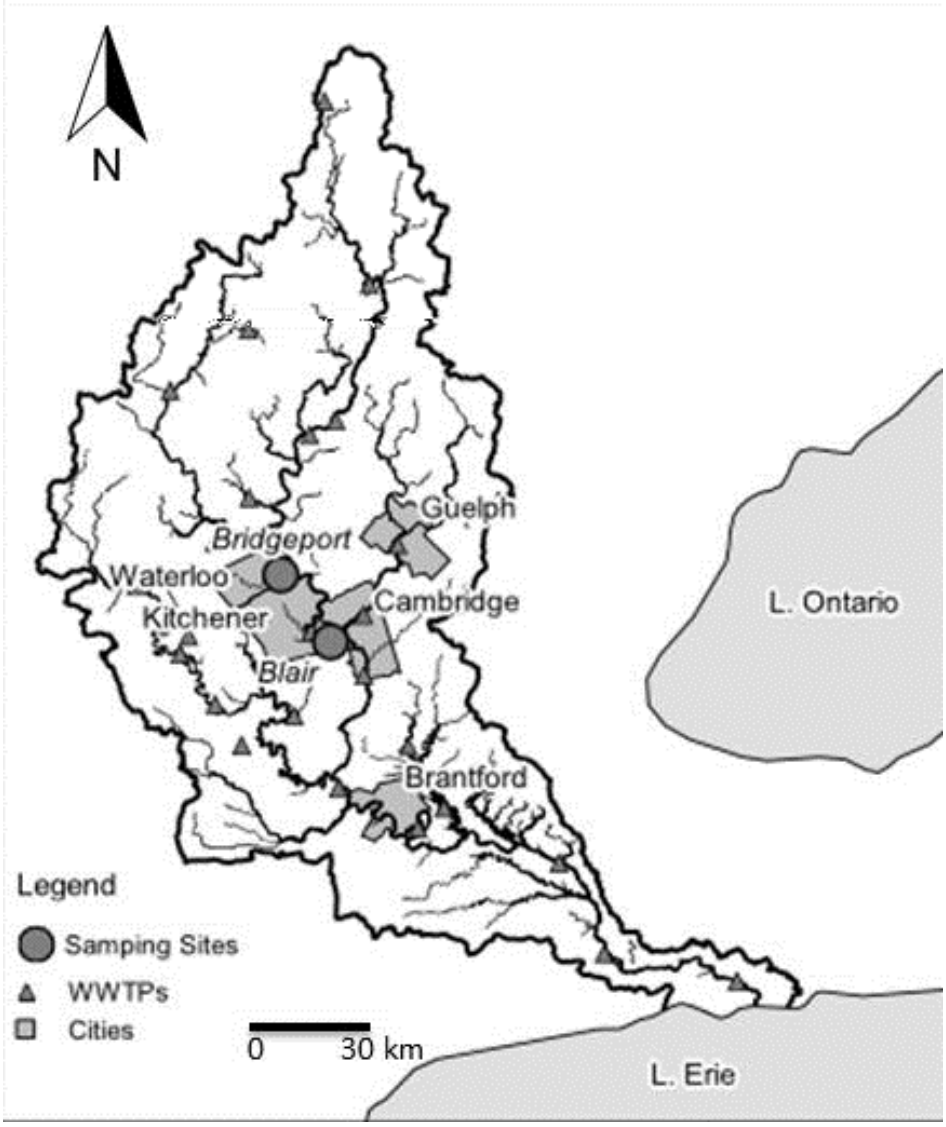

Figure 5.2: Map of the Grand River, Ontario, Canada, showing the sites were sediments were collected for incubations. Bridgeport is upstream of the central urban area, and Blair is 5 km downstream of the largest WWTP. Blair regularly experiences night-time hypoxia and high night-time N_2O fluxes in summer (see Chapter 2).

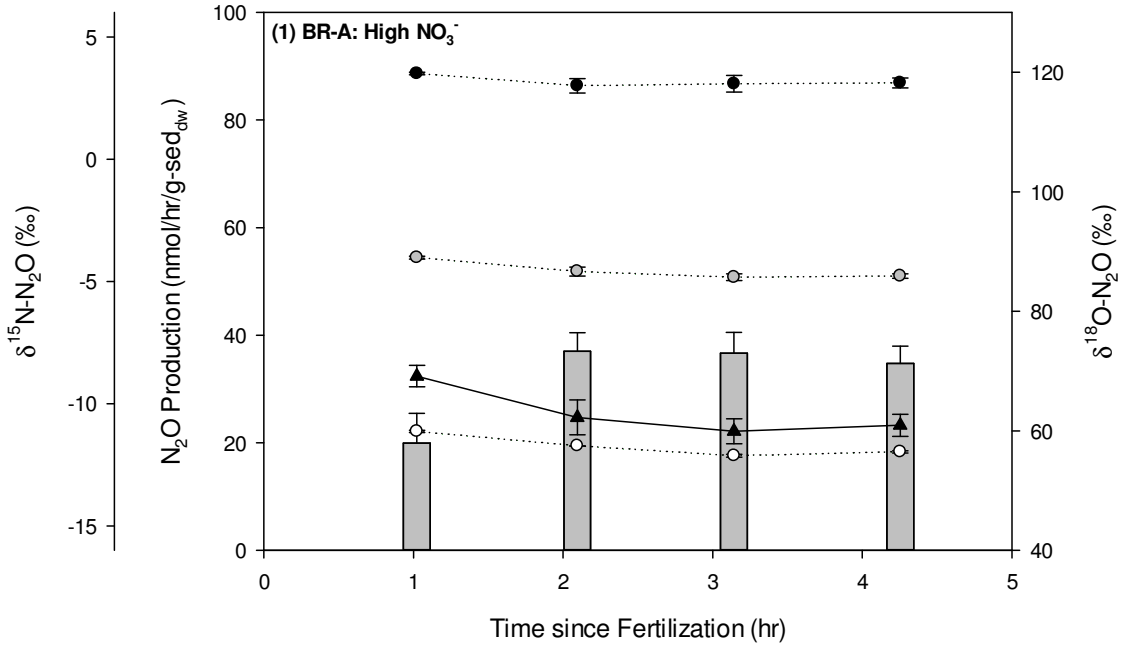
(1) BR-A: High NO3-
δ15N-N2O (‰)
N2O Production (nmol/hr/g-sedDW)
δ18O-N2O (‰)
Time since Fertilization (hr)

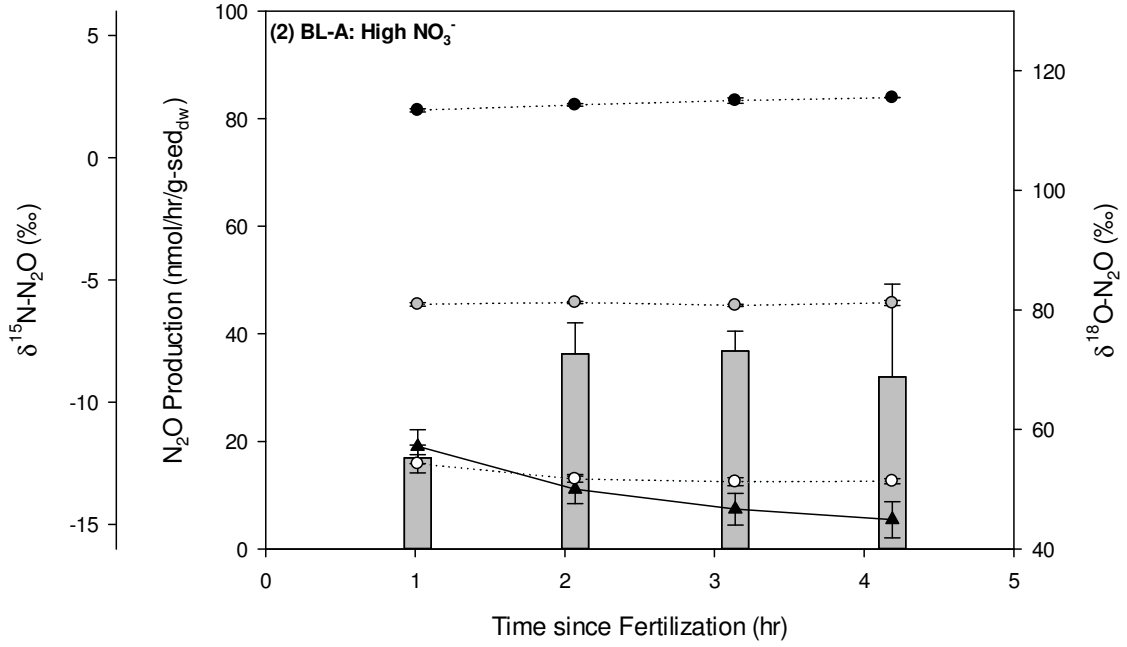
(2) BL-A: High NO3-
δ15N-N2O (‰)
N2O Production (nmol/hr/g-sedDW)
δ18O-N2O (‰)
Time since Fertilization (hr)

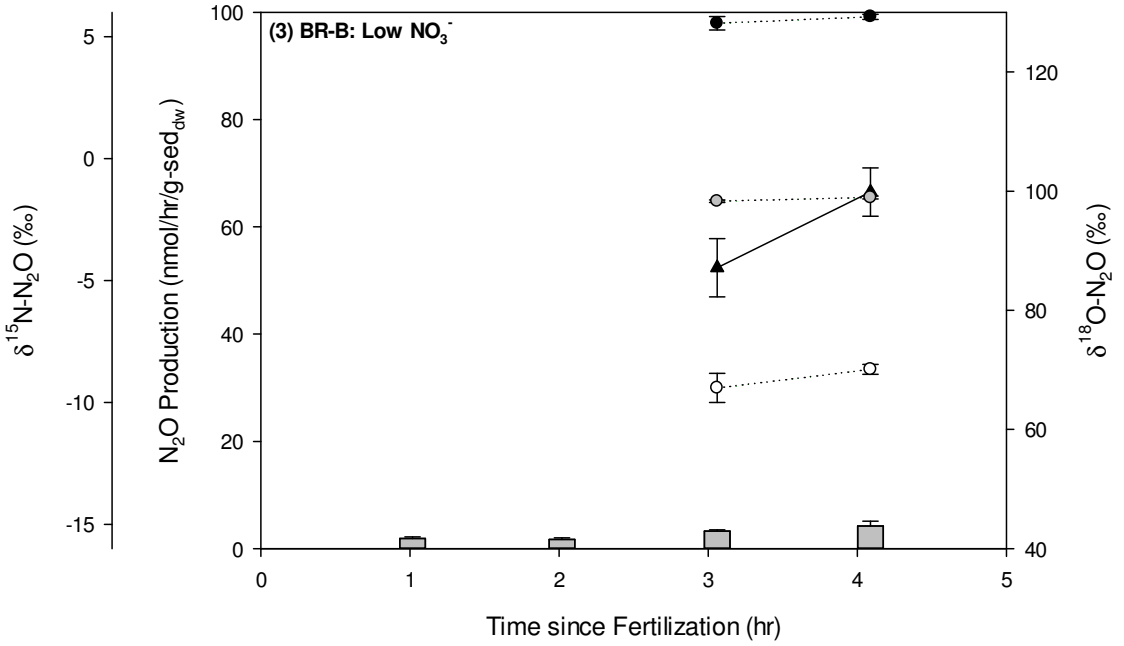
(3) BR-B: Low NO3-
δ15N-N2O (‰)
N2O Production (nmol/hr/g-sedDW)
δ18O-N2O (‰)
Time since Fertilization (hr)

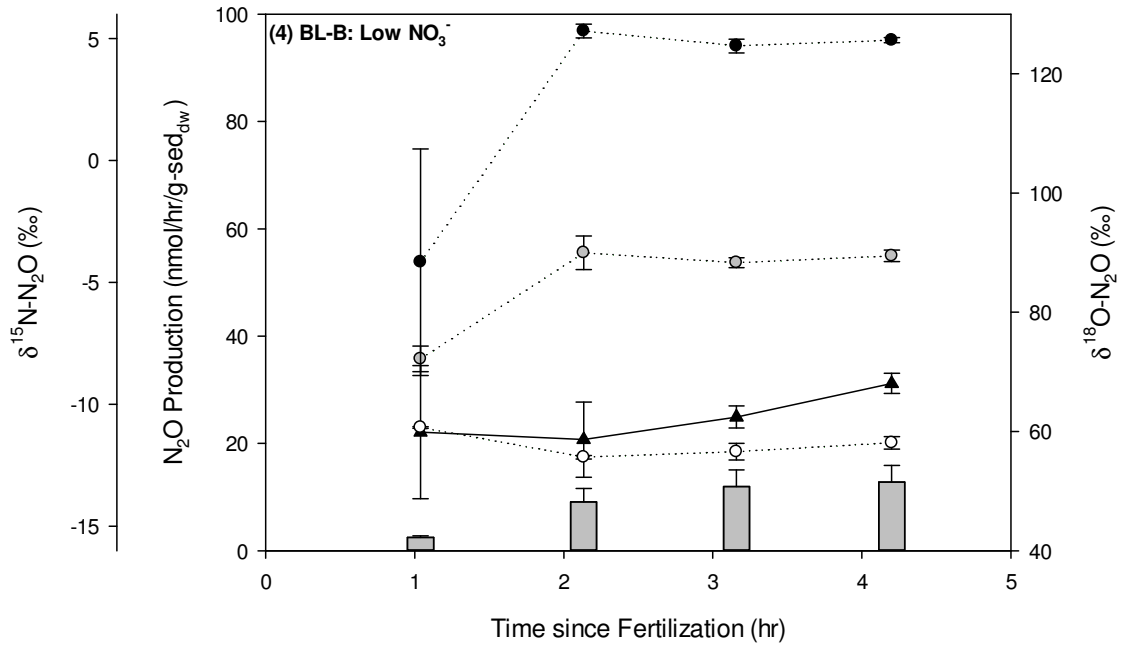
(4) BL-B: Low NO3-
δ15N-N2O (‰)
N2O Production (nmol/hr/g-sedDW)
δ18O-N2O (‰)
Time since Fertilization (hr)

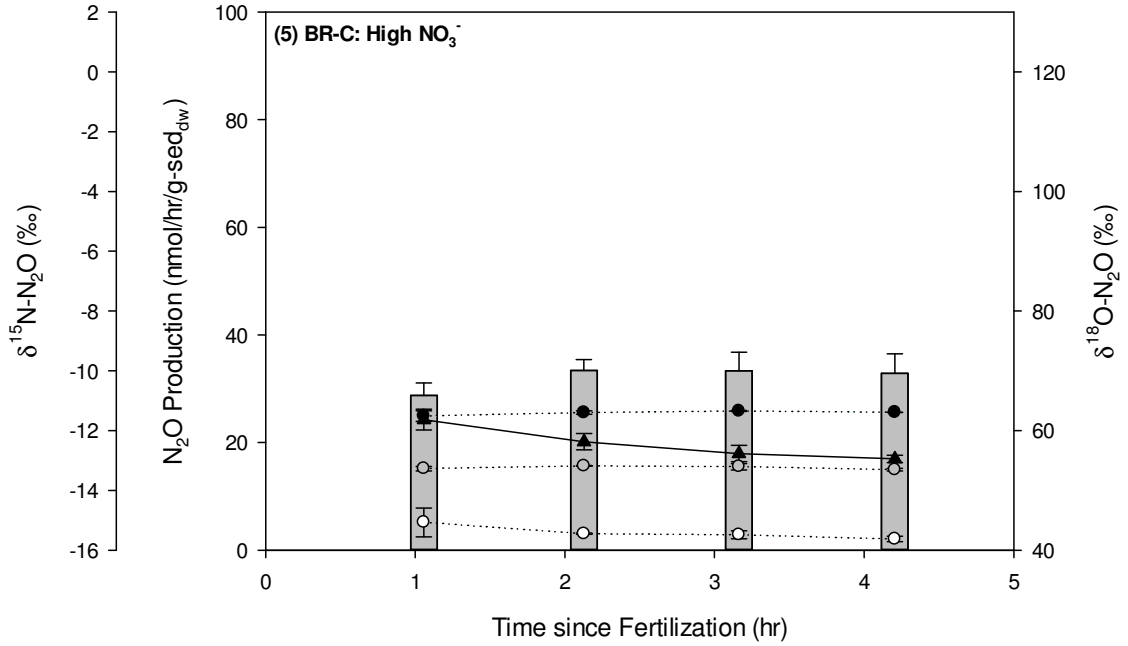
(5) BR-C: High NO_3^-
$\delta^{15}N\text{-}N_2O$ (‰)
N_2O Production (nmol/hr/g-sed_{dw})
$\delta^{18}O\text{-}N_2O$ (‰)
Time since Fertilization (hr)

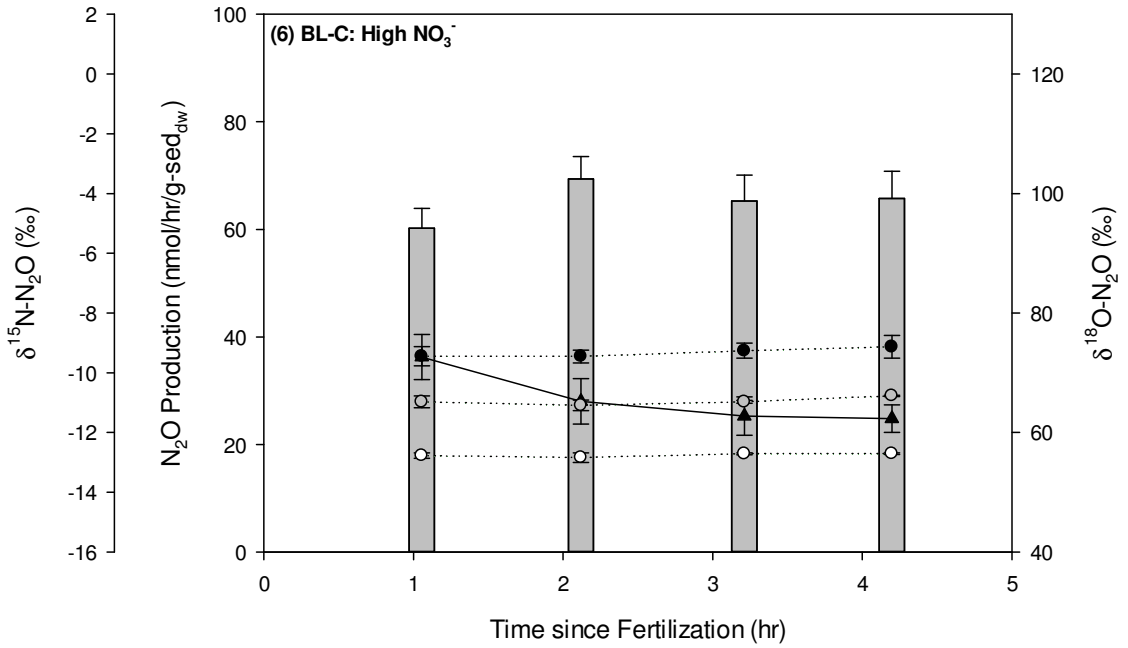
(6) BL-C: High NO_3^-
$\delta^{15}N\text{-}N_2O$ (‰)
N_2O Production (nmol/hr/g-sed_{dw})
$\delta^{18}O\text{-}N_2O$ (‰)
Time since Fertilization (hr)

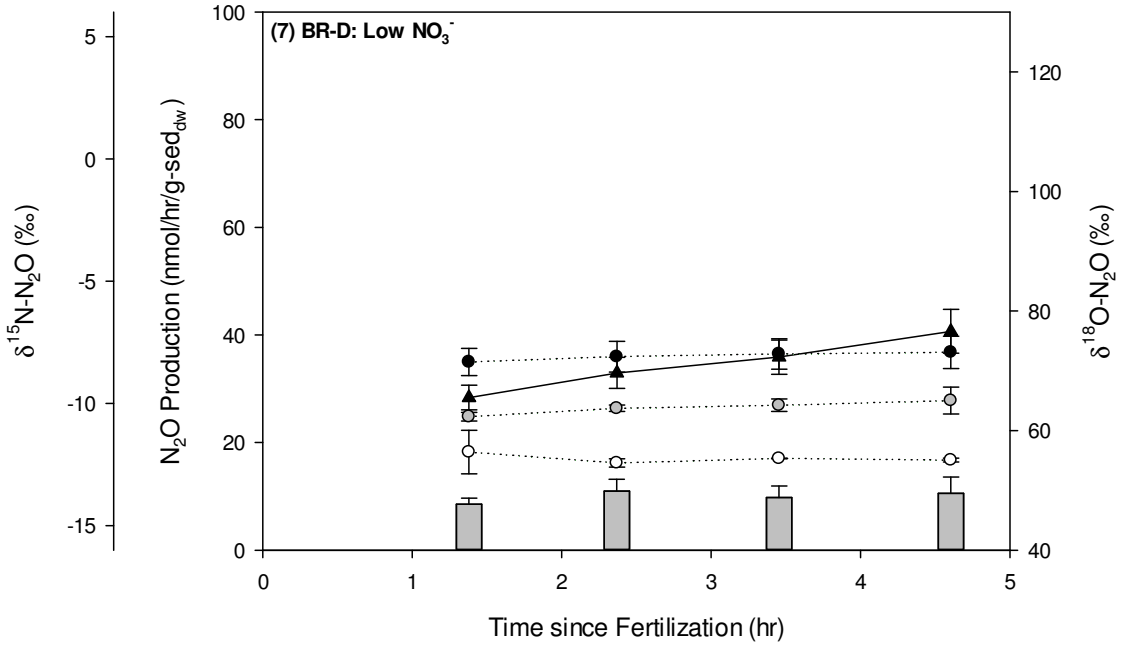
(7) BR-D: Low NO_3^-
N_2O Production (nmol/hr/g-sed_{dw})
$\delta^{15}N$-N_2O (‰)
$\delta^{18}O$-N_2O (‰)
Time since Fertilization (hr)

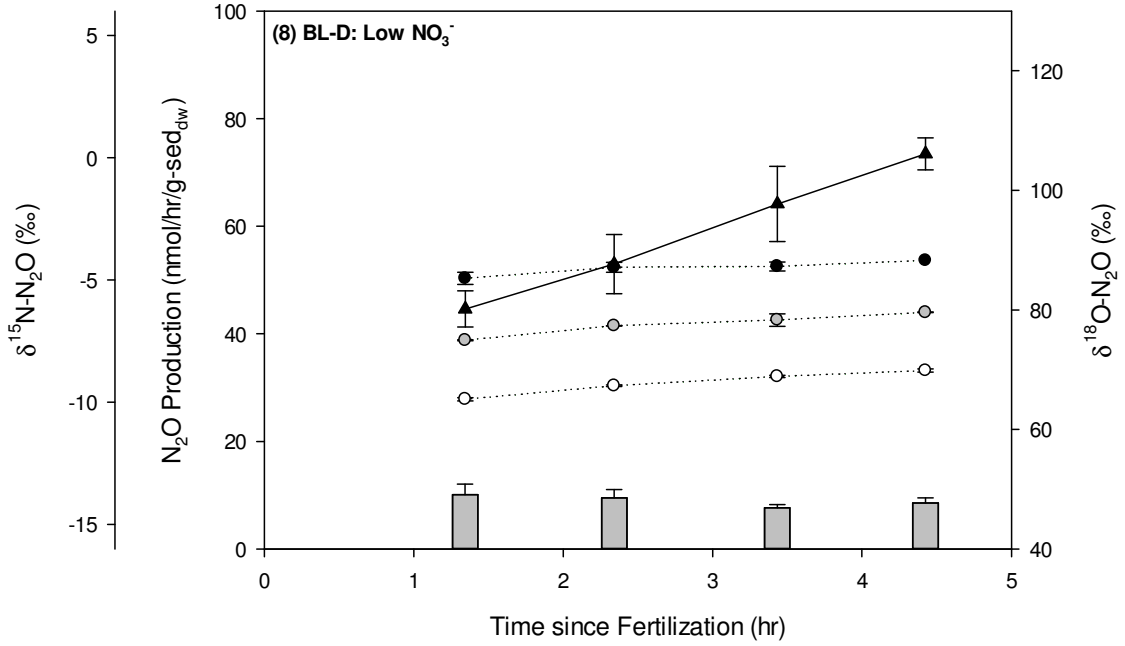
(8) BL-D: Low NO_3^-
N_2O Production (nmol/hr/g-sed_{dw})
$\delta^{15}N$-N_2O (‰)
$\delta^{18}O$-N_2O (‰)
Time since Fertilization (hr)

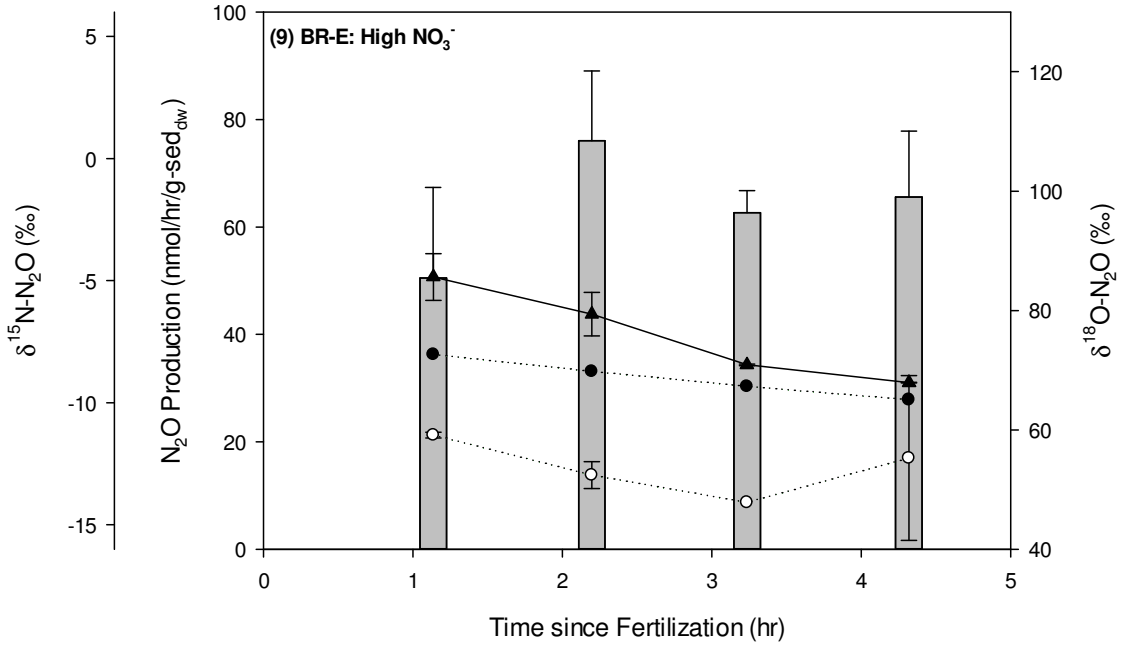
(9) BR-E: High NO_3^-
$\delta^{15}N\text{-}N_2O$ (‰)
N_2O Production (nmol/hr/g-sed_{dw})
$\delta^{18}O\text{-}N_2O$ (‰)
Time since Fertilization (hr)

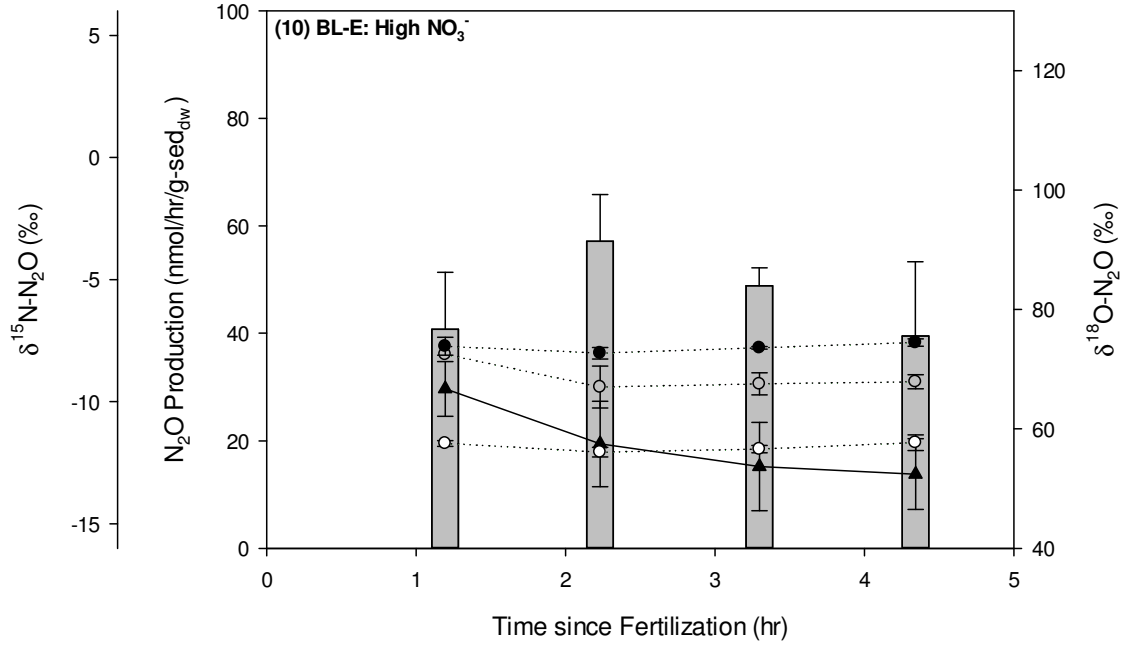
(10) BL-E: High NO_3^-
$\delta^{15}N\text{-}N_2O$ (‰)
N_2O Production (nmol/hr/g-sed_{dw})
$\delta^{18}O\text{-}N_2O$ (‰)
Time since Fertilization (hr)

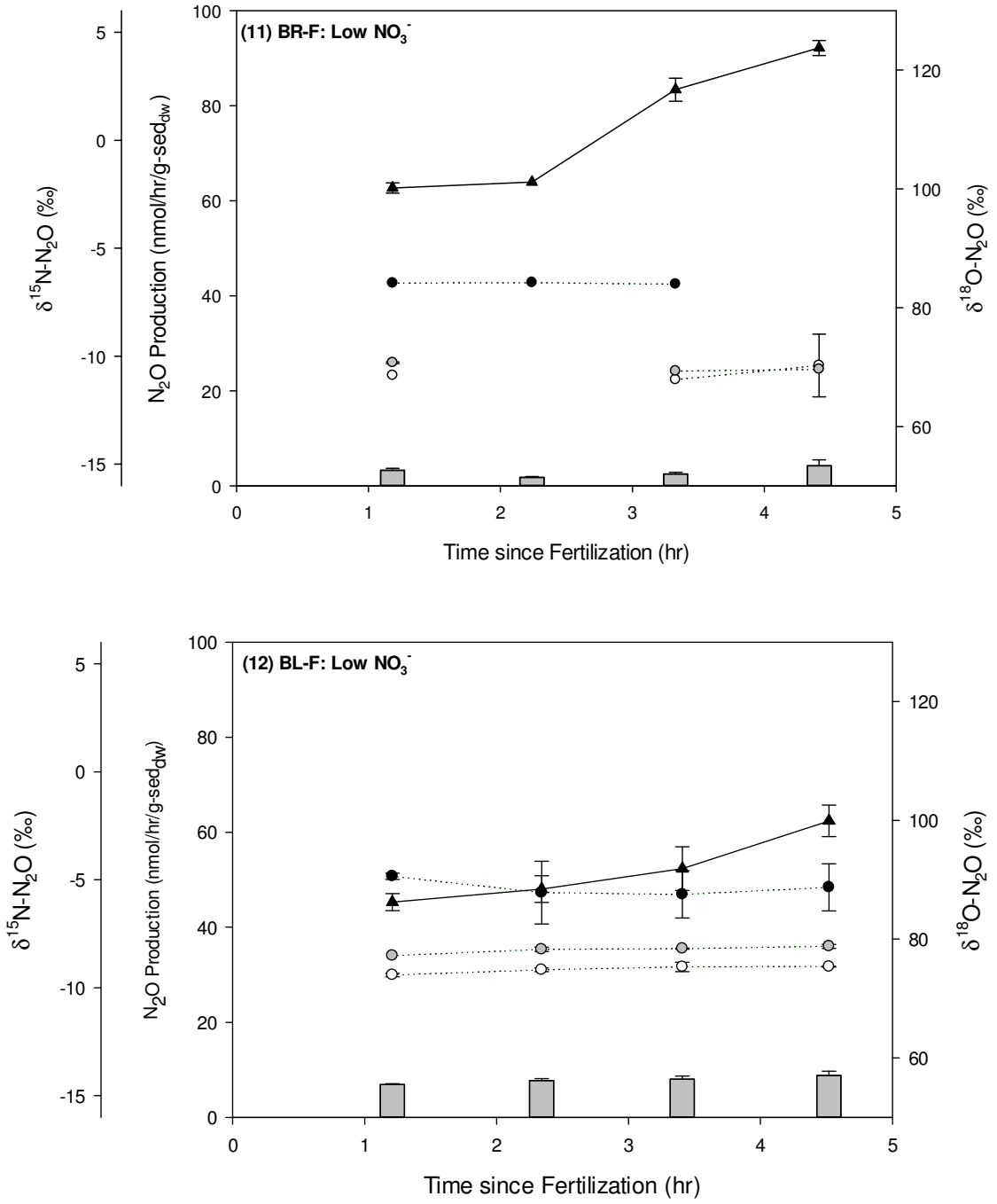

Figure 5.3: N_2O production rate (grey bars), $\delta^{15}N$-N_2O (rel. AIR) (black triangles) and $\delta^{18}O$-N_2O (rel. VSMOW) (white, grey and black circles) versus time for denitrification incubations of Grand River sediment collected at Bridgeport and Blair. Error bars represent standard deviation (n = 6 for N_2O production and $\delta^{15}N$, n = 2 for $\delta^{18}O$). White circles represent low $\delta^{18}O$-

H_2O addition; grey circles represent medium $\delta^{18}O$-H_2O addition, and black circles represent high $\delta^{18}O$-H_2O addition. Spring (panels 1 to 4), summer (panels 5 to 8) and summer (panels 9 to 12) incubations are shown.

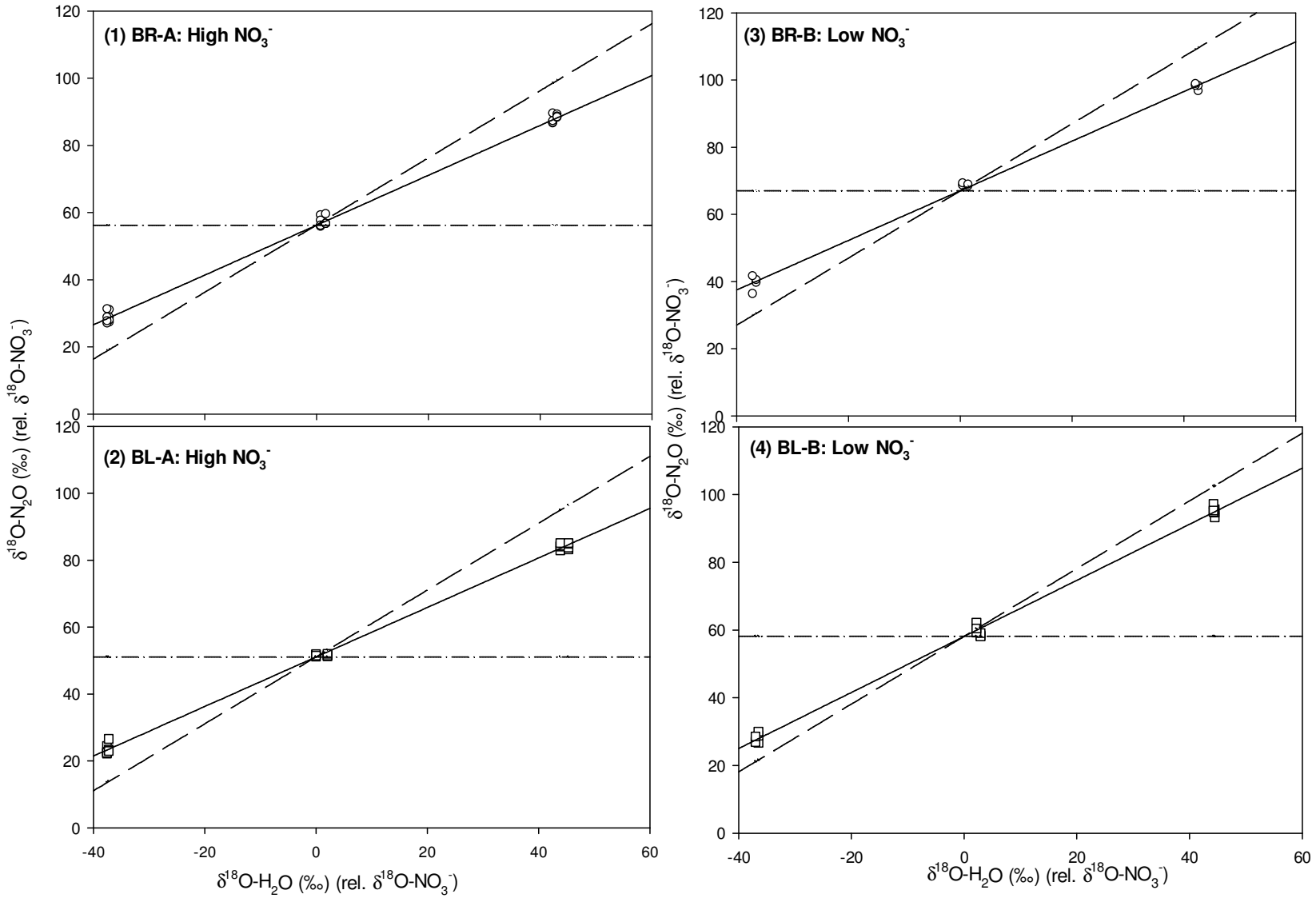
(1) BR-A: High NO3-
(2) BL-A: High NO3-
(3) BR-B: Low NO3-
(4) BL-B: Low NO3-
δ18O-N2O (‰) (rel. δ18O-NO3-)
δ18O-H2O (‰) (rel. δ18O-NO3-)
120
100
80
60
40
20
0
-40
-20
0
20
40
60

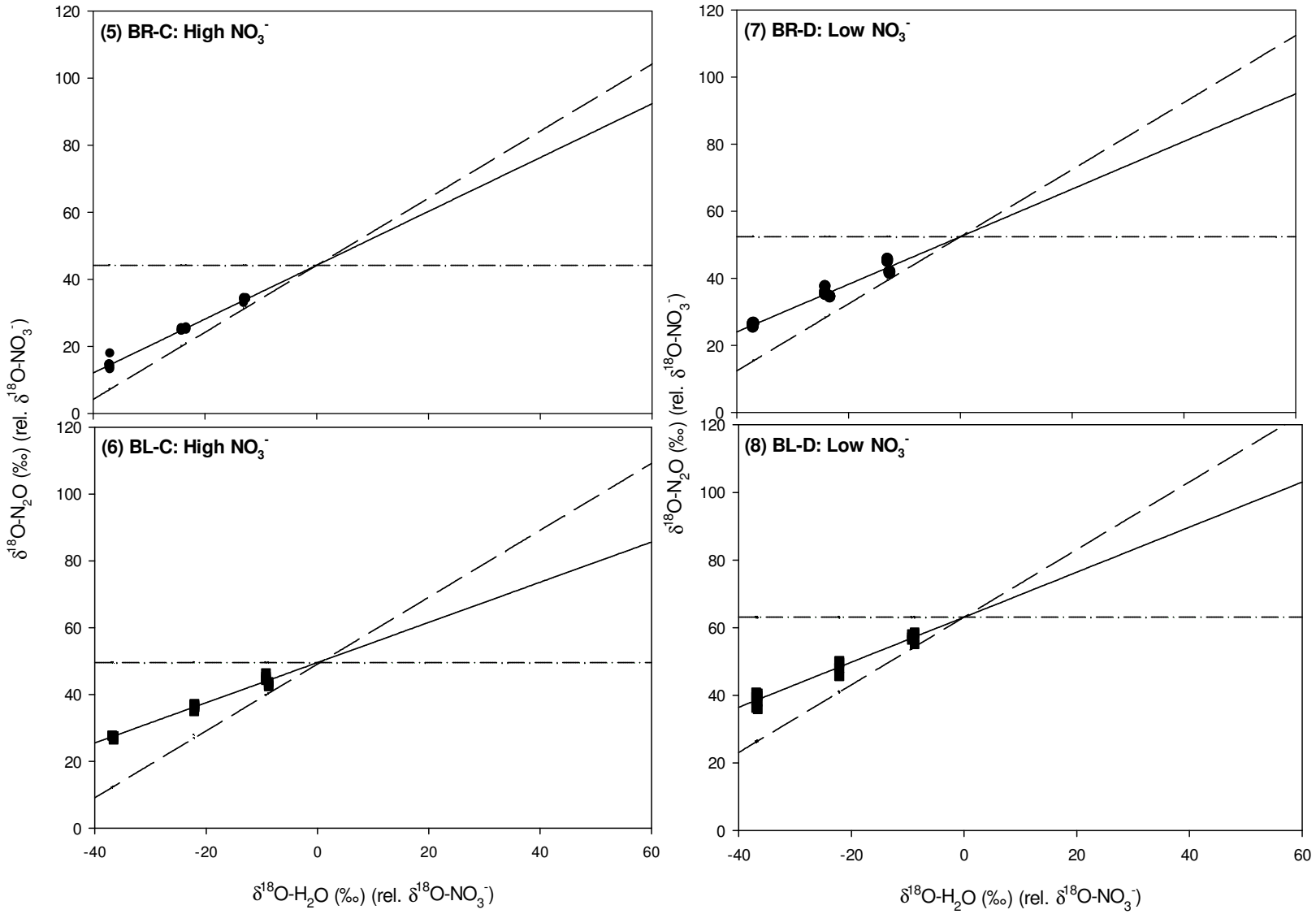
(5) BR-C: High NO3-
(6) BL-C: High NO3-
(7) BR-D: Low NO3-
(8) BL-D: Low NO3-
δ18O-N2O (‰) (rel. δ18O-NO3-)
δ18O-H2O (‰) (rel. δ18O-NO3-)
0
20
40
60
80
100
120
-40
-20
0
20
40
60

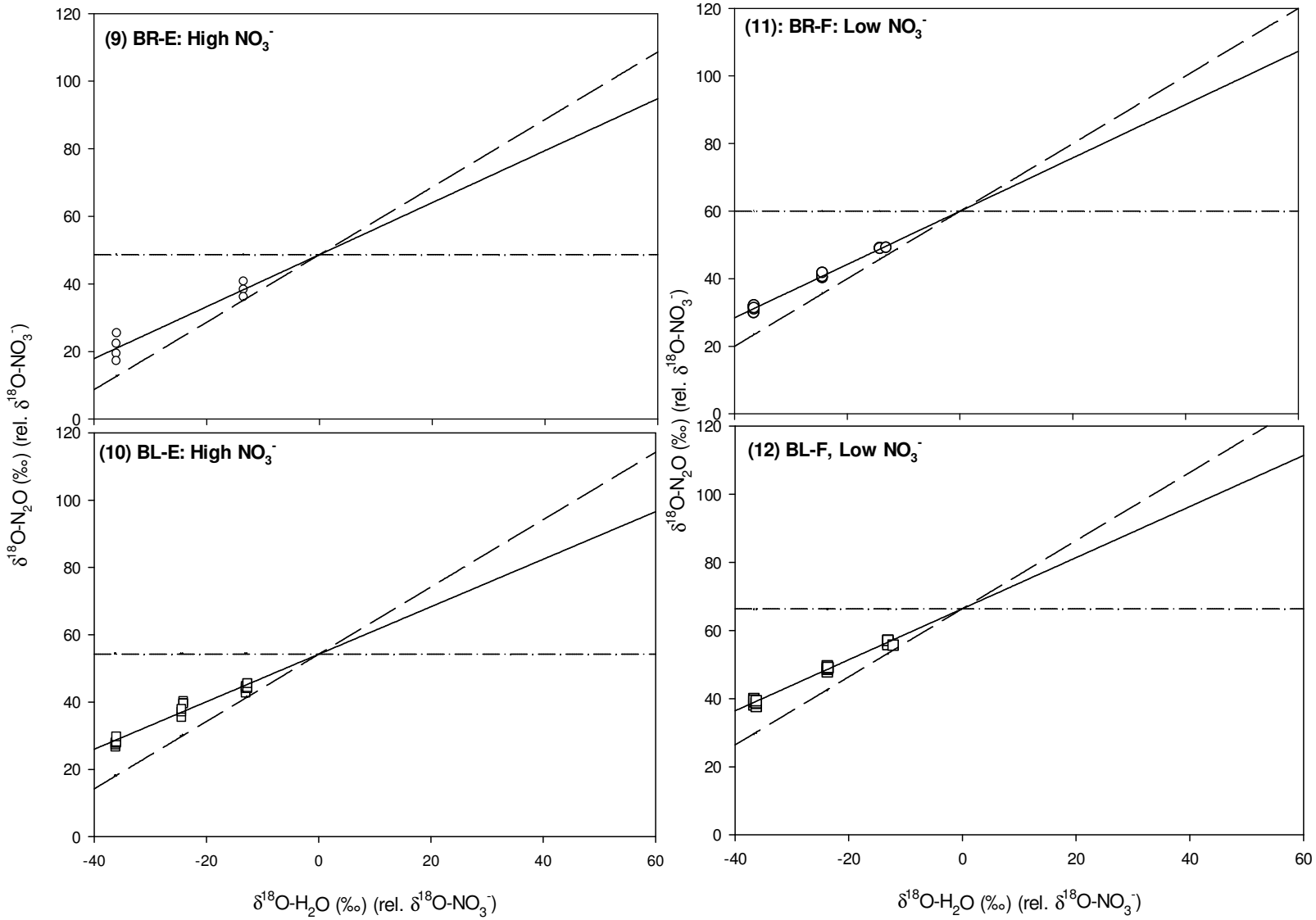
(9) BR-E: High NO_3^-
(10) BL-E: High NO_3^-
(11): BR-F: Low NO_3^-
(12) BL-F, Low NO_3^-
$\delta^{18}O$-N_2O (‰) (rel. $\delta^{18}O$-NO_3^-)
$\delta^{18}O$-H_2O (‰) (rel. $\delta^{18}O$-NO_3^-)
0
20
40
60
80
100
120
-40
-20
0
20
40
60

Figure 5.4: The relationship between $\delta^{18}O\text{-}H_2O$ and $\delta^{18}O\text{-}N_2O$ in denitrification incubations, indicating that O exchange occurs. Horizontal lines represent no O exchange. Angled dashed lines represent 100% O exchange. The slope of the best-fit line is the fraction O exchange and the y-intercept is the $\varepsilon_{net}{}^{18}O$ (with O exchange removed). Spring (panels 1 through 4), summer (panels 5 to 8) and autumn (panels 9 to 12) are shown. High-NO_3^- incubations (1.3 mg N/g-seddw) are shown on the left and lower-NO_3^- incubations (0.8 mg N/L) are shown on the right. $\varepsilon_{net}{}^{18}O$ values and fraction O exchange are summarized in Table 5.4.

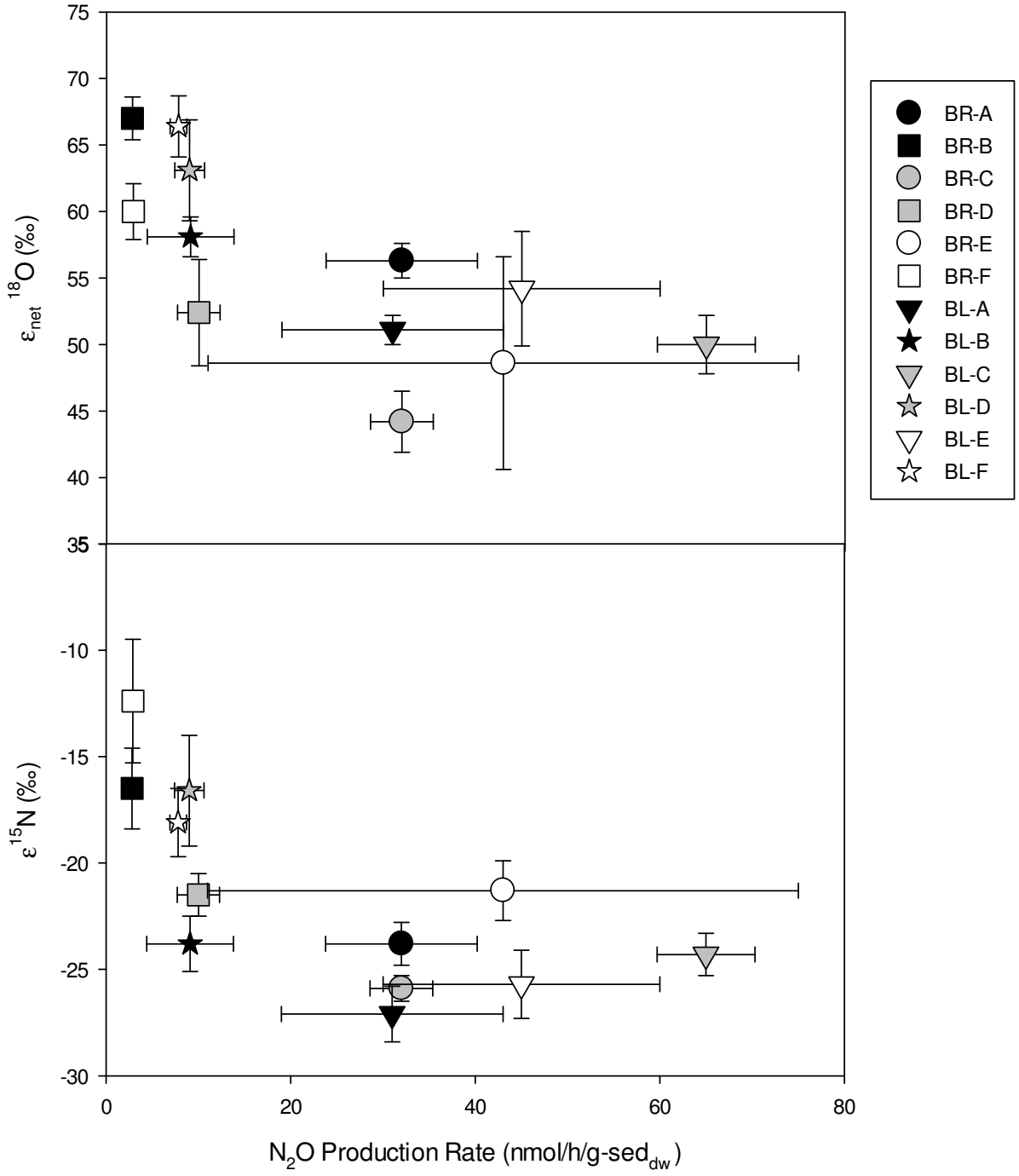

Figure 5.5: Net N_2O production rate versus $\varepsilon^{15}N$ (top) and $\varepsilon_{net}{}^{18}O$ (bottom) in incubations. Spring: grey; summer: black; autumn: white. Circles and triangles: high NO_3^- additions; squares and stars: low NO_3^- additions.

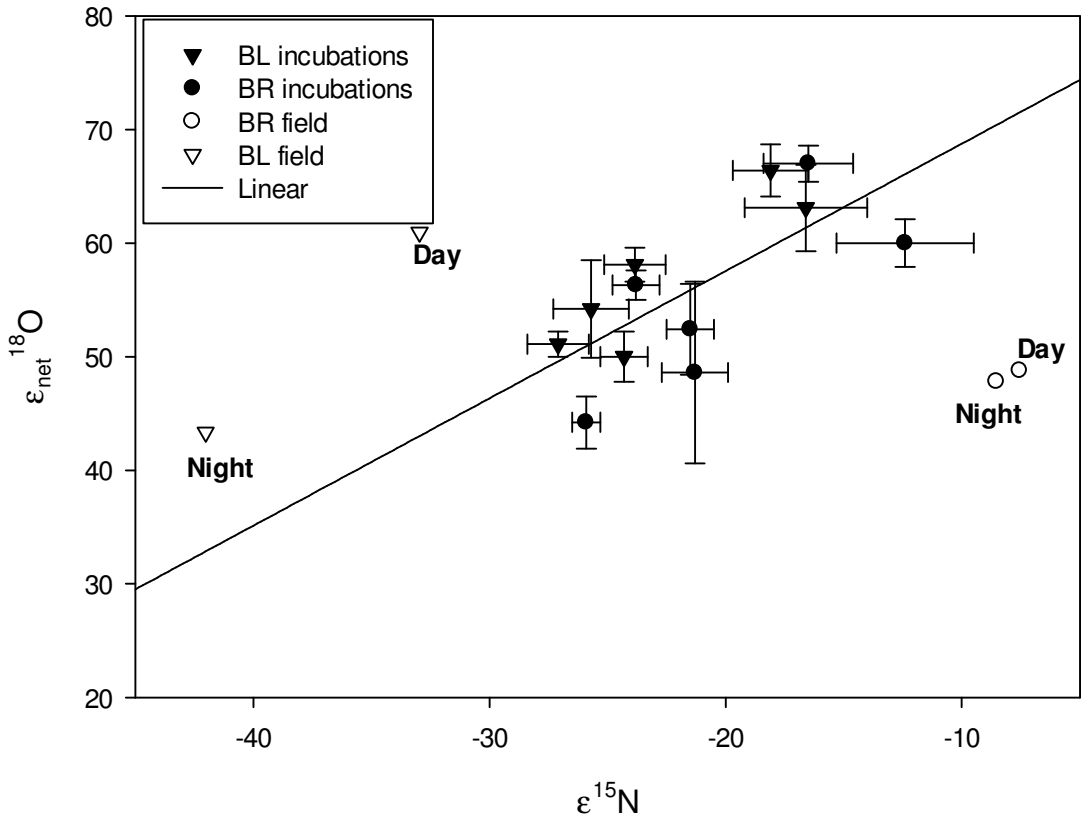

Figure 5.6: Denitrification isotopic fractionations ($\varepsilon^{15}N$ and $\varepsilon_{net}{}^{18}O$) for all incubations and for estimated field values from Bridgeport and Blair. Day and night isotopic fractionation values are shown because of diel changes in the isotopic ratios of NO_3^- and N_2O in the Grand River. The linear relationship (all incubation points) has a slope of 1.1 ($r^2 = 0.51$).

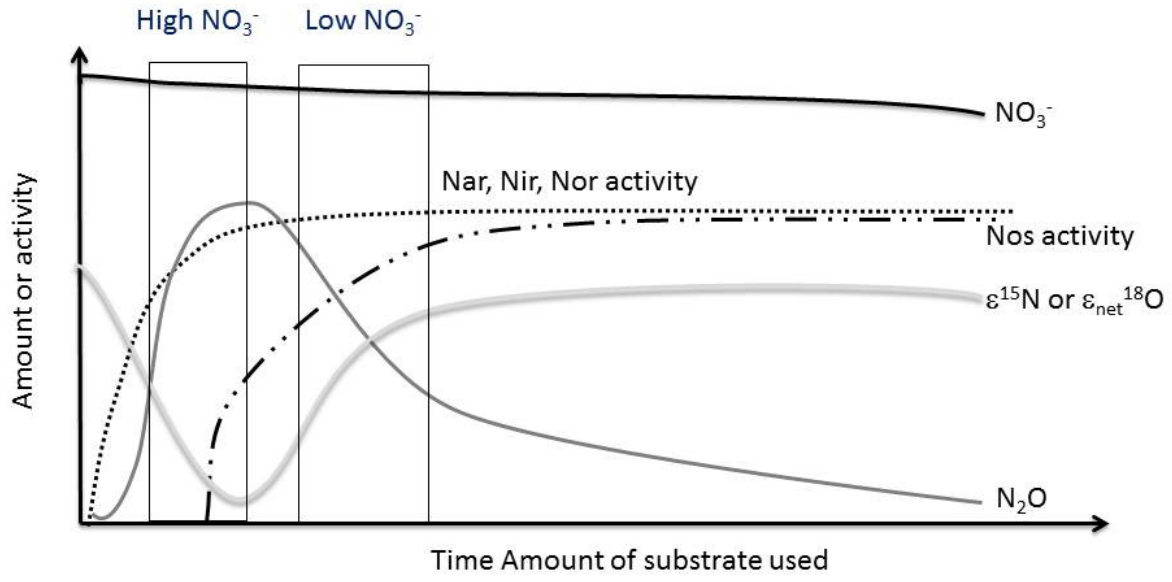

Figure 5.7: Conceptual model showing a possible mechanism for lower N_2O yield and higher $\varepsilon^{15}N$ and $\varepsilon_{net}{}^{18}O$ values in low-NO_3^- incubations. Denitrification enzymes and concentrations of N compounds are known to vary over time on the onset of conditions favouring denitrification (i.e. anoxia, NO_3^- supply).The lag in N_2O reductase (Nos) results in an initial peak, then decline, of N_2O. The temporal locations of high- and low-NO_3^- incubations discussed in this study are shown in boxes. A positive relationship between Nos lag time and NO_3^- substrate concentration has not been demonstrated but is required to validate this model.

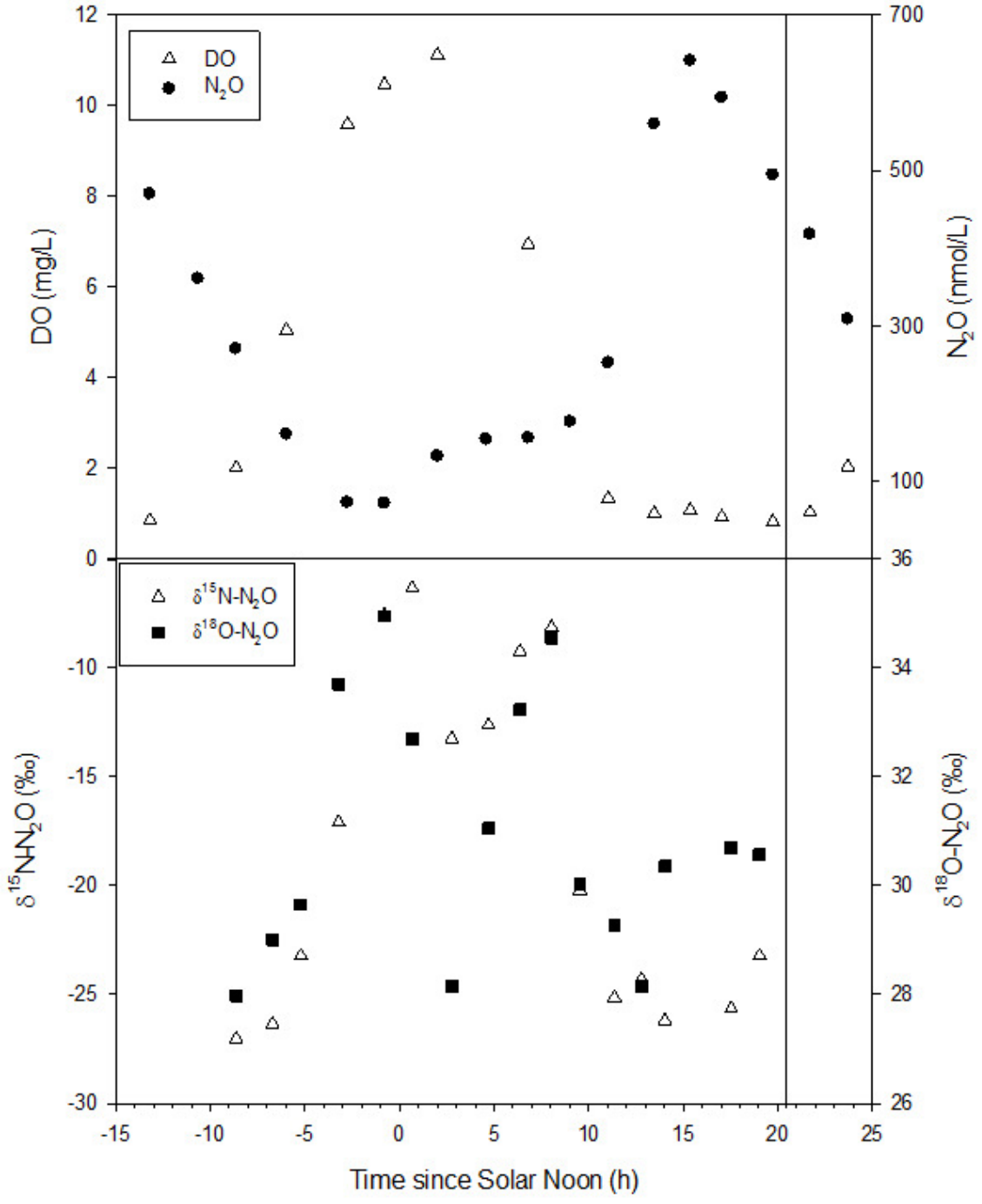

Figure 5.8: Diel changes in DO, N_2O concentration, $\delta^{15}N$-N_2O and $\delta^{18}O$-N_2O at Blair on June 26-27, 2009. The vertical line indicates dawn (5:45 AM, EDT). Note that N_2O concentrations peak around the onset of minimum DO concentration.

Chapter 6: NO_3^- Inputs, Losses and Stable Isotopic Values in the Grand River, Ontario

Abstract

Nitrate (NO_3^-) can contaminate drinking water and impact riverine ecological health. Though rivers in agricultural catchments are susceptible to high NO_3^-, watershed NO_3^- dynamics are variable and difficult to predict. NO_3^- concentrations and $\delta^{15}N$ values were measured at 23 sites along the entire Grand River in early summer, later summer and spring. Using flow and surface area information for each reach, a NO_3^- mass balance was created. Denitrification was estimated by multiplying areal N_2O flux with a range of values representing N_2O:(N_2O+N_2) ratios produced during denitrification. The river was divided into four sections based on land use and geomorphology (Upper Agricultural, Urban, Groundwater Recharge and Lower Agricultural). The river almost always gained NO_3^- in each reach. However, areal NO_3^- gains were lowest in the Upper Agricultural section. Denitrification and other NO_3^- losses were low relative to other fluxes but were highest in the Urban and Lower Agricultural sections. Estimated $\delta^{15}N$-NO_3^- values of NO_3^- added to the river were generally consistent with previously measured $\delta^{15}N$-NO_3^- values for inputs to the Grand River, such as tributaries in the Upper Agricultural section, WWTP effluent in the Urban section, and groundwater in the Groundwater Recharge section. Estimated NO_3^- inputs were much lower than watershed-scale NO_3^- leaching, indicating that 68% to 83% of NO_3^- loss occurs in smaller streams, wetlands and riparian zones in this watershed and never enters the Grand River. 5% to 19% of watershed NO_3^- was lost in the river, and 13% was exported to Lake Erie. Denitrification and other NO_3^- losses reduce NO_3^- concentration in the Grand by < 2 mg N/L at most sites and times. This study underestimates annual NO_3^- export to Lake Erie (because storms and snowmelt were not included), indicating that the Grand River denitrifies an even smaller percentage of incoming NO_3^- than estimated. Low denitrification rates are surprising, given that the Grand River has ideal conditions for high denitrification rates (high NO_3^-, high dissolved organic carbon, low dissolved oxygen and high sediment surface-to-volume ratio). Low in-river denitrification rates and undesirable side effects of hypoxia in rivers suggest that effective NO_3^- reduction on the watershed scale involves reducing NO_3^- application to the watershed (via agricultural best management practices) and creating denitrification hotspots on the landscape such as wetlands and riparian zones.

6.1 Introduction

Nitrate (NO_3^-) is often the most common form of inorganic, biologically reactive nitrogen in freshwaters (Burgin and Hamilton 2007). It is an important macronutrient, and can limits primary productivity in freshwater environments, particularly in high-phosphate systems (Davidson and Seitzinger 2006). Excess NO_3^- can contribute to eutrophication of freshwaters, which can cause algal blooms, hypoxia (dissolved oxygen (DO) < 2 mg/L), fish kills and reduced biodiversity (Cameron et al. 2013).

The Grand River watershed, southern Ontario, Canada is dominated by agriculture and has several large urban wastewater treatment plants (WWTPs). The river has moderate to high nitrate (NO_3^-) concentrations (below detection to ~10 mg N/L). NO_3^- concentration generally increases downstream, and NO_3^- can approach or exceed drinking water limits (10 mg N/L, (Health Canada 2012)) especially in the Upper Agricultural area, which has been attributed to N leaching from agriculture (Cooke 2006).

High riverine NO_3^- (and NH_4^+) can affect communities that rely on the Grand River for drinking water, such as Brantford (population: 90 000). Additionally, The Grand River is the largest Canadian river entering Lake Erie, which has impacted water quality, including algal blooms resulting in hypoxia and fish kills (Vanderploeg et al. 2009). The Saint Lawrence River and estuary, downstream of Lake Erie, also experience eutrophication, and hypoxia-related fish kills (Ouellet et al. 2010).

There is therefore much interest in the assimilative capacity of nutrients of the Grand River. Large WWTPs in the watershed are currently scheduled to upgrade from ammonium (NH_4^+) to NO_3^- effluent release in 2018 (Ouellet et al. 2010). Simulations run on the Grand River Simulation Model (GRSM) have indicated that NO_3^- concentrations will increase dramatically in winter after this change (Ouellet et al. 2010).

Currently, it is unclear how NO_3^- sources to the Grand River (agricultural fertilizers and manure, WWTP effluent, etc.) change spatially and temporally. NO_3^- use and production in the river is also not well-understood. NO_3^- is likely being continually assimilated and released by organisms in river, but net changes in river NO_3^- resulting from biological cycling are unknown. Similarly, denitrification (sequential anoxic reduction of NO_3^- to N_2O and N_2) occurs, indicated by high N_2O fluxes during hypoxia events in the Grand River (Chapters 2 and 3), but the rates and spatial distribution are

unknown. Denitrification occurs continually at relatively low rates in oxic water systems, likely in anoxic sediments (Chapters 3 and 5). Net nitrate loss (attributed to denitrification) and gain can occur in reservoirs in the Grand River, but this depends on season and reservoir management (B. De Baets, personal communication).

Denitrification rates in rivers can be difficult to measure because they are spatially and temporally variable (Baulch et al. 2010), requiring good sampling coverage, and because N_2 is difficult to measure without atmospheric contamination. In small streams, ^{15}N tracers can be added, and any $^{15}N_2$ or $^{15}N_2O$ produced attributed to denitrification (Mulholland et al. 2004, Mulholland et al. 2008). This is impractical for large rivers. Instead, previous studies in large rivers have used N mass balances in rivers, measuring concentrations of NO_3^- and N_2, and attributing all N_2 above atmospheric saturation to denitrification (Pribyl et al. 2005). This approach tends to produce large errors because rivers are seldom at atmospheric equilibrium, particularly as water temperatures change on a diel scale. This problem is addressed by a denitrification model measuring the ratio of dissolved N_2 to dissolved argon (Ar) in the river, which corrects for temperature-based disequilibrium with biologically-inert Ar (Laursen and Seitzinger 2002). The model requires very precise sampling to avoid contamination with air and a specialized membrane-inlet mass spectrometer (MIMS). It was unsuccessfully attempted at two sites in the Grand River in 2007 and 2008. Ar and N_2 concentrations increased with temperature instead of decreasing, suggesting that external Ar sources (e.g. groundwater) were more significant than temperature effects. N_2-Ar sampling can also be compromised by N_2 losses via biological N_2 fixation, and N_2 production by other biological reactions such as anammox.

Other approaches include measuring natural abundance $\delta^{15}N\text{-}NO_3^-$ in rivers and calculating NO_3^- loss when the isotopic fractionation factor is known using the Rayleigh equation (Johannsen et al. 2008). However, this approach cannot detect low denitrification rates. For example, if the initial $\delta^{15}N\text{-}NO_3^-$ value is 10‰ and a typical isotope fractionation factor (α) of 0.985, losing 10% of the original pool of NO_3^- results in a change in $\delta^{15}N\text{-}NO_3^-$ of 1.6‰, which may well be within natural variability of NO_3^- sources to the river. The Rayleigh equation describes systems that are closed to substrate (i.e. no NO_3^- is added as denitrification occurs) and in which products (N_2O, N_2) are instantaneously removed; these conditions are unlikely in rivers dominated by multiple non-point sources of NO_3^-. This approach also ignores completed denitrification in sediments, in which no NO_3^- remains for measurement (Mayer et al. 2002).

One by-product of denitrification unused by the methods above is nitrous oxide (N_2O). N_2O is an obligate intermediate in denitrification and is relatively easy to measure with an electron capture detector on a gas chromatograph. Assuming steady state N_2O production, N_2O flux to the atmosphere equals N_2O production rate. N_2O flux rates can be converted to denitrification rates by estimating an N_2O:N_2 ratio for denitrification production. This ratio has been shown to vary with redox conditions (Silvennoinen et al. 2008), NO_3^- and nitrite (NO_2^-) concentration (Firestone et al. 1980, Silvennoinen et al. 2008) and temperature (Silvennoinen et al. 2008), as discussed in Chapter 5. However, a range of ratios can be used to estimate likely minimum and maximum denitrification rates.

A benefit of using N_2O to estimate denitrification is that N_2O is almost exclusively produced by denitrification (as nitrification yields of N_2O are low), while N_2 is produced by other biological reactions such as anammox (anaerobic ammonia oxidation) and is used by N_2 fixing organisms (e.g. cyanobacteria, heterotrophic bacteria and fungi). Likewise, NO_3^- loss in rivers could be due to biological reactions such as assimilation and dissimilatory nitrate reduction to ammonia (DNRA). N_2O is also produced by hydroxylamine oxidation during nitrification (oxidation of NH_4^+ to NO_3^-) (see Section 1.21). However, N_2O production by this pathway in rivers is typically low for a variety of reasons. NH_4^+ concentrations are low in rivers (Stief et al. 2003) because of rapid biological uptake, which has much higher rates than nitrification (Webster et al. 2003). Little N_2O is produced per mole NH_4^+ nitrified under oxic conditions (Klemedtsson et al. 1988). N_2O is produced at higher rates by "nitrifier-denitrification", or NO_2^- reduction by nitrifiers in anoxic conditions (see Section 1.2.4); this is considered part of denitrification in this study. Therefore, N_2O production in the Grand River is entirely attributed to denitrification in this study.

Denitrification rates in rivers are not well-quantified, even though there is much interest in using rivers (as well as wetlands, riparian zones, groundwater, etc.) to naturally attenuate NO_3^- before it enters coastal areas (Groffman et al. 2006). Similarly, it is difficult to quantify N inputs on the watershed scale. A common approach is NANI (Net Anthropogenic Nitrogen Inputs), in which anthropogenic N inputs to a watershed are tallied. There is a linear relationship between NANI (normalized to watershed surface area) and N export (normalized to surface area) in temperate watersheds ($r^2 = 0.60$, $n = 154$, (Howarth et al. 2012)), which is used to estimate watershed N export from watersheds. NANI includes N from fertilizers, manure, N fixation by crops, atmospheric N deposition and net movement of N in human and animal feed to or from the watersheds. The last two

parameters can be difficult to measure. Predictability can be increased slightly by including discharge (Q) and splitting data at a NANI value of 1070 kg N/km^2/yr. However, this this method does not address in-stream N processing or examine N export on a seasonal and spatial scale within a watershed.

Additionally, the amount of N entering large rivers from watersheds is not well understood because the amount of N lost or stored in soils, wetlands, groundwater and tributaries is not well quantified. This value can be estimated with mechanistic watershed models (e.g. SWAT, RiverStrahler), but these require significant input data. For instance, mandatory inputs for SWAT are a digital elevation model, a land cover/crop database, soil layers, a tillage database, sub-basin parameters, and land management scenarios (Arnold et al. 2011). Mandatory inputs for RiverStrahler are physical parameters (slope, length of rivers and tributaries; area of ponds and reservoirs, and total watershed area) and meteorological data (rainfall, evapotranspiration, snow and air temperature) (Sferratore et al. 2005). However, a NO_3^- isotope mass balance using river NO_3^- masses and $\delta^{15}N\text{-}NO_3^-$ values and denitrification estimates from N_2O fluxes can predict the amount of N entering the river for comparison with watershed N application with minimal inputs. This approach can shed light on the efficiency of the watershed versus the main stem river for removing NO_3^- as well as address NO_3^- exports from the watershed compared to watershed NO_3^- loading.

Thus, the purpose of this study is to create a NO_3^- mass balance for the entire Grand River. Denitrification will be estimated using N_2O fluxes as described above, and sources and sinks of NO_3^- in the river will be investigated. Because mass balances only examine net fluxes to and from the river, a companion NO_3^- isotope mass balance was also created. This is useful, as $\delta^{15}N\text{-}NO_3^-$ values can be distinct for different NO_3^- sources (e.g. synthetic fertilizer vs. manure or sewage). When NO_3^- is lost from a reach, the apparent isotopic fractionation between NO_3^- in the reach and the net loss can be calculated. This can help determine the method of loss, as no isotopic fractionation is known to occur with biological assimilation of NO_3^- but denitrification has a strong isotopic fractionation. Similarly, the isotopic ratios of net NO_3^- gain can be calculated; this can be compared to isotopically characterized sources of NO_3^- to the river (e.g. tributaries, groundwater, WWTP effluent) to determine important sources of NO_3^- to river.

The last purpose of this study is to tally estimated NO_3^- sources to the river (WWTP effluent, N leaching from agricultural fertilizers, manure and crop residue) and compare to NO_3^- losses from and

gain to the Grand River. This could provide valuable information on relative rates of NO_3^- loss in the main river channel versus in smaller tributaries, wetlands and riparian zones in the watershed, thus helping focus N management policy.

6.2 Methods

6.2.1 Site Descriptions

The Grand River is a 300 km-long, seventh-order river in southern Ontario, with an average annual discharge of 56 m^3/s to Lake Erie (Aquaresource 2009). The watershed substrate is mostly calcite-rich glacial till and glaciolacustrine clay. In some areas, limestone bedrock is exposed. About 70% of the 7000 km^2 watershed is used for agriculture. Corn, soybeans and alfalfa are the most common crops (2006 Canada Census data clipped to the Grand River Watershed, Grand River Conservation Authority, personal communication). Over half of the 975 000 watershed residents live in cities with wastewater treatment plants (WWTPs).

For this study, the entire river from headwaters to mouth was sampled. Twenty-three sampling sites along the river (Figure 6.1) were chosen to correspond to Provincial Water Quality Monitoring Network (PWQMN) sites (Sites 3, 5, 6, 8, 9, 10, 11, 13, 20 and 22), Grand River Conservation Authority water quality monitoring sites (Sites 6, 9, 11, 13, 16, 20, 23) or flow gauged sites (Sites 1, 3, 6, 8, 9, 20, 22), or are influenced by points of interest such as dams (Sites 6, 12 and 21), WWTPs (Sites 10, 11, 12, 15 and 17) and tributaries (Sites 9, 12, 15 and 18) (Table 6.1). The sites can be grouped based on geomorphology and land use as follows:

Upper Agricultural Section (Sites 1 to 9):

This section is characterized by compacted glacial diamict and hummocky topography (Karrow and Morgan 2004). Regional groundwater input is minimal due to the low permeability of the diamict though local groundwater inputs in sandy and gravelly areas exist (Cooke 2006). Land use is primarily agricultural. Small WWTPs on the Grand River are found in the towns of Dundalk (population: 2000), Grand Valley (population: 2700), Fergus (population: 19 000), Elora (population: 4 500) and Conestogo (population: 1300). Nitrogen sources are expected to be primarily from agricultural sources (fertilizer and manure) and septic beds. Site 6 is located immediately downstream of the bottom-draw Shand Dam on Bellwood Lake reservoir. The Conestogo River, a sixth-order major tributary of the Grand River, enters the Grand between Sites 8 and 9.

Urban Section (Sites 10 to 12)

This section is dominated by the Kitchener-Waterloo-Cambridge urban area (combined population: 450 000). Another large city, Guelph (population: 127 000) is upstream on the Speed River, which joins the Grand River between Sites 11 and 12. N sources are expected to be almost entirely from WWTPs and urban runoff. Groundwater input is minimal due to the compacted clay diamict and urban impervious surfaces (Cooke 2006). Site 10 is downstream of the Waterloo WWTP, and Sites 11 is downstream of the Kitchener WWTP, and Site 12 is downstream of the Preston WWTP (Table 6.1). This reach is known for summer night-time hypoxia (Chapter 2) due to high macrophyte biomass and respiration, particularly at Site 11 (Jamieson 2010). Site 12 was sampled in the Park Hill reservoir.

Groundwater Recharge Section (Sites 13 to 16):

This section experiences significant groundwater input due to the porous sands and gravels of the Paris Moraine (Westberg 2012). Land use is mostly agricultural. Site 13 is downstream of the Hespeler WWTP (Table 6.1). Paris (population: 12 000) is upstream of Site 15 and has a small WWTP. Expected N sources are agricultural runoff and groundwater and septic beds. The Nith River, which has an agriculture-dominated subwatershed, enters the Grand River upstream of Site 15. Nighttime hypoxia has not been observed (minimum measured: 3.7 mg/L, n = 236) in any sampling from May 2006 to December 2012.

Lower Agricultural Section (Sites 17 to 23):

This section is characterized by glaciolactustine clays and flat topography. Agriculture dominates the landscape. The low permeability of the clay suggests that groundwater input is minimal. The city of Brantford's WWTP discharges upstream of Site 17. The Caledonia WWTP is upstream of Site 19 and the Cayuga WWTP is upstream of Site 22. The Fairchild Creek confluence is upstream of Site 18. Site 22 is in the Dunnville reservoir and is deep and slow moving (Cooke 2006).

6.2.2 Sampling Protocol

Three sampling sessions were conducted: June 14, 2007; September 5, 2007 and April 24, 2009. The sessions were chosen to represent the early summer growing season, the late summer with low flow and high production, and the high flow, early growing season where epilithion but little macrophyte growth had occurred.

Each site was sampled multiple times to capture diel variability. Every site was sampled before sunrise and close to solar noon. Additionally, several sites (Sites 1, 4, 8, 12, 16, 20 and 23) were sampled between these two times, around 10:30 AM.

At each sampling time, water temperature was measured with a multiprobe (YSI 556 MPS) or thermometer. All sample bottles were filled at wrist-depth (~ 10 cm), in moving water. 125 mL opaque HDPE bottles were filled with water for later pH and specific conductivity analysis. 300 mL glass BOD bottles with ground glass stoppers were used to collect water for dissolved oxygen concentration and fixed with Winkler reagents (American Public Health Association 1995). 1 L HDPE Nalgene bottles were used for NO_3^- concentration and isotope analyses. 125 mL glass serum bottles were used for N_2O concentration analysis and 500 mL borosilicate glass jars were used for N_2O isotope analysis. Both N_2O bottles were capped with stoppers underwater using a needle to remove any air bubbles and were preserved in the field with 2 mL saturated mercuric chloride solution per litre sample. All samples were kept cool and dark until analysis.

6.2.3 Chemical Analyses

Conductivity and pH and conductivity were measured in the laboratory with a multiprobe (YSI 556 MPS). Dissolved oxygen concentration was determined using Winkler titration (standard deviation of multiple potassium biiodate standards, hereafter called "precision": 0.2 mg/L, detection limit: 0.2 mg/L) (American Public Health Association 1995). NO_3^- concentration and isotope samples were filtered to 0.45 μm. NO_3^- concentrations were run on a Dionex ICS-90 ion chromatograph (precision: 0.07 mg N/L, detection limit: 0.05 mg N/L). N_2O concentration samples were prepared with a headspace overpressurization method (after (Lide and Frederikse 1995)). Headspace was then extracted with a syringe and run on a Varian 3800 CP gas chromatograph with an electron capture detector designed for greenhouse gas analysis. Precision was 6% or less.

6.2.4 Isotopic Analyses of NO_3^- and N_2O

NO_3^- isotope samples were run with three methods: silver nitrate ($AgNO_3$) burning, chemical denitrification and biological denitrification. Due to sample collection size and budget limits, many samples were only run by one or two methods. When available, $\delta^{15}N\text{-}NO_3^-$ values from multiple methods and time points (i.e. pre-dawn and solar noon) were averaged for each site for each sampling occasion. Linear correlations existed between $\delta^{15}N$ determined by AgNO3 and chemical denitrifier

methods (r^2 = 0.60, n = 4, Figure 6.2) and between chemical and biological denitrifier methods (r^2 = 0.82, n =16, Figure 6.2). Correlations similar for $\delta^{18}O\text{-}NO_3^-$ (r^2 = 0.98 and 0.86, respectively). However, the methods are different in their handling of NO_2^-, which typically has a $\delta^{18}O$ value near water due to rapid chemical oxygen exchange (Casciotti et al. 2007). The measureable presence of NO_2^- was noted but not quantified at some locations in the Grand River, particularly at Site 11 at night in summer when dissolved oxygen is > 2 mg/L. Because $\delta^{18}O\text{-}NO_3^-$ values may be influenced by NO_2^-, $\delta^{15}N\text{-}NO_3^-$, not $\delta^{18}O\text{-}NO_3^-$, was used in the isotope mass balance.

For the $AgNO_3$ method, NO_3^- was concentrated using an anion exchange resin (BioRad AG 1-X8, 100-100 mesh, chloride form), then reacted with silver chloride (AgCl) to from $AgNO_3$, then freeze-dried (Silva et al. 2000). The resulting $AgNO_3$ was analyzed using a breakseal method (Spoelstra et al. 2001) and a VG PRISM mass spectrometer at the Environmental Isotope Lab, University of Waterloo. Precision of $\delta^{15}N\text{-}NO_3^-$ values was 0.3‰.

The chemical denitrification method reduces NO_3^- to NO_2^- using cadmium, which is then converted to N_2O using sodium azide (McIlven and Altabet 2005). Resulting N_2O was then run on a continuous flow-isotope mass spectrometer (CF-IRMS) in line with a TraceGas gas chromatograph pre-concentrator system (GV instruments, Thermo Electron Corp., Manchester, UK). NO_2^- present in the original sample is included in this analysis. Precision of $\delta^{15}N\text{-}NO_3^-$ values was 0.3‰.

NO_3^- isotope samples run by biological denitrification filtered to 0.2 µm to remove microbes, frozen in 30 mL plastic bottles, and analyzed at University of California Davis Stable Isotope Facility, where samples were consumed by denitrifying bacteria with no N_2O reductase (Sigman et al. 2001). The resulting N_2O was then analysed on a ThermoFinnigan GasBench + PreCon trace gas concentration system interfaced to a ThermoScientific Delta V Plus isotope-ratio mass spectrometer (Bremen, Germany) at the Environmental Isotope Lab, University of Waterloo. Precision was 0.3‰ (John Spoelstra, personal communication).

Dissolved N_2O samples were collected with a purge and trap system (Thuss 2008), and analyzed with the CF-IRMS described above. $^{15}N/^{14}N$ and $^{18}O/^{16}O$ ratios in N_2O samples were reported in delta (δ) notation in parts per thousand (permil, ‰):

$$\delta = (R_{sample}/R_{standard} - 1) \qquad \textbf{Equation 6.1}$$

where R is the ratio of the heavy to light isotope (e.g. $^{15}N/^{14}N$). All data are reported relative to international standards for N (atmospheric N_2: AIR: $^{15}N/^{14}N = 0.0036765$ (Coplen et al. 2002)) and O (Vienna Standard Mean Ocean Water, or VSMOW; $^{18}O/^{16}O = 0.0020052$ (Coplen et al. 2002)).

6.2.5 Grand River NO_3^- Isotope Mass Balance

In order to estimate NO_3^- loading to the Grand River, and $\delta^{15}N\text{-}NO_3^-$ of NO_3^- inputs and losses to the river, an isotope mass balance of the Grand River was created for each sampling date. In the isotope mass balance, the river was divided into 23 reaches, each of which was represented by one sampling station. Each reach was represented as a box in a 23-box model, where upstream NO_3^- and any NO_3^- gain or loss was combined and fully mixed. Each mixed pool then underwent denitrification and the remainder became the flux to downstream box (Figure 6.3).

Reaches of the river were divided as in Chapter 3, except that one more reach was added to the end (23) by splitting Reach 22 into equal portions. This allowed the most downstream portion of the river, exporting to Lake Erie, to be modeled. Each reach is represented by a sampling point of the same number (Figure 6.1, Table 6.1). Reach surface areas and depths were estimated by field work (Reaches 1 to 6), the Grand River Simulation Model (Anderson 2012) (Reaches 7 to 18), and the Waterbody Segment GIS layer of Natural Resource and Values Information System (Ontario Ministry of Natural Resources) (reaches 19 to 23) (Table 6.1). Depth data were estimated similarly, except for Reaches 19 to 23, where appropriate GIS data did not exist. There, an exponential discharge-depth relationship for each sampling day was used ($r^2 = 0.5$ to 0.7, Figure 6.4).

6.2.5.1 Estimation of Denitrification Rates

To construct a NO_3^- model, denitrification rates were estimated for each reach by assuming a constant $N_2O:(N_2+N_2O)$ ratio for denitrification and using average daily N_2O emission (Chapter 3). N_2O production is assumed to occur on a daily scale at steady state; thus N_2O production rate equals N_2O emission rate. Literature values for $N_2O:(N_2O+N_2)$ produced in denitrification vary dramatically from 0.001 to 0.833 with a mean value of 0.11 (Table 6.2). However, very high values (> 0.10) have only been noted in soil experiments, not natural systems; the mean value of river sediment experiments is 0.01 (Table 6.2). The IPCC assumes a ratio of 1:400 (0.0025) for N_2O from denitrification in rivers, which is used here as the low-end estimate. For the high-end estimate, a 1:11 (0.0909) ratio is used, similar to the mean literature value, including soils.

Denitrification rates were estimated for each section as:

DEN = N_2O emission*R **Equation 6.2**

Where DEN is the rate of denitrification (mg N/m^2/h), N_2O emission is the rate of emission of N_2O to the atmosphere (mg N/m^2/h), and R is the ratio of N_2O to (N_2O + N_2) produced during denitrification (0.0025 and 0.0909 for the low and high estimates, respectively). Note that a positive value for DEN indicates the removal of NO_3^- from the reach via denitrification.

Daily average N_2O emission was rarely negative (Reach 2 in June; Reaches 2 and 3 in September). When N_2O emissions were negative, DEN could not be estimated and was set to zero.

6.2.5.2 NO_3^- Mass Balance

A mass balance was used to solve for residual gain or loss of NO_3^- in each reach as:

GAIN or LOSS = EXP – UPS + DEN **Equation 6.3**

where EXP is the NO_3^- export from the reach (measured reach NO_3^- concentration multiplied by reach discharge, divided by reach surface area), UPS is the NO_3^- export from the reach above, and DEN is the rate of denitrification in the reach. The residual is termed GAIN when positive (indicating a net gain of NO_3^- to the reach) and LOSS when negative (indicating a net loss of NO_3^- from the reach, not including denitrification). All are in units of mg N/m^2/h. UPS is set to zero for Reach 1, the uppermost reach of the river.

6.2.5.3 Isotopic Mass Balance

An isotope mass balance of NO_3^- was completed as a check on the NO_3^- mass balance, and to provide information about the sources of NO_3^- added to the river and NO_3^- removal processes in the river. Because $\delta^{18}O$-NO_3^- in the Grand River has been shown to change not only due to addition and processing (removal) of NO_3^-, but also by O exchange between water and NO_2^- (Snider 2011), only $\delta^{15}N$-NO_3^- was used in the mass balance.

$\delta^{15}N$-NO_3^- values for EXP (δEXP) and UPS (δUPS) are the measured values for the reach in question and the reach above, respectively. $\delta^{15}N$ values of the net gain or loss of NO_3^- (δGAIN and δLOSS) were solved using the Rayleigh distillation equation. The Rayleigh equation was determined for open systems in which the product (here, N_2O + N_2) does not react with the substrate (NO_3^-) and in which the substrate pool is finite and closed (not replenished during the reaction). The first

assumption is valid. However, in this model, the combined pool of UPS and GAIN (or LOSS) undergo denitrification and the remaining NO_3^- is exported (EXP) Figure 6.3. A literature review shows a range of fractionation factor (α) values for complete denitrification ($NO_3^- \rightarrow N_2$) between 0.980 and 0.998 (Table 6.3); a moderate value 0.985 is used here. Fractionation factors obtained from sediment incubations (Chapter 5) were not used here because they only represent partial denitrification ($NO_3^- \rightarrow N_2O$). The Rayleigh equation applied to the box model is as follows:

$$\delta\mathbf{EXP} = \left[\frac{\delta\mathbf{UPS}\times\mathbf{UPS} + \delta\mathbf{GAIN}\times\mathbf{GAIN}}{\mathbf{UPS}+\mathbf{GAIN}}\right] \times \boldsymbol{f}^{(\boldsymbol{\alpha}-\mathbf{1})} \qquad \textbf{Equation 6.4}$$

where UPS and GAIN are as described in Equation 6.3, δEXP is the $\delta^{15}N\text{-}NO_3^-$ value for EXP, δUPS is the $\delta^{15}N\text{-}NO_3^-$ value for UPS, f is the fraction remaining after denitrification, and α is the isotopic fractionation factor for denitrification. The equation is identical when there is a net loss of NO_3^- (not including denitrification losses) to the reach, but GAIN and δGAIN are replaced by LOSS and δLOSS, respectively.

The fraction remaining after denitrification is:

$$\boldsymbol{f = EXP/(UPS + GAIN)} \qquad \textbf{Equation 6.5}$$

To find δGAIN, Equation 6.4 is rearranged to:

$$\boldsymbol{\delta GAIN} = \left[(\boldsymbol{UPS + GAIN}) \times \frac{\boldsymbol{\delta EXP}}{\boldsymbol{f^{\alpha-1}}} - (\boldsymbol{\delta UPS \times UPS})\right]\boldsymbol{/GAIN} \qquad \textbf{Equation 6.6}$$

δLOSS is computed identically, with the GAIN term replaced by LOSS.

δDEN, or the $\delta^{15}N$ value of the $N_2O + N_2$ products of denitrification, is calculated using an isotope mass balance:

$$\boldsymbol{\delta DEN} = (\boldsymbol{\delta UPS \times UPS} + \boldsymbol{\delta GAIN \times GAIN} - \boldsymbol{\delta EXP \times EXP})\boldsymbol{/DEN} \qquad \textbf{Equation 6.7}$$

where GAIN and δGAIN are replaced by LOSS and δLOSS if applicable.

6.2.6 Watershed-Scale NO_3^- Mass Balance

NO_3^- mass fluxes were summed from each section to give total fluxes for the Grand River. These values were then time-weighted to give annual average values for DEN and RES. For time-weighted averages, June was assigned 2.5 months (May through July 15), September was assigned 2.5 months (July 16 through Sept) and April was assigned 7 months (October through April) based on a visual

inspection of annual discharge and NO_3^- concentration data at West Montrose in the year 2007 (Figure 6.5). Discharge-weighted averages were not used because discharge was often low in fall, winter and spring 2007 while NO_3^- concentrations were high and were best represented by April NO_3^- values. Note that this approach underestimates annual NO_3^- export from the Grand River because sampling did not capture high-flow events when NO_3^- concentration was high (e.g. snowmelt, Figure 6.5).

Instantaneous standing stock of NO_3^- in the river was calculated by summing NO_3^- concentration and water volume of each reach:

$$\boldsymbol{Standing\ Stock} = \sum_{i=1}^{23} \boldsymbol{C_i \times SA_1 \times D_i} \qquad \textbf{Equation 6.8}$$

where C_i is the daily average NO_3^- concentration of reach *i*, and SA_i and D_i are surface area and depth of reach *i*, from Table 6.1.

6.2.7 NO_3^- Loading to Watershed

GAIN fluxes, integrated over the whole river, were compared to (a) NO_3^- loading from WWTP effluent (from WWTP annual reports), (b) NO_3^- loading from septic beds and (c) NO_3^- loading from agricultural fertilizer use and manure from livestock in the watershed, from empirical equations published by the IPCC Fourth Assessment Report (IPCC 2007). Note that agricultural NO_3^- loading values are for the whole watershed, while GAIN and DEN values are calculated from the Grand River main channel only. The IPCC ignores NO_3^- in dry and wet atmospheric deposition.

6.2.7.1 NO_3^- Leaching from Septic Beds

NO_3^- leaching from septic beds was estimated by assuming all people not serviced by a WWTP had a septic bed. This results in a population of 141 000 people on septic beds in the watershed (total population: 950 000; total using WWTPs: 809 000, compiled WWTP annual reports; Mark Anderson, personal communication). A literature survey of N leaching per capita results in a range from 0.04 kg N/capita/year to 5.6 kg N/capita/year (Table 6.4). This range includes studies measuring NO_3^- only, dissolved inorganic nitrogen (DIN), total dissolved nitrogen (TDN) and total nitrogen (TN). A mean value of 2.5 kg N/capita/year was used in this study.

6.2.7.2 NO_3^- Leached from Fertilizers and Crop Residue

NO_3^- to the watershed via fertilizer and crop residue is calculated as (IPCC 2007):

$$NO_{3\,LEACH}^{-} = (F_{SN} + F_{ON} + F_{PRP} + F_{CR} + F_{SOM}) \times Frac_{LEACH} \quad \textbf{Equation 6.9}$$

Where F_{SN} is synthetic fertilizer N applied to soils (kg N/yr), F_{ON} is manure, compost and sewage sludge applied to soils (kg N/yr), F_{PRP} is urine and dung from grazing animals applied to pasture land (kg N/yr), F_{CR} is N in crop residues returned to soils (kg N/yr), F_{SOM} is N mineralization from soil organic matter due to changes in land use or management (kg N/yr) and $Frac_{LEACH}$ is the fraction of all N added to soils that is lost through leaching and runoff (IPCC 2007). $Frac_{LEACH}$ has a default value of 0.3, which is used here (IPCC 2007).

$F_{SN} + F_{ON}$ was calculated using area under cultivation of specific crops (corn, wheat, soybeans, alfalfa, hay, and beans) provided by Canada Census 2006 data clipped to the Grand River Watershed (Zoe Green, GRCA, personal communication) and by fertilizer recommendations given by Ontario Ministry of Agriculture and Food (Ontario Ministry of Agriculture and Food 2011). F_{PRP} was estimated from total area of pastureland (distinct from hay crops) in the watershed (GRCA, personal communication) and a value of 41.48 kg N/ha/yr applied as manure from grazing animals (Huffman et al. 2008). Land use change, and therefore $F_{SOM,}$ were assumed to be zero.

F_{CR} was estimated as a sum of residues for specific crops (T, i.e. corn, wheat, soybeans, alfalfa, hay, and beans) grown in the Grand River watershed (IPCC 2007):

$$F_{CR} = \sum_T \{Crop_{(T)} \times (Area_{(T)} - Area\ burnt_{(T)} \times C_f) \times Frac_{Renew(T)} \times [R_{AG} \times N_{AG} \times (1 - Frac_{Renew(T)} + R_{BG(T)} \times N_T]\} \quad \textbf{Equation 6.10}$$

Where $Crop_{(T)}$ is the dry-mass yield for crop T (kg/ha), $Area_{(T)}$ is the total annual area harvested of crop T (ha/y), Area $burnt_{(T)}$ is the area of crop T burnt (ha/y, set to zero for this watershed as burning residue is not common in Southern Ontario), $Frac_{Renew(T)}$ is the fraction of total area renewed annually (for annual crops: 1), $R_{AG(T)}$ is the ratio of above-ground dry residue to harvested yield for crop T (IPCC 2007), $N_{AG(T)}$ is the N content of above-ground crop residues (kg N/kg dry matter), $Frac_{Remove(T)}$ is the fraction residue removed (kg N/kg crop N, assumed to be zero in the absence of information), $R_{BG(T)}$ is the ratio of below-ground residue to harvested crop yield (kg N/kg dry mass, IPCC literature values used), $N_{BG(T)}$ is the N content of below-ground residues for crop T (kg N/kg dry mass). Crop types and areas were provided by the Grand River Information Network (Grand River Conservation Authority 2008).

6.2.7.3 NO_3^- Leached from Manure Management Systems

NO_3^- leached from livestock manure management systems is estimated as (IPCC 2007):

$$\boldsymbol{NO_{3\,LEACH}^{-} = \sum N_{(T)} \times N_{ex(T)} \times MS_{(T,S)} \times Frac_{LEACHMS(T,S)}} \qquad \textbf{Equation 6.11}$$

where $N_{(T)}$ is the number of livestock in each species (T), $N_{ex(T)}$ is the annual average N excretion per head of species (T) (kg N/yr), $M_{S(S,T)}$ is the fraction of total annual nitrogen excretion that is managed in manure management systems per species and livestock type (S), $Frac_{LEACHMS}$ is the fraction of managed manure N losses in categories T and S.

Equation 6.11 was modified slightly because $MS_{(T,S)}$ for the Grand River watershed is unknown. Therefore, any manure that is not directly deposited on pastures (F_{PRP}, Equation 6.9) is assumed to be included in $MS_{(T,S)}$. To avoid counting manure on pastures twice, $F_{PRP} \times Frac_{LEACH}$ was removed from Equation 6.11:

$$\boldsymbol{NO_{3\,LEACH}^{-} = \sum (N_{(T)} \times N_{ex(T)} \times MS_{(T,S)} - F_{PRP}) \times Frac_{LEACHMS(T,S)}} \qquad \textbf{Equation 6.12}$$

$NO_3^-{}_{LEACH}$ was calculated for multiple livestock species (cattle, poultry, pigs and horses). $N_{(T)}$ data was provided by 2006 census data clipped to the watershed (GRCA, personal communication). $N_{ex(T)}$ values were taken from Table 10.19 (IPCC 2007) in excretion/100 kg livestock biomass, which was multiplied by average livestock masses from a variety of sources (Dairy Farmers of Ontario 2013, Dougherty and Young 2005, Farm Animal Shelters 2013, Kaberia et al. 2003, National Research Council Canada 1982, Ontario Cattlemen's Association 2012, Ontario Sheep Marketing Agency 2013, Richards 2011, Sendel 2010, Stevenson 2007, Wezyk et al. 2013). There is no default value for $Frac_{LEACHMS(T,S)}$, but a range of 1% to 20% is given (IPCC 2007); in the absence of other information, a moderate value of 10% is used in this study. Other sources of NO_3^- to the watershed, such as atmospheric N deposition, were ignored.

6.2.8 Checks on Isotopic Mass Balances

To ascertain if the NO_3^- isotope mass balance for the Grand River yielded reasonable results, calculated δGAIN for net gains to the river section, and δLOSS for net losses were compared to published data from the literature and measured values for inputs and outputs to the Grand River. It is very likely that NO_3^- gains (e.g. NO_3^- input from tributaries, WWTPs, septic beds, and/or groundwater, and NO_3^- produced by in-river nitrification and/or mineralization) and NO_3^- losses (e.g. biological

assimilation, denitrification not accounted for in DEN) occur in every reach. Therefore, δGAIN and δLOSS represents multiple NO_3^- sources and losses but can still provide some information, especially if one source or loss dominates a reach. δGAIN values were compared to tributary and groundwater $\delta^{15}N\text{-}NO_3^-$ values collected in the Grand River watershed.

To remove the effect of changing $\delta^{15}N\text{-}NO_3^-$ values in the river, δLOSS values were converted to an isotopic fractionation (ε) between $\delta^{15}N\text{-}NO_3^-$ measured in each reach (δEXP) and δLOSS, with the following equation:

$$\boldsymbol{\varepsilon LOSS} = \left(\frac{\boldsymbol{\delta LOSS}}{\mathbf{1000}} + \mathbf{1}\right)/\left(\frac{\boldsymbol{\delta EXP}}{\mathbf{1000}} + \mathbf{1}\right) \qquad \textbf{Equation 6.13}$$

where εLOSS is reported in ‰. Isotopic fractionations were then compared to reported values for denitrification and biological assimilation.

6.2.9 Error Propagation

Error was propagated for each component of the mass balance. Machine precisions were used for NO_3^- concentration, $\delta^{15}N\text{-}NO_3^-$, and N_2O concentration. Uncertainty on discharge was unknown and a value of 10% was chosen. Uncertainty was assumed to be zero for surface area, reach length and depth measurements.

For addition and subtraction (e.g. GAIN = EXP – UPS – DEN), error was calculated as (Luna 2013):

$$\boldsymbol{Error} = \sqrt{\sum_{\boldsymbol{i=1}}^{\boldsymbol{N}} \boldsymbol{e_i}} \qquad \textbf{Equation 6.14}$$

Where e_i is the error on term i.

For multiplication and division (e.g. EXP = NO_3^- concentration × discharge/reach surface area), error is calculated as (Luna 2013):

$$\boldsymbol{Error/Value} = \sqrt{\sum_{\boldsymbol{i=1}}^{\boldsymbol{N}} (\boldsymbol{e_i/v_i})} \qquad \textbf{Equation 6.15}$$

Where v_i is the measured value for term *i*.

6.2.10 Statistical Analyses

To determine if denitrification rate, net NO_3^- gain or loss to each reach, δGAIN and εLOSS varied significantly by season (June, September and April) or by Section (1 through 4), one-way ANOVA tests were conducted using SigmaPlot 12.0 (Systat Software Inc., Chicago, IL). When data were not normally distributed, Kruskal-Wallis one-way ANOVA tests were used. P values < 0.05 were considered significant.

6.3 Results

6.3.1 In-River Denitrification Rates (DEN)

Measured NO_3^- concentration and $\delta^{15}N\text{-}NO_3^-$ values are shown in Figure 6.6. Denitrification rate estimates varied widely depending on the N_2O: (N_2 + N_2O) ratio used. Areal rates using the 1:11 ratio will be shown first with the rate using the 1:400 ratio following in brackets. Denitrification rates were moderate in June, ranging from 0 to 13.4 mg $N/m^2/h$ (0 to 487.8 mg $N/m^2/h$); high in September, ranging from 0 to 20.7 mg $N/m^2/h$ (0 to 224.4 mg $N/m^2/h$); and low in April, ranging from 0.02 to 0.1 mg $N/m^2/h$ (0.2 to 11.4 0.1 mg $N/m^2/h$) (Figure 6.7). Because almost all sampling events had positive daily N_2O emissions (66/69), denitrification rate was almost always greater than zero. The only exceptions were Reach 2 in June and September and Reach 3 in September; where NO_3^- was low and N_2O was undersaturated. Negative emissions likely occurred because changes in water temperature were rapid over the diel scale, causing changes in N_2O solubility, rather than N_2O consumption resulting in net negative N_2O production.

Denitrification rates were typically low in the Upper Agricultural section (0 to 1.0 mg $N/m^2/h$ (0 to 38.1 mg $N/m^2/h$)), high in the Urban section (0.4 to 13.4 mg $N/m^2/h$ (3.5 to 487.7 mg $N/m^2/h$) and moderate in the Groundwater Recharge Section (0.2 to 2.0 mg $N/m^2/h$ (1.3 to 72.9 mg $N/m^2/h$) and 4 Lower Agricultural Section (0.4 to 3.4 mg $N/m^2/h$ (4.4 to 101.0 mg $N/m^2/h$). Denitrification rates had no relationship with NO_3^- concentration but peaked when NO_3^- was moderate (Figure 6.8)

6.3.2 Net NO_3^- Gain and Loss (GAIN and LOSS)

GAIN and LOSS values ranged from -35.8 (LOSS) to 235.7 (GAIN) mg $N/m^2/h$ (-0.3 to 511.8 mg $N/m^2/h$) in June; -27.9 to 19.1 mg $N/m^2/h$ (-18.5 to 303.7 mg $N/m^2/h$) in September, and -57.5 to 729.8 mg $N/m^2/h$ (-36.4 to 743.1 mg $N/m^2/h$) in April. GAIN values were much larger using the

1:400 N_2O:(N_2+N_2O) ratio because they had to balance out larger denitrification rates. This is especially noticeable in September when N_2O fluxes (and thus DEN) were highest. GAIN values were highest in April and lowest in September.

Net GAIN values occurred throughout the river but net LOSS values predominantly occurred in the Groundwater Recharge and Lower Agricultural sections of the river (with the exception of Sites 4 and 8 in the Upper Agricultural section in September).

6.3.3 Whole Watershed Mass Balance

The annual average export of NO_3^- from the river to Lake Erie was 5.6 Gg N/year. Denitrification and LOSS summed to 2.0 (8.1) Gg N/year and net inputs (GAIN) summed to 7.5 (13.7) Gg N/year (Figure 6.9). The net inputs were compared to whole-watershed inputs of WWTPs (from annual reports, 1.5 Gg N/year), septic beds (0.4 Gg N/yr), fertilizer leaching and crop residues (using Equations 6.9 and 6.10, 36.9 Gg N/year), and leaching from livestock manure (using Equation 6.11, 4.7 Gg N/yr). Thus, total watershed NO_3^- inputs were 43.4 Gg N/year, resulting in an estimated NO_3^- loss and/or storage of 37.1 Gg/yr between the watershed and the mouth of Grand River, only 2.0 (8.1) Gg N/yr of which occurred in the Grand River itself. The annual average standing stock of NO_3^- in the river was estimated as 0.137 Gg N. This results in an estimated average annual residence time for NO_3^- in the river (NO_3^- standing stock divided by the sum of export to Lake Erie, DEN and LOSS) was 6.6 (3.6) days; this is similar to the residence time of water in the river (~3 days not including reservoirs, Mark Anderson, personal communication).

6.3.4 δGAIN and δLOSS

NO_3^- concentrations and $\delta^{15}N\text{-}NO_3^-$ measured in tributaries, WWTP effluent and groundwater in the Grand River watershed are shown in Figure 6.10. δGAIN and δLOSS estimates had a wide range. The two denitrification rate assumptions (1:11 and 1:400) resulted in different flux values and isotopic values of GAIN and LOSS. Therefore, both values will be shown here, with the 1:11 value first and the 1:400 value following in parentheses.

δGAIN ranged from -8.5‰ to 19.2 ‰ (-23.7‰ to 39.0‰) (Figure 6.11). δLOSS ranged from -279.2‰ to 13.4‰ (-0.8‰ to 13.7‰) (Figure 6.12). Very low δLOSS values (< -50‰) occurred in Reach 20 in September.

δGAIN (1:10) values were significantly linearly related to distance in the Upper Agricultural section in June ($r^2 = 0.56$, p = 0.037, n = 8) and September ($r^2 = 0.86$, p = 0.014, n =7) but not April. Values using the 1:400 ratio were similar (June: $r^2 = 0.51$, p = 0.047, n = 8; September: $r^2 = 0.73$, p = 0.004, n = 9; April: not significant). No significant correlations between δGAIN and distance are found in the other three sections.

6.3.5 $\varepsilon^{15}N$ for LOSS

$\varepsilon^{15}N$ values for δEXP (measured) → δLOSS ranged from -287.2‰ to 6.4‰ (-8.7‰ to 6.5‰). There were fewer values for the 1:400 estimate and the range in values was much smaller. Values were lowest (most negative) in June, moderate in September and highest in April, which had several positive values. There were insufficient data to determine spatial trends though $\varepsilon^{15}N$ values did decrease in the Groundwater Recharge section in June and September (Reaches 17 and 15, respectively).

6.4 Discussion

6.4.1 Grand River Denitrification Rates Compared to Literature Values

Estimated denitrification rates for rivers in the literature vary widely, from 1 to 100 mg $N/m^2/h$ (Table 6.5). Estimates of denitrification in the Grand River using the 1:11 $N_2O:(N_2O+N_2)$ ratio fall in the low end of this range (0 to 13.4 mg $N/m^2/h$). However, denitrification estimates using the 1:400 ratio are often higher than the published range (0 to 487.7 mg $N/m^2/h$), especially in September when flow was low and N_2O fluxes were high. The Grand River has near-ideal conditions for denitrification – warm summer temperatures, moderate to high NO_3^- concentrations (especially in the Urban, Groundwater Recharge and Lower Agricultural sections), periods of hypoxia in the Urban section and abundant biofilm (Hood 2012). This suggests that denitrification rates should fall in the moderate to high end of the published range. The mean $N_2O:(N_2O+N_2)$ ratio in river sediments is 0.01 (Table 6.2); this value is intermediate between the values used here and may give more accurate denitrification estimates in the absence of direct measurement. Using this ratio yields denitrification rates in the Grand River of 1 to 121.9 mg $N/m^2/h$, encompassing the literature range. However, $N_2O:(N_2O+N_2)$ ratios in river sediment also change over time (Chapter 5) and with temperature and DO, NO_3^- and NO_2^- concentration (Firestone et al. 1979, Firestone et al. 1980, Silvennoinen et al. 2008, Silvennoinen et al. 2008). Denitrification rates in rivers are difficult to measure, resulting in scant published data. It is

possible that the published range of denitrification rates does not adequately capture the global range of rates and more studies are needed over a large variety of rivers of varying climate, redox conditions, NO_3^- concentration, etc. It is unclear how to average the ratio over space and time in a complex river system, but the reasonable denitrification rate estimates obtained with a 1:100 N_2O:(N_2O+N_2) ratio suggest that this type of sampling (multiple sites over whole river, two or three times a day for three seasons) can provide a good first estimate of N cycling rates.

6.4.2 Comparing GAIN and LOSS with Estimated N Uptake Rates

To determine if unaccounted for NO_3^- losses in some reaches (LOSS) could be attributed to biological N assimilation, assimilation rates were estimated. Macrophyte biomass has been estimated in some stretches of the Grand River (Hood 2012), but epilithion biomass has not, although it likely makes up a significant portion of the primary producing community in the river (Cejudo et al., in submission). N assimilation is related to net primary production (NPP), the difference between gross primary production and respiration by primary producers. N assimilation was estimated using the following equation, modified from Sundback et al. (2004) and Alsterberg et al. (2012):

$$\boldsymbol{Gross\ N\ assimilation} = \frac{\boldsymbol{GPP}\times(\frac{\boldsymbol{NPP}}{\boldsymbol{GPP}})}{\boldsymbol{PQ}}/(\boldsymbol{C}:\boldsymbol{N}) \qquad \textbf{Equation 6.16}$$

where GPP is gross primary productivity (estimated using the PoRGy model and DO concentration and δ^{18}O-DO in the Grand River (Venkiteswaran et al. in submission)) in moles $O_2/m^2/h$. The NPP/GPP ratio is estimated at 0.8 (Alsterberg et al. 2012, Sundback et al. 2004). PQ is the photosynthetic quotient, or number of moles O_2 produced per moles CO_2 fixed (typically 1.25 in freshwater (Falkowski and Raven 2007)), and C:N is the ratio of C to N atoms in biomass. A C:N ratio of 9.26 (molar) was used here, based on measurements of epilithion in the Grand River (Cejudo et al. in submission). GPP estimates were available from Sites 1, 4, 8, 16, 20 and 23 for all three sampling events (June, September and April) discussed here. Note that the variability in GPP:NPP ratios in aquatic systems (Howarth et al. 1996) adds uncertainty to this estimate.

Estimates of N assimilation ranged from 1.1 to 51.0 mg $N/m^2/h$ (Table 6.6). This range is larger than that for LOSS values from these reaches (-3.1 to -0.3 mg $N/m^2/h$). Thus it is possible that net loss of N from reaches is due to N assimilation.

There were no significant linear relationships between GAIN and LOSS and N assimilation using either the 1:11 or 1:400 ratios. This suggests that GAIN and LOSS are likely driven by N point

sources (e.g. tributaries, WWTPs) and hot spots (e.g. groundwater, denitrification) rather than N assimilation.

6.4.3 Comparing $\delta^{15}N\text{-}NO_3^-$ of GAIN with Known Tributary, Groundwater and WWTP Values

The estimated $\delta^{15}N\text{-}NO_3^-$ values of net NO_3^- gain (GAIN) from each reach were compared to three possible sources: tributaries, WWTP effluent, and groundwater. Mean values are reported plus or minus standard deviation. Tributaries were represented by the Conestogo River, Boomer Creek, Cox Creek and Swan Creek, collected in October 2012 ($\delta^{15}N\text{-}NO_3^-$: 10.3 ± 1.9‰, n = 22, T.F. Cummings, unpublished data). WWTP effluent from the Kitchener WWTP ($\delta^{15}N\text{-}NH_4^+$: 5.1±1.7, n=11; $\delta^{15}N\text{-}NO_3^-$: 4.2±0.0, n=2) and Waterloo WWTP ($\delta^{15}N\text{-}NH_4^+$: 12.7± 2.1‰, n=9; $\delta^{15}N\text{-}NO_3^-$: 14.4 ±8.3‰, n=9) was characterized in more detail in Chapter 4. Groundwater was characterized in the Groundwater Recharge section downstream of Site 13 and includes domestic wells, seeps into the Grand River, and groundwater from 1 m below the river bed in summer (mean $\delta^{15}N\text{-}NO_3^-$: 8.0 ± 6.2‰, n = 25 (Westberg 2012)). Additionally, the literature range for $\delta^{15}N$ of NH_4^+ and NO_3^- fertilizers was used because these were not measured directly in this study (range of one standard deviation: -2.0 to 6.0, (Xue et al. 2009)). Thus, the mean plus one standard deviation of all three sources is pooled to a total range of -2.0‰ to 22.7‰. However, inputs with very high $\delta^{15}N\text{-}NO_3^-$ values (>15‰) have low concentration (< 5 mg N/L) (Figure 6.10). Therefore, δGAIN values are likely to be similar to high-concentration inputs (NO_3^- > 5 mg N/L, $\delta^{15}N$ range: 2.4‰ to 11.4‰).

In general, most δGAIN values fell within the expected range for tributaries, groundwater and WWTP effluent. Very low (< -2‰) and very high (> 23‰) δGAIN values occur when GAIN values are low (< 2 mg N/m^2/h) but change in $\delta^{15}N\text{-}NO_3^-$ over the reach is high, due to very large propagated error. The only very low value occurs in Reach 19 in September (-8.5‰, 1:10 ratio, GAIN = 0.5 mg N/m^2/h). High values occur in Reach 15 in September (26.0‰, 1:400, GAIN = 0.6 mg N/m^2/h) and Reach 17 in September (38.9‰, 1:400, GAIN = 1.4 mg N/m^2/h).

Similarly, δGAIN values were not significantly different by section using 1:11 values (one way ANOVA: f = 0.09, p = 0.97). Using the 1:400 ratio, δGAIN in the Upper Agricultural section was significantly lower than in the Lower Agricultural section (non-normal data, Kruskal-Wallis ANOVA, p < 0.05). This suggests that the net incoming NO_3^- was less processed prior to entering the river in the Upper Agricultural section.

Annual average values for δGAIN again show that the majority of the reaches have δGAIN values consistent with expected source values. The annual average is heavily weighted to April values because GAIN fluxes were higher and because it represented the largest portion of the year. Very high or low (> 23 or < -3) δGAIN values occur in Sections 3 and 4 only, where GAIN values are small. This indicates that these reaches have lower areal NO_3^- inputs and more losses than the other sections.

6.4.4 Comparing $\varepsilon^{15}N$ (River NO_3^- → LOSS) with Denitrification and Assimilation $\varepsilon^{15}N$

Net loss of NO_3^- from river reaches that is not accounted for by N_2O could result from (a) denitrification with a lower N_2O:(N_2O+N_2) than expected, (b) biological assimilation, or (c) other biological processes such as dissimilatory NO_3^- reduction to ammonia (DNRA) or anammox. NO_3^- sorption to clay colloids in sediment is minimal (Brady and Weil 2002) and therefore will be ignored. The isotopic fractionation ($\varepsilon^{15}N$) helps distinguish the first two loss mechanisms. $\varepsilon^{15}N$ for denitrification is expected to range from -20‰ to -1.5‰ in rivers (Table 6.3). $\varepsilon^{15}N$ for denitrification when NO_3^- is not limiting is likely very negative (-30‰ to -20‰ (Snider et al. 2009, Chapter 5)). NO_3^- limitation (e.g. by NO_3^- diffusion into sediment from the water column) typically results in $\varepsilon^{15}N$ values dominated by diffusion effects (~ -4‰). Therefore, a moderate value of -15‰ was used here. Biological assimilation appears to have a slightly negative or zero $\varepsilon^{15}N$ (see Section 1.3.5); a value of 0‰ is used here.

Most calculated εLOSS values (including propagated error) fall with the expected range of -15‰ to 0‰ in June and September (Figure 6.12). The exception at Reach 20 in September (-287.2‰) occurs when LOSS is very close to zero (0.3 mg N/m^2/h) due to large propagated error. Because propagated uncertainty is large, it is not often possible to distinguish between the denitrification and assimilation end members, or apportion LOSS between the two, especially in the Groundwater Recharge and Lower Agricultural sections of the river, where uncertainty can be > 10‰. This suggests that εLOSS is not sufficiently sensitive to separate assimilation and denitrification. In order to estimate these rates, direct measurement may be required.

6.4.5 Seasonality of NO_3^- Inputs and Losses in the Grand River

Significant seasonal differences were found in denitrification rates. Using the 1:11 ratio, June DEN rates were significantly higher than September and April denitrification rates (one-way Kruskal

Wallis ANOVA, p= 0.011). Using the 1:400 ratio, April DEN rates were significantly lower than both June and September rates (Kruskal-Wallis ANOVA, $p < 0.001$). Total denitrification (sum of all reaches) was highest in June (1.4 mg N/m^2/h (53.9 mg N/m^2/h)), followed by September (0.9 mg N/m^2/h (33.9 mg N/m^2/h) and April (0.5 mg N/m^2/h (18.2 mg N/m^2/h). Low denitrification rates in April are expected due to low temperature, even when NO_3^- concentrations are high. However, high June rates are unexpected, as DO was slightly lower in September (range: 0.8 to 15.1 mg/L) than June (range: 1.3 to 15.5 mg/L) and water temperatures were higher (September range: 17.2° C to 28.0° C; June range: 12.7° C to 27.8° C), both of which promote denitrification. Nitrate concentrations were similarly moderate in both September (range: BD to 3.7 mg N/L) and June (0.2 to 3.2 mg N/L). This could indicate that N_2O:(N_2O+N_2) ratios for denitrification were lower in September, and thus denitrification may have been underestimated. Denitrification rates could also have been influenced by the quantity and lability of organic carbon in sediments but this was not quantified. Total organic C in sediments did not change significantly by season at Sites 9 and 11 (Chapter 5).

Seasonal patterns in net gain or loss of NO_3^- were different using the 1:11 and 1:400 ratios. Using the 1:11 ratio, GAIN values were significantly higher in April than in September (one-way Kruskal-Wallis ANOVA, $p = 0.025$) though not significantly different than in June. NO_3^- inputs are expected to increase in winter and early spring, when shallow groundwater discharge is high and biological removal of NO_3^- (via assimilation, denitrification, etc.) is minimal. Measured NO_3^- concentrations are also highest in winter and early spring in the Grand River. However, no significant changes in GAIN or LOSS (1:400 ratio) occur between seasons. This is because the 1:400 ratio predicts much higher denitrification rates and GAIN rates are therefore all higher (and more similar) to compensate.

The stable isotopic ratios of net NO_3^- gain to the river (δGAIN) were not always significantly different by season (1:11: one way ANOVA, $f = 0.57$, $p = 0.57$; 1:400: Kruskal-Wallis ANOVA: April has a lower median δGAIN value than September, $p < 0.05$). Lower δGAIN values in April may suggest that incoming NO_3^- is less biologically processed (e.g. by denitrification, NH_4^+ nitrification) and less chemically processed (e.g. NH_4^+ volatilization and subsequent biological nitrification) due to lower temperatures reducing biological rates and lower pH inhibiting volatilization. Lower δGAIN values may also indicate more NO_3^- input from inorganic fertilizers, which have low δ^{15}N-NO_3^- values (-2.0‰ to 6.0‰ (Xue et al. 2009)) as they are produced from atmospheric N_2 (0‰).

Using lower denitrification rate estimates (i.e. the 1:11 N_2O:(N_2O+N_2) ratio) results in more reaches with net NO_3^- loss after denitrification. There were so few εLOSS values using the 1:400 ratio that seasons could not be statistically compared. εLOSS (1:11) values were not significantly different by season (Kruskal-Wallis ANOVA, $p = 0.191$).

6.4.6 Spatial changes in NO_3^- Inputs and Losses in the Grand River

NO_3^- inputs and losses in the Grand River show spatial patterns as well as seasonal changes. NO_3^- concentrations in the headwaters are very low (< 0.1 mg N/L). Areal NO_3^- additions (GAIN) were low throughout the Upper Agricultural section until the site downstream of the large Bellwood Lake reservoir (Site 6). The reservoir can act as a NO_3^- source or sink, depending on the complex interaction of reservoir management and seasonal effects (B.J. De Baets, unpublished data). GAIN fluxes are high in the headwater sites (Reaches 1 through 5) of the Upper Agricultural section in April, likely due to high flows from groundwater and tributaries in spring. Downstream sites (Reaches 7 to 9) have higher NO_3^- inputs, likely due to non-point agricultural sources of NO_3^- as well as the confluences of the Conestogo River and Laurel Creek, upstream of the urban centre (Site 9). WWTPs in this reach are small. Effluent NO_3^- and NH_4^+ loads represent a small portion (< 0.05) of incoming NO_3^- in most cases (Table 6.7). The exception, Reach 2 in September, had very low GAIN. It is downstream of the Dundalk WWTP, which releases effluent from a sewage lagoon only a few times a year, likely not during sampling. Denitrification rates in the Upper Agricultural section were significantly lower than those in the Urban and Lower Agricultural sections, but not the Groundwater Recharge section (Kruskal-Wallis one-way ANOVA, $p < 0.001$ for both 1:11 and 1:400 estimates). Low denitrification rates were likely due the oxic water column, which reduces anoxic sediment habitat for denitrifiers, and low NO_3^- concentrations. δGAIN values typically suggest tributary, groundwater or WWTP effluent sources. Net NO_3^- loss is rare in this section, and occurs mostly in September. $\varepsilon^{15}N$ values are -5‰ and higher, suggesting that net NO_3^- removal was heavily influenced by biological NO_3^- assimilation, with some denitrification. $\varepsilon^{15}N$ values did not vary significantly between sections of the river (Kruskal-Wallis ANOVA, $p = 0.222$).

Net NO_3^- inputs (GAIN) were very high in the Urban section of the Grand River. No reaches have net NO_3^- losses (LOSS) in addition to denitrification in any season. WWTP effluent contributes < 1% to 16% of net NO_3^- gain to reaches in this reach (Table 6.7). This is a surprisingly low fraction, and more work is needed on other sources (urban runoff, NO_3^- from the Speed River) to determine urban

NO_3^- sources. It is possible that overestimating denitrification losses results in overestimating NO_3^- gain to the reach; this may have occurred because low DO concentrations and relatively high NO_2^- concentrations in this reach (up to 0.5 mg N/L, unpublished data) promote high N_2O:(N_2O+N_2) ratios in denitrification. Denitrification rates were significantly higher in the Urban section than in the Upper Agricultural and Groundwater Recharge sections but not the Lower Agricultural section (Kruskal-Wallis one-way ANOVA, $p < 0.001$). Denitrification rates were especially high in Reaches 11 (downstream of Kitchener WWTP) and 12 (downstream of Preston WWTP), where hypoxic conditions at night in summer promote denitrification and high N_2O production. δGAIN values were within the $\delta^{15}N$ range of sources used. Reach 10 in June had high δGAIN values (18.2‰ (14.7‰)), which may be influenced by high $\delta^{15}N$-NO_3^- values in effluent from the upstream Waterloo WWTP (range in summer: 24.2‰ to 26.6‰, n = 3, Chapter 4). Reach 11 in September, on the other hand, had low δGAIN values (0.9‰ (3.8‰)), possibly because NH_4^+ was only partially nitrified to NO_3^- in the river by Reach 11, allowing partial expression of the $\varepsilon^{15}N$ for nitrification (-20‰ to -3‰ (Snider et al. 2009)) to be expressed.

The Groundwater Recharge section had a large range of both net GAIN and LOSS values that were not significantly different than any other sections (Kruskal-Wallis one-way ANOVA, $p > 0.05$). There was a large increase in NO_3^- in the reach downstream of the Nith River (Reach 15) in all seasons. The Nith River has a heavily agricultural subcatchment and typically has high NO_3^- concentrations (Cooke 2006). WWTP effluent makes up 7% or less of GAIN downstream of the Galt and Paris WWTPs (Reaches 13 and 15) (Table 6.7), suggesting that other sources (agriculture, septic beds) are significant. Areal denitrification rates were higher than in the Upper Agricultural section ($p < 0.001$) but not significantly different than in the Urban and Lower Agricultural sections ($p > 0.005$). Groundwater flux is highly spatially variable in this area, and its chemistry varies widely in both DO and NO_3^- (Westberg 2012), making large changes in the NO_3^- budget between sites possible. ALL δGAIN and εLOSS values were consistent with expected ranges.

Lastly, the Lower Agricultural section had the most instances of net NO_3^- losses (LOSS). GAIN and LOSS values were significantly lower than in the Urban section but not the Upper Agricultural or Groundwater Recharge sections ($p < 0.001$ and > 0.05, respectively). The reach immediately downstream of the Brantford WWTP (Reach 17) consistently had net NO_3^- loss even though the Brantford WWTP contributed 0.26 mg N/m^2/h as effluent NO_3^- + NH_4^+ (Table 6.7). The clay plain is

relatively impervious to groundwater inputs (Aquaresource 2009), suggesting that NO_3^- additions come from tributaries, WWTPs, and other rural sources such as tile drains and septic beds. δGAIN and εLOSS values are as expected although large uncertainty makes source apportionment impossible, except for one anomalous εLOSS value which occurs when LOSS is very close to zero.

6.4.7 Conceptual Model for NO_3^- Gain and Loss in the Grand River

The data above suggest that GAIN, LOSS and their isotopic values should change in a predictable fashion based on river section. The differences in the sections are clearly shown when GAIN and LOSS is plotted against δGAIN or εLOSS (Figure 6.13). Most points plot within expected ranges (black boxes), especially when error bars are included. The Upper Agricultural section is dominated by low to moderate GAIN rates; well-constrained, moderate δGAIN values and no LOSS values. The Urban section has high GAIN values, highly variable δGAIN values due to large fluxes in from WWTP effluent and no LOSS values. The Groundwater Recharge section may show either net NO_3^- gain or loss and has variable δGAIN and εLOSS values. Lastly, the Lower Agricultural section shows both high net GAIN values and the most net LOSS values. This method makes it clear that almost all reaches have a net gain in NO_3^-. It also indicates where denitrification may be higher than expected from N_2O fluxes (indicating that using a 1:11 or 1:400 N_2O:(N_2O+N_2) ratio is inadequate), i.e. where εLOSS is similar to expected values for denitrification. Lastly, it can indicate where biotic assimilation may be a significant NO_3^- sink, i.e. where $\varepsilon^{15}N \sim 0‰$. Annual average values are not shown in Figure 6.13 as they are similar to April.

6.4.8 Losses in the Grand River Relative to Inputs

Annually, denitrification removes 3% (56%) of NO_3^-entering the Grand River (Figure 6.9). Unaccounted-for NO_3^- losses (LOSS) (N assimilation, denitrification accounted for by N_2O emissions) remove a further 23% (4%). Figure 6.14 shows concentrations of NO_3^- in the Grand River if no denitrification and LOSS occurred but NO_3^- inputs to the river stayed the same. These hypothetical values are < 2 mg N/L higher than measured values at the most downstream site (Site 23) when the 1:11 denitrification rate is used. However, the values are very large, often greater than the drinking water limit for NO_3^- (10 mg N/L) when the 1:400 ratio is used. Even though denitrification and LOSS remove a modest amount of NO_3^- in the Grand River (26% to 59% of net

NO_3^- entering), this can be enough to prevent NO_3^- concentrations from exceeding the drinking water limit, especially in summer when denitrification rates are high.

The modest estimated denitrification values are surprising, considering that the Grand River seems ideal for high denitrification rates: biofilm biomass is high (Hood 2012), NO_3^- concentrations are moderate to high, DO can be low, DOC is high (~7 mg/L) and there is high sediment area-to-volume ratio because the river is shallow. This may be due to the river's short water residence time, low sediment organic content (see Chapter 5) and cold annual average water temperature. Denitrification estimates are uncertain because of uncertainty in the N_2O:(N_2O+N_2) ratio. However, a 1:11 N_2O:(N_2O+N_2) ratio is relatively high for river denitrification (Table 6.2), suggesting it is a reasonable minimum estimate of denitrification. The N_2O:(N_2O+N_2) ratio is understood to increase immediately upon the onset of conditions favourable to denitrification (e.g. hypoxia) due to a lag in the activity of N_2O reductase relative to other enzymes involved in denitrification (Codispoti 2010, Firestone and Tiedje 1979). The increase in the ratio is temporary. Additionally, NO_2^- has been shown to be an effective inhibitor of N_2O reductase (Firestone et al. 1979), even at low concentrations. Thus, denitrification may be overestimated in Reach 11 in June and September, where night-time hypoxia is common and night-time water column NO_2^- concentrations of up to 0.5 mg/L have been measured (unpublished data). On the other hand, denitrification may be underestimated in other reaches of the river if the 1:11 N_2O:(N_2O+N_2) ratio is too high. This is especially likely in low-NO_3^-, well-oxygenated reaches in the Upper Agricultural section, where NO_3^- must diffuse into sediments from the water column in order to be denitrified.

Much more NO_3^- is added to the watershed than enters the river. Only 13% of total watershed NO_3^- inputs are exported to Lake Erie, less than the average for temperature watersheds estimating using NANI (25%, (Howarth et al. 2012). This is typical of rivers with low discharge and short residence time (Howarth et al. 2012). NANI was not calculated for the Grand River because atmospheric NO_3^- deposition and N import and export data were not available. However, the sum of fertilizer, manure, septic bed and WWTP DIN loading in the watershed (including all inputs, not just those that leach into freshwaters), is 25 290 kg N/km^2/y. This is a high value relative to published values from Europe and the USA (Howarth et al. 2012), suggesting that N losses (e.g. export of crops from the watershed) may be underestimated. TN export from the river was not calculated, but NO_3^- export was only 3% of total N inputs. This is likely because NH_4^+ and organic N are not included in export calculations and

because annual NO_3^- export is underestimated because no high-discharge events were included in sampling.

Because NO_3^- export was underestimated, the proportion of NO_3^- entering the river that is denitrified is even lower than predicted in the model. More research is needed to determine if denitrification rates in the Grand River are low, and if this is typical of other high-NO_3^-, low-DO rivers.

High N_2O production, and likely denitrification, occur in the Grand River when DO < 1.4 mg/L (Venkiteswaran et al, in submission) and when temperatures are high (> 25 °C). DO- and temperature-limited denitrification presents difficulties for river managers. Highest NO_3^- concentrations occur in winter when denitrification rates are low due to low temperature and high DO. Population and economic predictions for the Grand River watershed suggest increased urban populations (Schultz 2005) and therefore increased WWTP inputs to the river. Additionally, intensification of agriculture, including high density livestock production, is predicted in Canada (Council of Canadian Academies 2013). These activities may well result in increased NO_3^- load to the river, but denitrification rates likely will not increase significantly unless hypoxia increases. Hypoxia may increase if community respiration rates increase with increased nutrient loading and gas exchange is not rapid enough to reaerate the water column (Venkiteswaran et al. 2008). Hypoxia in rivers is considered extremely undesirable by river managers (Conley et al. 2009, Shields and Knight 2012) because it severely inhibits ecological function, and can result in fish kills and decreased biodiversity. Thus, the Grand River is unlikely to increase its denitrification capacity and still maintain a healthy, oxic ecosystem. If NO_3^- inputs continue to increase in the watershed, the proportion of inputs that the river can remove may decrease over time.

The annual watershed-scale box model presented here suggests that most NO_3^- entering the watershed (83% (68%)) is lost by denitrification, assimilation and other biological processes and/or stored in soil and groundwater before it enters the river. Therefore, reducing NO_3^- loading to the watershed and increasing denitrification potential in the watershed before NO_3^- enters the river are sensible courses of action. NO_3^- source reduction techniques include WWTP upgrades (especially in-plant denitrification) and agricultural best management practices (BMPs) such as conservation tilling, reduced N fertilizer applications, raised tile outlets, etc. (Makarewicz et al. 2009, Passeport et al. 2013). Best management practices (BMPs) that encourage landscape denitrification include

restoration and maintenance of riparian zones (Ranalli and Macalady 2010), creation of storm water retention ponds (Bettez and Groffman 2012, Rosenzweig et al. 2011), and restoring wetlands on the landscape (Batson et al. 2012). These practices have complex results that are difficult to predict (Passeport et al. 2013, Ranalli and Macalady 2010). BMPs can also have environmental trade-offs such as anoxia, toxic methylmercury production, and greenhouse gas (CO_2, CH_4 and N_2O) production (Passeport et al. 2013).

6.4.9 Sources of Uncertainty and Recommendations

There are many possible sources of uncertainty in this study, and most are difficult to quantify. First, sampling only three times over the annual cycle likely does not fully capture seasonal variability. Peaks in discharge and NO_3^- concentration at some sites during snowmelt were not captured by the spring (April) sampling event (Figure 6.5). Storm events with high discharge are also missed; these can have high NO_3^- concentrations, though not consistently (T.F. Cummings, unpublished data). Therefore, average annual NO_3^- concentrations, standing stock and export to Lake Erie are severely underestimated because of poor winter and storm coverage. Interannual changes in the river are also not addressed in this study.

Denitrification rates are poorly estimated in this study. Direct measurement by N_2:Ar (after (Laursen and Seitzinger 2002)) failed. Other techniques such as whole-river ^{15}N tracer addition are best suited to small streams where mixing is rapid and reasonable amounts of tracers are needed (Mulholland et al. 2008). ^{15}N tracer additions are also labour-intensive. Better understanding of constraints on N_2O:(N_2O+N_2) ratios would also help constrain estimates of denitrification. Some N_2O likely enters the river from groundwater, although only a few measurements have been made near Site 13 (range: 37.3 nmol/L to 281.1 nmol/L, n = 5) (Encalada Romero 2008). N_2O concentrations in tributaries of the Grand River can be high, especially from small, agricultural creeks (Rempel 2008) but further study is needed to quantify N_2O loads to the Grand River.

Spatial coverage of the river could also be improved in future studies by increasing the number of sampling sites. For instance, sites could include only one large tributary, WWTP, dam or other influence on the river. Additionally, discharge was estimated at some sites (especially in the Lower Agricultural section) by adding gauged tributary flow to river flow. This results in underestimation of flow because groundwater and ungauged tributaries are not included. Better in-field measurements that change to reflect changing water level would increase certainty of flux measurements.

Stable isotopic measurements of NO_3^- in this study could also be improved. Due to a laboratory switch in methods during through the sampling period, $\delta^{15}N\text{-}NO_3^-$ was measured with three different methods ($AgNO_3$, chemical denitrification and biological denitrification). The methods do not always have strong linear correlations (Figure 6.2) and may bias measurements. It is unknown if the $AgNO_3$ method incorporates any sample NO_2^- in the $\delta^{15}N\text{-}NO_3^-$ measurement but the other two methods do. Additionally, samples from both pre-dawn and solar noon were used for isotope analysis. Typically $\delta^{15}N\text{-}NO_3^-$ does not change much on the diel scale in the Grand River except at a site immediately downstream of the Kitchener WWTP (Site 11, (Thuss 2008)). However, to improve consistency of the isotope mass balance results, one method of preparing $\delta^{15}N\text{-}NO_3^-$ should be used, with either samples from approximately the same time of day, or an average of pre-dawn and solar noon samples.

The whole-watershed annual box model also contains many potential sources of uncertainty. The IPCC estimates for NO_3^- leached from agricultural sources (fertilizers, crop residues and manure) could not be independently verified in this study. Additionally, local values of emission factors and fraction leached were not known, and global averages were used. Some inputs to the equations, such as percentage crop residue removed, and average mass of livestock species were estimated due to lack of direct measurements. It is likely that these relationships do not hold in this watershed, and/or that the factors used are not appropriate for the area. Research on the accuracy of these equations is scarce but the few published studies agree that the IPCC overestimates NO_3^- leaching from N fertilizer application, crop residue and manure management (Brown et al. 2001, Delgado et al. 2010, Silgram et al. 2001). The whole-watershed model could not differentiate between NO_3^- losses (e.g. assimilation, denitrification) and NO_3^- storage (e.g. in soil, organic matter and groundwater) in the watershed. This is an important distinction, as NO_3^- storage may become a legacy problem in future while NO_3^- loss is permanent. More research is needed to quantify NO_3^- storage in the watershed and determine NO_3^- residence time for each reservoir in the watershed.

The high uncertainty of several inputs results in large propagated uncertainty in this NO_3^- isotope box model, especially for δGAIN and δLOSS in downstream reaches. However, the model is useful in that it provides a first estimate of net NO_3^- gains and losses throughout the Grand River and does not require a large number of inputs, unlike mechanistic river water quality models (e.g. SWAT, RiverStrahler). The estimated NO_3^- stable isotopic ratios of net NO_3^- gains and losses to the river provide a check on the model – values very different than expected indicate a problem with the model

and/or with the assumed NO_3^- inputs and losses. The model provides the first estimate of a "big picture" N cycle for the Grand River watershed, allowing comparison of watershed NO_3^- loading, NO_3^- mass entering the river, NO_3^- mass lost in the river, and NO_3^- mass exported to Lake Erie, on the seasonal and annual scale.

6.5 Conclusions

NO_3^- concentration and areal mass flux in the Grand River increased with distance downstream year-round, with very few exceptions. NO_3^- removal in the river overall was low. The river's four distinct sections characterized by land use and geomorphology receive and remove NO_3^- differently. High flows and NO_3^- concentrations in April dominated annual average fluxes.

Denitrification is estimated to remove 3% to 56% of annual NO_3^- gain to the river. Total net NO_3^- losses, including assimilation and other biological NO_3^- removal, are slightly higher (26% to 59%). Areal denitrification rates were highest in the Urban and Lower Agricultural sections and most net NO_3^- loss occurs in the Lower Agricultural section. NO_3^- is added throughout the entire river, but areal inputs are high in the Urban, Groundwater Recharge and Lower Agricultural sections. Estimated inputs to the entire watershed, including WWTPs, septic beds and agricultural N runoff (from crop residue, fertilizer and manure) are high (43.1 Gg N/year) but only a fraction (7.5 (12.9) Gg N/year) enter the river itself as NO_3^-. Thus, 68% to 83% of watershed NO_3^- loading to freshwater is removed before entering the river, 5% to 19% is lost in the Grand River, and 13% is exported to Lake Erie. Promoting NO_3^- loss is important for ecosystem health (both for the Grand River and waterbodies downstream) and for drinking water quality (NO_3^- limit: 10 mg N/L). NO_3^- concentrations are highest in the Grand River in winter and snowmelt but in-river NO_3^- removal (by assimilation and denitrification) is low in winter due to low temperatures and high DO. This research suggests that promoting NO_3^- loss (denitrification, assimilation, etc.) in the Grand River itself will have a small effect on in-river NO_3^- concentrations and N export to Lake Erie. Therefore, focus should be placed on reducing NO_3^- use in the watershed (e.g. by reducing and correctly timing agricultural fertilizer application, and upgrading WWTPs to denitrify sewage within the plant). NO_3^- removal efforts should focus on denitrification hotspots (wetlands, riparian zones) throughout the watershed. Additionally, NO_3^- removal mechanisms that are effective at low surface temperature, such as denitrification in groundwater, can also be considered.

Table 6.1: Reaches of the Grand River used in the NO_3^- isotope mass balance. Surface area and depth of each station were determined by field work (white boxes), the GRSM (light grey boxes) and the Waterbody Segment GIS layer (Ontario Ministry of Natural Resources) (dark grey boxes). Missing depth values (black box) were estimated used exponential discharge vs. depth relationships (Figure 6.4). Important point sources (tributaries, WWTPs, dams) are also noted.

Reach Number	Distance from sampling point to headwaters (km)	Depth (m)	surface area (m^2)
	2.93	0.17	34112.5
2	21.43	0.20	150177.5
3	33.18	0.50	233073.5
4	40.45	0.45	178823.3
5	53.11	0.50	534419.6
6	71.01	0.45	5397190
7	83.91	0.45	546846.9
8	98.05	0.52	1024904
9	119.24	0.45	721351
10	135	0.60	1364206
11	145.82	0.52	605830.4
12	153.07	1.90	349824.1
13	164.13	0.71	885836.9
14	175.45	0.59	925347.9
15	181.76	0.62	633333.4
16	187.89	1.12	1357354
17	216.64	1.84	1723444
18	232.29	2.13	808803.5
19	250.6	4.03	2871105
20	253.6	4.12	1176707
21	263.05	4.12	3222960
22	288.12	4.13	2665846
23	295.66	4.14	2665846
Grand Valley WWTP	44.86		
Shand Dam	69.68		

Fergus WWTP	75.38
Elora WWTP	80.84
Canagagigue Creek Confluence	99.85
Conestogo Confluence	106.78
Waterloo WWTP	119.47
Kitchener WWTP	140.29
Speed River Confluence	147.46
Galt WWTP	155.93
Nith Confluence	176.04
Paris WWTP	179.3
Fairchild Creek Confluence	228.28
Caledonia WWTP	246.34
Cayuga WWTP	264.42
Dunnville WWTP	289.01

Table 6.2: N_2O:(N_2O+N_2) ratios produced during denitrification in laboratory experiments. WHC = water holding capacity. WFPS = water-filled pore space. ND = no data.

Medium	Moisture	Oxygen concentration	Temperature conditions (°C)	N_2O:(N_2O+N_2)	Notes	Citation
Soil	1 mL water/g soil	0	room temp.	0.46	3-5 h	(Firestone and Tiedje 1979)
Soil	1 mL water/g soil	0	room temp.	0.48	7-12 h	
Soil	1 mL water/g soil	0	room temp.	0.48	18-23 h	
Soil	1 mL water/g soil	0	room temp.	0.48	26-29 h	
Soil	1 mL water/g soil	0	room temp.	0.2	33-37 h	
Soil	1 mL water/g soil	0	room temp.	0.91	3-4 h	
Soil	1 mL water/g soil	0	room temp.	0.82	5-10 h	
Soil	1 mL water/g soil	0	room temp.	0.26	22-25 h	
Soil	ND	0	ND	0.31		(Firestone et al. 1980)
Soil	ND	0.016 atm	ND	0.47		
Soil	ND	0.163 atm	ND	0.59		
Soil	ND	ND	ND	0.02	0 ppm NO_2^-	
Soil	ND	ND	ND	0.15	0.5 ppm NO_2^-	
Soil	ND	ND	ND	0.31	2 ppm NO_2^-	
Soil	ND	ND	ND	0.86	20 ppm NO_2^--	
Soil	ND	ND	ND	0.01	0 ppm NO_3^-	
Soil	ND	ND	ND	0.06	0.5 ppm NO_3^-	
Soil	ND	ND	ND	0.11	2 ppm NO_3^-	
Soil	ND	ND	ND	0.19	20 ppm NO_3^-	
Soil	ND	ND	ND	0.06	pH 4.9	

Soil	ND	ND	ND	0.04	pH 6.5	
Soil	ND	ND	ND	0.71	pH 4.9+10 ppm NO_3^-	
Soil	ND	ND	ND	0.14	pH 6.5+10 ppm NO_3^-	
Soil	ND	ND	ND	0.13	0.1-1.7 h	
Soil	ND	ND	ND	0.36	2-4 h	
Soil	ND	ND	ND	0.57	5-12 h	
Soil	ND	ND	ND	0.008	23-28 h	
Soil	ND	ND	ND	0	33-51 h	
Soil	60% WHC	ND	ND	0.222	9-15 days	(Klemedtsson et al. 1988)
Soil	80% WHC	ND	ND	0.200	0-2 days	
Soil	80% WHC	ND	ND	0.083	3-6 days	
Soil	80% WHC	ND	ND	0.054	9-15 days	
Soil	90% WHC soil	ND	ND	0.667	0-2 days	
Soil	90% WHC soil	ND	ND	0.212	3-6 days	
Soil	90% WHC soil	ND	ND	0.039	9-15 days	
Soil	100% WHC soil	ND	ND	0.477	0-2 days	
Soil	110% WHC soil	ND	ND	0.014	3-6 days	
Sandy Soil	60% WFPS	ND	ND	0.833		(Weier et al. 1993)
Sandy Soil	90% WFPS	ND	ND	0.002		
River sediment	Saturated	ND	ND	0.010	0.14 mg N/L NO_3^-	(Silvennoinen et al. 2008)
River sediment	Saturated	ND	ND	0.027	0.42 mg N/L NO_3^-	
River sediment	Saturated	ND	ND	0.038	1.4 mg N/L NO_3^-	
River sediment	Saturated	ND	ND	0.033	4.2 mg N/L NO_3^-	
River sediment	Saturated	< 0.2 mg/L	5	0.017		(Silvennoinen et al. 2008)
River sediment	Saturated	< 0.2 mg/L	10	0.005		
River sediment	Saturated	< 0.2 mg/L	15	0.002		
River sediment	Saturated	< 0.2 mg/L	20	0.001		

River sediment	Saturated	5 mg/L	5	0.008
River sediment	Saturated	5 mg/L	10	0.001
River sediment	Saturated	5 mg/L	15	0.003
River sediment	Saturated	5 mg/L	20	0.002
River sediment	Saturated	10 mg/L	5	0.011
River sediment	Saturated	10 mg/L	10	0.003
River sediment	Saturated	10 mg/L	15	0.002
River sediment	Saturated	10 mg/L	20	0.001
Mean (± standard deviation), all samples				0.22 ± 0.27
Mean (± standard deviation), river samples				0.01 ± 0.01

Table 6.3: $\varepsilon^{15}N$ values for denitrification in rivers and river-groundwater systems. Both laboratory sediment incubations and in-stream measurements are included. R = Rayleigh equation (using $\delta^{15}N\text{-}NO_3^-$), D = difference between $\delta^{15}N\text{-}NO_3^-$ and $\delta^{15}N\text{-}N_2$.

Field Site	Method	$\varepsilon^{15}N$ (‰)	Citation
Morgan Creek, MD	In-stream, D	-10	(Böhlke and Denver 1995)
South Platte River, CO	In-stream, D	-20 to -10	(McMahon and Böhlke 1996)
Agricultural streams, QC	In-stream, R	-10.0	(Kellman and Hillaire-Marcel 1998)
Seine River sediment (diffusion-limited)	Laboratory incubation, R	-3.6 to -1.5	(Sebilo et al. 2003)
Seine River (not diffusion-limited)	Laboratory incubation, R	-18	(Sebilo et al. 2003)
Agricultural creeks, NY	In-stream, R	-4	(Burns et al. 2009)
Beijiang River, China	In-stream, R	-14.8	(Chen et al. 2009)
Seine River	In-stream, R	-3	(Curie et al. 2009)
Khura R., Trang R., Thailand	In-stream, R	-16.3 to -6.6	(Miyajima et al. 2009)
Rainforest stream, Ecuador	In-stream, R	-3.9 to -1.5	(Schwarz et al. 2011)
R. Wensum, UK	In-stream, R	-11.1 to -5.1	(Wexler et al. 2011, Wexler et al. 2012)
Ichetucknee River, FL	In-stream, R	-3.1	(Cohen et al. 2012)

Table 6.4: N leaching rates from septic beds. Note that various N compounds are measured: NO_3^-, dissolved inorganic nitrogen (DIN), total dissolved nitrogen (TDN) and total nitrogen (TN).

Site	Compound measured	Minimum leaching rate (kg N/capita/yr)	Mean leaching rate (kg N/capita/yr)	Maximum leaching rate (kg N/capita/yr)	Citation
Literature review	NO_3^-		5.6		(Ontario Ministry of the Environment 1996)
Rhode Island	DIN		2.3		(Gold et al. 1990)
Virginia	DIN	2.4		2.9	(Reay 2004)
Long Island, NY	TDN		2.3		(Koppelman 1978)
Massachusetts	TDN	1.6		2.7	(Weiskel and Howes 1991)
Chesapeake Bay area	TDN	2.4		3.4	(Maizel et al. 1997)
Sandy soil	TDN		1.41		(Humphrey et al. 2012)
Sandy loam soil	TDN		0.33		(Humphrey et al. 2012)
Sandy clay loam soil	TDN		0.04		(Humphrey et al. 2012)

Literature average	TN	4.5	(Hoffman and Canace 2004)
Mean (all values)		4.5	

178

Table 6.5. Denitrification rates from rivers worldwide. Only field measurements are included.

Site	Minimum Denitrification Rate (mg $N/m^2/d$)	Mean Denitrification Rate (mg $N/m^2/d$)	Maximum Denitrification Rate (mg N/m2/d)	Method	Citation
Chiangjiang R., China	39.5		80.4	N_2:Ar open channel	(Yan et al. 2004)
Connecticut R., USA		2.8		N_2:Ar open channel	(Smith et al. 2008)
Delaware River, USA	1.6		4.8	N_2 flux	(Seitzinger and Kroeze 1998)
Potomac River, USA	2.9		3.3	N_2 flux	(Seitzinger and Kroeze 1998)
San Francisco Creek, USA		0.4		C_2H_2	(Duff et al. 1984)
Sangamon R., USA	0.1	13.6	15.0	C_2H_2	(Royer et al. 2004)
Seine R., France	7.0		42.0	N mass balance	(Chesterikoff et al. 1992)
South Platte R., USA		221.8		N_2 open channel	(McCutcheon 1989)
South Platte R., USA		67.5		Open channel	(Pribyl et al. 2005)
South Platte R., USA		87.9		N mass balance	(Pribyl et al. 2005)
South Platte R., USA	2.0		100.0	N mass balance	(Sjodin et al. 1997)
Sugar Creek., USA		3.8		N_2:Ar	(Laursen and Seitzinger 2002)
Sugar Creek, USA		1.7		^{15}N addition	(Böhlke et al. 2004)
Swale River, UK		3.5		C_2H_2	(Pattinson et al. 1998)
Walker Branch, USA		0.2		^{15}N addition	(Mulholland et al. 2004)
Wiske R., UK		11.9		C_2H_2	(Pattinson et al. 1998)

Table 6.6: Areal N assimilation rates (ASM) estimates from the Grand River using community productivity rates from the PoRGy model (Venkiteswaran et al. in submission) and Equation 6.16. Net NO_3^- gains to each reach (GAIN) are also shown. Negative values for GAIN indicate a net NO_3^- loss (LOSS). GAIN and ASM rates are in mg N/m^2/h. Only sites with three samplings per day were modeled with PoRGy. ND = no data (no acceptable PoRGy runs).

	June			September			April		
Reach	GAIN (1:11)	GAIN (1:400)	ASM	GAIN (1:11)	GAIN (1:400)	ASM	GAIN (1:11)	GAIN (1:400)	ASM
1	2.5	15.6	6.6	0.0	0.4	ND	55.1	61.2	1.1
4	1.0	10.5	12.8	-0.6	10.2	7.7	43.1	49.9	3.4
8	4.4	40.8	25.6	-1.2	17.5	33.2	50.8	59.0	22.3
12	238.8	427.2	22.3	190.1	225.5	ND	729.8	743.1	ND
16	19.7	63.2	25.4	8.4	16.8	20.6	91.6	103.3	18.2
20	-0.3	30.0	18.2	-3.1	17.9	ND	101.1	123.6	17.3
23	4.1	50.9	49.0	2.2	82.0	51.1	99.9	127.3	ND

Table 6.7: Annual average WWTP effluent NO_3^- and NH_4^+ loads to the Grand River (Environment Canada 2010) as a fraction of net NO_3^- gain (GAIN). Negative values in the GAIN columns are net losses (LOSS). Effluent loads and RES in mg N/m^2/h. (A) 1:11 ratio, (b) 1:400) ratio. Only WWTPs with available data are shown. ND = no data.

A. 1:11 ratio

				June			September			April		
Reach	WWTP Name	Effluent NO_3^- Load	Effluent NH_4^+ load	GAIN	NO_3^- /GAIN	(NO_3^- + NH_4^+) /GAIN	GAIN	NO_3^- /GAIN	NO_3^- + NH_4^+)/ GAIN	GAIN	NO_3^- /GAIN	NO_3^- + NH_4^+) /GAIN
2	Dundalk	ND	0.01	-0.30	ND	-0.04	0.00	ND	3.66	3.42	ND	0.00
7	Fergus, Elora	ND	0.02	9.08	ND	0.00	9.18	ND	0.00	27.32	ND	0.00
10	Waterloo	0.19	0.36	16.94	0.01	0.03	22.39	0.01	0.02	31.66	0.01	0.02
11	Kitchener	0.15	1.83	37.60	0.00	0.05	85.41	0.00	0.02	12.21	0.01	0.16
12	Preston	0.45	0.00	238.76	0.00	0.00	190.11	0.00	0.00	729.82	0.00	0.00
13	Galt	0.60	0.01	33.76	0.02	0.02	9.35	0.06	0.07	-57.48	-0.01	-0.01
15	Paris	ND	0.01	50.63	ND	0.00	-3.34	ND	0.00	157.01	ND	0.00
17	Brantford	0.15	0.11	-6.30	-0.02	-0.04	-17.40	-0.01	-0.01	-51.31	0.00	-0.01

B. 1:400 ratio

				June			September			April		
Reach	WWTP Name	Effluent NO_3^- Load	GAIN	NO_3^- /GAIN	(NO_3^- + NH_4^+) /GAIN	GAIN	NO_3^- /GAIN	(NO_3^- + NH_4^+) /GAIN	GAIN	NO_3^- /GAIN	(NO_3^- + NH_4^+) /GAIN	NO_3^- + NH_4^+) /RES
2	Dundalk	ND	0.01	-0.30	ND	-0.04	0.00	ND	3.66	4.19	ND	0.00

7	Fergus/Elora	ND	0.02	16.97	ND	0.00	15.48	ND	0.00	34.20	ND	0.00
10	Waterloo	0.19	0.36	95.05	0.00	0.01	59.97	0.00	0.01	71.67	0.00	0.01
11	Kitchener	0.15	1.83	511.84	0.00	0.00	303.66	0.00	0.01	37.00	0.00	0.05
12	Preston	0.45	0.00	427.20	0.00	0.00	225.51	0.00	0.00	743.06	0.00	0.00
13	Galt	0.60	0.01	104.61	0.01	0.01	26.11	0.02	0.02	-36.37	-0.02	-0.02
15	Paris	ND	0.01	92.83	ND	0.00	3.68	ND	0.00	167.96	ND	0.00
17	Brantford	0.15	0.11	44.44	0.00	0.01	2.96	0.05	0.09	-35.95	0.00	-0.01

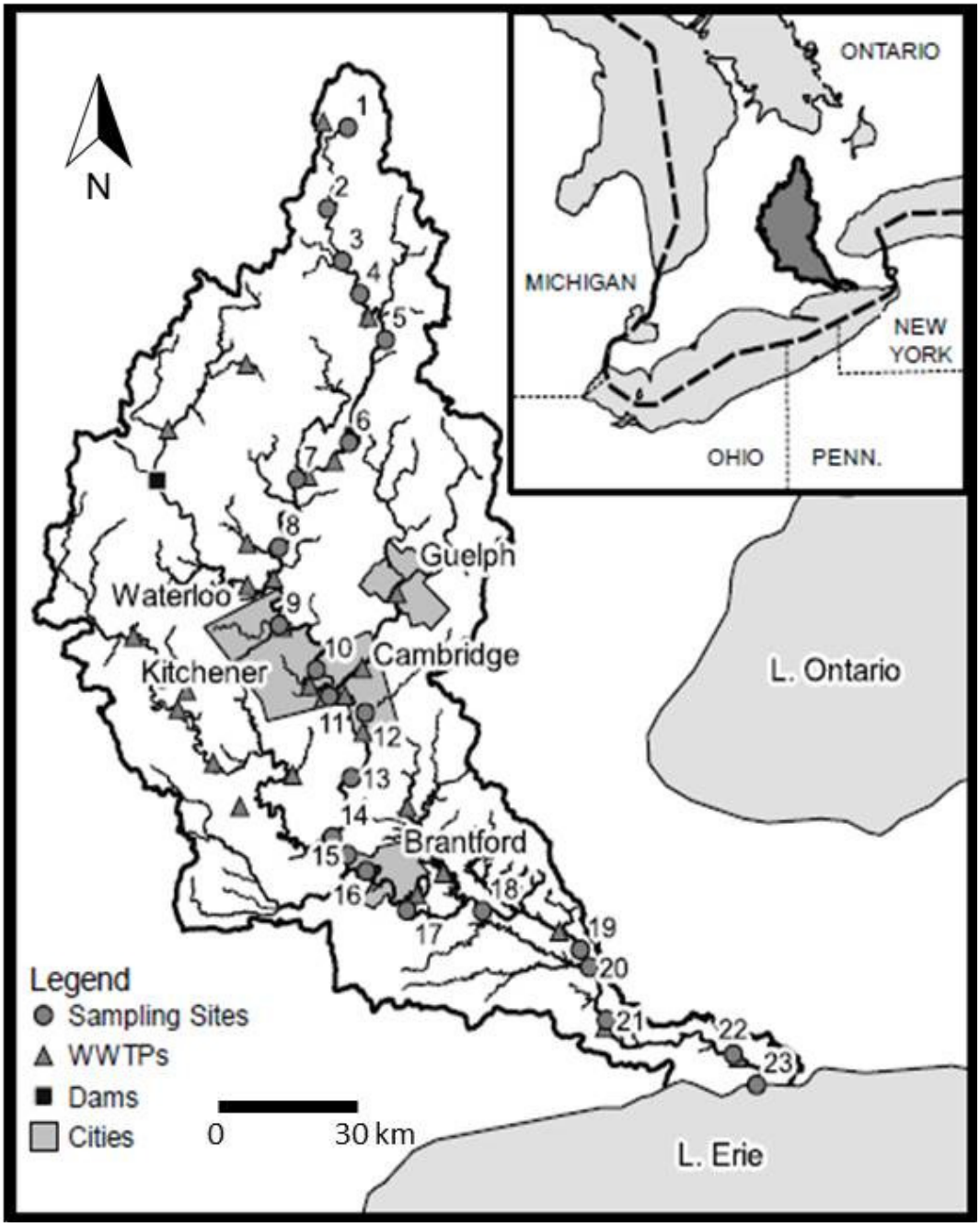

Figure 6.1: Map showing 23 sampling sites (circles) on the Grand River. Wastewater treatment plants (WWTPs) (triangles) and dams (black squares) are also shown. Image courtesy of Jason Venkiteswaran.

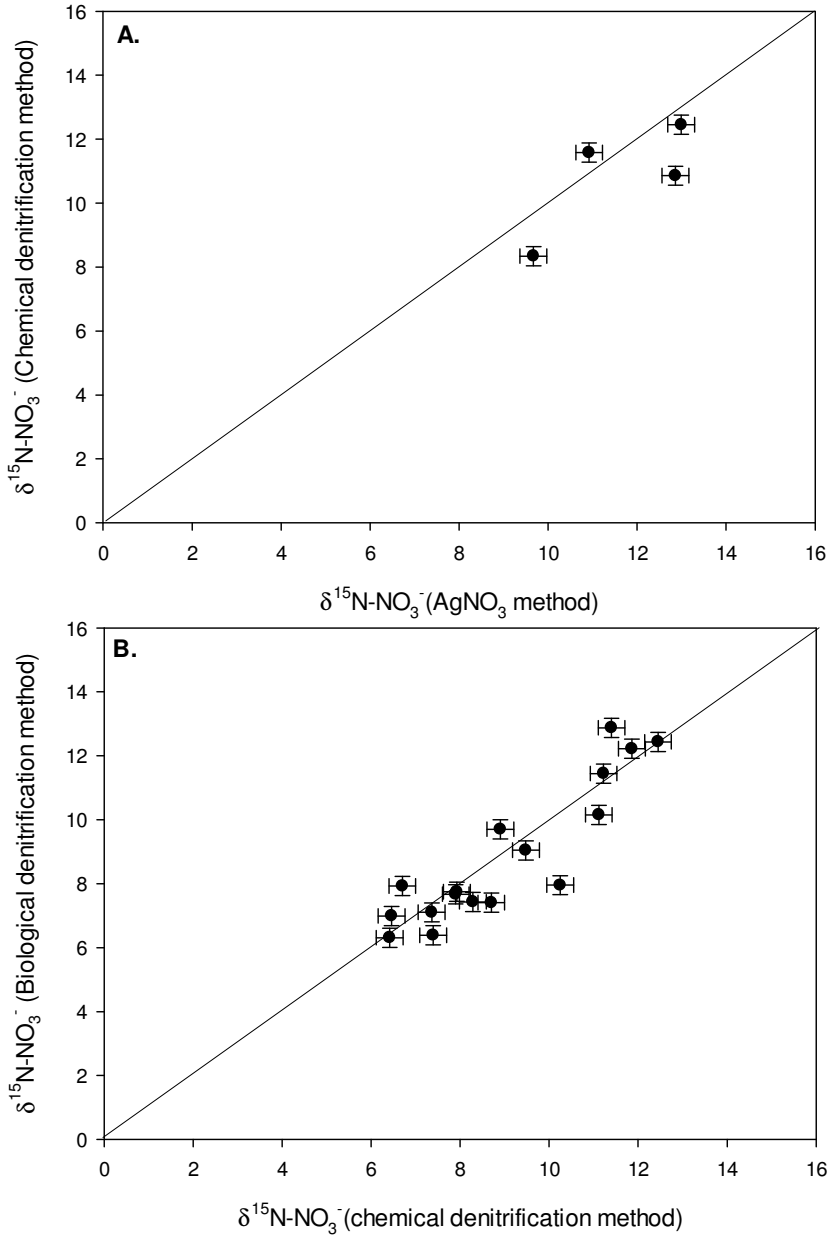

Figure 6.2: Relationships between $\delta^{15}N\text{-}NO_3^-$ measured with the $AgNO_3$ method and the chemical denitrification methods (top) and the chemical denitrification and bacterial denitrification methods (bottom), using Grand River samples only. The 1:1 line is shown in black. Error bars represent standard deviation of multiple standards.

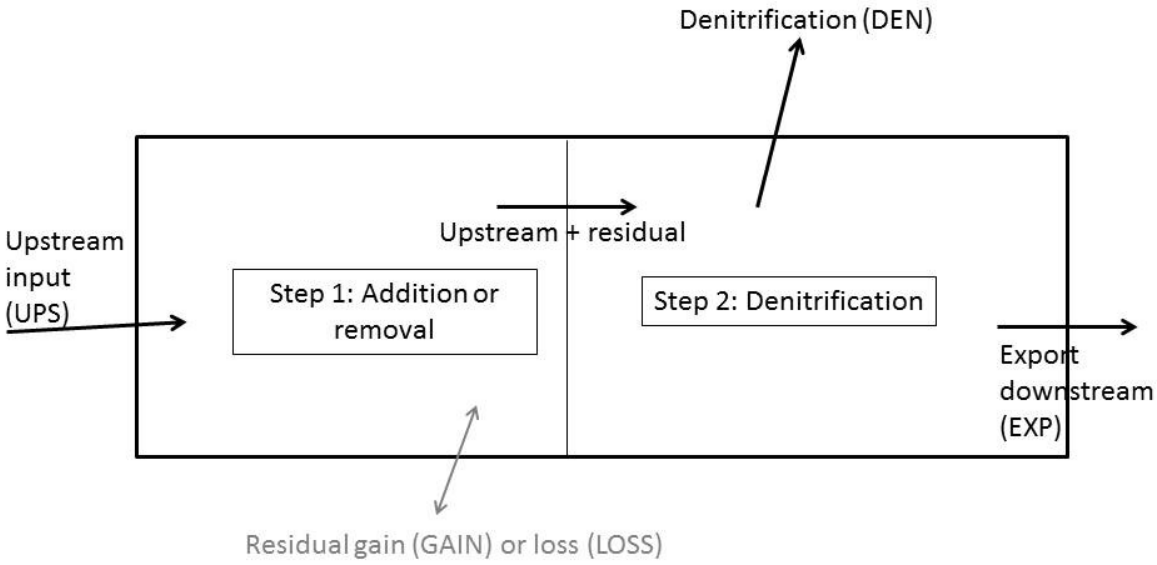

Figure 6.3: Box model schematic of one reach represented by a sampling. For each box, NO_3^- added or removed via tributaries, groundwater, assimilation etc. and fully mixed with upstream NO_3^-. The combined NO_3^- pool is then denitrified. Grey text indicates the solved-for flux.

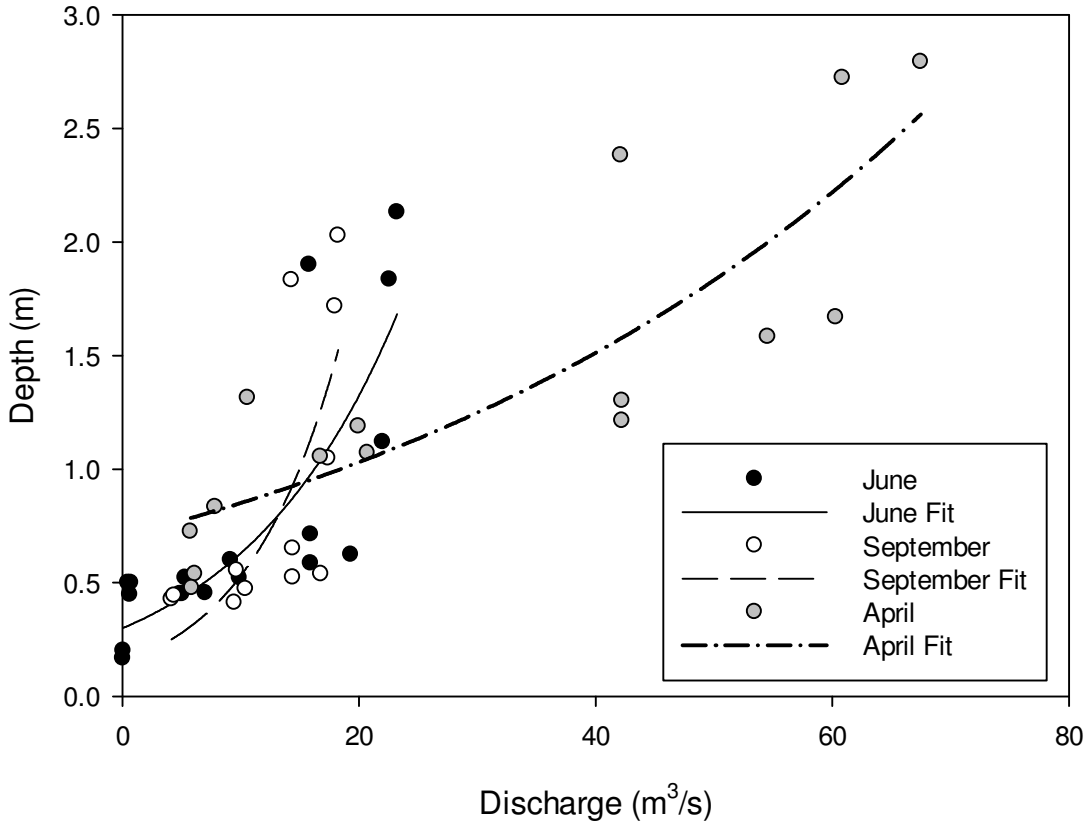

Figure 6.4: Discharge-depth relationships for June (top), September (middle) and April (bottom). Discharge data is from GRCA and National Water Survey field gauges. Depth is from field measurement during sampling events (sites 1-9) and from the Grand River Simulation Model (Mark Anderson, personal communication). All data are fit with exponential growth curves. R^2 values are 0.68 (June), 0.49 (September) and 0.73 (April).

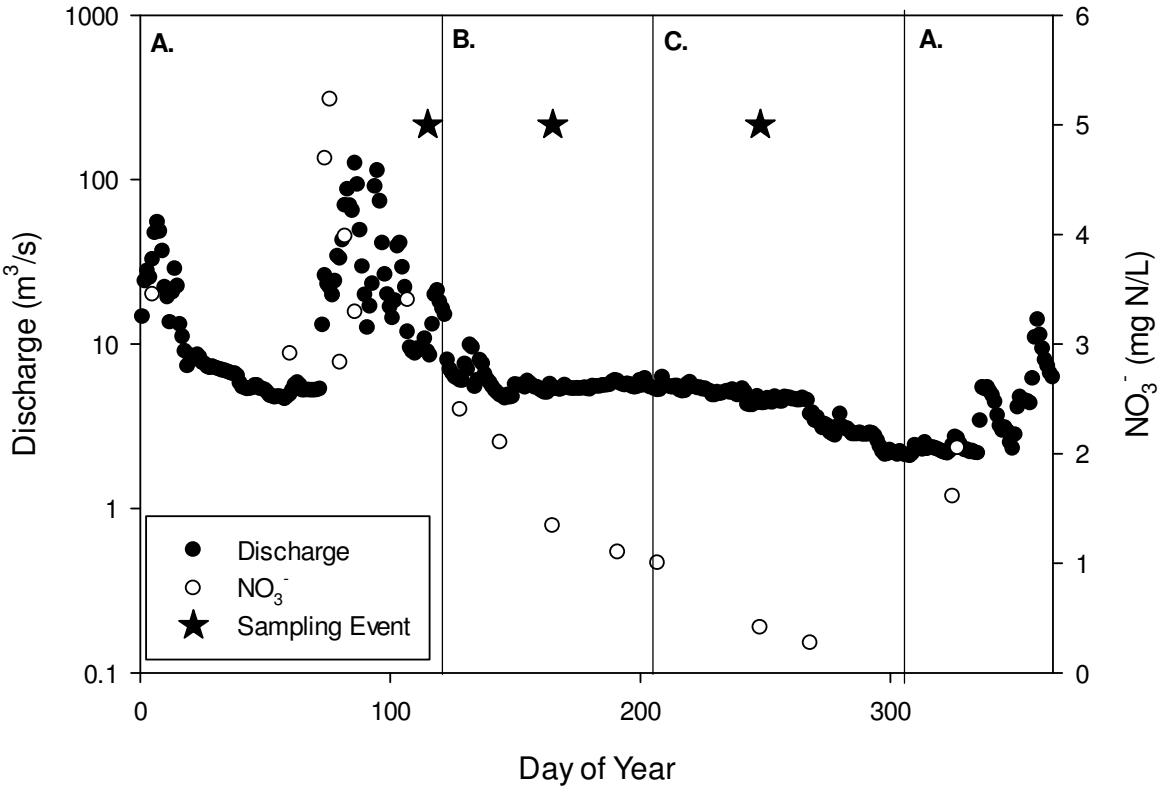

Figure 6.5: Daily average discharge (Water Survey of Canada 2010) and NO_3^- concentration at West Montrose (Site 8) in 2007. The vertical bars separate time periods represented by (A) April sampling, (B) June sampling, and (C) September sampling. Stars indicate sampling events.

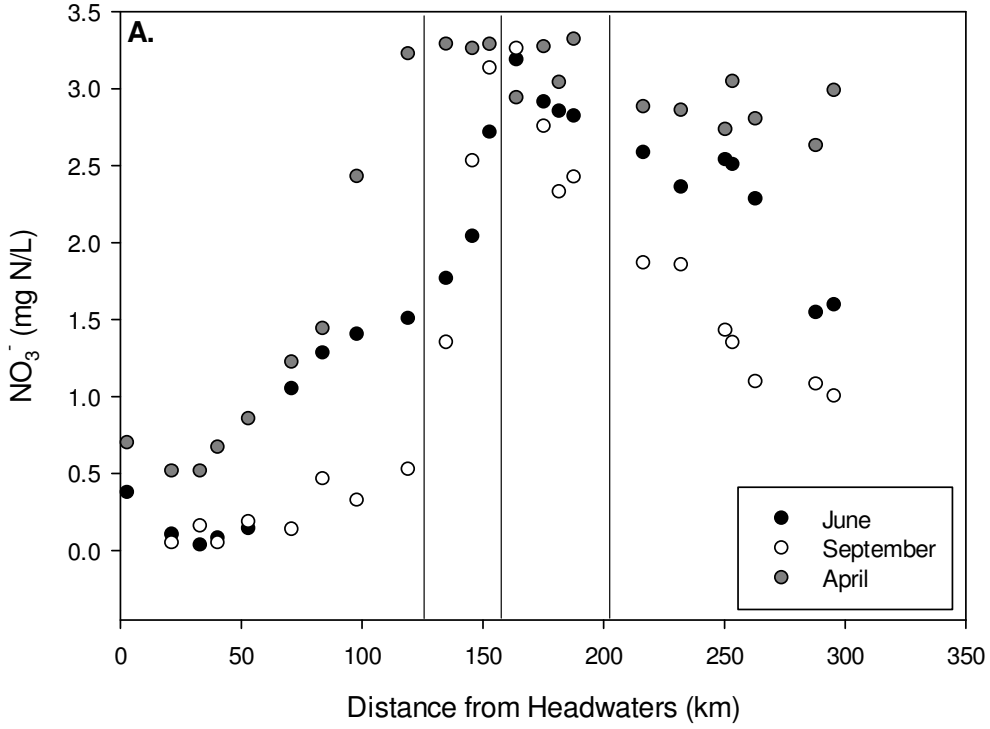
A.
NO_3^- (mg N/L)
3.5
3.0
2.5
2.0
1.5
1.0
0.5
0.0
0
50
100
150
200
250
300
350
Distance from Headwaters (km)
June
September
April

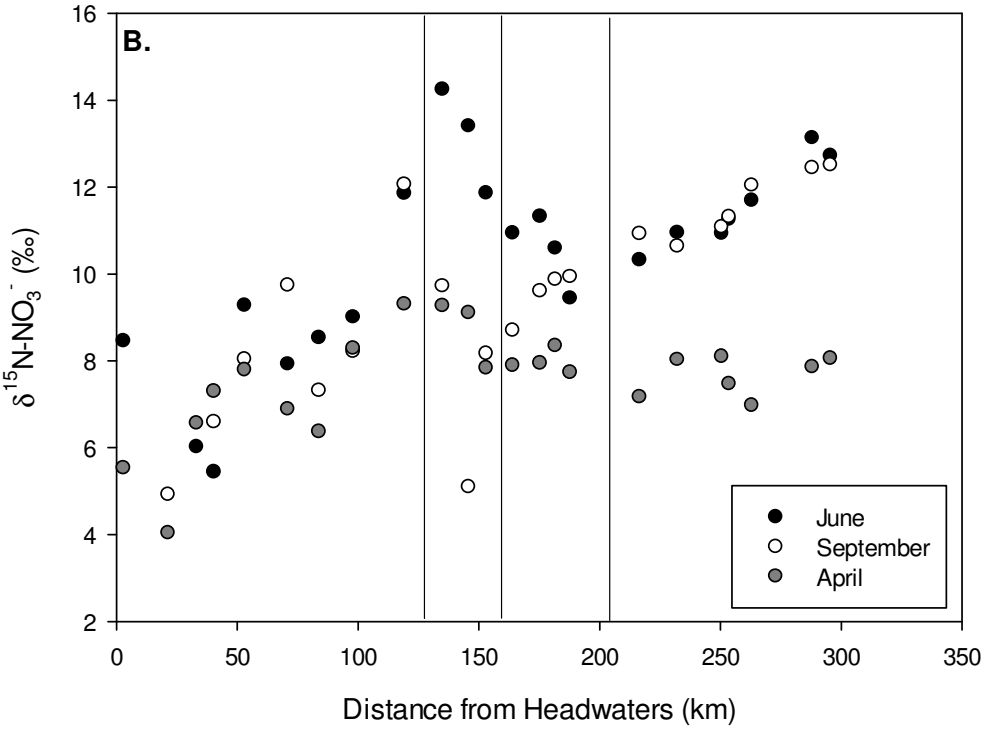
B.
$\delta^{15}N\text{-}NO_3^-$ (‰)
16
14
12
10
8
6
4
2
0
50
100
150
200
250
300
350
Distance from Headwaters (km)
June
September
April

Figure 6.6: NO_3^- concentration (Panel A) and $\delta^{15}N\text{-}NO_3^-$ (Panel B) in the Grand River in June 2007, September 2007 and April 2007. NO_3^- concentrations are the mean of pre-dawn and solar noon samplings. These values are used as the EXP component for each river section. Vertical lines separate the river into four sections described in Section 1.2.1: From upstream to downstream, Upper Agricultural, Urban, Groundwater Recharge, and Lower Agricultural.

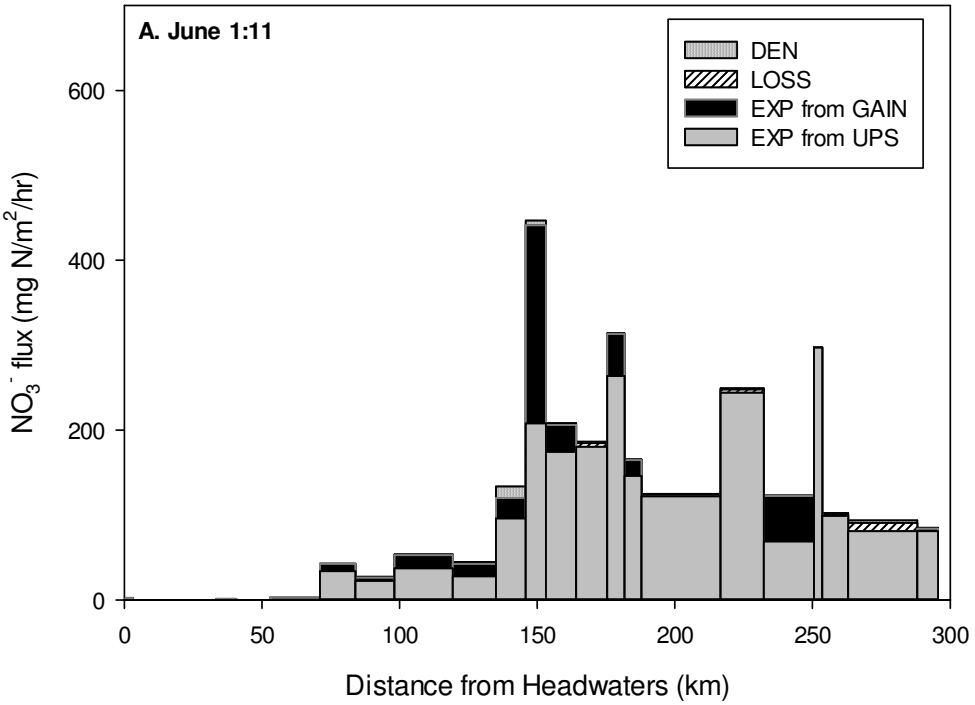
A. June 1:11
DEN
LOSS
EXP from GAIN
EXP from UPS
600
400
200
0
0
50
100
150
200
250
300
NO3- flux (mg N/m2/hr)
Distance from Headwaters (km)

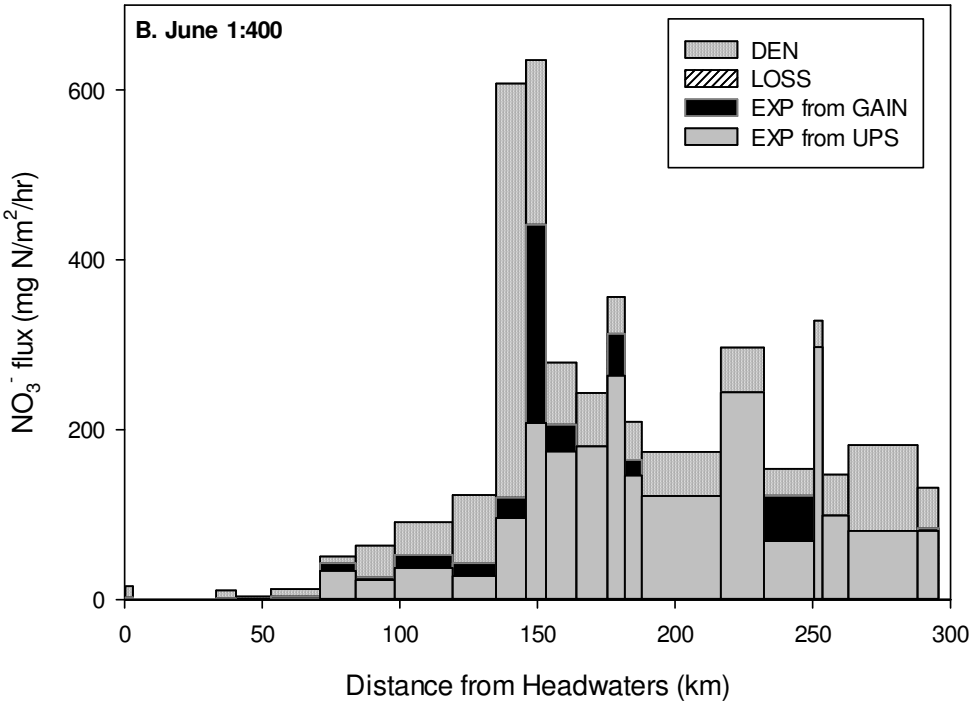
B. June 1:400
DEN
LOSS
EXP from GAIN
EXP from UPS
600
400
200
0
0
50
100
150
200
250
300
NO3- flux (mg N/m2/hr)
Distance from Headwaters (km)

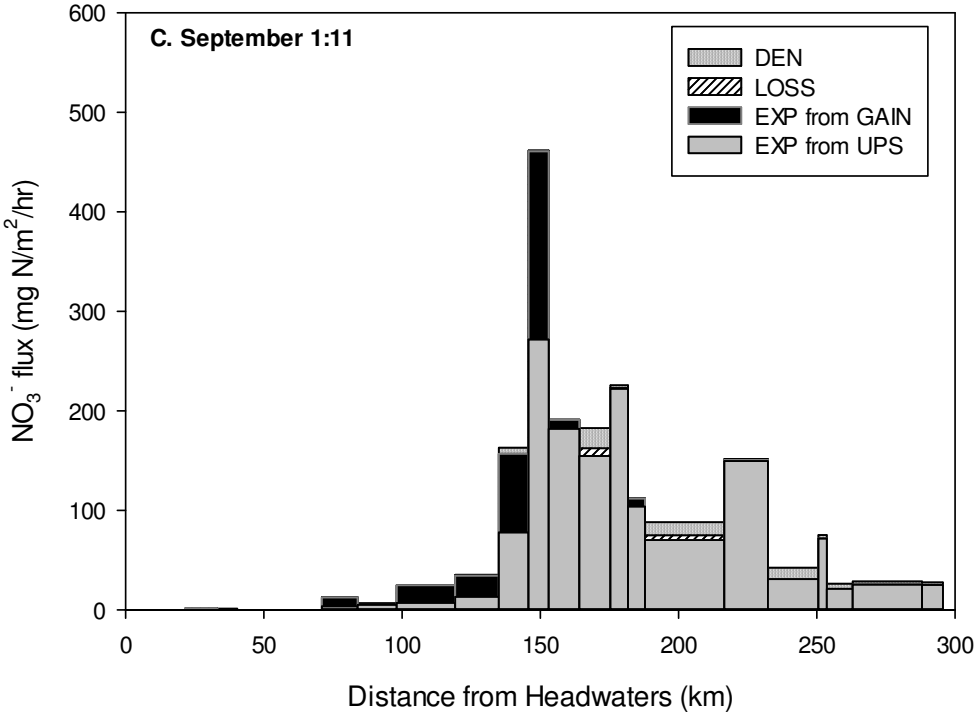
C. September 1:11
DEN
LOSS
EXP from GAIN
EXP from UPS
NO_3^- flux (mg N/m^2/hr)
Distance from Headwaters (km)
0
100
200
300
400
500
600
0
50
100
150
200
250
300

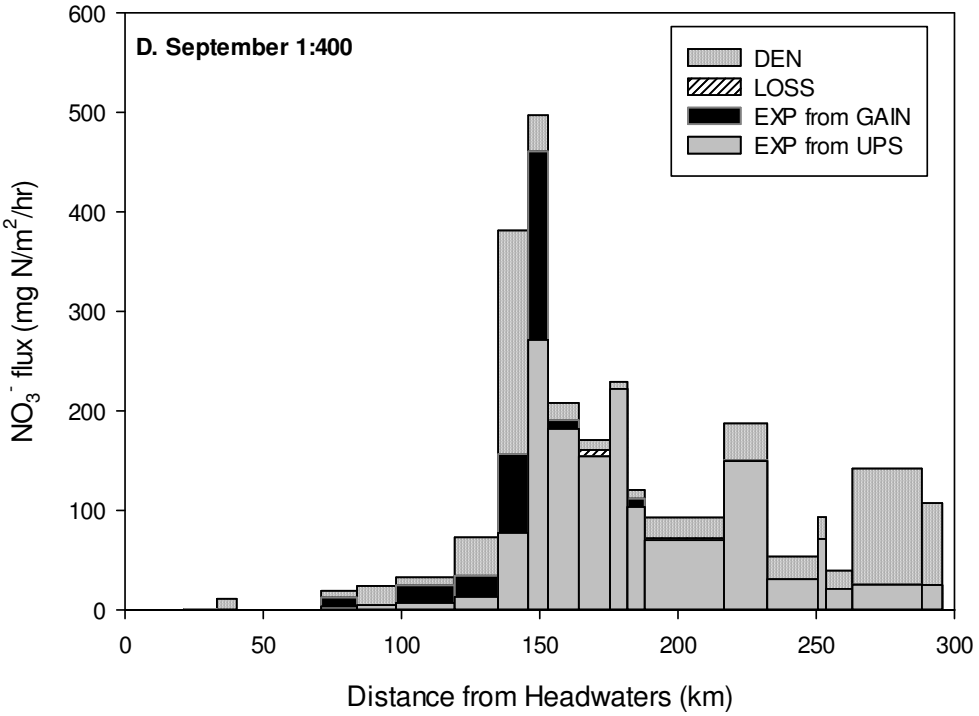
D. September 1:400
DEN
LOSS
EXP from GAIN
EXP from UPS
NO_3^- flux (mg N/m^2/hr)
Distance from Headwaters (km)
0
100
200
300
400
500
600
0
50
100
150
200
250
300

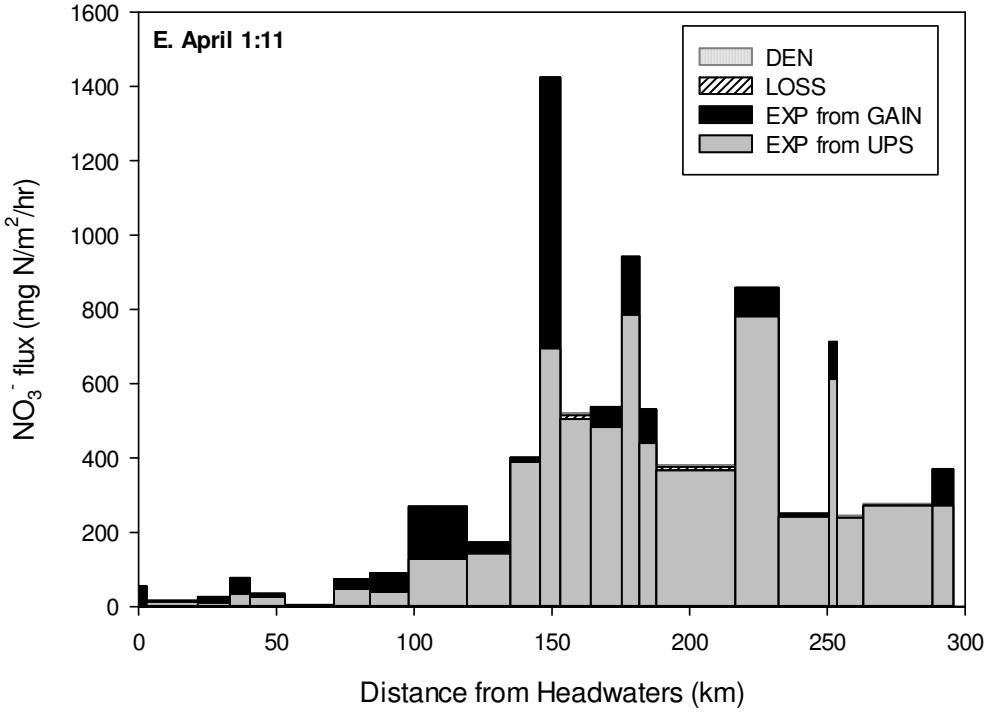
E. April 1:11
DEN
LOSS
EXP from GAIN
EXP from UPS
NO_3^- flux (mg N/m^2/hr)
Distance from Headwaters (km)
0
200
400
600
800
1000
1200
1400
1600
0
50
100
150
200
250
300

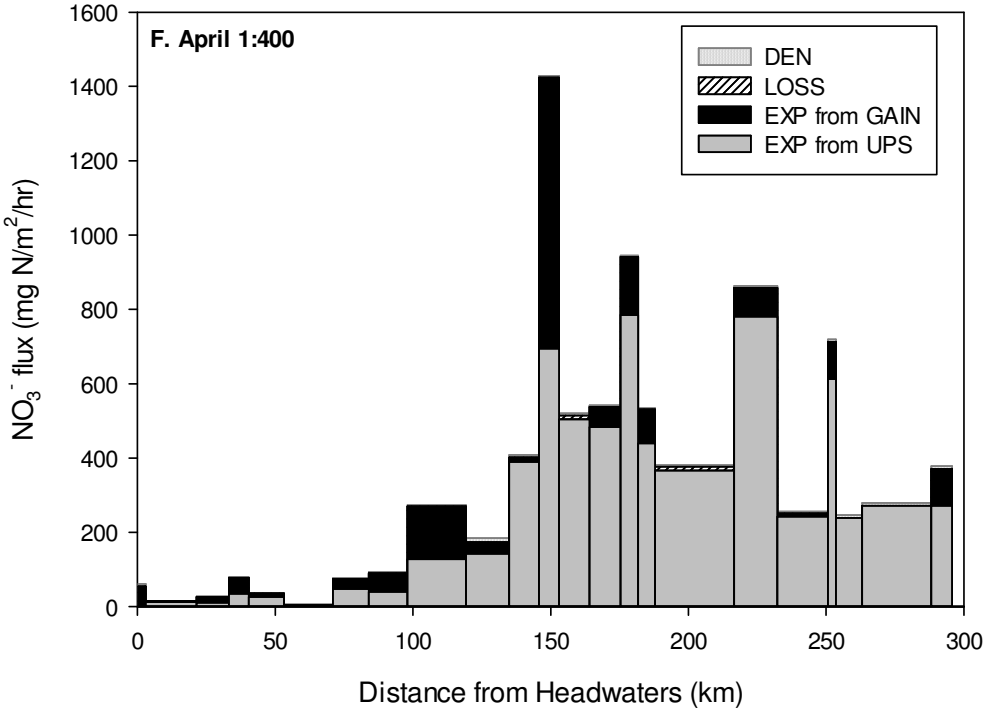
F. April 1:400
DEN
LOSS
EXP from GAIN
EXP from UPS
NO_3^- flux (mg N/m^2/hr)
Distance from Headwaters (km)
0
200
400
600
800
1000
1200
1400
1600
0
50
100
150
200
250
300

Figure 6.7: NO_3^- fluxes per section in the Grand River in June 2007 (A and B), September 2007 (C and D) and April 2009 (E and F). Note different y axes between sampling events. DEN = denitrification, LOSS = negative residual (loss per section not associated with denitrification), EXP = export to next section, GAIN = positive residual (gain per section), and UPS = flux from upstream. EXP is shown in light colours, and is divided into upstream sources (UPS) and inputs to the reach (RES). Losses are shown in dark colours (DEN and LOSS). Adding all fluxes gives a hypothetic NO_3^- export if no losses occurred. All fluxes are normalized to surface area.

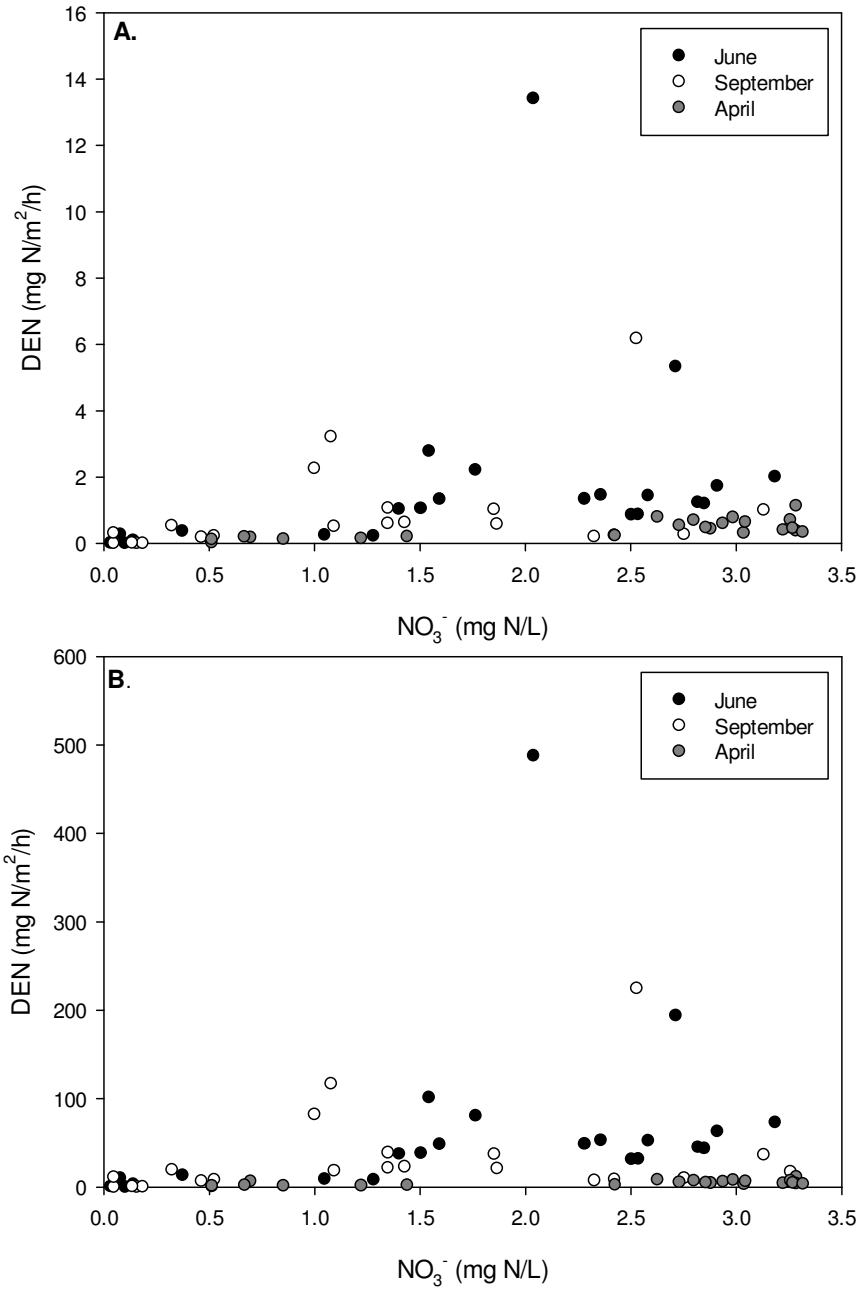

Figure 6.8. Denitrification rates versus NO_3^- concentration in the Grand River. Panel A: DEN estimated using a 1:11 N_2O:(N_2O+N_2) ratio; Panel B: DEN estimated using a 1:400 N_2O:(N_2O+N_2) ratio.

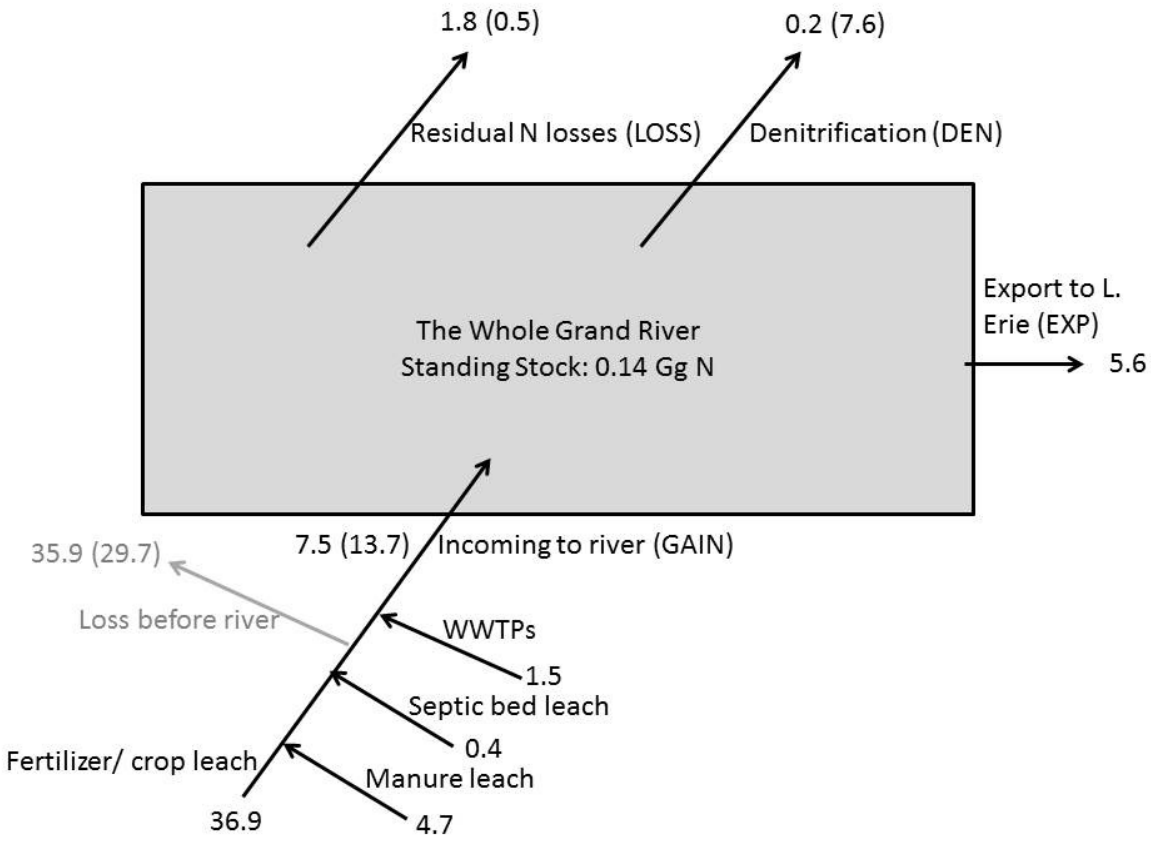

Figure 6.9: NO_3^- mass balance for the entire Grand River watershed, on an annual scale, assuming steady state. Grey text indicates solved-for variables. All fluxes are in Gg N/year. Numbers in brackets represent estimates using a 1:400 N_2O:(N_2O+N_2) ratio. Fluxes entering and leaving the Grand River were annual averages of the Grand River mass balance described above. WWTP inputs were obtained from annual reports. NO_3^- from septic beds was estimated with values from Table 6.3. NO_3^- from fertilizers, crops and manure were estimated using Equations 6.8 to 6.10. Note that the location of removal or storage of NO_3^- from watershed sources is not known.

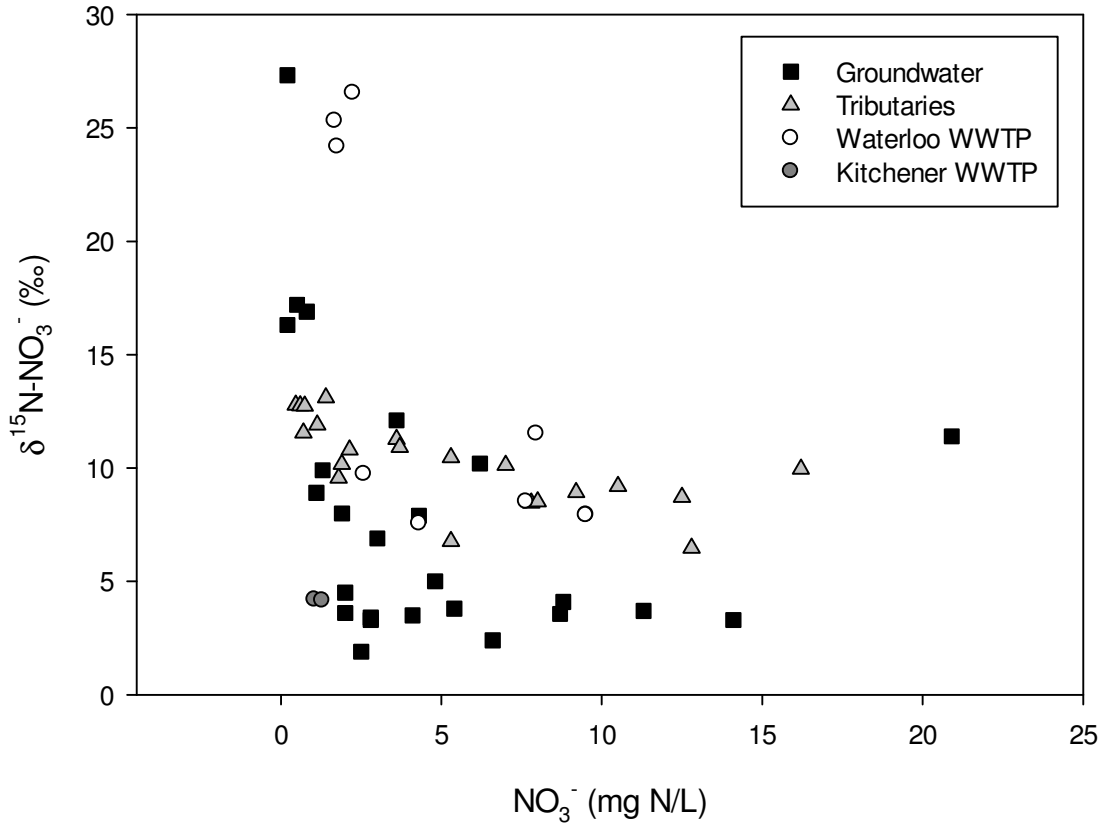

Figure 6.10: Concentration and δ^{15}N-NO_3^- values for NO_3^- inputs to the Grand River. Groundwater data are from the Groundwater Recharge section (between Sites 12 and 14) (Westberg 2012). Tributary data are from the Upper Agricultural area (between Sites 8 and 9) and include Conestogo River, Boomer Creek, Cox Creek and Swan Creek (T.F. Cummings, unpublished data). WWTP data are from Chapter 4. The range of δ^{15}N-NO_3^- of high-NO_3^- samples (> 5 mg N/L) is 2.4‰ to 11.4‰.

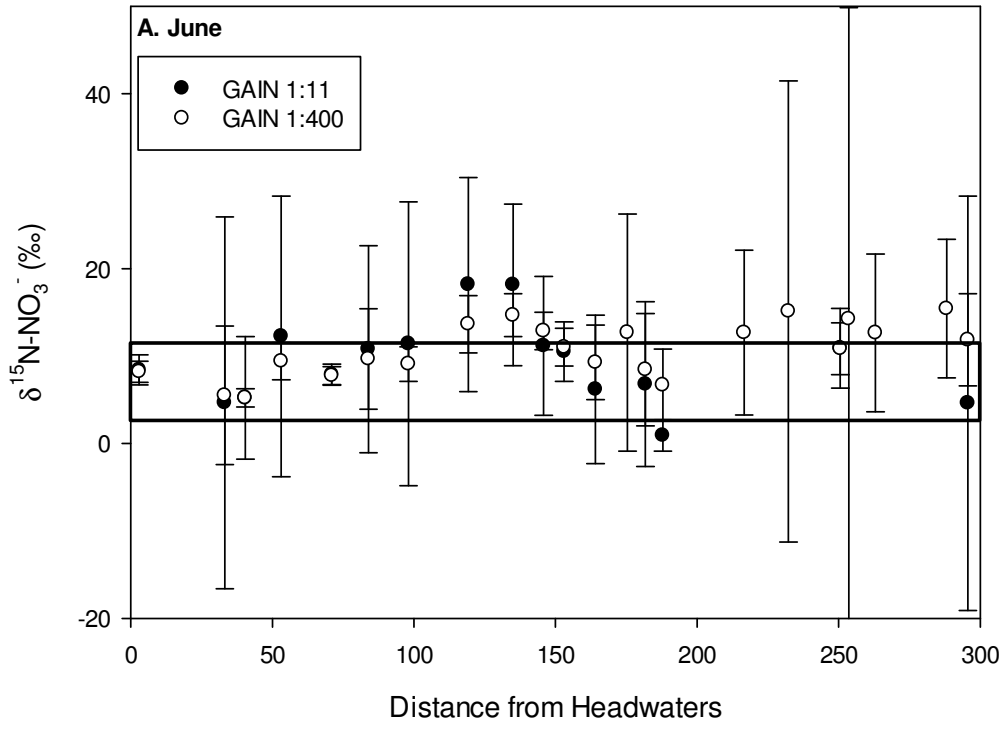
A. June
GAIN 1:11
GAIN 1:400
40
20
0
-20
0
50
100
150
200
250
300
δ15N-NO3- (‰)
Distance from Headwaters

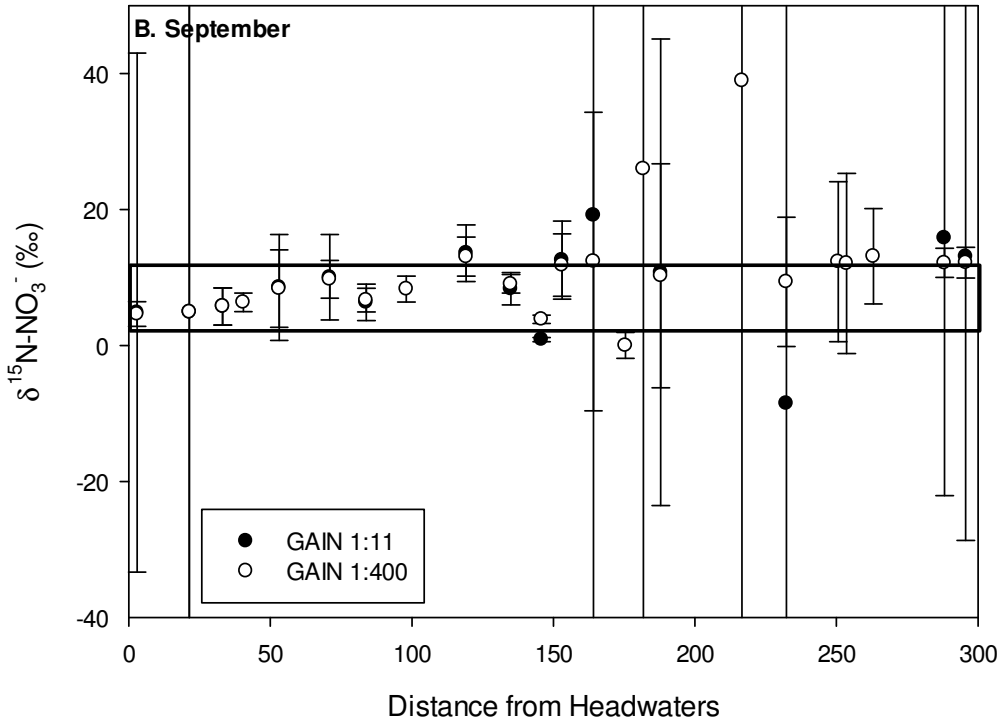
B. September
40
20
0
-20
-40
GAIN 1:11
GAIN 1:400
0
50
100
150
200
250
300
δ15N-NO3- (‰)
Distance from Headwaters

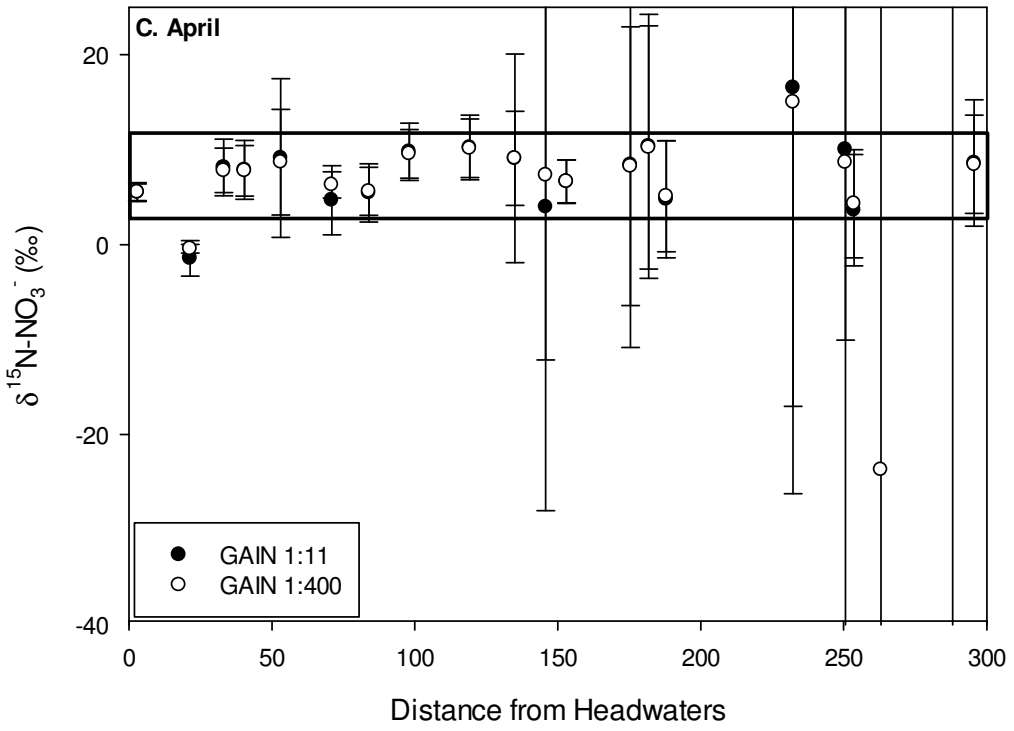
C. April
20
0
-20
-40
0
50
100
150
200
250
300
GAIN 1:11
GAIN 1:400
δ15N-NO3- (‰)
Distance from Headwaters

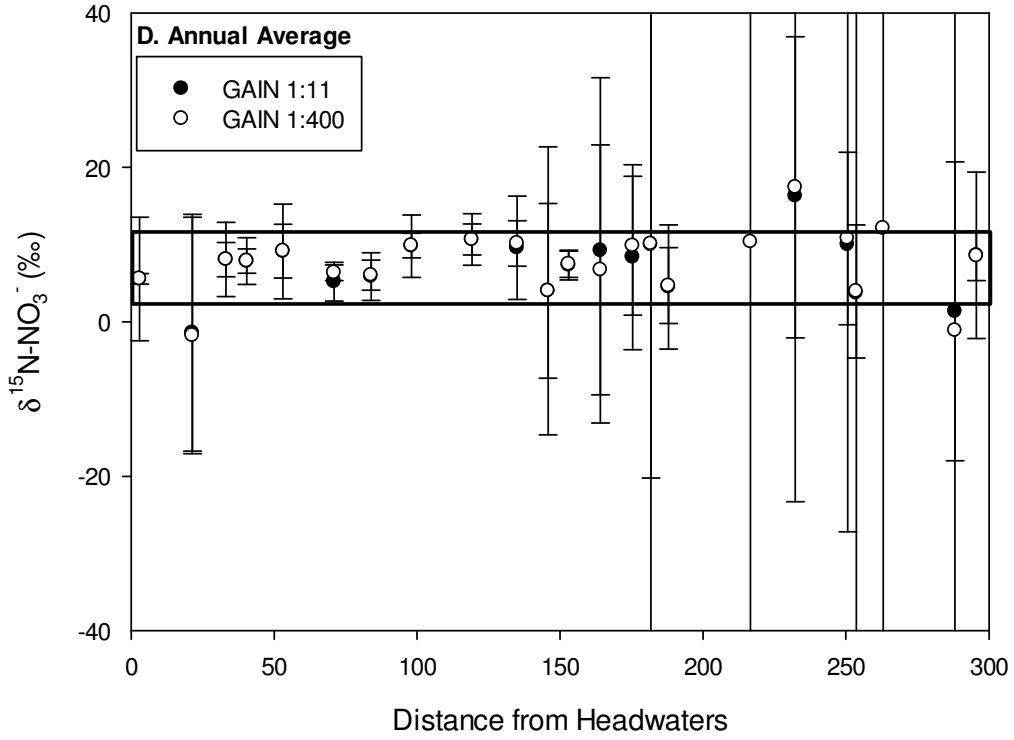
D. Annual Average
40
20
0
-20
-40
0
50
100
150
200
250
300
GAIN 1:11
GAIN 1:400
δ15N-NO3- (‰)
Distance from Headwaters

Figure 6.11: Estimated $\delta^{15}N\text{-}NO_3^-$ of net NO_3^- gain (δGAIN) in the Grand River. Black boxes show the range of $\delta^{15}N\text{-}NO_3^-$ of high-NO_3^- inputs (tributaries, WWTP effluent and groundwater > 5 mg N/L: 2.4‰ to 11.4‰). Error bars represent propagated uncertainty. Annual averages are shown in panel D.

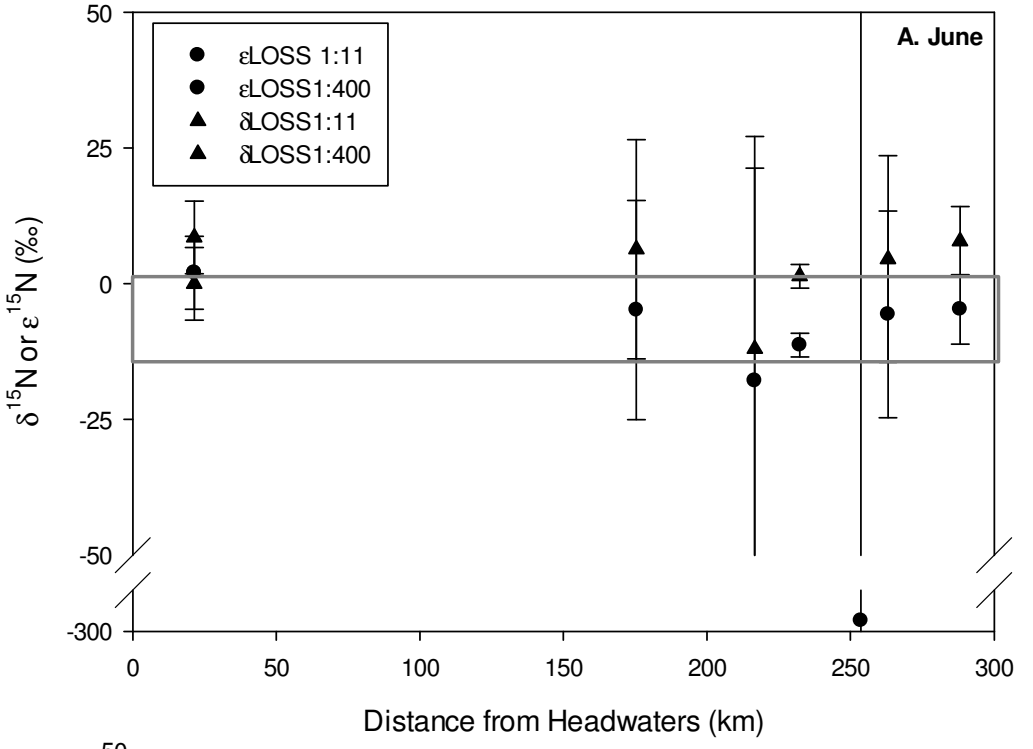
A. June
εLOSS 1:11
εLOSS1:400
δLOSS1:11
δLOSS1:400
δ15N or ε15N (‰)
Distance from Headwaters (km)

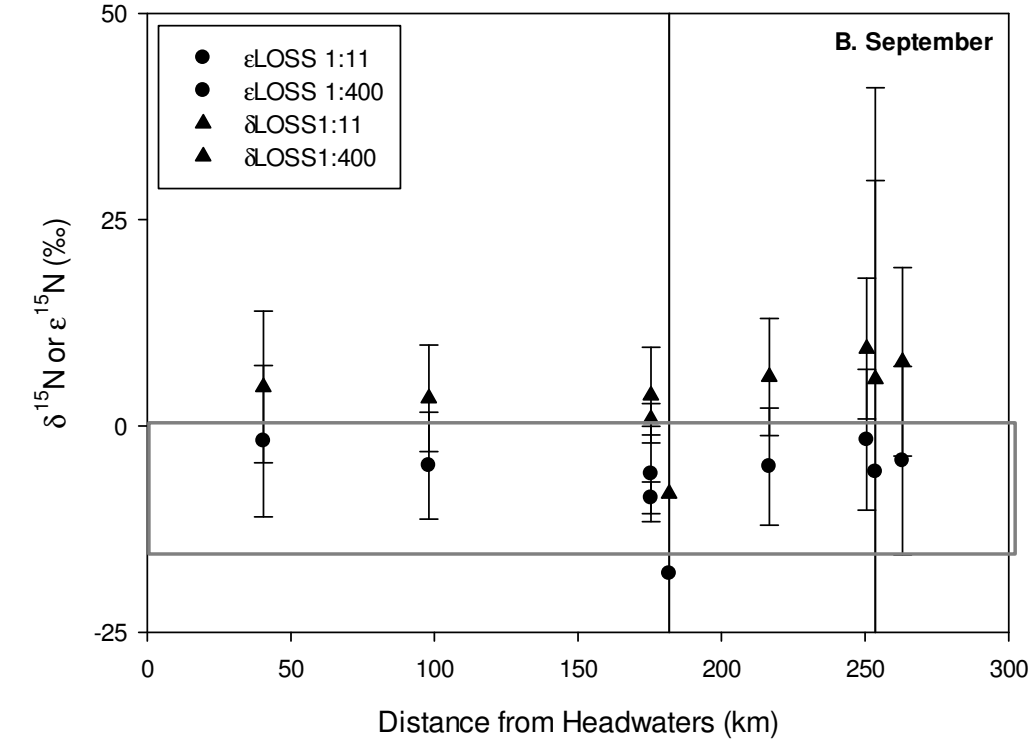
B. September
εLOSS 1:11
εLOSS 1:400
δLOSS1:11
δLOSS1:400
δ15N or ε15N (‰)
Distance from Headwaters (km)

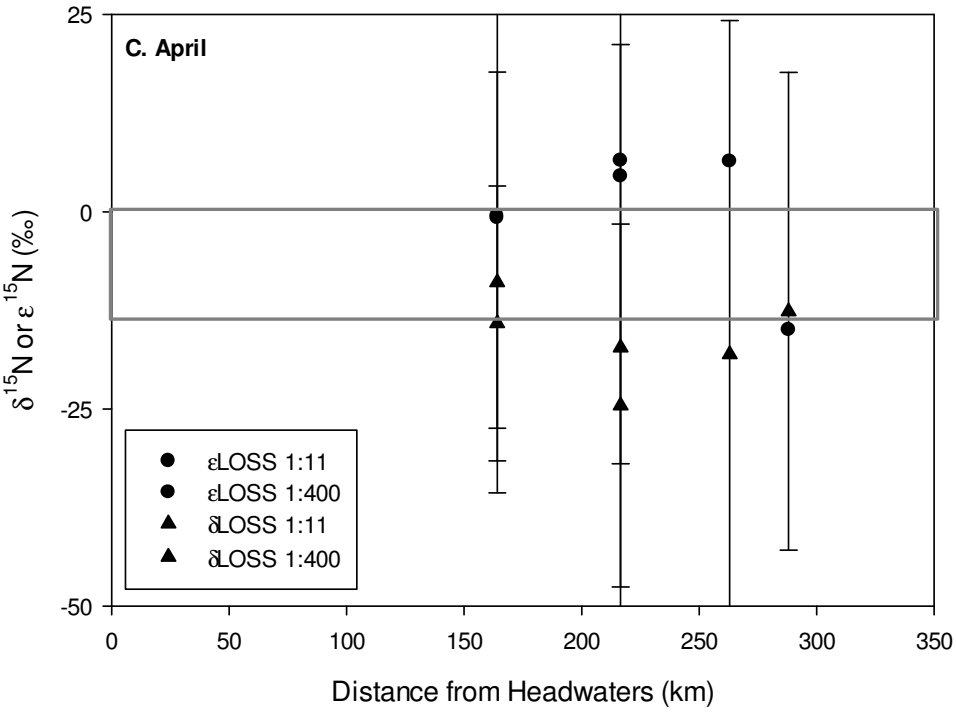
C. April
25
0
-25
-50
0
50
100
150
200
250
300
350
δ15N or ε15N (‰)
Distance from Headwaters (km)
εLOSS 1:11
εLOSS 1:400
δLOSS 1:11
δLOSS 1:400

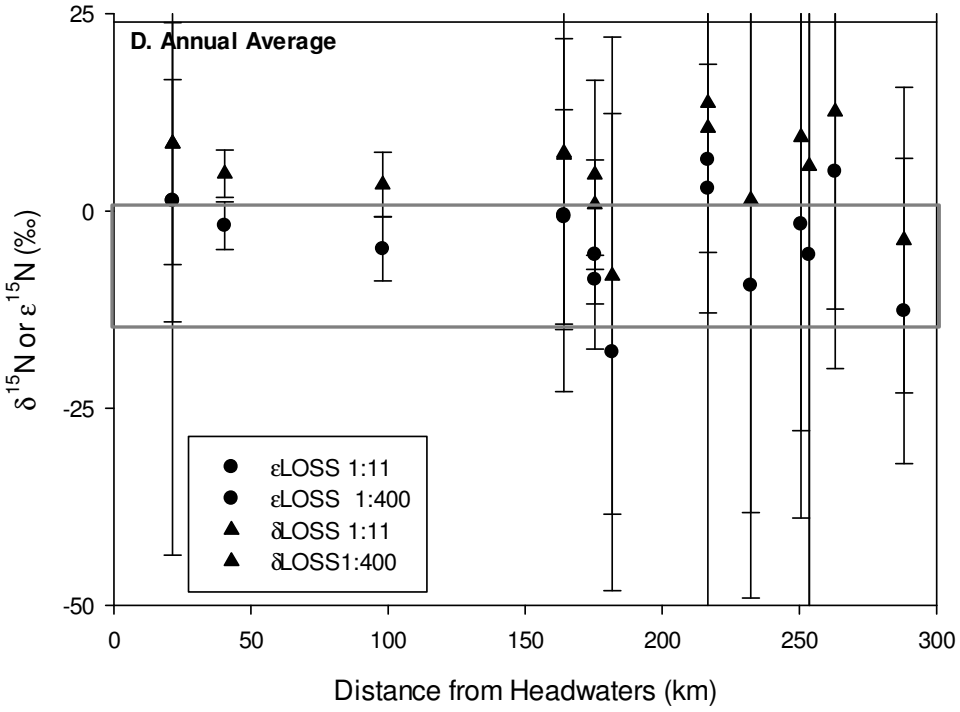
D. Annual Average
25
0
-25
-50
0
50
100
150
200
250
300
δ15N or ε15N (‰)
Distance from Headwaters (km)
εLOSS 1:11
εLOSS 1:400
δLOSS 1:11
δLOSS1:400

Figure 6.12: Isotope effects (ε) between measured NO_3^- and δLOSS. The grey boxes represent expected values for assimilation by biomass (~0‰) and for denitrification (~15‰).

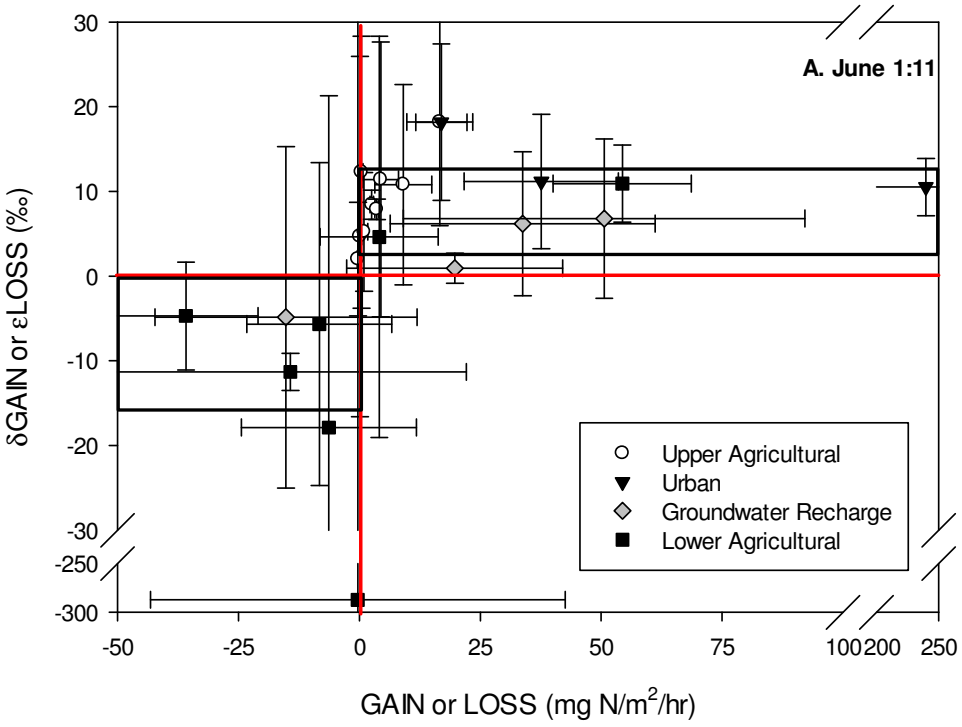
A. June 1:11
δGAIN or εLOSS (‰)
GAIN or LOSS (mg N/m2/hr)
Upper Agricultural
Urban
Groundwater Recharge
Lower Agricultural
30
20
10
0
-10
-20
-30
-250
-300
-50
-25
0
25
50
75
100
200
250

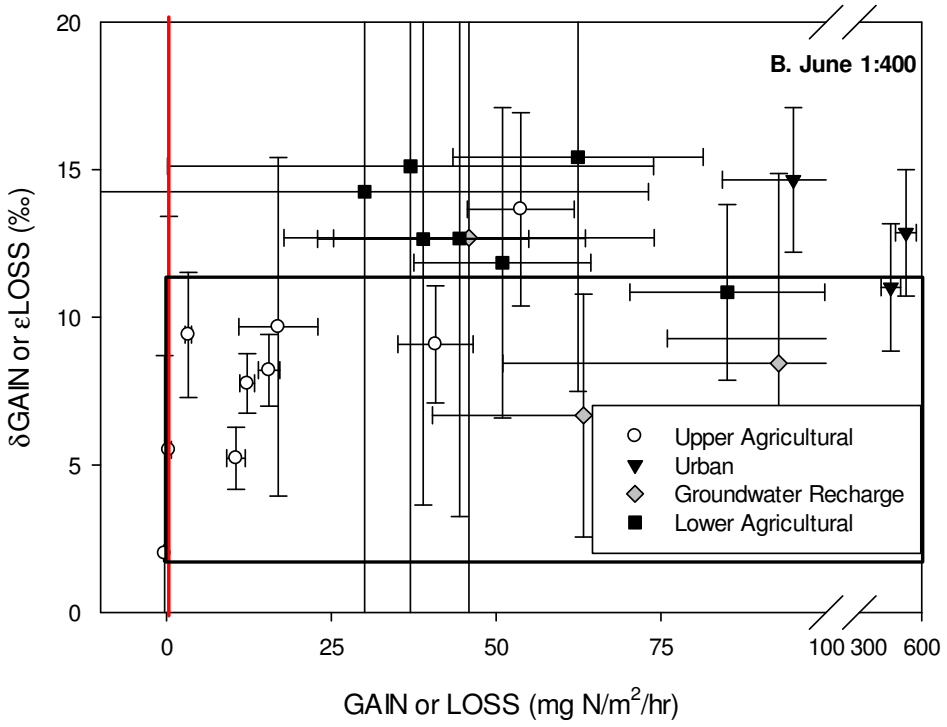
B. June 1:400
δGAIN or εLOSS (‰)
GAIN or LOSS (mg N/m2/hr)
Upper Agricultural
Urban
Groundwater Recharge
Lower Agricultural
20
15
10
5
0
0
25
50
75
100
300
600

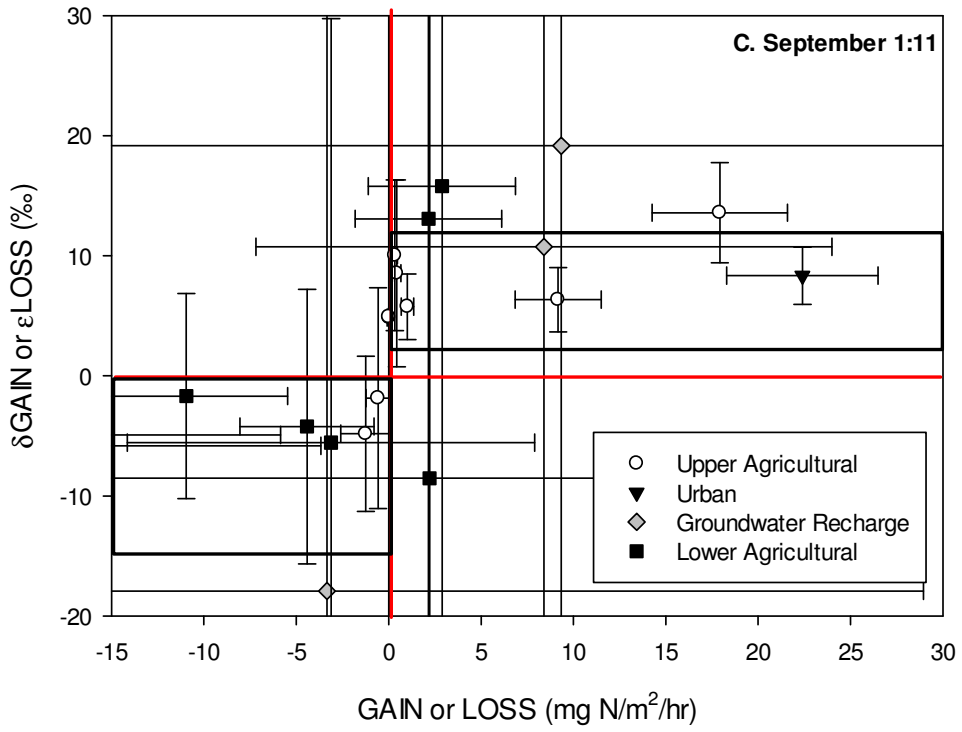
C. September 1:11
δGAIN or εLOSS (‰)
GAIN or LOSS (mg N/m2/hr)
Upper Agricultural
Urban
Groundwater Recharge
Lower Agricultural

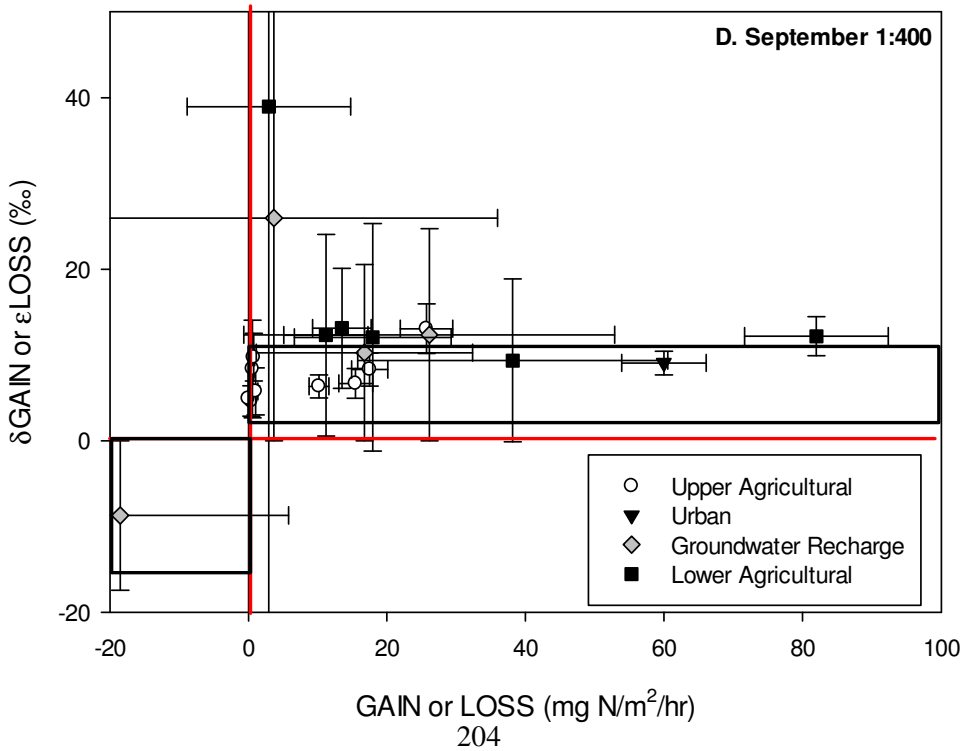
D. September 1:400
δGAIN or εLOSS (‰)
GAIN or LOSS (mg N/m2/hr)
Upper Agricultural
Urban
Groundwater Recharge
Lower Agricultural

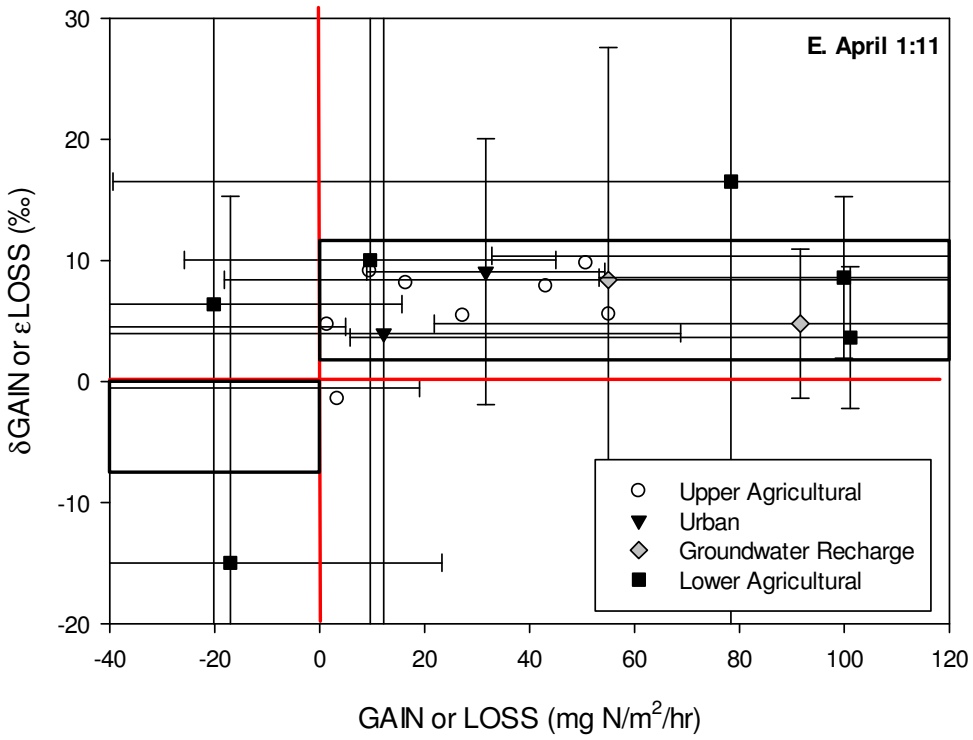
E. April 1:11
δGAIN or εLOSS (‰)
GAIN or LOSS (mg N/m2/hr)
Upper Agricultural
Urban
Groundwater Recharge
Lower Agricultural

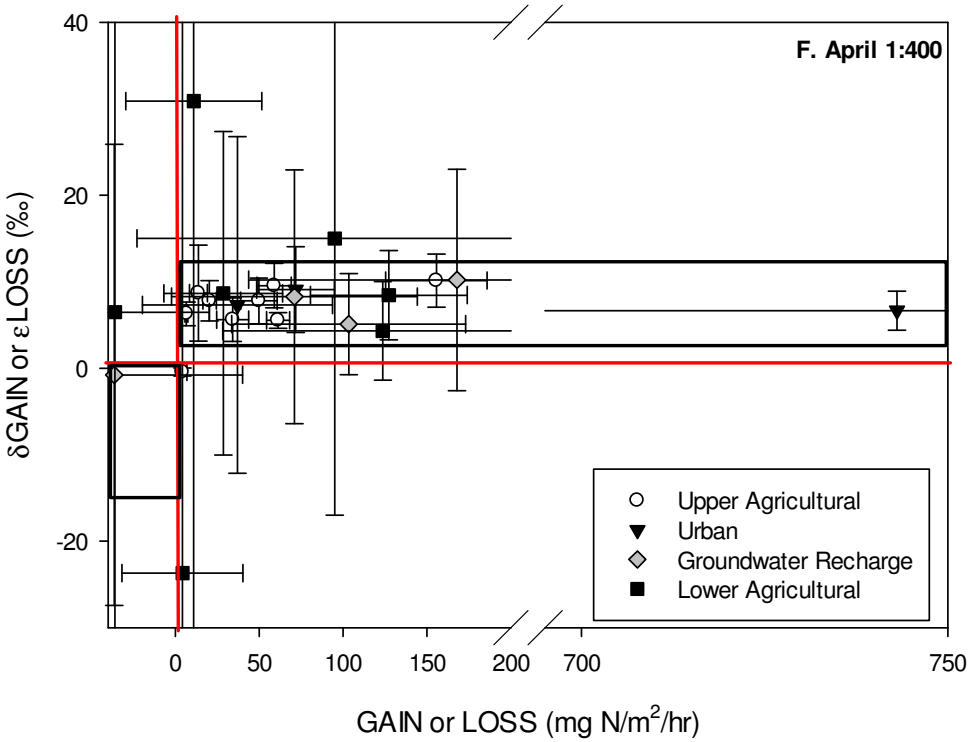
F. April 1:400
δGAIN or εLOSS (‰)
GAIN or LOSS (mg N/m2/hr)
Upper Agricultural
Urban
Groundwater Recharge
Lower Agricultural

Figure 6.13. Net NO_3^- gain or loss rates (GAIN, LOSS) versus $\delta^{15}N\text{-}NO_3^-$ (δGAIN or εLOSS) by river section. June (A and B), September (C and D) and April (E and F) are shown. Annual averages are similar to April. Black boxes constrain δGAIN values to a range of 2.4‰ to 11.4‰ (Figure 6.10) and δLOSS values to -15‰ to 0‰ (expected range for denitrification and N assimilation). Horizontal lines divide GAIN and LOSS. Vertical lines divide expected δGAIN and δLOSS values.

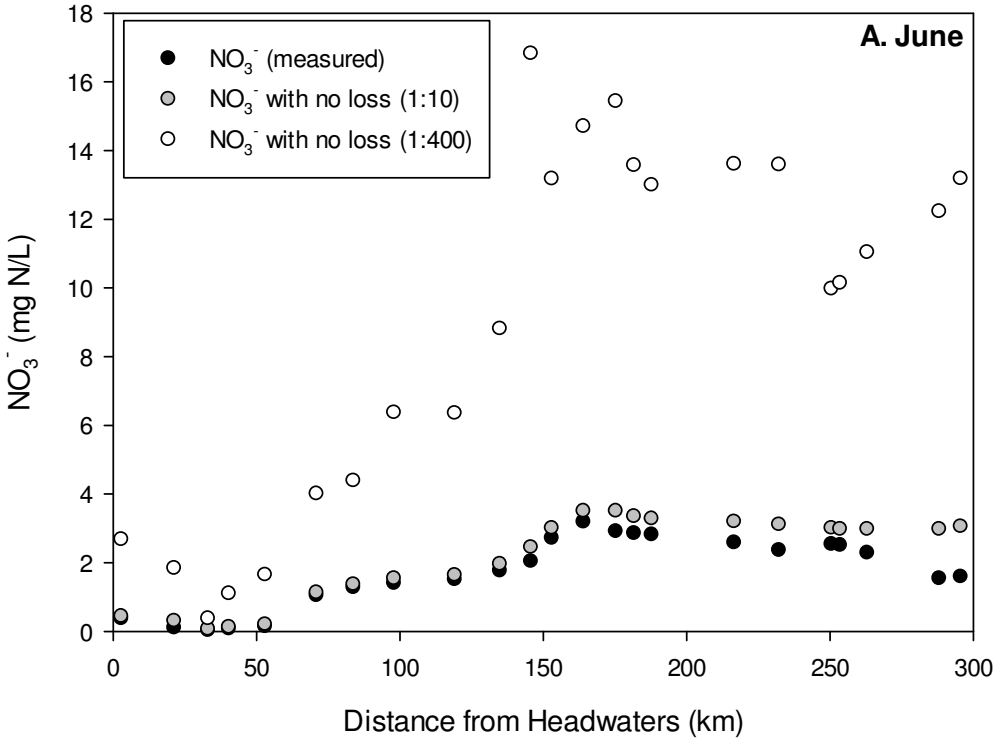
A. June
NO_3^- (measured)
NO_3^- with no loss (1:10)
NO_3^- with no loss (1:400)
NO_3^- (mg N/L)
Distance from Headwaters (km)
0
2
4
6
8
10
12
14
16
18
0
50
100
150
200
250
300

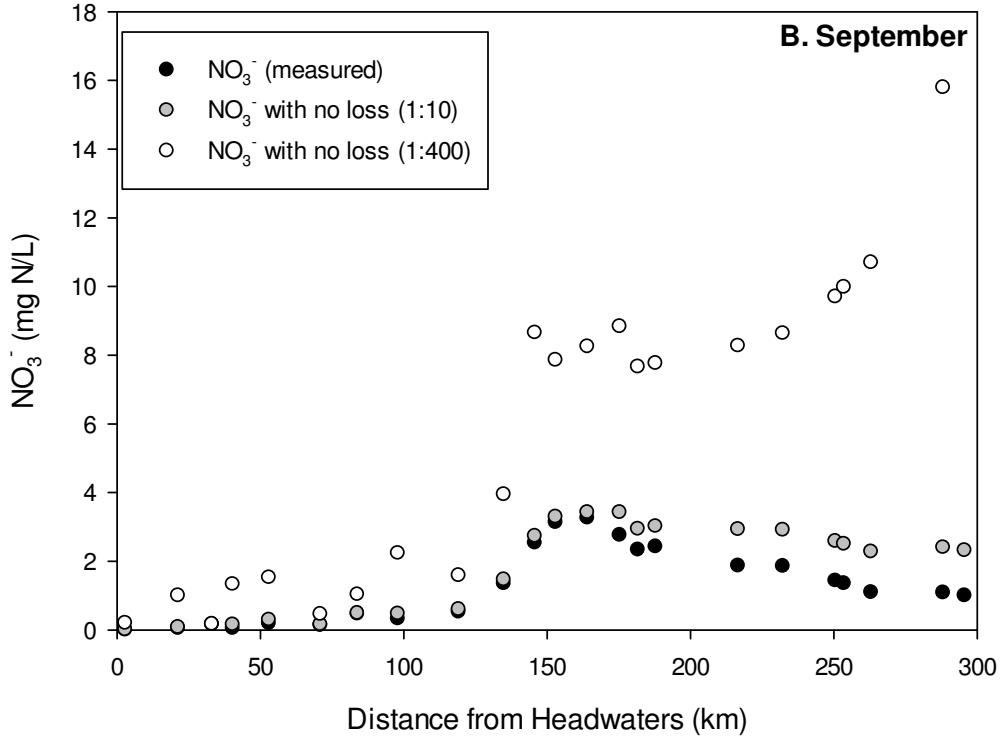
B. September
NO_3^- (measured)
NO_3^- with no loss (1:10)
NO_3^- with no loss (1:400)
NO_3^- (mg N/L)
Distance from Headwaters (km)
0
2
4
6
8
10
12
14
16
18
0
50
100
150
200
250
300

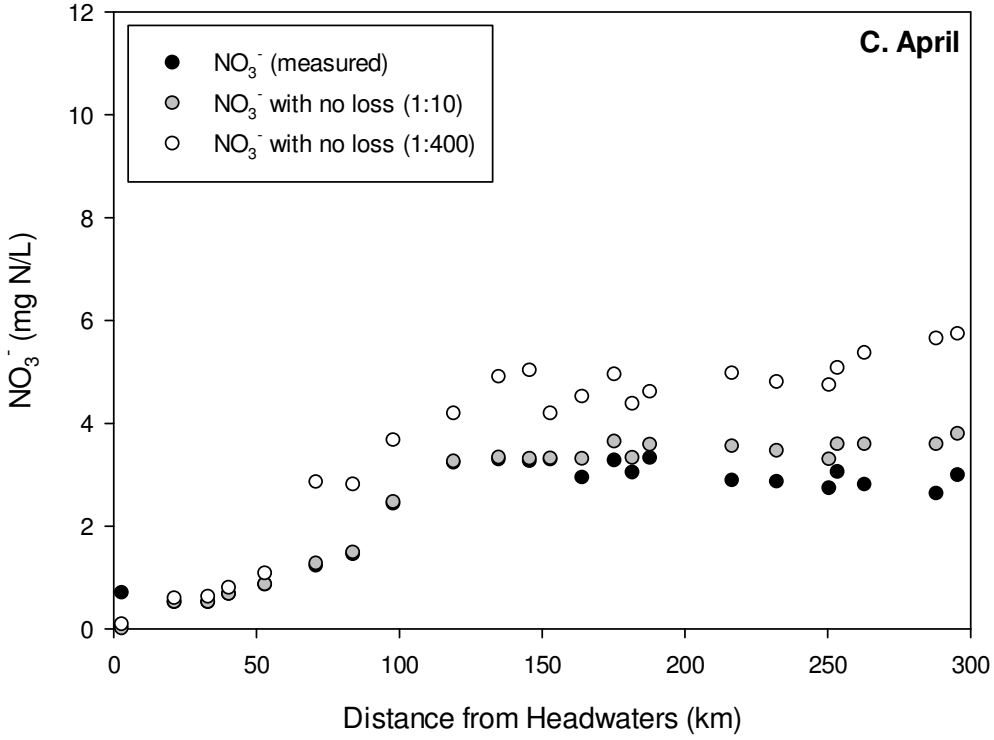
C. April
NO_3^- (measured)
NO_3^- with no loss (1:10)
NO_3^- with no loss (1:400)
NO_3^- (mg N/L)
Distance from Headwaters (km)
0
2
4
6
8
10
12
0
50
100
150
200
250
300

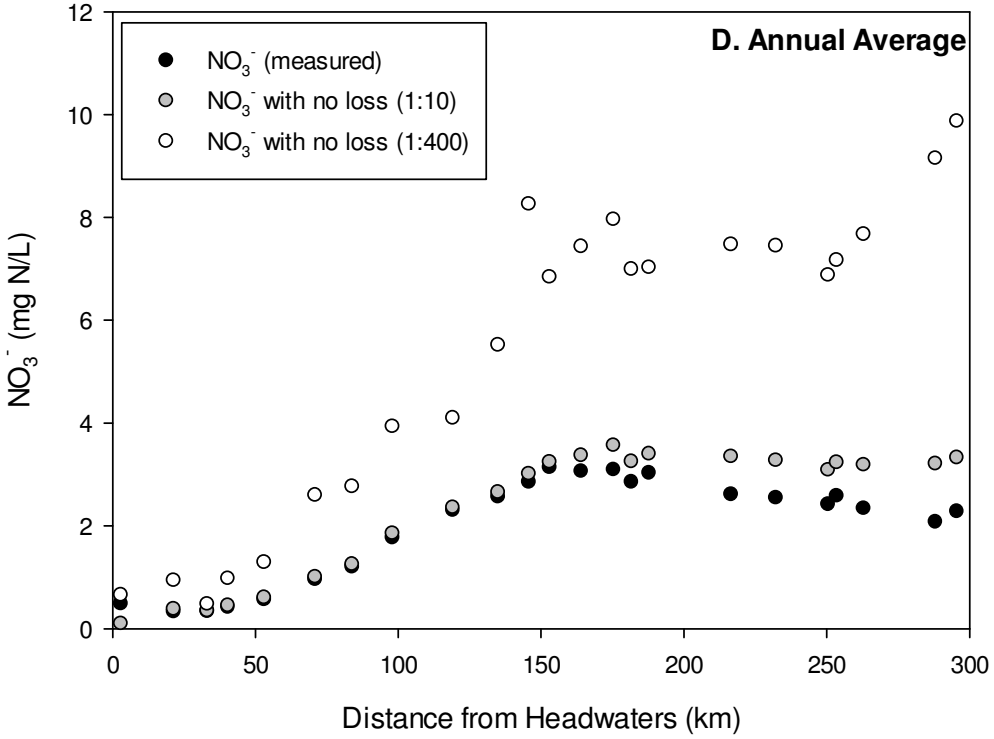
D. Annual Average
NO_3^- (measured)
NO_3^- with no loss (1:10)
NO_3^- with no loss (1:400)
NO_3^- (mg N/L)
Distance from Headwaters (km)
0
2
4
6
8
10
12
0
50
100
150
200
250
300

Figure 6.14. Modelled NO_3^- concentrations in the Grand River if denitrification and other net NO_3^- losses (LOSS) did not occur. June (A), September (B), April (C) and Annual Average (D) concentrations are shown.

Chapter 7: N_2O- NO_3^- Relationships in Streams and Rivers, Ontario, and Worldwide

Abstract

Previous work (Chapters 2 and 3) showed that N_2O emissions from the Grand River are very high during hypoxic events. However, predictability of N_2O emissions under oxic conditions was poor. Therefore, we examined N_2O-NO_3^- relationships in 24 streams and rivers in southern Ontario when dissolved oxygen (DO) was always high (> 3 mg/L). Similar to the Grand River, there was a weak but significant relationship between instantaneous NO_3^- concentrations and N_2O emissions. Regression trees predicted N_2O emissions better than linear regressions. Using all available data on both the annual and instantaneous scale, NO_3^- was a weak but significant predictor of N_2O emissions. However, N_2O emissions spiked at moderate NO_3^- concentration when temperature was high and DO was low. The data fit a Probability Triangle conceptual model, which posits that the range of possible N_2O emissions rises with NO_3^- concentrations. Interestingly, no strong linear relationship between NO_3^- and N_2O emission was noted, even at low NO_3^-, where NO_3^- limitation of N_2O production would be expected. The paucity of data from streams and rivers with very high NO_3^- concentrations (> 5 mg N/L) may be responsible for the lower variation in N_2O emissions seen in the literature. Alternatively, N_2O emissions may be lower at high NO_3^- because these streams are likely to be oxic (or NO_3^- would be removed via denitrification). The weak to non-existent N_2O-NO_3^- relationship in streams and rivers indicates that new techniques for modelling N_2O emissions are necessary. Since N_2O emissions during hypoxia are very high, quantifying hypoxia on the annual scale is the first step to quantifying N_2O emissions. Hypoxia may be estimated in some systems using ecosystem metabolism models. Local DO, NO_3^- and water temperature data can be used to create local non-linear relationships with regression trees. Caution should be applied as local N_2O-NO_3^--DO-temperature relationships may change over time due to changes in microbial community, substrate availability, etc. Climate change may alter microbial habitat and local species composition as well as geochemical parameters.

7.1 Introduction

Nitrous oxide (N_2O) is a potent greenhouse (~300 times more warming potential than CO_2 over 100 years (Zafiriou 1990) and the primary stratospheric ozone destroyer (Ravishankara et al. 2009). The global N_2O budget is not well-understood (Syakila and Kroeze 2011), but the United Nations

Intergovernmental Panel on Climate Change (IPCC 2007) estimates that 17.7 Tg N/yr N_2O is released to the atmosphere, 6.7 Tg N/yr of which is anthropogenic. Forty-two percent of anthropogenic N_2O (2.8 Tg N/yr) is produced by microbial metabolism of agricultural nitrogen fertilizers in soils, via metabolism of NO_3^- (via denitrification) and NH_4^+ (via nitrification) (Forster et al. 2007). Leached agricultural and sewage N enters rivers, estuaries and coastal zones, where another 25% of anthropogenic N_2O (1.7 Tg N/yr) is produced (Forster et al. 2007).

N_2O is currently responsible for about 5% of climate forcing (Zafiriou 1990). However, it may become more significant in the future. While many strategies for CO_2 emission reduction are being studied (Farrelly et al. 2013) and may be implemented, N_2O emissions are difficult to mitigate. World population is expected to plateau at 9.2 billion people by 2075 (United Nations Department of Economic and Social Affairs 2004). This, along with increased meat consumption in developing countries (Rosegrant et al. 2001) suggests that global food production, agricultural intensity, N fertilizer application and manure production will increase. N_2O emissions may increase because of increased substrate availability, but also because climate change-induced aquatic hypoxia and higher temperatures promote denitrification (Veraart et al. 2011). Few N_2O mitigation strategies have been proposed, probably because (a) agricultural and aquatic N_2O emissions are typically diffuse, non-point sources and very difficult to treat on the landscape scale and (b) microbial reactions that produce N_2O may be desired (even actively promoted) because they reduce toxic substances (NH_4^+, via nitrification) and reduce biologically reactive nitrogen (NO_3^-, via denitrification) which can result in eutrophication. Additionally, both NH_4^+ and NO_3^- are drinking water contaminants.

Despite these challenges, some mitigation strategies have been proposed (e.g. (Desloover et al. 2012, Rees et al. 2013)). These typically take advantage of the fact that (a) N_2O emissions, like denitrification rates, can be high in "hotspots" such as wetlands, stormwater retention ponds, manure lagoons, and other areas with high NO_3^- and low dissolved oxygen (DO) ((Davidson and Seitzinger 2006)) and (b) emission rates depend not only on heterogeneous denitrification (or nitrification) rates, but on the fraction of N_2O produced per total product (denitrification: $N_2O:(N_2O+N_2)$, nitrification: $N_2O:(NO_3^-+N_2O)$), which changes due to temperature, redox conditions and substrate (NO_3^-, NO_2^- and organic carbon) availability (Chapters 5 and 6). Unfortunately, $N_2O:(N_2O+N_2)$ ratios tend to be lowest when NO_3^- and NO_2^- are scarce (Firestone et al. 1979) and DO is low (Silvennoinen et al. 2008). Thus, mitigation strategies for N_2O emissions are not very useful for high-NO_3^- systems

or oxic ecosystems, even as agricultural and sewage NO_3^- and NH_4^+ increase on the landscape. If the production and use of N fertilizers increase in the future and N_2O mitigation remains insignificant, N_2O may become a more important climate forcer in the future.

Quantifying N_2O emissions and understanding controls and predictors of N_2O production are crucial. Currently, global N_2O emissions are estimated by self-reporting from countries that have signed the United Nations Framework Convention on Climate Change (UN FCCC) and must report annual N_2O emissions. Canada and many other countries use default equations provided by the IPCC, which assume N_2O emissions linearly increase with N leached from agriculture or released from wastewater treatment plants (WWTPs) as effluent (IPCC 2007):

$$\boldsymbol{N_2O\ emission = N_{LEACH} \times EF_{5-R}} \qquad \textbf{Equation 7.1}$$

$$\boldsymbol{N_2O\ emission = N_{EFF} \times EF_{EFF}} \qquad \textbf{Equation 7.2}$$

Where N_2O emissions are in kg N/yr, N_{LEACH} is the amount of inorganic N (NO_3^-, NH_4^+) leached from agricultural sources (see Chapter 6) in kg N/yr, N_{EFF} is the amount of inorganic N (NO_3^-, NH_4^+) released from WWTP effluent per year in kg N/yr, $EF_{5\text{-}R}$ is emission factor for agriculture (default value: 0.0025) and EF_{EFF} is the emission factor from effluent (default value: 0.0075) (IPCC 2007). These equations assume that increased N loads to rivers necessarily increase annual N_2O emissions.

Previous work has focused on appropriate values for $EF_{5\text{-}R}$, which was lowered from 0.0075 in 2006 based on to field studies in streams and rivers that indicated it was too high (Clough et al. 2006, Reay et al. 2005). Since then, a large study of 27 streams in the United States indicated that the higher value was correct (Beaulieu et al. 2011). Many of these studies examined instantaneous N_2O emissions and NO_3^- concentrations, although the IPCC equations represent annual totals. In contrast, there is no significant linear relationship between N_2O concentration or emission and NO_3^- in the Grand River on an instantaneous or annual scale (Chapters 2 and 3). Negative exponential relationships between DO and N_2O emission were significant ($r^2 = 0.54$, $p < 0.001$, $n = 689$, Chapter 3) using data collected over two years at 23 sites in the Grand River.

Because DO-N_2O relationships appear to be related but not linearly related (Chapter 3), a regression tree approach was used on an expanded dataset of Grand River data (Venkiteswaran et al. in submission). Regression trees are statistical tools allowing the identification of structure in datasets without requiring assumptions about the type or nature of the structure. They do not require linear

relationships in the data and allow for interactions between variables. Essentially, the data are divided into two groups so each group is as different as possible. Then each group is divided again into two groups until no improvement can be made. Using all Grand River all river data, N_2O fluxes were significantly higher when DO was low (< 1.4 mg/L) than when DO was high. Low-DO samples were further subdivided by temperature > 24 ℃ (mean N_2O emissions: 2862 and 1474 μmol/m^2/d, respectively). High-DO samples were subdivided again by DO < 3.7 mg/L (mean N_2O emissions: 497 and 63 μmol/m^2/d respectively). However, this relationship was driven by very low-DO and high-N_2O samples in the urbanized section of the Grand River. When only non-urban sites were used, temperature and NO_3^- were important predictors of N_2O (r^2 = 0.44, n = 406) (Venkiteswaran et al. in submission). The low predictability of N_2O in these areas likely results from a complex interplay of limits to microbial N_2O production rates, changes in the N_2O:(N_2O+N_2) ratio, N_2O emission rate, NO_3^- uptake and production rate, etc. However, the limited number of sites (19) and samples (406) used in the "non-urban" sections of the river indicates that the N_2O:NO_3^- (and N_2O:DO and N_2O:temperature) relationship bears further investigation in non-hypoxic river systems. Additionally, NO_3^- concentrations were relatively low (< 3 mg N/L) in almost all of these sampling events; this may affect N_2O predictability if NO_3^- is limiting.

Therefore, the purpose of this study is threefold. The first purpose is to examine N_2O:NO_3^- relationships in oxic streams and rivers using (a) 24 streams and rivers in Southern Ontario, across a variety of trophic levels, NO_3^- concentrations and temperatures and (b) the river and stream literature. The second purpose is to present a conceptual model of likely N_2O emission rates over a range of NO_3^- concentrations, including other geochemical constraints (temperature, DO) when possible, based on the global literature. The last purpose is to make recommendations for N_2O emissions sampling protocols. A strong linear relationship between N_2O and NO_3^- globally is unlikely, given the variability previously seen in the Grand River (Chapters 2 and 3). However, this study aims to constrain the range of potential N_2O emissions based on NO_3^- concentration in rivers and determine how physical (e.g. temperature) and geochemical (e.g. DO) factors aid or hinder prediction of N_2O flux with NO_3^- concentration. N_2O:NO_3^- relationships will be examined using regression tree analysis, and on an instantaneous and annual scale, where data are available.

7.2 Methods

7.2.1 Site Descriptions

Twenty-four streams and rivers from fourth to sixth Strahler order were chosen in four Southern Ontario watersheds to represent a wide range of NO_3^- concentrations (Figure 7.1). All sites had oxic water columns (DO> 3 mg/L). Most sites were active or inactive Provincial Water Quality Monitoring Network Stations, meaning that historical water quality data was available. Sites were located in five watersheds or watershed areas, discussed below.

7.2.1.1 Conestogo-Speed Subwatersheds

The Conestogo-Speed (CS) area encompasses subwatersheds in the central portion of the Grand River watershed. Land use in the Grand River Watershed is primarily agricultural (71%), followed by wetlands (12%) and urban (8%) (SOLRIS and CAADMIN GIS layers, Ontario Ministry of Natural Resources, 2003 and 2008 respectively). These subwatersheds are underlain primarily by calcite-rich diamict with some glacial outwash gravel near stream and riverbeds (Surficial Geology of Southern Ontario GIS layer, Ontario Ministry of Northern Development and Mines, 2010). Sites in this section are Laurel Creek at Bridgeport Rd (CS-1, Strahler order: 4), Conestogo River at St. Jacobs (CS-2, Strahler order: 6), Canagagigue Creek (CS-3, Strahler order: 5), Irvine Creek (CS-4, Strahler order: 5) and the Speed River (CS-5, Strahler order: 5) (Table 7.1).

7.2.1.2 Nith-Whitemans Subwatersheds

The Nith-Whitemans (NW) area includes subwatersheds of the southern Grand River watershed. The subwatersheds are underlain primarily by calcitic glaciolacustrine clays and some diamict (Surficial Geology of Southern Ontario GIS layer, Ontario Ministry of Northern Development and Mines, 2010). Sites in this area are the Nith R. (NW-1, Strahler order: 5), Horner Creek (NW-2, Strahler order: 5), Whitemans Creek (NW-3, Strahler order: 6) and Fairchild Creek (NW-5, Strahler order: 5) (Table 7.1).

7.2.1.3 Maitland River Watershed

Land use in the Maitland River (ML) watershed is primarily agricultural (79%), followed by wetland (11%) and forest (6%) (SOLRIS and CAADMIN GIS layers, Ontario Ministry of Natural Resources, 2003 and 2008 respectively). The watershed is underlain by calcitic glacial gravels, sands and diamict

(Surficial Geology of Southern Ontario GIS layer, Ontario Ministry of Northern Development and Mines, 2010). Sites are the Middle Maitland R. (ML-1, Strahler order: 6), Beauchamps Drain (ML-2, Strahler order: 4), South Maitland R. (ML-3, Strahler order: 6), Blyth Brook (ML-4, Strahler order: 4) and Maitland R. (ML-4, Strahler order: 5).

7.2.1.4 Saugeen River Watershed

The Saugeen River watershed is less agricultural than the previous watersheds (67% land use), with more wetland (17%) and forest (9%) (SOLRIS and CAADMIN GIS layers, Ontario Ministry of Natural Resources, 2003 and 2008 respectively). The watershed is underlain by calcite-rich glacial gravels and diamicts (Surficial Geology of Southern Ontario GIS layer, Ontario Ministry of Northern Development and Mines, 2010). Sampling sites in this area are the South Saugeen R. (SA-1, Strahler order: 5), the Beatty Saugeen R. (SA-2, Strahler order: 5), the Upper Main Saugeen R. (SA-3, Strahler order: 6), the Saugeen R. (SA-4, Strahler order: 7) and the Chepstow Mill Pond Stream (SA-5, Strahler order: 3).

7.2.1.5 Upper Thames Watershed

Lastly, the Upper Thames River watershed is highly agricultural (77% land use), with high urban (10%) and forest (6%) land use (SOLRIS and CAADMIN GIS layers, Ontario Ministry of Natural Resources, 2003 and 2008 respectively). The watershed is underlain primarily by calcitic diamict and has some glacial gravels and sands (Surficial Geology of Southern Ontario GIS layer, Ontario Ministry of Northern Development and Mines, 2010). Sampling sites are the Avon R. (UT-1, Strahler order: 4), Trout Creek (UT-2, Strahler order: 5), Middle Thames R. (UT-3, Strahler order: 6), South Thames R. (UT-4, Strahler order: 5) and Trout Creek (UT-5, Strahler order: 4).

7.2.2 Physical Characterization of Streams

Sampling sites were characterized for depth, width, and stream velocity on August 6, 2009. Stream depth and width were measured with measuring tapes. Water velocity was measured with Swoffer 3000 Current Velocity Meters (Swoffer Instruments, Seattle, WA). Water velocity was measured at 60% of total depth, measured from the top, to capture average velocity. Velocities were then averaged across multiple sections. Discharge was calculated as:

$$\boldsymbol{Q = \sum_i^n V_i \times d_i \times w_i} \qquad \textbf{Equation 7.3}$$

Where Q is discharge in m^3/s, V_i is velocity (m/s) in section i, d_i is depth (m) in section i, w_i is the width of each section (m), and n is the total number of sections.

Gas exchange coefficient (k) was estimated from depth and velocity measurements (Jha et al. 2004):

$$k_{O2} = 0.603286 \times V^{0.4} \times S^{-0.173} \times d^{0.8} \quad \textbf{Equation 7.4}$$

Where k_{O2} is the gas exchange coefficient for oxygen (day^{-1}), V is velocity (m/s), S is slope of streambed (unitless, measured in Google Maps), and d is depth (m). To convert k_{O2} to k_{N2O}, Schmidt numbers, which are unitless descriptors of fluid flow, were first calculated for both O_2 and N_2O (Wanninkhof 1992) :

$$Sc = A - B \times T + C \times T^2 - D \times T^3 \quad \textbf{Equation 7.5}$$

Where Sc is the Schmidt number, A, B, C and D are constants for each gas (Wanninkhof 1992), and T is water temperature in ℃.

This gas exchange coefficient for N_2O was determined as (Wanninkhof 1992):

$$k_{N2O} = k_{O2} \times \left(\frac{Sc_{N2O}}{Sc_{O2}}\right)^{-0.5} \quad \textbf{Equation 7.6}$$

Where k_{N2O} is the gas exchange coefficient for N_2O (day^{-1}), k_{O2} is as described in Equation 7.4, and Sc_{N2O} and Sc_{O2} are the Schmidt numbers for N_2O and O_2, respectively (unitless). The -0.5 exponent is an empirically derived value for rough water (Wanninkhof 1992).

7.2.3 Water Chemistry Sampling Protocol

Water samples were collected at each site twice a day: once, before sunrise and once at or after solar noon. All sample bottles were filled at wrist-depth (~ 10 cm), in moving water. The sampling times were chosen to capture as much of the diel range in DO and other geochemical variables as possible. Water temperature was measured with a multiprobe (YSI 556 MPS) or thermometer. Water samples for pH and specific conductivity were collected in 125 mL dark HDPE plastic bottles and stored on ice until laboratory analysis. DO samples were collected in 300 mL glass BOD bottles (cite) and fixed with Winkler reagents (American Public Health Association 1995). 1 L HDPE Nalgene bottles were used for total phosphorous (TP) samples. NO_3^- concentration and isotope samples were also collected in 1 L HDPE Nalgene bottles. 125 mL glass serum bottles were used for N_2O

concentration analysis and 500 mL borosilicate glass jars were used for N_2O isotope analysis. Both N_2O bottles were capped with stoppers underwater using a needle to remove any air bubbles and were preserved in the field with 2 mL saturated mercuric chloride solution per litre of sample. All samples were kept cool and dark until analysis. All water chemistry samples were measured at both sampling times (pre-dawn and afternoon) except TP (afternoon only) and NO_3^- isotopic analyses (pre-dawn only).

7.2.4 Chemical and Isotopic Analyses

Conductivity and pH and conductivity were measured in the laboratory with a YSI 556 MPS multiprobe. Dissolved oxygen concentration was determined using Winkler titration (standard deviation of multiple potassium biiodate standards: 0.2 mg/L, detection limit: 0.2 mg/L) (American Public Health Association 1995). TP samples were unfiltered and analyzed by molybdate colorimetry (Cary Bio UV-Visible Spectrophotometer, Aigilent Technologies, Mississauga, ON). Precision and detection limit were both 5 µg P/L. NH_4^+ concentration was determined by the salicylate and nitroprusside colorimetric method (American Public Health Association 1995) on a Technicon Auto spectrophotometric analyzer (wavelength: 660 nm). Precision and detection limit were 0.005 mg N/L and detection limit of 0.01 mg N/L respectively. NO_3^- concentration and isotope samples were filtered to 0.45 µm. NO_3^- concentrations were run on a Dionex ICS-90 ion chromatograph (precision: 0.07 mg N/L, detection limit: 0.05 mg N/L). Stable isotopic composition of NO_3^- ($\delta^{15}N\text{-}NO_3^-$ and $\delta^{18}O\text{-}NO_3^-$) was determined using a modified version of the chemical denitrification method (McIlven and Altabet 2005), in which NO_3^- is reduced to N_2O using cadmium and sodium azide. The N_2O was then analyzed on a continuous flow-isotope mass spectrometer (CF-IRMS) in line with a TraceGas gas chromatograph pre-concentrator system (GV instruments, Thermo Electron Corp., Manchester, UK). Standard deviation of multiple standards was 0.3‰ for $\delta^{15}N\text{-}NO_3^-$ and 0.5‰ for $\delta^{18}O\text{-}NO_3^-$.

N_2O concentration samples were prepared with a headspace overpressurization method. Headspace was then extracted with a syringe and run on a Varian 3800CP gas chromatograph with an electron capture detector designed for greenhouse gas analysis. Precision was 6% or less. N_2O isotopic composition ($\delta^{15}N\text{-}N_2O$ and $\delta^{18}O\text{-}N_2O$) were determined as above.

7.2.5 N_2O emission measurements

N_2O emissions to the atmosphere were calculated using the thin boundary layer equation (Wanninkhof 1992):

$$\boldsymbol{N_2O\ emission = k_{N2O} \times d \times (C_m - C_s)} \qquad \textbf{Equation 7.7}$$

Where N_2O emission is in μmol/m^2/d, k_{N2O} was determined as in Equation 7.6 (d^{-1}), d is depth (m), C_m is measured concentration of N_2O (μmol/m^3) and C_s is N_2O concentration at atmospheric equilibrium (μmol/m^3), assuming an atmospheric N_2O concentration of 320 ppb (European Environment Agency 2013).

7.2.6 Statistical Analyses

Differences in geochemistry by region were assessed by one-way ANOVA tests. When data were not normally distributed, Kruskal-Wallis one-way ANOVA tests on ranks were used. Linear relationships between N_2O emissions and possible predictive factors (temperature, pH, DO, NO_3^-, NH_4^+, total dissolved nitrogen (TDN), dissolved organic carbon (DOC) and TP) were also assessed. When slopes between variables were determined, linear II (Deming's) regressions were used, which take into account different uncertainties in the variables. Data was transformed if constant variance was not achieved. When multiple transformations were run, the transformation with the lowest p value with constant variance was chosen. Both linear and ANOVA tests were performed in SigmaPlot 12.0 (Systat Software Inc., Chicago) and in both, p values < 0.05 were considered significant.

To group bivariate data by watershed, standard ellipses were determined in R, which contain about 40% of the data (Jackson et al. 2011). The long and short semi-axes of the ellipses are one standard deviation of the bivariate data.

To understand the relationship between N_2O fluxes and independent variables, regression tree analysis of N_2O fluxes was performed. Analysis was performed with the *mvpart* package in R (Therneau and Atkinson 2012). Regression trees are used for regression analyses where no obvious linear relationship between dependent and independent variables is present. They are non-parametric, and create "thresholds" or "breakthrough points" by splitting the dataset using the independent variable (e.g. NO_3^- or DO concentration) in order to effectively maximize the between-groups sum-of-squares (De'ath and Fabricius 2000). The total variance in the dependent variable (N_2O flux) explained is reported as the R^2 (1 minus the resubstitution error). A 10-fold cross-validation was

applied, and each tree was pruned such that the smallest tree whose cross-validated relative error (CVRE) is less than 1 standard error of the minimum CVRE was kept (Breiman et al. 1984). Independent variables entered into regression tree model were: temperature, NO_3^-, DO, TP, TDN, NH_4^+, DON, DOC, TSS and Strahler order. See Venkiteswaran et al. (in submission) for more details.

7.3 Results

7.3.1 Descriptive Geochemistry of Field Sites

Water temperature ranged from 14.5 °C to 23.7 °C between all sites and conductivity had a large range (401 to 1367 µS). pH had a narrow range of 7.7 to 8.8 due to extensive carbonate mineral buffering. There were no statistical differences in temperature, conductivity or pH with region though highest conductivity values occurred in the Upper Thames region (Figure 7.2A).

DO ranged from 3.8 to 14.2 mg/L (39% to 145% saturation). DO values were both lowest and highest in the Maitland watershed (pre-dawn and afternoon samples, respectively). DO had a weakly positive linear relationship with temperature ($r^2 = 0.251$, $p < 0.001$, $n = 24$) (Figure 7.2B). NO_3^- concentrations ranged from below detection (BD, < 0.07 mg N/L) to 6.5 mg N/L while NH_4^+ ranged from 0.001 mg N/L to 0.028 mg N/L (Figure 7.3A). Total phosphorus (TP) ranged from 48 µg/L to 368 µg/L (Figure 7.3B). The TP concentrations result in a range of trophic status from mesotrophic to eutrophic (Dodds et al. 1998) (Table 7.1).

$\delta^{15}N\text{-}NO_3^-$ values ranged from 5.1‰ to 22.7‰ and $\delta^{18}O\text{-}NO_3^-$ values ranged from -2.1‰ to 6.5‰ (Figure 7.4A). There was a weak linear relationship between the two with a slope ($\delta^{18}O/\delta^{15}N$) of 0.353 ($r^2 = 0.436$, $p < 0.001$, $n = 12$).

N_2O concentrations ranged from 9.3 nmol/L to 53.0 nmol/L (100% to 620% saturation) and CH_4 concentrations ranged from 60 nmol/L to 1741 nmol/L (2200% to 60700% saturation) (Figure 7.4B).

7.3.2 N_2O flux and NO_3^- in streams

Gas exchange coefficients for N_2O (k_{N2O}) ranged from 0.09 to 0.67 day^{-1}. Daily average N_2O emissions ranged from 0.02 to 43 $nmol/m^2/d$. N_2O emissions and NO_3^- concentrations appeared to clump by watershed (Figure 7.5A). To assess if NO_3^-—N_2O ratios are significantly different by watershed, standard ellipses were calculated showing the mean and one standard deviation of data from each region (Figure 7.5B). Some overlap between ellipses is evident. One-way ANOVA tests

showed that NO_3^- concentrations were significantly different by region (except for Conestogo-Speed, Maitland and Saugeen, which were not different from each other) (p values < 0.001 to 0.031). N_2O emission data were not normally distributed but most regions were significantly different ($p< 0.05$), however, Maitland was not significantly different than Conestogo-Speed or Upper Thames.

NO_3^- concentration and N_2O flux by region were compared to land-use in the subwatersheds. Land use for the whole watershed was used, rather than land use upstream of each site, due to a scarcity of data (SOLRIS and CAADMIN GIS layers, Ontario Ministry of Natural Resources, 2010). Highest NO_3^- concentrations were found in the Upper Thames, which had the lowest wetland fraction of all catchments, while highest N_2O emissions occurred in the Maitland watershed, where agricultural land use was highest (Figure 7.6).

7.3.3 Linear Correlations between N_2O and predictive factors (NO_3^-, DO, temperature etc.)

Of the predictor variables tested (temperature, DO, NO_3^-, NH_4^+, total dissolved nitrogen (TDN), TP) only NO_3^- and TDN had significant relationships with N_2O emissions ($p < 0.001$, Table 7.2). Both had moderate r^2 values (0.31 and 0.37, respectively).

7.3.4 Regression Tree Analysis

The regression tree analysis shows that there is a NO_3^- concentration threshold of 2.7 mg N/L, above and below which, N_2O emissions are significantly different ($r^2 = 0.35$) (Figure 7.7). Mean N_2O emission rate when $NO_3^-< 2.7$ mg N/L is 0.87 ± 1.0 nmol/m^2/h and is 2.8 ± 1.4 nmol/m^2/h when $NO_3^- \geq 2.7$ mg N/L. No other inputs (temperature, DO, NH_4^+, TDN, DOC or TP) were significantly correlated to N_2O emissions.

7.4 Discussion

7.4.1 Sources of N_2O in Small, Oxic Streams

This study was not designed to determine the main pathways of N_2O production in small streams. However, the positive relationship between NO_3^- and N_2O suggests that N_2O is primarily produced by denitrification. For that reason, we might expect that N_2O concentration increases as $\delta^{15}N\text{-}NO_3^-$ increases, as high $\delta^{15}N\text{-}NO_3^-$ may indicate denitrification. However, N_2O peaks at relatively low $\delta^{15}N\text{-}NO_3^-$ values (~6‰ to 9‰) (Figure 7.8) at three points in the Maitland and Saugeen watersheds. These

sites also have low NO_3^- concentration (Figure 7.8). The Maitland watershed has the highest fraction agricultural land of any watershed – this appears to correlate to high N_2O but not high NO_3^- (Figure 7.6). The Saugeen site with high N_2O and low $\delta^{15}N\text{-}NO_3^-$ was sampled immediately downstream of a mill pond, were N_2O was likely produced in fine sediment.

Even when the three peak N_2O samples are removed, there is no significant positive linear relationship between $\delta^{15}N\text{-}NO_3^-$ and N_2O concentration ($p = 0.287$).

7.4.2 Relationships between NO_3^- and N_2O in Small, Oxic Streams

The data presented above agree generally with the conclusions of a regression tree analysis on a larger Grand River dataset (Venkiteswaran et al. in submission) – in non-hypoxic rivers, DO does not predict N_2O fluxes. In the Grand River dataset, temperature is the first regression tree "branch" (i.e. the most important predictor of N_2O emission) in non-urban sites, followed by NO_3^- (4.9 mg N/L). Temperature is not significant in this study, probably because only summer samples were collected and temperature has a relatively narrow range of 9°C. In both studies, NH_4^+ did not correlate with N_2O emissions, suggesting that nitrification of NH_4^+ was not an important source of N_2O relative to denitrification.

In both datasets, predictability (i.e. r^2 value) is improved by using regression trees over linear regressions (this study: $r^2 = 0.35$ vs. 0.31; Grand River non-urban: $r^2 = 0.13$ vs. 0.35) which indicates that thresholds or breakthroughs give a better representation of N_2O dynamics in streams and rivers than do linear relationships. These results may indicate that N_2O production is NO_3^- limited when $NO_3^- < 2.7$ mg N/L. It is clear from previous work on the Grand River (Chapters 2 and 3) that N_2O production can be very high when NO_3^- concentration is < 2.7 mg N/L, but generally only when DO is low. High N_2O:NO_3^- ratios during hypoxia might be explained by two factors. First, when the water column is oxic, denitrification occurs lower in the sediment, in the anoxic zones or in anoxic microsites. NO_3^- diffusion into the sediment may limit denitrification and higher NO_3^- concentrations in the water column results in a higher diffusional gradient between water column and sediment and therefore higher NO_3^- fluxes to the sediment. When the water column is hypoxic, the sediment oxic layer is shallower and the diffusion distance between the water column and anoxic sediment is shorter. The second factor is the N_2O:(N_2O+N_2) ratio produced during denitrification. The N_2O:(N_2O+N_2) ratio is generally high on the onset of hypoxia due to a lag in N_2O reductase activity (Codispoti 2010). Thus, high N_2O emissions can occur even when NO_3^- (and denitrification rate) is

relatively low. Additionally, N_2O:(N_2O+N_2) ratios typically stay relatively elevated in hypoxic conditions even after N_2O reductase is activated, unless NO_3^- is low and N_2O reduction is favoured (e.g. (Silvennoinen et al. 2008)). More work on characterizing the N_2O:(N_2O+N_2) ratio under different and changing conditions (redox, NO_3^-, temperature, etc.) is needed to fully understand how much this ratio affects NO_3^- thresholds for N_2O emissions in oxic rivers.

While regression trees improve explanatory power of N_2O emissions over linear regressions, they can still only explain less than 40% of variability in N_2O emissions in these systems. This speaks to the difficulty in predicting N_2O emissions, which are likely controlled by a complex interplay of upstream redox conditions, sediment conditions, organic carbon availability, and/or denitrifying community. The difference in NO_3^- concentration threshold between this study (2.7 mg N/L) and the Grand River (4.9 mg N/L, Venkiteswaran et al., in submission) indicates that NO_3^- controls on N_2O production are not well understood in these systems. The difference may relate to winter data in the Grand Rive study (typically: higher NO_3^- and lower N_2O than in summer; S.L. Schiff, unpublished). However, more research is needed to understand differences in NO_3^- thresholds for N_2O production in different systems.

7.4.3 Comparison to N_2O:NO_3^- Relationships in Global Streams and Rivers

7.4.3.1 The Probability Triangle Concept

Previous work (Chapters 2 and 3) and this study show that N_2O:NO_3^- relationships in rivers and streams are unlikely to be linear, especially when the water column is hypoxic. Predictability is poor. Thus, the linear model described the IPCC (IPCC 2007) must be replaced by a new conceptual model.

One possible model is the Probability Triangle (Figure 7.9). This maps out possible N_2O emission rates with NO_3^- concentrations. Assuming steady state production of N_2O, emissions are equal to N_2O production rates in this diagram. Below a certain (undefined) NO_3^- concentration, N_2O emissions are expected to be limited by water column NO_3^- concentration, and thus linearly increase with NO_3^-. Above this threshold is the Probability Triangle. The triangle's upper slope is defined as the maximum N_2O production rate possible based on NO_3^- diffusion from the water column into the sediment. The bottom line of the triangle is equal to N_2O emission limited by NO_3^- concentration. Of course, complete reduction of NO_3^- to N_2O in aquatic systems is unlikely; this triangle represents maximum possible values. The location of N_2O emissions within the triangle can be narrowed by

considering other predictive factors for N_2O emissions: dissolved oxygen and temperature (Chapter 3; Venkiteswaran et al., in submission). Hypoxia (DO<2 mg/L) and high temperature will place N_2O emissions toward the top of the triangle (Chapters 2 and 3, Venkiteswaran et al., in submission).

7.4.3.2 The Global Dataset and the Probability Triangle

To assess the ability of the Probability Triangle conceptual model to predict N_2O emission ranges from NO_3^- concentrations, a literature review of annual average and instantaneous N_2O emissions and NO_3^- concentrations was conducted, to which data from this study and all Grand River data collected and analysed (2006 to 2012) were added. When possible, temperature and DO values were also collected. IPCC estimates for N_2O flux from NO_3^- loading is done on an annual scale, and where possible, annual average values were used. However, more studies collect NO_3^- and N_2O data for only part of the year, and instantaneous data are also shown. These instantaneous data may be most useful for understanding N_2O production under geochemical conditions and for determining N_2O hotspots, while annual data may elucidate long-term trends. Studies include streams and rivers in a variety of climates (temperate to tropical) and watershed land uses (non-agricultural, agricultural and urban).

Fifteen studies reporting annual NO_3^- concentrations and N_2O emissions from 36 unique rivers and streams are reported here, along with the Grand River (n = 41, Figure 7.10). While data is relatively scarce, N_2O emissions at the same NO_3^- concentration range by between four and ten times. N_2O variability increases with NO_3^- concentration, as predicted in the Probability Triangle concept, but this is driven by one Japanese stream exiting a rice paddy (Hasegawa et al. 2000) with very high NO_3^- and N_2O concentrations. When this point is removed, N_2O variability is highest at moderate NO_3^- concentrations (1 – 2 mg N/L), driven by high N_2O emissions from Mexican agricultural canals which have periods of hypoxia (Harrison and Matson 2003). N_2O emission data could not be transformed to fulfill the constant variance assumption of the linear regression model and thus linear regressions should be interpreted with caution. Using both N_2O emission and logged N_2O emission, r^2 was low but relationships were significant ($r^2 = 0.186$, $p = 0.006$ and $r^2 = 0.162$ and $p = 0.006$, respectively, n = 41).

More work is needed on the global scale to add more rivers with high NO_3^- concentrations to determine if N_2O emission variability is very high in these conditions. Additionally, more work is needed to quantify other geochemical parameters that could improve predictive power on the annual scale, such as temperature, DO and TP.

Instantaneous N_2O emission and NO_3^- concentration data from twelve studies of rivers and streams worldwide were graphed along with Grand River data (divided into four sections based on land use and geomorphology; see Chapter 6) and data from this study (total: n = 1297) (Figure 7.11). A LOESS (locally weighted scatterplot smoothing) fit was applied to assess local means. There is a much larger range of NO_3^- concentration in this dataset (maximum: 21.2 mg N/L) than in the annual data. N_2O emissions also had a larger range, almost 2 orders of magnitude. Variability in N_2O emissions peaked around 2 mg N/L NO_3^- and again at around 8 mg N/L NO_3^-. It is likely that N_2O variability would also be high between 2 mg N/L and 8 mg N/L but insufficient data exists. The high N_2O variability at high NO_3^- concentration is mostly driven by agricultural streams in New Zealand (Wilcock and Sorrell 2008). Similar to the annual dataset, constant variance could not be obtained and r^2 values were low but significant (linear: $r^2 = 0.02$, $p < 0.001$; logged N_2O: $r^2 = 0.07$, $p < 0.001$, n = 1297).

Other predictive factors (temperature, DO) could add predictive ability to NO_3^-. This was tested with a multiple linear regression. Only data points with all three predictive variables were used (n = 951). Data were from the Grand River, the Neuse River watershed, North Carolina (Stow et al. 2005) and the Xin'an Tang River, China (Xia et al. 2013). Constant variance requirements were not met, and r^2 values were low whether or not N_2O emissions were log-transformed but results were significant ($r^2 = 0.197$ and $r^2 = 0.194$, respectively; both $p < 0.001$).

Relationships between DO, temperature, NO_3^- and N_2O emissions were visually examined by sorting data by temperature (Figure 7.12) and DO (Figure 7.13). This allows the inclusion of data points that include only temperature or DO. Temperature data were given for the Neuse River watershed, North Carolina (Stow et al. 2005), the LII River in New Zealand (Clough et al. 2007), the 72 streams of the LINX II experiment in the United States (Beaulieu et al. 2011), and the Xin'an Tang R., China (Xia et al. 2013) as well as the Grand River data and this study. Highest N_2O emissions always occur at high temperatures (> 20℃). However, not all low emissions occur at low temperatures. The highest temperature category (> 24℃) has N_2O emissions ranging from -1 μmol/m^2/d to 3749 μmol/m^2/d. This suggests that temperature alone is not an accurate predictor of N_2O emissions.

DO concentrations were given in the Neuse watershed (Stow et al. 2005) and the Xin'an Tang R. (Xia et al. 2013) as well as in the Grand River and in this study (Figure 7.12). Highest N_2O emissions

occur when DO is lowest (< 2 mg/L). Unlike temperature, low DO (< 2 mg N/L) occurs with a narrower and higher N_2O emission range (52 to 3549 μmol/m^2/d).

Thus, the current global dataset on N_2O emissions and NO_3^- concentrations in rivers and streams do not refute the Probability Triangle conceptual. Interestingly, there appears to be no region where low NO_3^- limits N_2O emissions, even though NO_3^- concentrations ranged from below detection to 21 mg N/L. This could be because N_2O (but not NO_3^-) enters streams from groundwater, or because N_2O production is limited by NO_3^- in sediment, which may not be in equilibrium with NO_3^- in the sediment column. High N_2O emissions (i.e. the upper portion of the triangle) are most likely to occur when DO is low (< 2 mg/L) and temperatures are high (> 20 mg/L) regardless of NO_3^- concentration. This is likely because the rate of denitrification and/or N_2O:(N_2O+N_2) ratios are highest in these conditions. Lower N_2O fluxes are harder to predict because they can occur at any temperature but do occur at high DO (> 2 mg/L).

This conceptual model can be further refined by future studies in other streams and rivers worldwide. Tropical rivers are particularly underrepresented, as are rivers with high NO_3^- concentrations (> 4 mg/L). Agricultural streams with high NO_3^- and moderate N_2O emissions are included (Wilcock and Sorrell 2008) but streams or rivers with high NO_3^- and very high N_2O have yet to be reported. This may be merely because such systems are rare or understudied. However, it is also possible that very high N_2O emissions are incompatible with high-NO_3^- systems. These emissions occur via denitrification in hypoxic systems, but high denitrification could also significantly lower NO_3^- concentrations. For example, hypereutrophic canals with extensive night-time hypoxia in Mexico removed all NO_3^- present (~ 1mg/L) before night-time was over (Harrison et al. 2005). If this is the case, the Probability Triangle can be modified to include a decreasing slope at high NO_3^- concentration (Figure 7.14).

The model could also be refined by improving the comparability and quality of the global dataset. N_2O emissions measured in different ways (e.g. modeled k, chambers, SF_6 addition, etc.) may produce different results because they measure k on different time scales (Howarth et al. 2013, Jha et al. 2001, Jha et al. 2004, Raymond and Cole 2001). Additionally, many studies do not include night-time sampling, even though N_2O can be much higher than in daytime, even when no hypoxia exists (Chapter 2, (Harrison et al. 2005)).

Lastly, the model includes the confounding variable of stream depth because it compares N_2O emissions per surface area to NO_3^- mass per volume. Since depth can vary dramatically, especially between streams and rivers, normalizing N_2O emissions to volume would be wise. This also allows more direct comparison to the IPCC equations, which deal only with masses of NO_3^- and N_2O on an annual scale. However, most published studies do not include depth measurements and depth measurements were not collected for most Grand River samples.

7.4.4 Implications for IPCC Methodology and River Management

It is clear from the data shown above that there is, at best, a very weak ($r^2 = 0.186$) relationship between annual average NO_3^- concentrations and N_2O emissions from rivers and streams. The paucity of global datasets including dissolved oxygen and temperature make it impossible to determine if trends seen on the instantaneous scale in the Grand River (Venkiteswaran et al. in submission) and in southern Ontario streams and rivers (this study) occur on the annual and global scales. However, instantaneous N_2O emissions do not correlate with NO_3^- concentrations ($r^2 < 0.10$) when all available instantaneous data is used.

Thus, a new method of estimating annual N_2O emissions from rivers is needed. Figures 7.12 and 7.13 suggest that warmer, low-oxygen rivers with moderate NO_3^- concentrations are more likely to emit more N_2O to the atmosphere. It also appears that N_2O emission variability is very high, even at low NO_3^- concentrations, but peaks at moderate NO_3^- concentrations. It is therefore of primary importance to determine the extent of hypoxia in rivers on an annual scale, as this relates best to N_2O emissions (Chapter 3). Hypoxia is also an important indicator of ecosystem health, so hypoxia data may be collected by local ecosystem managers and could be used for greenhouse gas inventories. DO concentrations can be modeled in river systems if the gas exchange coefficient, ecosystem respiration and primary productivity can be measured (Venkiteswaran et al. 2007). Regression tree analyses have been shown to increase predictability of N_2O emissions from rivers using DO, NO_3^- and temperature (Venkiteswaran et al. in submission, this study). NO_3^- thresholds identified by regression trees appear to change by region (this study: $NO_3^- = 2.7$ mg N/L; non-urban Grand River sites: $NO_3^- = 4.9$ mg/L). This suggests that as much data as possible should be used in trees so branches are not skewed by outliers. Further analysis of more streams and rivers worldwide will indicate how much NO_3^-–DO-temperature relationships change by region.

N_2O-NO_3^- relationships may also change over long time periods. Climate change predictions for warmer water temperatures, more hypoxia and higher denitrification rates (Veraart et al. 2011, Whitehead et al. 2009) will probably lead to increases in N_2O production. Higher temperatures alone may reduce N_2O predictability (Figure 7.12) but hypoxia may increase predictability (Figure 7.13). It is currently unknown if or how these two factors will interact in N_2O production rates. Recent changes in dissolved organic carbon (DOC) quantity and quality in many rivers, lakes and streams (Evans et al. 2005) may affect food sources for heterotrophic denitrifiers. Additionally, climate change could result in changes to habitat ranges of many species (Van der Putten et al. 2010), including denitrifying organisms. This is especially important for denitrifiers who lack N_2O reductase and therefore process 100% of NO_3^- substrate into N_2O (Philippot et al. 2011). Additionally, the newly discovered N_2O fixation pathway in cyanobacteria (Farías et al. 2013) could also be influenced by climate. Therefore, it is unknown if, but unlikely that, relationships between N_2O emission and predictors (temperature, DO, NO_3^-) will remain constant over time. Careful N_2O sampling, taking potential hotspots (hypoxic and warm areas) into account, will be necessary to fully understand the N_2O budget.

7.5 Conclusions

A survey of 24 streams and rivers in southern Ontario was conducted to examine NO_3^-:N_2O relationships on the instantaneous scale in oxic systems. The linear relationship between NO_3^- and N_2O was weak (r^2 =0.31) but a non-linear regression tree analysis improved predictability (r^2 = 0.37). No other predictive factors that significantly improved fit were found. This dataset was compared to the global published dataset, including an extensive dataset from the Grand River, of NO_3^- concentrations and N_2O emissions from streams and rivers, on both the annual and instantaneous scale. In both cases, N_2O emissions are highest and most variable at moderate NO_3^- concentrations. This relationship can be examined further on the instantaneous scale, where some simultaneous temperature and DO data exists. The linear relationship between NO_3^- and N_2O emission is very weak (r^2 < 0.10) on the instantaneous scale. Highest N_2O emissions occur at high temperature and low DO. However, low DO (< 2 mg/L) occurs with relatively high N_2O emissions (> 50 μmol/m^2/d) while high temperature occurs with large range of N_2O emissions (> -1 μmol/m^2/d). This suggests that high temperature alone is not enough to drive N_2O emissions very high, but low DO resulting from high community respiration rates can drive high N_2O production rates.

The data were compared to a conceptual model, the Probability Triangle, which posits that N_2O variability increases with NO_3^- concentration except at very low NO_3^- concentrations, where NO_3^- limits N_2O production. Interestingly, the low threshold is not obvious in the global dataset, suggesting that low NO_3^- concentrations in sediments may be poorly coupled to NO_3^- in the water column. Additionally, N_2O variability appears to peak at moderate NO_3^- concentrations (~2 mg N/L). This may be an artifact of data scarcity. Alternatively, it could be that high NO_3^- concentrations occur in areas poorly suited to denitrification, resulting in low N_2O emissions. Further research on more rivers and streams worldwide is needed to determine these relationships.

NO_3^- and N_2O emissions are, at best, very weakly linearly related in rivers and streams. This indicates that a new approach is needed to estimate N_2O emissions from these systems. One possibility is to quantify hypoxia (DO < 2 mg/L) on an annual scale, possibly with the aid of DO models such as PoRGy (Venkiteswaran et al. 2007) and then conduct regression tree analysis with other variables (NO_3^-, temperature). Hypoxia is also a concern for river ecosystem health; it is therefore recommended that greenhouse gas inventories pool data with ecosystem managers. However, greenhouse gas inventories must continually monitor and measure N_2O emissions, NO_3^-, DO and temperature, as N_2O-NO_3^- relationships are likely influenced by changes in organic carbon quantity and quality, hypoxia, and other factors affecting the denitrifying community.

Table 7.1: Site names and physical and trophic characteristics. E = eutrophic, M = mesotrophic, based on TP concentrations after (Dodds et al. 1998). PWQMN = Provincial Water Quality Monitoring Network Site. I = inactive site, A = active site.

Site Code	Site Name	Latitude and Longitude	Stream Order	Trophic Status	PWQMN Site?
CS-1	Laurel Creek	43.4823783886 N 80.4833468575 W	4	M	Y, I
CS-2	Conestogo	43.54114301370 N 80.55331623260 W	6	M	Y, I
CS-3	Canagagigue Creek	43.5847483887 N, 80.5346244826 N	5	E	Y, A
CS-4	Irvine Creek	43.6954463888 N 80.4478219825 W	5	M	Y, A
CS-5	Speed R.	43.6399308888 N 80.2701321073 W	5	E	Y, A
NW-1	Nith R.	43.3754790135 N 80.6788787327 W	5	E	Y, A
NW-2	Horner Creek	43.162061 N 80.540942 W	5	E	Y, I
NW-3	Whitemans Creek	43.126078 N 80.383606 W	6	E	Y, A
NW-4	Fairchild Creek	43.2308733884 N 80.2424814823 W	5	E	Y, I
MA-1	Middle Maitland River	43.7242838889 N 81.2457202332 W	6	E	Y, I
MA-2	Beauchamps Drain	43.7044357638 N 81.2487102333 W	4	E	Y, A
MA-3	South Maitland River	43.6846218888 N 81.5409024835 W	6	E	Y, A
MA-4	Blyth Brook	43.7488695139 N 81.4459168584 W	4	M	Y, A
MA-5	Maitland River	43.895497639 N 81.3534972334 W	5	M	Y, A
SA-1	South Saugeen R.	44.098272 N 80.984956 W	5	E	Y, I
SA-2	Beatty Saugeen	44.1309828892 N 80.96736535800 W	5	M	Y, A
SA-3	Upper Main Saugeen R. at Hanover	44.15136451430 N 81.03917298310 W	6	E	Y, I
SA-4	Saugeen R.	44.132764 N, 81.144136 W	7	M	Y

SA-5	Mill Pond Stream	44.154219 N, 81.274658 W	3	M	N
UT-1	Avon R.	43.36606 N 81.01867 W	4	E	Y, A
UT-2	Trout Creek	43.251367 N 80.984211 W	5	E	Y, A
UT-3	Middle Thames R.	43.059458 N 80.994814 W	6	M	N
UT-4	South Thames R.	43.01864 N 80.92691 W	5	E	Y, A
UT-5	Reynolds Creek	42.969158 N 80.949758 W	4	E	Y, I

Table 7.2: Results of linear regressions on survey sites, N_2O emissions versus temperature, DO, NH_4^+, NO_3^-, total dissolved nitrogen (TDN) and total phosphorus (TP). Where noted, data were transformed to improve fit and/or produce constant variance. Bolded values are significant (p< 0.005).

Dependent Variable	N_2O transformation	Dependent variable transformation	r^2	p
Temperature	log(N_2Oemission+10)	None	0.003	0.704
DO	None	None	0.035	0.203
NO_3^-	log(N_2Oemission+10)	None	**0.31**	**<0.001**
NH_4^+	log(N_2Oemission+10)	log(NH_4^+)	0.037	0.192
TDN	log(N_2Oemission+10)	None	**0.37**	**<0.001**
TP	log(N_2Oemission+10)	None	0.09	0.146

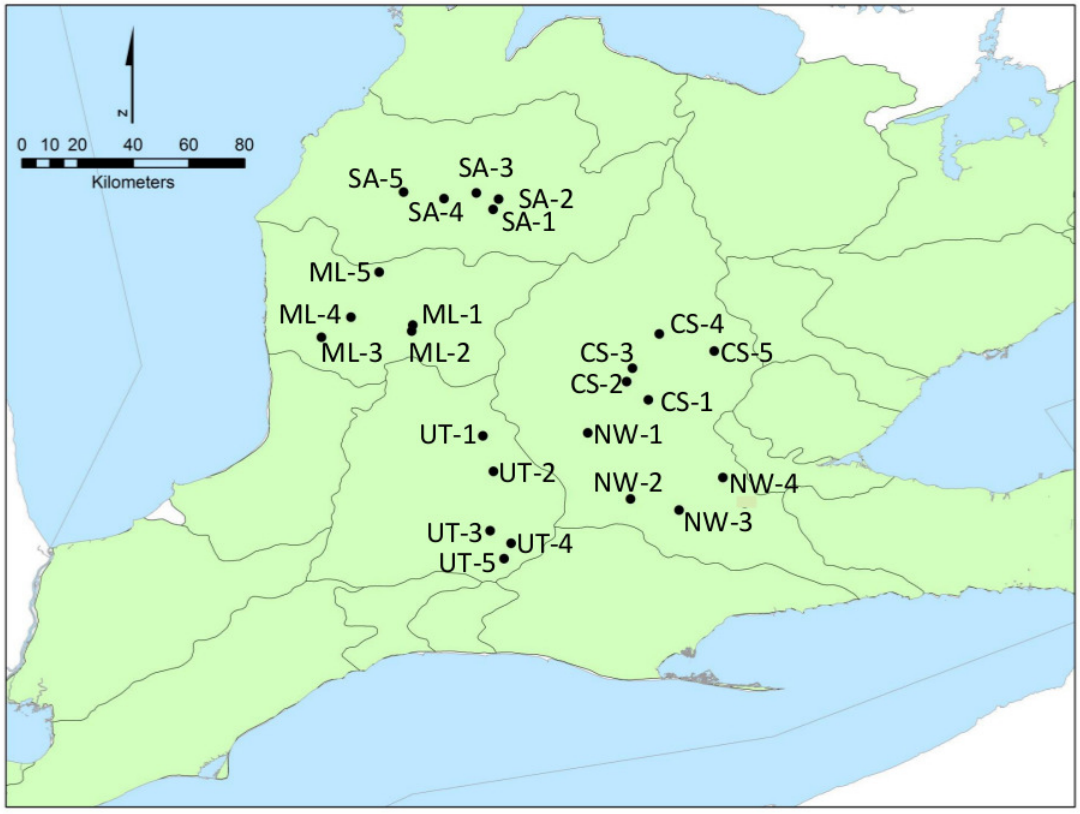

Figure 7.1: Map of southern Ontario showing the 24 stream and river sites. See Table 7.1 for site descriptions and names. Grey lines indicate watershed boundaries.

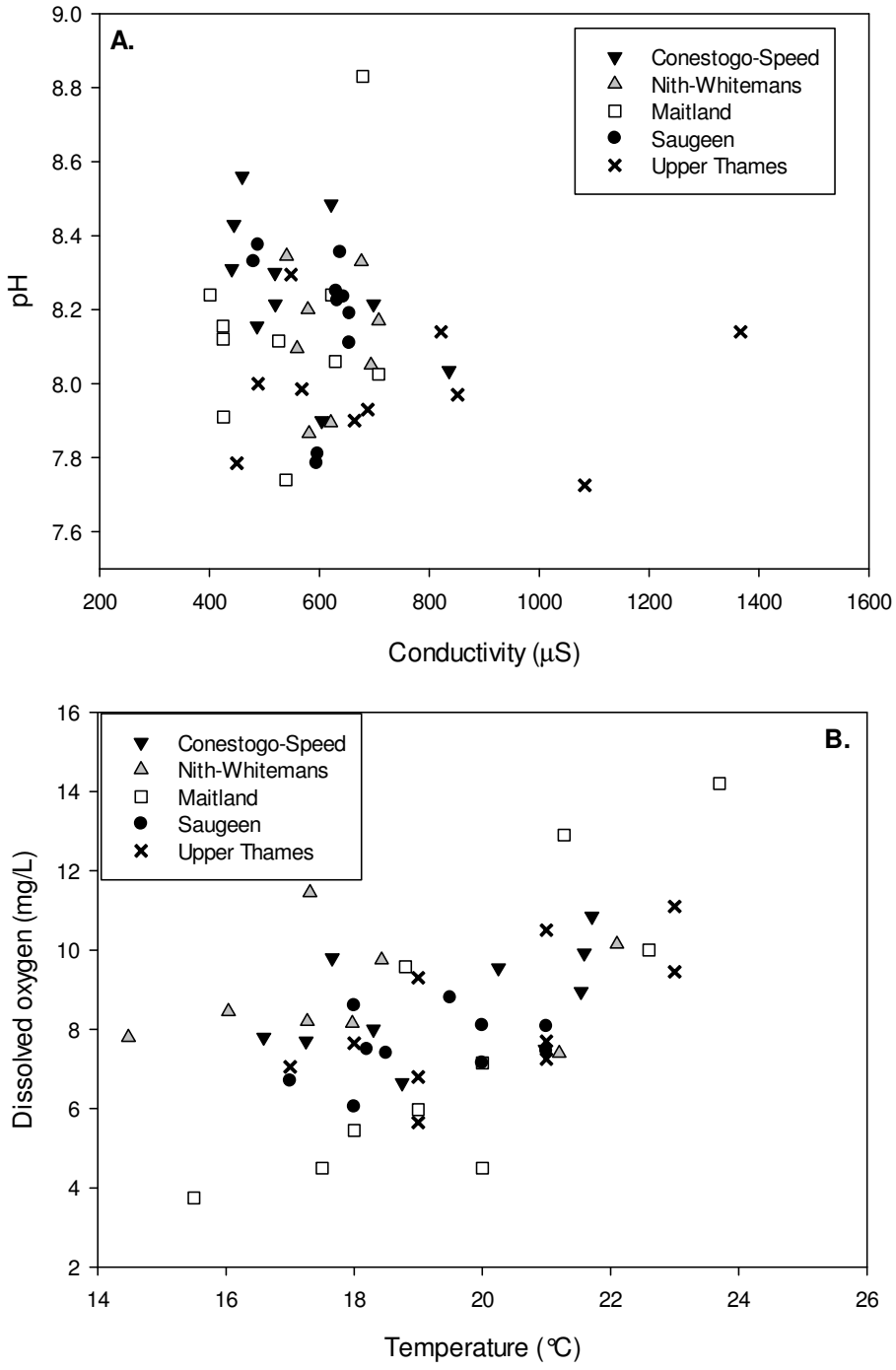

Figure 7.2: pH, specific conductivity (panel A), water temperature and dissolved oxygen (DO) (panel B) at the 24 sites surveyed, grouped by watershed.

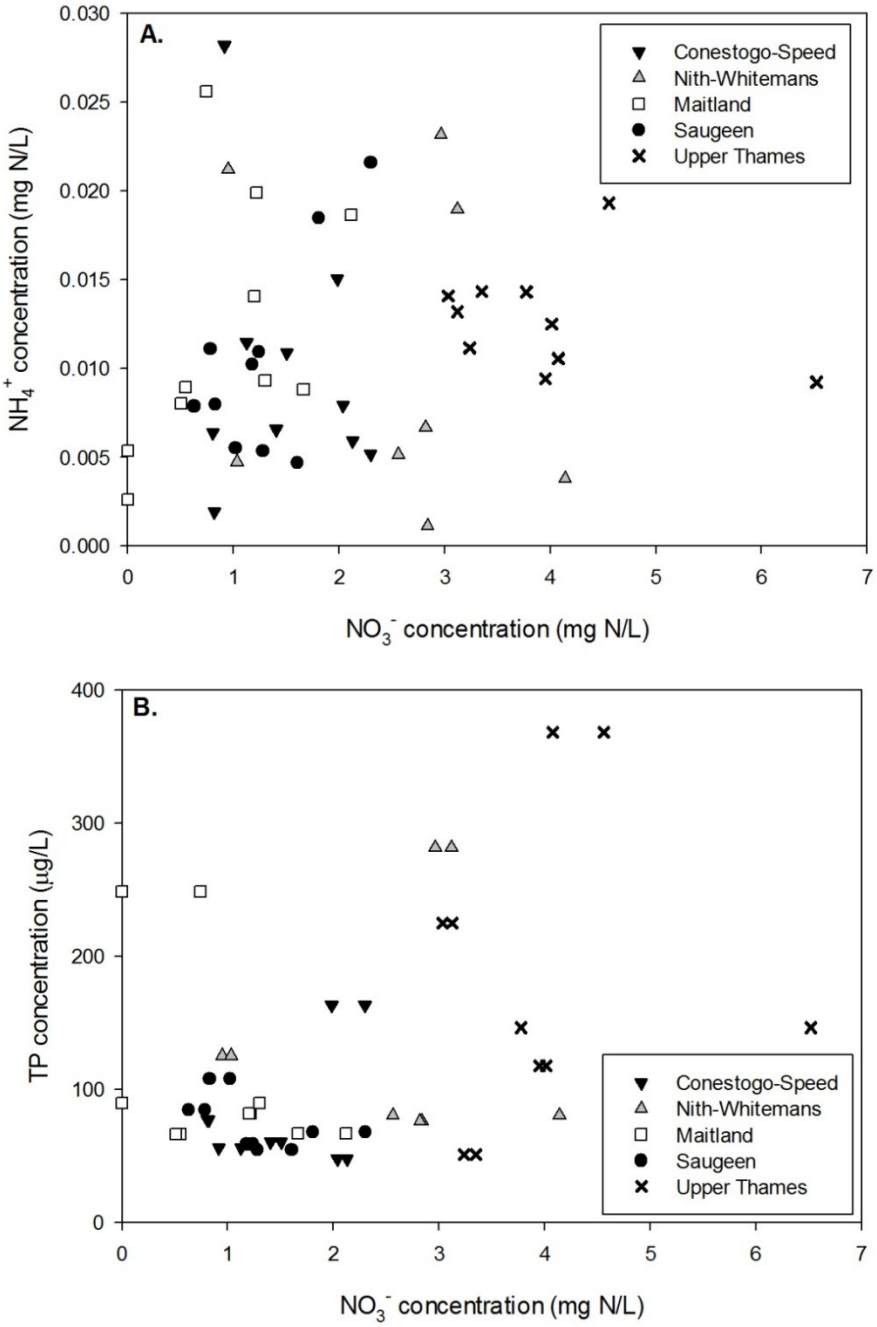

Figure 7.3: NO_3^-, NH_4^+ and total phosphorus (TP) concentrations at the 24 sites surveyed, grouped by watershed.

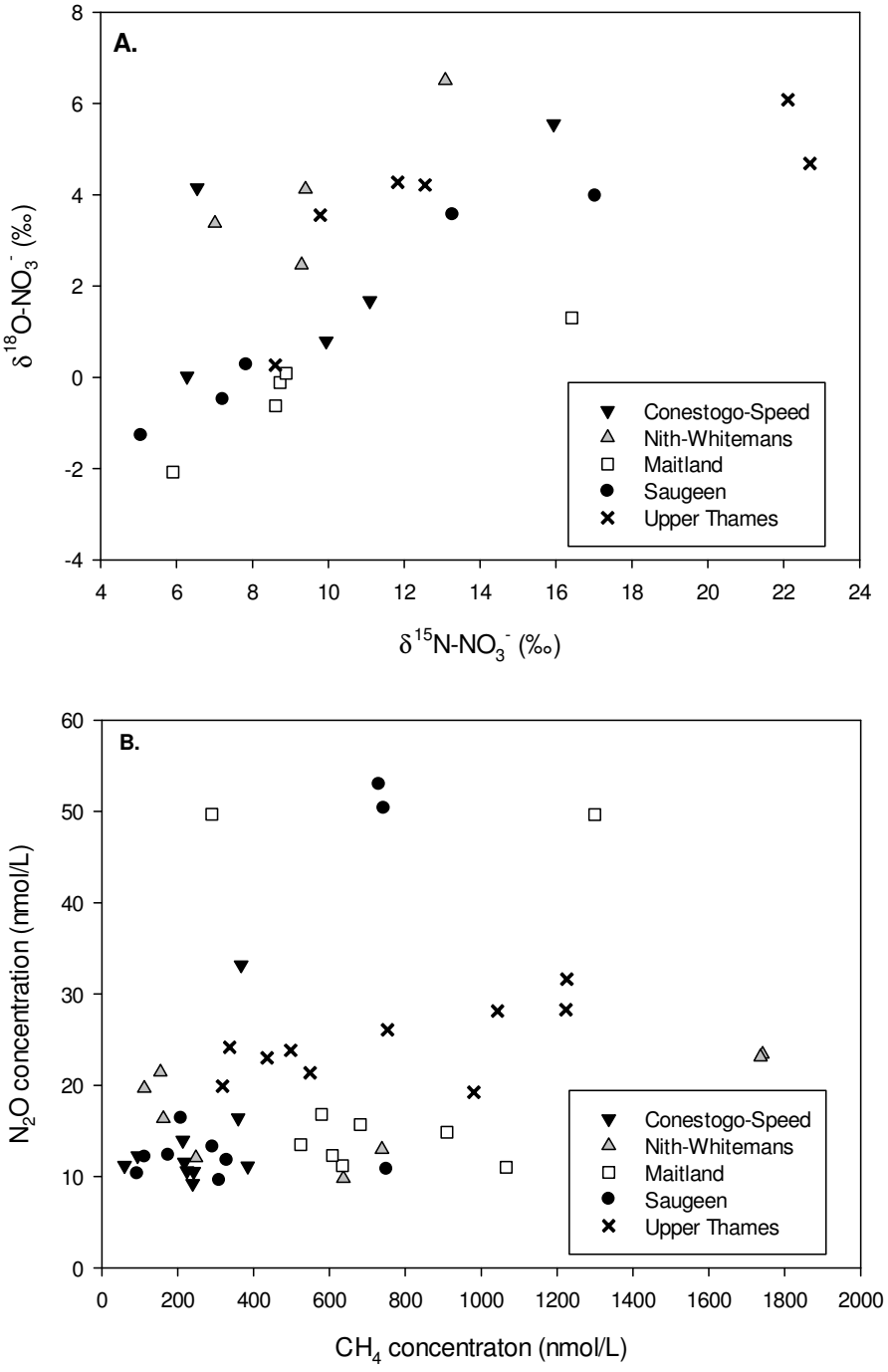

Figure 7.4: $\delta^{15}N\text{-}NO_3^-$, $\delta^{18}O\text{-}NO_3^-$ values (panel A) and N_2O and CH_4 concentrations (panel B) in the 24 sites surveyed, grouped by watershed.

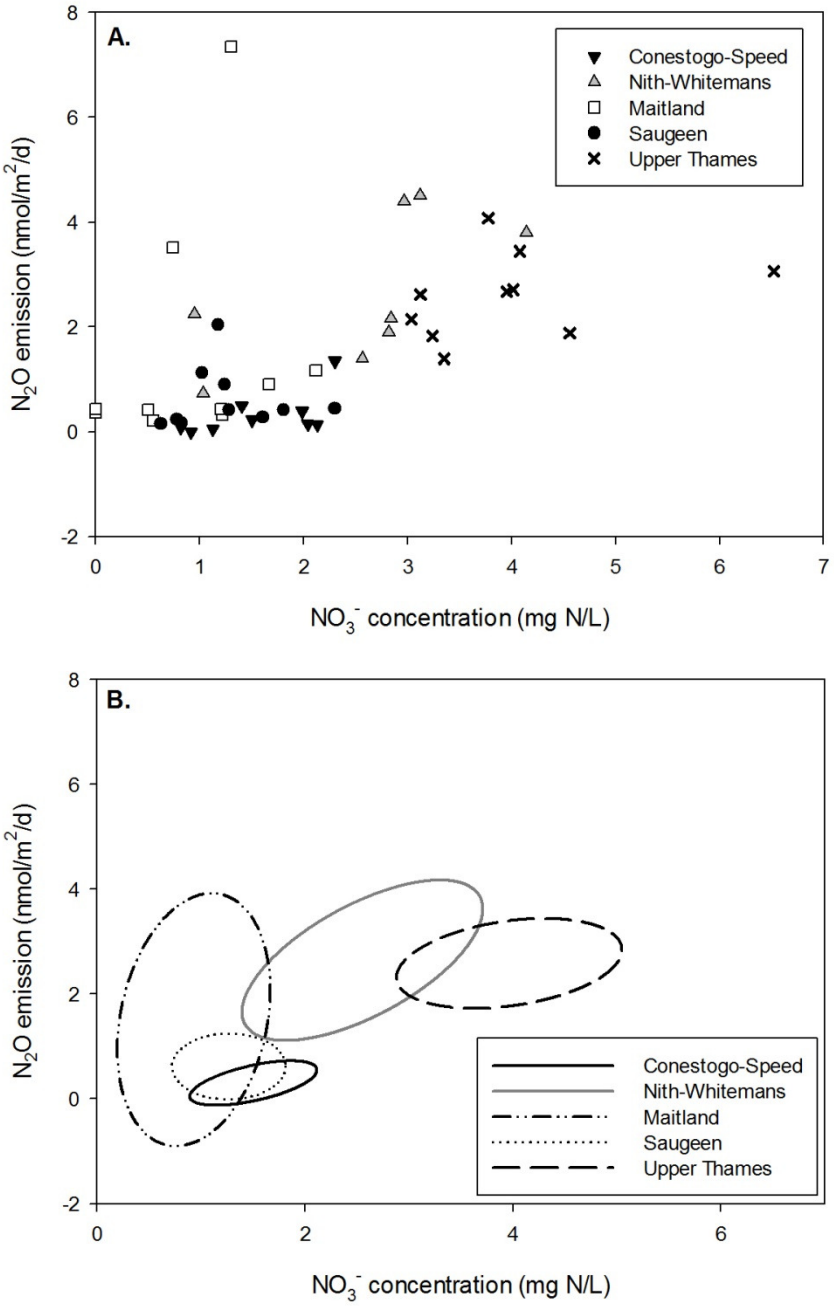

Figure 7.5: NO_3^- concentration and N_2O emissions at the 24 surveyed sites, by watershed area. A: Data, B: standard ellipses.

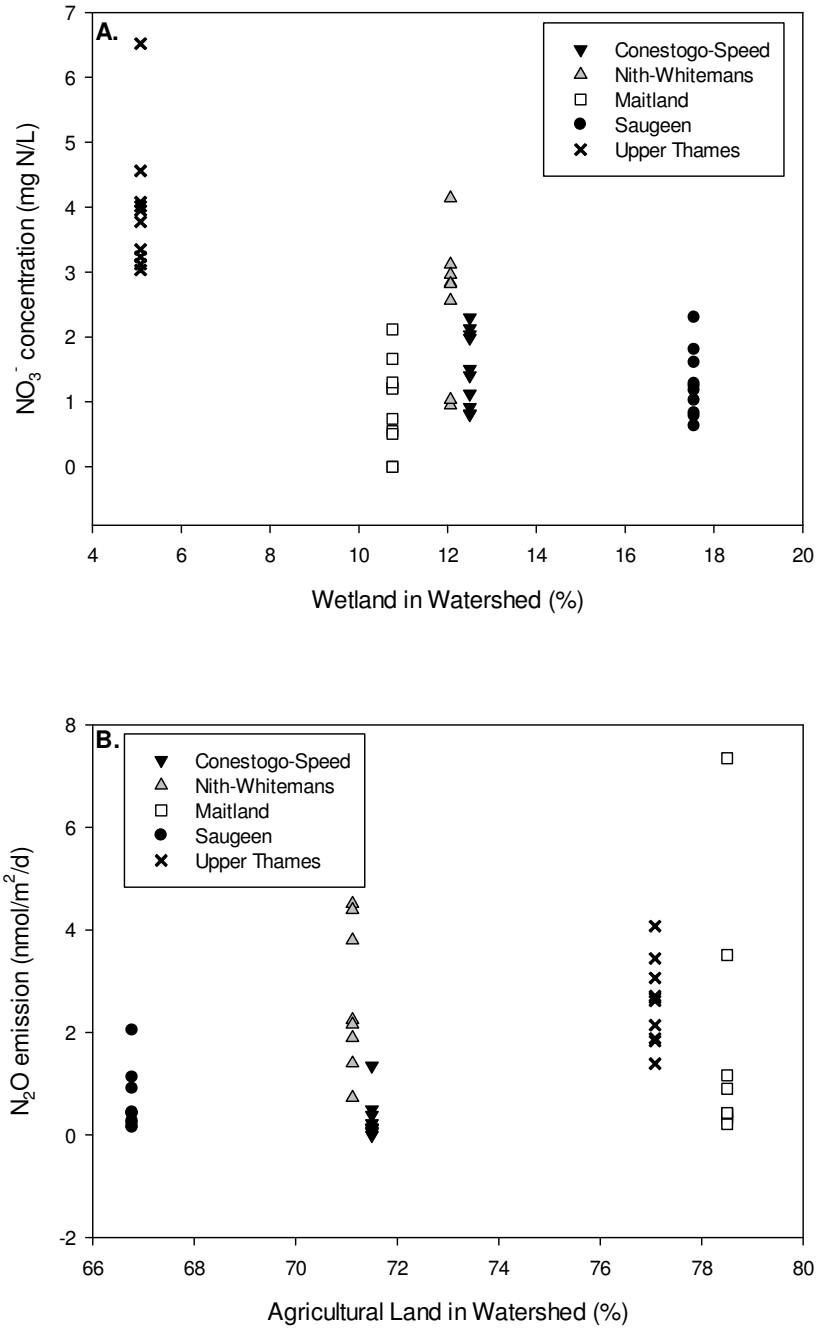

Figure 7.6: Watershed land use versus NO_3^- concentrations (A) and N_2O emissions (B). CS and NW are in the same watershed and have the same fraction land use, but values in CS are increased by 0.5% for clarity.

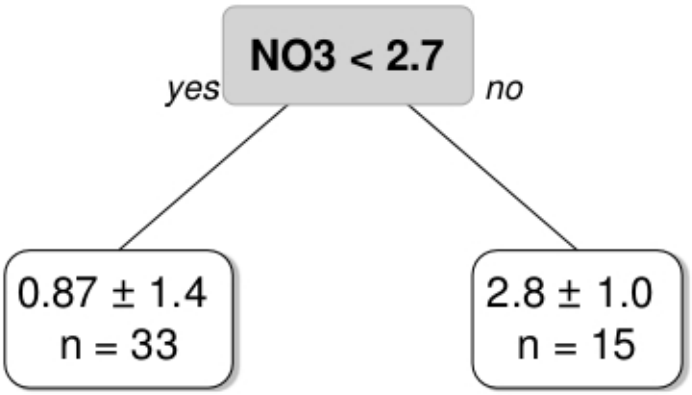

Figure 7.7: Regression tree for the 24 surveyed sites. Inputs were temperature, DO, NO_3^-, TDN, DOC, TP and total suspended solids (TSS). A NO_3^- concentration threshold of 2.7 mg N/L provided the most predictive power with the least number of inputs. $r^2 = 0.35$. When NO_3^- concentration is < 2.7 mg N/L, the average N_2O emission is 0.87 µmol/m^2/d (n = 33). When NO_3^- concentration is ≥ 2.7 mg N/L, the average N_2O emission is 2.8 µmol/m^2/d (n =15).

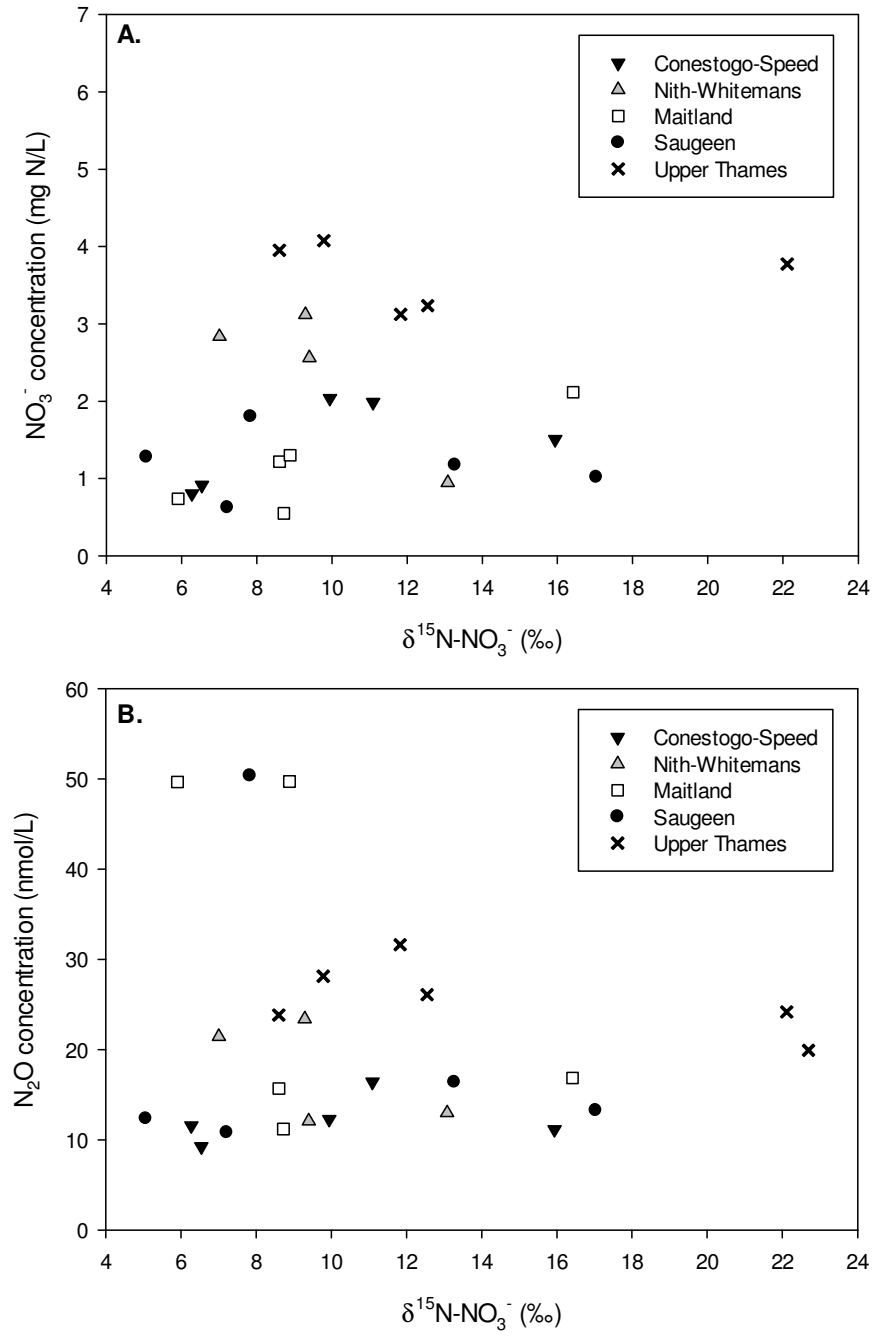

Figure 7.8: $\delta^{15}N\text{-}NO_3^-$ versus NO_3^- concentration (panel A) and N_2O concentration (panel B) at 24 field sites, by watershed area. Only one sample per day is shown (when $\delta^{15}N\text{-}NO_3^-$ samples were collected).

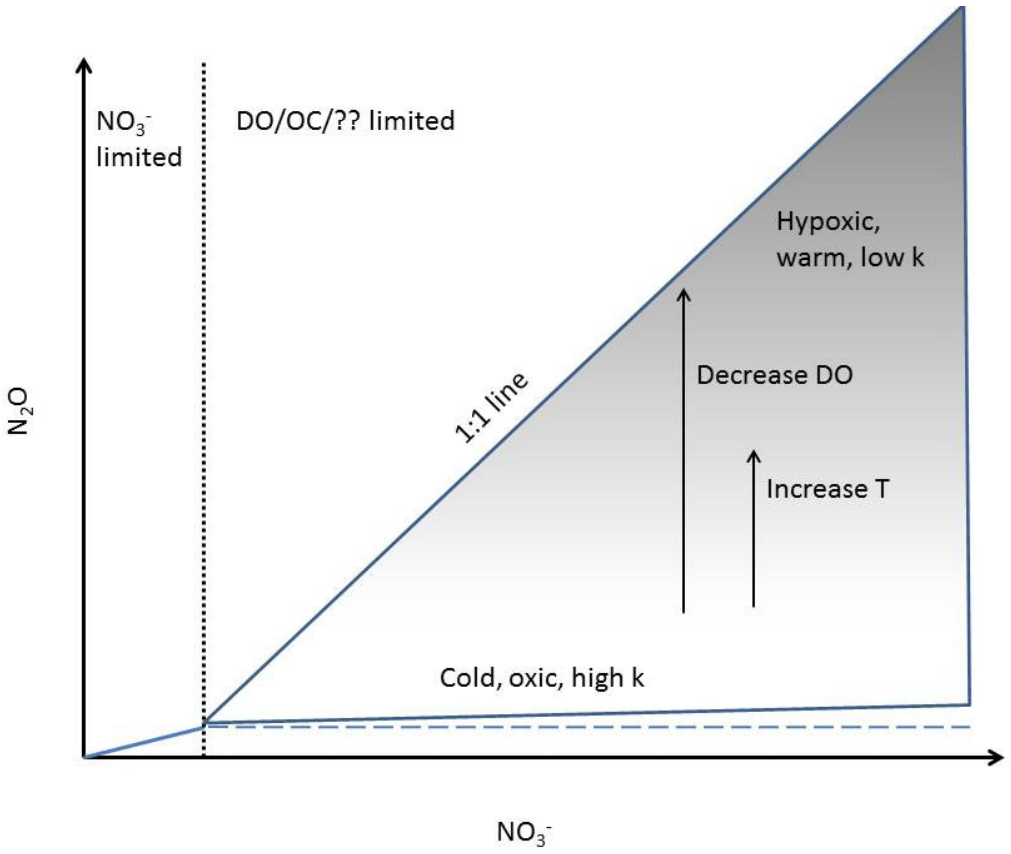

Figure 7.9: Conceptual diagram for the Probability Triangle, showing increasing variability in N_2O emissions with increasing NO_3^- concentration. Below a NO_3^- concentration threshold, N_2O emissions are expected to be linearly related to NO_3^- because NO_3^- is limiting. Based on previous work (Chapters 2 and 3, Venkiteswaran et al. in submission), high N_2O emissions (dark grey area) are expected to occur when temperature is high and DO is low; low emissions during low temperature and high DO.

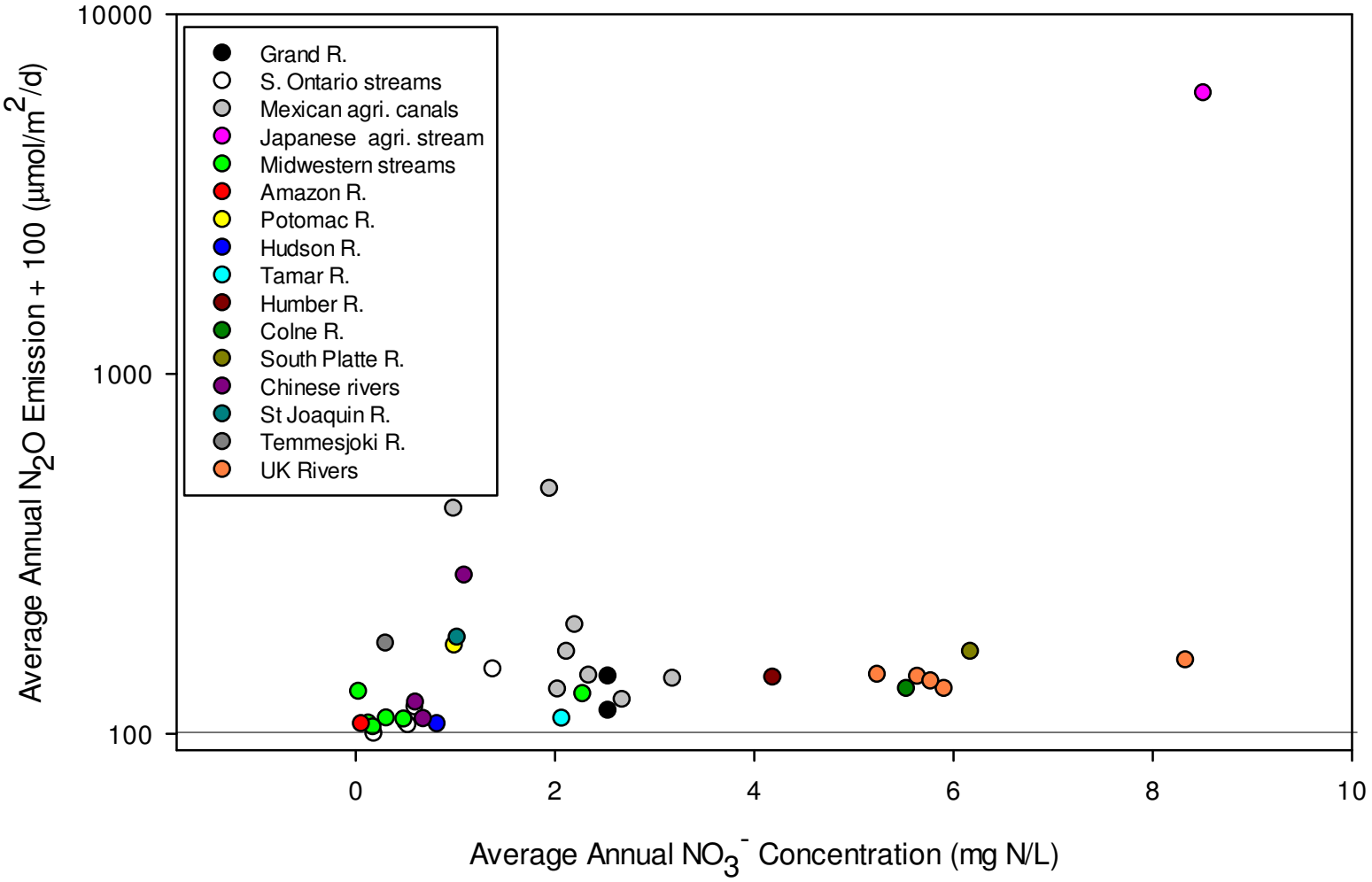
10000
1000
100
0
2
4
6
8
10
Average Annual N_2O Emission + 100 (µmol/m^2/d)
Average Annual NO_3^- Concentration (mg N/L)
Grand R.
S. Ontario streams
Mexican agri. canals
Japanese agri. stream
Midwestern streams
Amazon R.
Potomac R.
Hudson R.
Tamar R.
Humber R.
Colne R.
South Platte R.
Chinese rivers
St Joaquin R.
Temmesjoki R.
UK Rivers

Figure 7.10: Global dataset of annual average NO_3^- concentration and annual average N_2O emissions in streams and rivers. Data are from the Grand River (Chapter 3), S. Ontario streams (Baulch et al. 2011); Mexican agricultural canals (Harrison and Matson 2003); a Japanese agricultural stream (Hasegawa et al. 2000); Midwestern American streams (Beaulieu et al. 2008); the Amazon R. (Richey et al. 1988); the Potomac R. (Richey et al. 1988); the Hudson R. (Cole and Caraco 2001); the Tamar R., UK (Law et al. 1992); the Humber R. (Law et al. 1992); the Colne R. (Robinson et al. 1998); the South Platte R., CO (Robinson et al. 1998); three eutrophic Chinese rivers (Yang et al. 2011); the Temmesjoki R, Finland (Silvennoinen et al. 2008) ; and seven UK rivers (Dong et al. 2004). The horizontal line represents zero N_2O emissions.

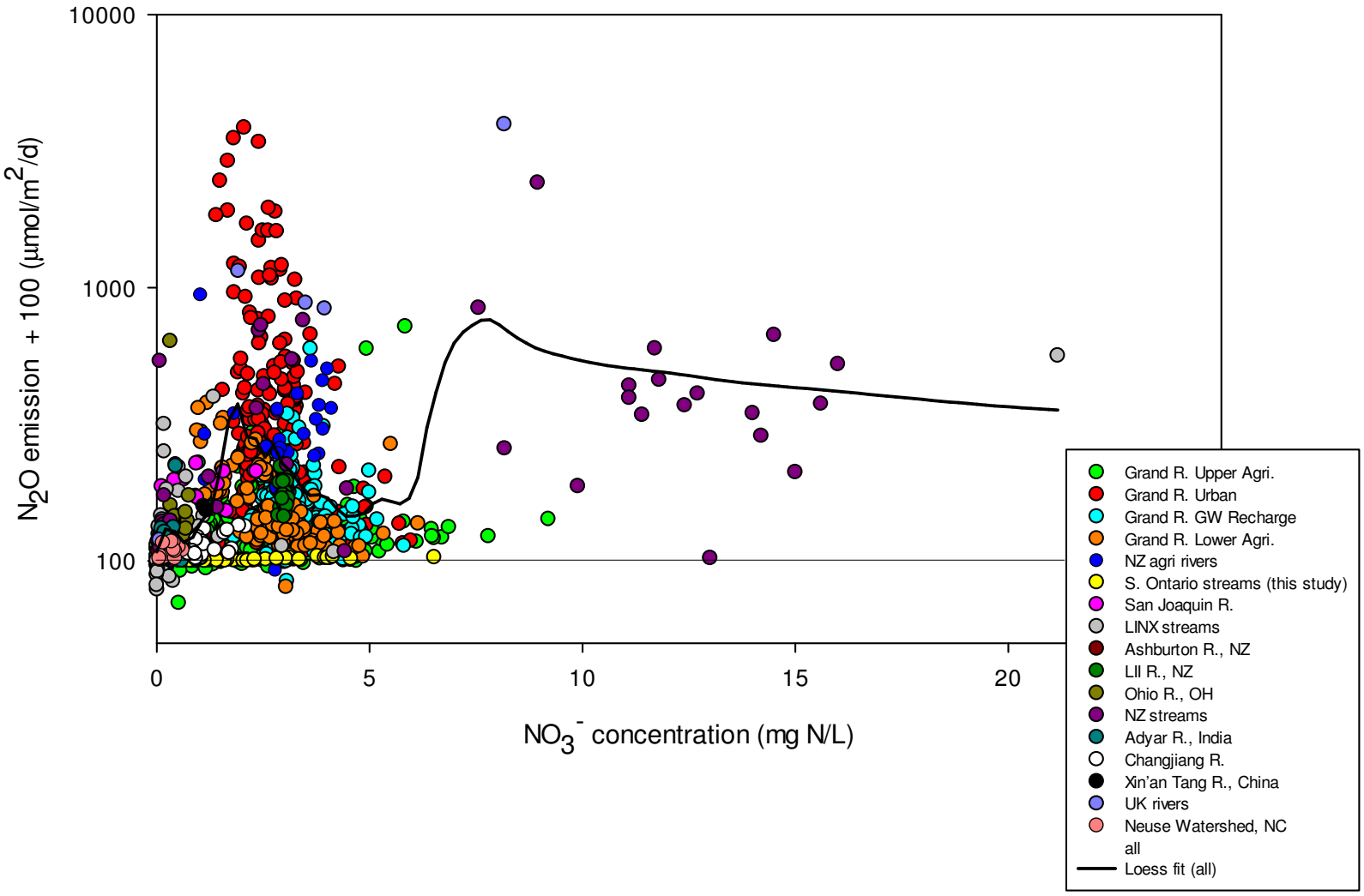
10000
1000
100
0
5
10
15
20
N_2O emission + 100 (µmol/m^2/d)
NO_3^- concentration (mg N/L)
Grand R. Upper Agri.
Grand R. Urban
Grand R. GW Recharge
Grand R. Lower Agri.
NZ agri rivers
S. Ontario streams (this study)
San Joaquin R.
LINX streams
Ashburton R., NZ
LII R., NZ
Ohio R., OH
NZ streams
Adyar R., India
Changjiang R.
Xin'an Tang R., China
UK rivers
Neuse Watershed, NC
all
Loess fit (all)

Figure 7.11: Global dataset of instantaneous NO_3^- concentrations and annual average N_2O emissions in streams and rivers, organized by site. Data are from the Grand River (Chapter 3), southern Ontario streams and rivers (this study), New Zealand streams (Wilcock and Sorrell 2008); the San Joaquin R, California (Hinshaw and Dahlgren 2013), 72 American streams from the LINXII experiment (Beaulieu et al. 2011); the Ashburton R., NZ (Clough et al. 2011); the LII R., NZ (Clough et al. 2007); the Ohio R. (Beaulieu et al. 2010); New Zealand rivers (Clough et al. 2006); the Adyar R., India (Nirmal Rajkumar et al. 2008); the Changjiang R., China (Yan et al. 2012); the Xin'an Tang R., China (Xia et al. 2013), UK rivers (Garcia-Ruiz et al. 1999) and the Neuse R. watershed (Stow et al. 2005). The thick black line represents the loess (locally weighted scatterplot smoothing) line of best fit for all data. The horizontal line represents zero N_2O emissions.

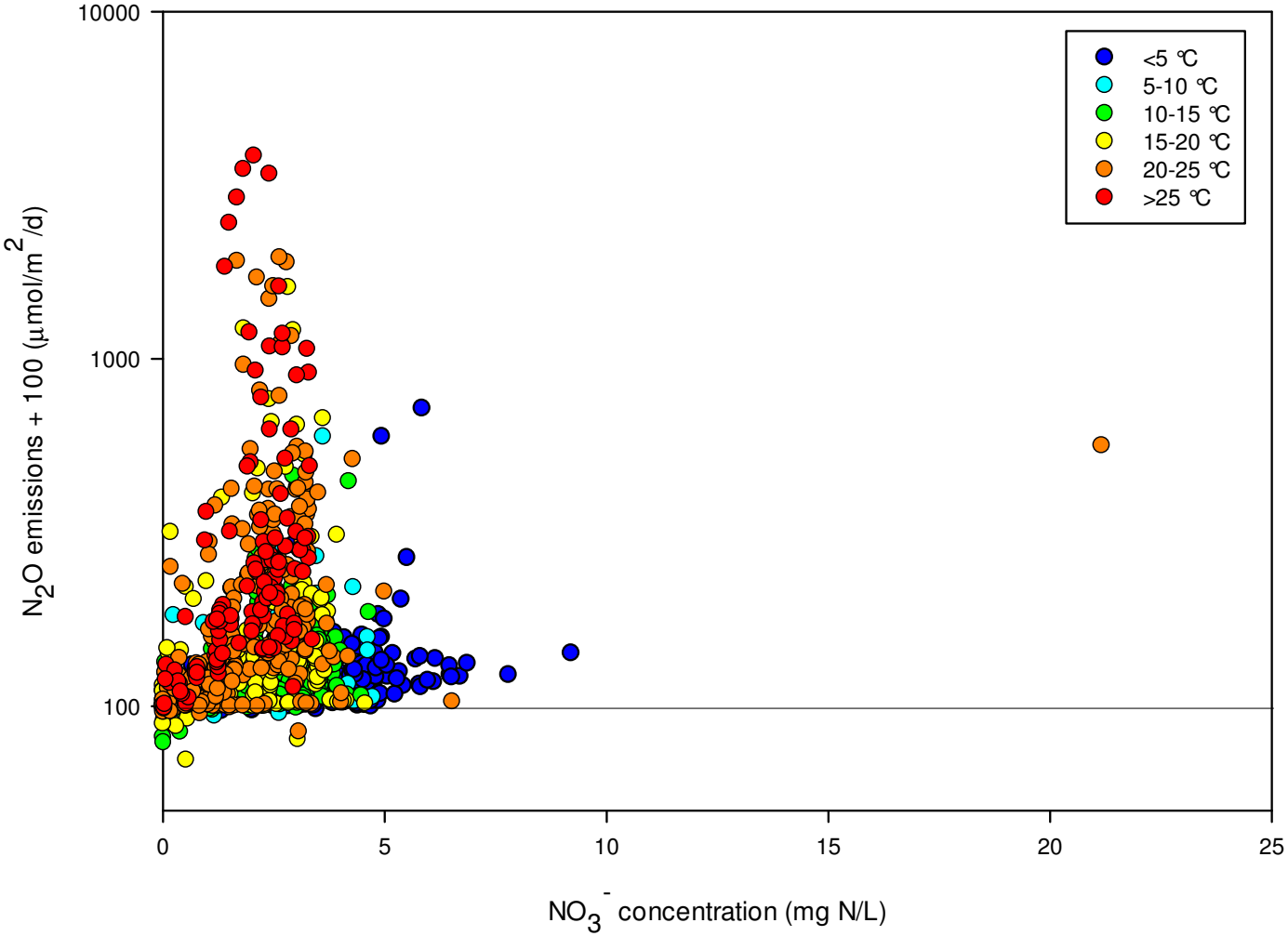
10000
1000
100
0
5
10
15
20
25
N_2O emissions + 100 (µmol/m^2/d)
NO_3^- concentration (mg N/L)
<5 ℃
5-10 ℃
10-15 ℃
15-20 ℃
20-25 ℃
>25 ℃

Figure 7.12: Global dataset of instantaneous NO_3^- concentrations and annual average N_2O emissions in streams and rivers, organized by water temperature. Data are from the Grand River (Chapter 3), southern Ontario streams and rivers (this study), the Neuse River watershed, North Carolina (Stow et al. 2005); the LII agricultural river in New Zealand (Clough et al. 2007); 72 pristine, agricultural and urban streams from the United States (Beaulieu et al. 2011) and the Xin'an River in China (Xia et al. 2013). Studies with no water temperature data reported were omitted. The horizontal line represents zero N_2O emissions.

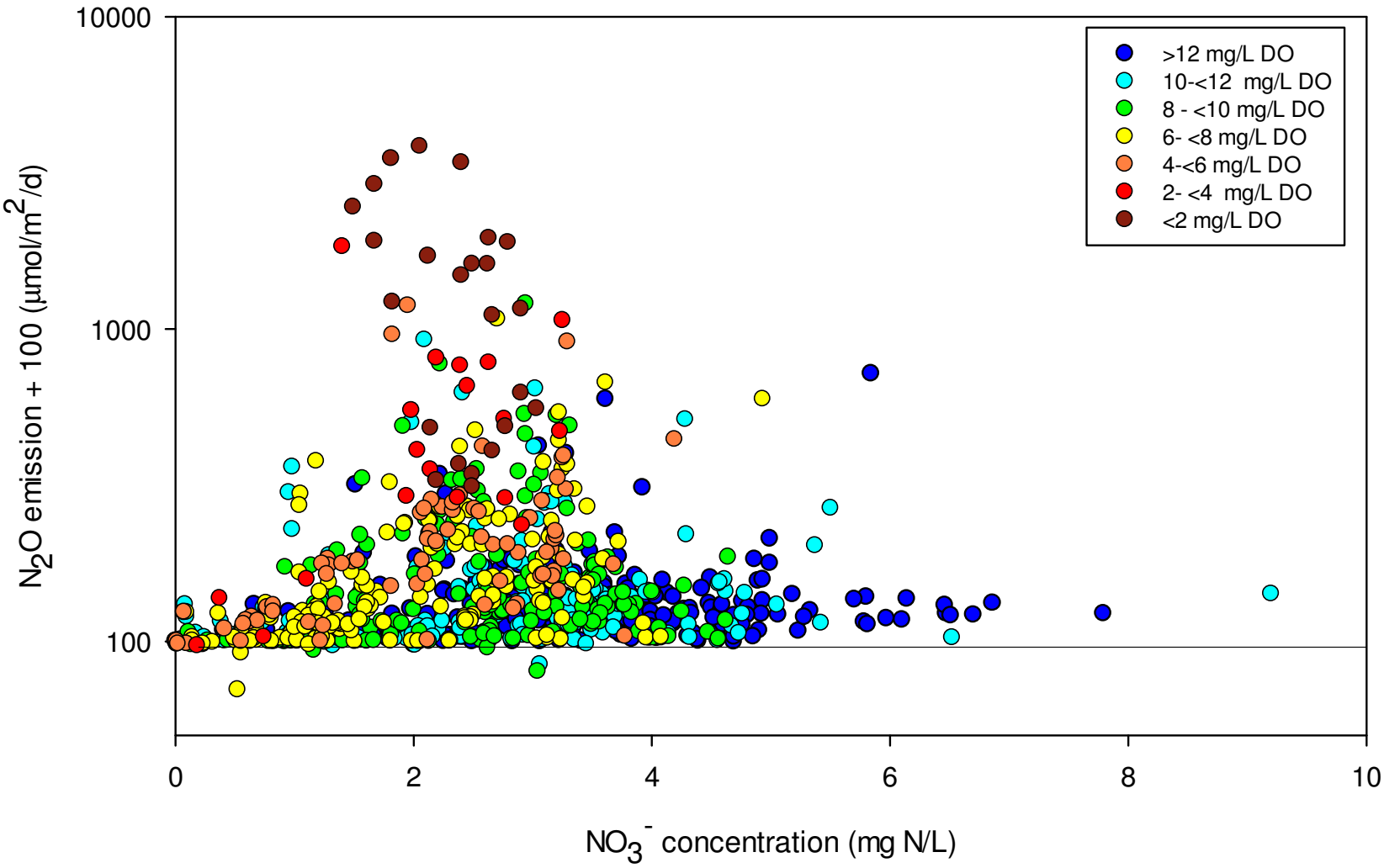
10000
1000
100
0
2
4
6
8
10
N_2O emission + 100 (µmol/m^2/d)
NO_3^- concentration (mg N/L)
>12 mg/L DO
10-<12 mg/L DO
8 - <10 mg/L DO
6- <8 mg/L DO
4-<6 mg/L DO
2- <4 mg/L DO
<2 mg/L DO

Figure 7.13: Global dataset of instantaneous NO_3^- concentrations and annual average N_2O emissions in streams and rivers, organized by DO concentration. Data are from the Grand River (Chapter 3), southern Ontario streams and rivers (this study), (Stow et al. 2005, Xia et al. 2013). Studies with no DO data reported were omitted. The horizontal line represents zero N_2O emissions.

.

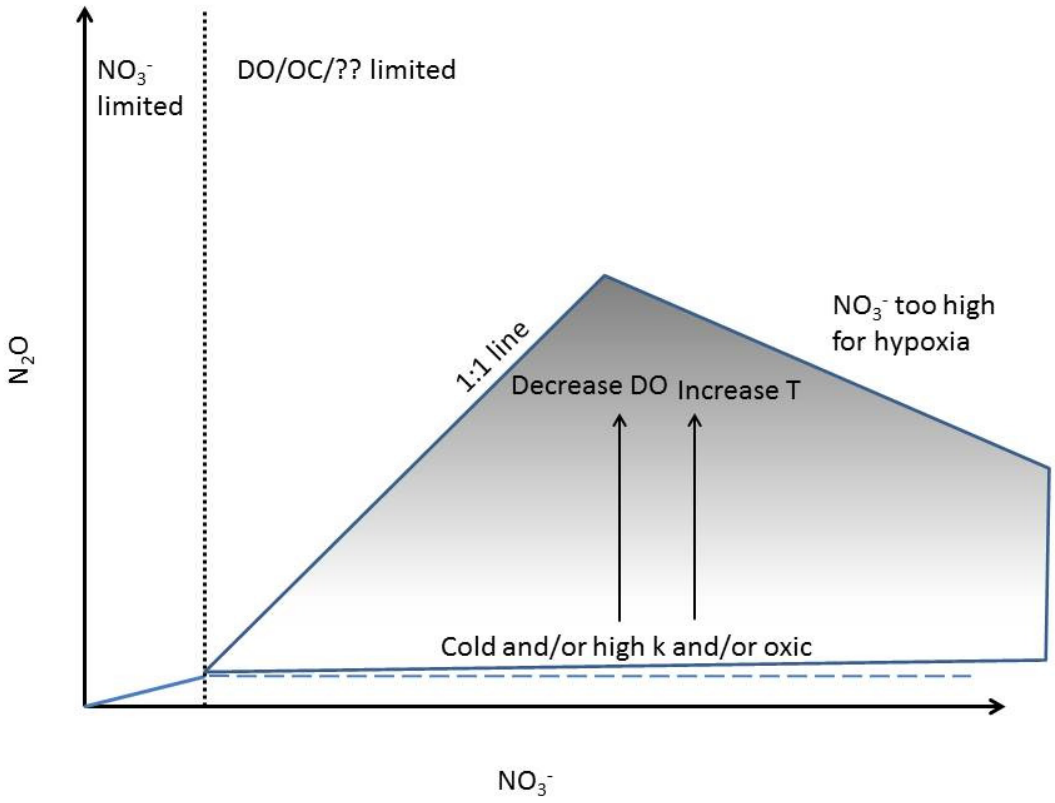

Figure 7.14: Alternative conceptual diagram of the Probability Triangle, where the range of N_2O emissions decreases above moderate NO_3^- concentrations, on the assumption that hypoxia will result in low NO_3^- due to rapid denitrification (e.g. (Harrison et al. 2005)). More research is needed in high-NO_3^- streams and rivers to see if this model best fits available data.

Chapter 8: Conclusions and Recommendations

8.1 Major Findings of this Research

The overall goal of this research was to increase understanding of N cycling in rivers, particularly controls on production and emission of the greenhouse gas N_2O. Six research chapters identify and address specific unknowns in the N cycle. They are described below with the most important results of each chapter.

The objective of Chapter 2 was to determine if diel N and DO cycles were coupled in the Grand River watershed, and, if so, how this changes by site, trophic status and season. Previous work had shown that DO has a diel cycle throughout the Grand River in spring and summer due to diel changes in photosynthesis and respiration rates by macrophytes and epilithion (Jamieson 2010). In other rivers, N_2O concentration had been shown to peak in daytime in low-N streams (Laursen and Seitzinger 2004) and peak at night in hypereutrophic systems with night-time hypoxia (Harrison et al. 2005) but it was unclear if and to what extent N_2O and DO cycles are coupled in the Grand River. Diel cycles of both N_2O and DO existed at all sites and sampling times (May, June, July, September). In low-nutrient sites with modest diel DO cycles on the Eramosa and Speed Rivers, N_2O peaked during daytime when DO was high. At all other sites, N_2O peaked at nighttime when DO was low. Diel N_2O concentration range was highest in summer and lower in spring and fall. The diel range in N_2O concentration was strongly negatively correlated with night-time minimum DO concentrations ($r^2 = 0.97$) and, contrary to IPCC N_2O estimates, did not correlate well with NO_3^-. Diel N_2O ranges were highest downstream of large wastewater treatment plants (WWTPs).

The relationship between NO_3^-, DO and N_2O is further examined in Chapter 3. The objective of this chapter was to quantify N_2O emissions from the entire length of the Grand River over two years, with good spatial and temporal coverage, and then to compare instantaneous and annual N_2O emission rates to NO_3^- and DO concentrations. Annual emissions were lower than or similar to emissions estimated with IPCC equations, but changed dramatically between years while IPCC estimates did not. Instantaneous emissions were significantly correlated to DO ($r^2 = 0.21$), not NO_3^- ($r^2 = 0.07$). Previous studies focused on picking an appropriate EF_5 value to linearly relate NO_3^- and N_2O emissions (Beaulieu et al. 2010, Beaulieu et al. 2011). However, this study is the first to show that the linear paradigm itself is not supported by field measurements.

N_2O emissions from rivers, as calculated by the IPCC, include N_2O produced by the microbial processing of inorganic N (NO_3^-, NH_4^+) from agricultural runoff and from human sewage effluent. The IPCC also tallies direct N_2O and CH_4 emissions from WWTPs. However, it was unknown if N_2O and CH_4 were dissolved in effluent upon its release to rivers and how significant this potential greenhouse gas source was. Two recent studies report stable isotopic ratios of N_2O and CH_4 in WWTPs (Townsend-Small et al. 2011, Toyoda et al. 2011), but do not compare these values to in-river values. The objectives of Chapter 4 were to quantify N_2O and CH_4 dissolved in effluent from three WWTP in the Grand River watershed, and to determine if $\delta^{15}N$-N_2O, $\delta^{18}O$-N_2O and $\delta^{13}C$-CH_4 values were distinct from upstream river sources and could be used as isotopic tracers of effluent. Three WWTPs with distinct processing methods were examined: a non-nitrifying plant releasing DIN as NH_4^+; a partially-nitrifying plant releasing a mix of NH_4^+ and NO_3^-; and a fully nitrifying plant releasing almost entirely NO_3^-. N_2O and CH_4 were supersaturated in all effluent at all times over the 24-hour cycle, in both summer and winter. CH_4 emissions from effluent (0.3 to 0.9 g CH_4/capita/yr) were much lower than direct CH_4 emissions from WWTPs (39 g CH_4/capita/yr) (Czepiel et al. 1993). However, N_2O emissions from effluent (1.1 to 2.0 g N_2O/capita/yr) were on the low end of emissions from WWTPs (0.1 to 1583) (Table 4.1). This suggests that the current IPCC estimate for N_2O emissions from wastewater (0.2 Tg N/yr) (IPCC 2007) would increase if N_2O dissolved in effluent were taken into account. However, this is a small portion of total anthropogenic N_2O emission (6.7 Tg N/yr) (IPCC 2007). Stable isotopic ratios of N_2O and CH_4 were distinct from river sources, suggesting they may be used as effluent tracers until they are degassed.

Stable isotopic ratios of N_2O can not only trace effluent in the Grand River, but potentially can trace N_2O production and consumption processes in the Grand River (Thuss 2008). In order to understand N_2O production pathways, isotopic fractionations ($\varepsilon^{15}N$ and $\varepsilon^{18}O$) for N_2O production by denitrification must be known. However, $\varepsilon^{15}N$ and $\varepsilon^{18}O$ values have been measured in pure culture experiments (Toyoda et al. 2005) and in soil incubations (Mariotti et al. 1982, Snider et al. 2009, Snider et al. 2013) but not in river sediment incubations. The objective of Chapter 5 was to measure $\varepsilon^{15}N$ and $\varepsilon^{18}O$ of N_2O produced by denitrification in river sediment at two sites in the Grand River (above and below the urban area) in spring, summer and fall. A second objective is to measure the fraction of O in N_2O that came from water, instead of NO_3^-. $\varepsilon^{15}N$ values ranged from -27.1‰ to -12.4‰, similar to the literature range of -39‰ to -10‰ (Snider et al. 2009). Net $\varepsilon^{18}O$ values (not

including O exchange with H_2O) ranged from 48.6‰ to 67.0‰, higher than values from soil incubations (Snider et al. 2009). The fraction O exchange ranged from 60% to 83%, similar to previous soil incubations (65% to 91%) (Snider et al. 2009). Surprisingly, $\varepsilon^{15}N$ and net $\varepsilon^{18}O$ were strongly negatively correlated with net N_2O production rate. This relationship is explained by N_2O reduction by N_2O reductase (Nos), which imparts a positive $\varepsilon^{15}N$ and $\varepsilon^{18}O$ on the remaining N_2O. Nos activity is suppressed in the high- NO_3^- incubations relative to the low-NO_3^- incubations either because (a) high NO_3^- or NO_2^- inhibits Nos (though NO_3^- is very high in both incubation types), and/or (b) the lag time in Nos activity is related to NO_3^- concentration, and is higher in the high-NO_3^- incubations. The latter has not been documented in the literature. Quantifying isotopic fractionations yields information on the N_2O:(N_2O+N_2) ratio while avoiding the difficulty of measuring N_2 directly.

N_2O production rates can also be used to estimate denitrification rates, if an appropriate N_2O:(N_2O+N_2) ratio can be determined. The objective of Chapter 6 was to create an annual NO_3^- isotope mass balance of the Grand River and estimate the relative importance of in-river denitrification as a NO_3^- removal mechanism. NO_3^- mass in the river, as well as inputs and outputs, were tallied and N_2O was used as a denitrification rate proxy. Watershed NO_3^- inputs and the portion of the watershed's annual NO_3^- load removed by the river were also estimated. Denitrification rates in the Grand River were almost always lower than NO_3^- inputs, resulting in relatively steady increases in dissolved NO_3^- mass downstream. The calculated stable isotopic ratios of incoming NO_3^- typically matched values measured in tributaries, WWTP effluent and groundwater. NO_3^- lost from the river (not accounted for by denitrification) typically fell in stable isotopic range for denitrification and biotic assimilation. On the watershed scale, denitrification in the Grand River accounts only for 5% to 19% of total annual watershed NO_3^- loading. 69% to 82% of watershed NO_3^- loading is lost or stored on the landscape and never enters the Grand River while 13% of total watershed NO_3^- loading is exported to Lake Erie annually.

While the previous chapters provide insight into N_2O dynamics in the Grand River, it is unclear how N_2O emissions are related to NO_3^-, DO and temperature in other streams and rivers, particularly where hypoxia does not occur. The first objective of Chapter 7 was to examine these relationships in 24 streams and rivers in southern Ontario which do no experience hypoxia, and determine if N_2O:NO_3^- relationships exist, as observed in other oxic systems (Baulch et al. 2011). The second objective was to use all available literature N_2O, DO, temperature and NO_3^- data from rivers and

streams and develop a conceptual model showing possible N_2O emission rates with NO_3^- concentration. N_2O emissions and NO_3^- concentration in southern Ontario streams had a weak, nonparametric relationship ($r^2 = 0.27$) using the regression tree method (Venkiteswaran et al. in submission). The global dataset was used to create the Probability Triangle concept, which posits that N_2O emissions should linearly increase with NO_3^- concentration at low NO_3^- concentration. When NO_3^- is too high to limit N_2O production, possible N_2O emission rates increase with NO_3^- concentration, creating a triangle. The top of the triangle coincides with high-temperature, low-DO conditions where N_2O is likely high due to both high denitrification rate and high N_2O:(N_2O+N_2) ratio. Annual and instantaneous global data fit in Probability Triangle, but there is very little data from high-NO_3^- systems that have high N_2O emissions. This may be because such systems have not been studied, or because most high-NO_3^- systems are probably oxic (decreasing denitrification rates) and thus are unlikely to have high N_2O emissions. It is therefore possible that N_2O emission variability decreases above a certain NO_3^- concentration; further study of high-NO_3^- streams and rivers is needed.

8.2 Recommendations for Further Research

The data in this thesis highlight questions to be addressed in future research. In Chapters 2 and 3, it is posited that N_2O fluxes are high in low-oxygen conditions because the sediment anoxic zone increases, which increases habitat of facultative denitrifiers and reduces the travel time for NO_3^- diffusion from the water column to the anoxic zone (Figure 8.1). When the sediment oxic boundary moves upward, NO_3^- can be present from previous nitrification. However, this conceptual model has not been tested *in situ* in rivers. Testing this model would require measuring DO and NO_3^- microprofiles *in situ*, using microelectrode sensors. This can be expensive and labour-intensive but could yield valuable insights into diel cycling in natural systems. Currently, there are no published studies examining NO_3^- microprofiles in river sediment, although NO_2^- has been observed accumulating at the sediment oxic boundary in a river in Japan (Nakamura et al. 2004).

Another possible approach is to conduct N and DO sediment microprofiles in the laboratory. Only two previous studies exist, and provide some insight: in one, sediment cores from an agricultural creek were incubated in light and dark conditions (Laursen and Carlton 1999). DO and NO_3^- microprofiles were determined with microelectrodes. DO concentrations were higher at the sediment surface under light conditions. However, DO penetration depth ranged from 2 to 4 mm and did not

always change between light and dark conditions (Laursen and Carlton 1999). NO_3^- concentration peaked at around 2 mm depth due to sediment nitrification, and NO_3^- peaks were higher in lighted conditions. There was no indication of a shift in denitrification habitat between light and dark incubations. Stream water NO_3^- concentrations were not reported but NO_3^- concentrations in the cores peaked at around 0.04 mg N/L (Laursen and Carlton 1999). A similar study used sediment from an estuary with a water column NO_3^- concentration of < 0.007 mg N/L (Porubsky et al. 2008). ^{15}N-labelled NO_3^- was added, allowing measurement of NO_3^- assimilation and dissimilation rates. Combined rates of denitrification and dissimilatory nitrate reduction to ammonium were ~6 times higher in dark incubations than light incubations but the sediment profiles showing the location of different N cycling processes were not shown (Porubsky et al. 2008).

These studies provide insight into N cycling in sediments but probably do not represent Grand River diel cycling because (a) water column DO and therefore sediment DO penetration depth depend on community respiration, which in the Grand River, is largely influenced by macrophytes and biofilm (Chen 2013), while sediment studies only consider benthic processes, and (b) ambient NO_3^- concentrations in the Grand River are higher than in those studies by at least an order of magnitude. Therefore, future work should test the conceptual model presented here to explain diel changes in N_2O production and denitrification rate by performing similar laboratory experiments in higher-NO_3^- systems, if field studies are impractical. Hypoxia (and high-oxygen conditions) may have to be artificially induced in laboratory studies if sediments are too high in oxygen because sediment respiration rates are lower than community respiration rates (including respiration by submerged macrophytes and water column algae).

In Chapter 4, WWTP effluent N_2O and CH_4 concentrations and stable isotopic ratios were quantified. N_2O emissions from the three WWTPs in the Grand River watershed were modest (range: 1.1 to 2.0 g N_2O/capita/y), but similar to direct N_2O emissions from WWTPs (0.1 to 1580 g N_2O/capita/y). Only one other study has estimated N_2O emissions from effluent (0.2 g N_2O/capita/year, (Toyoda et al. 2011)); more research is needed to determine how representative these values are. This will help determine if IPCC estimates of N_2O emissions from WWTPs (currently 0.2 Tg N/yr, (IPCC 2007)) need to be updated. Similarly, there are very few published stable isotopic ratios of N_2O and CH_4 in effluent (Townsend-Small et al. 2011, Toyoda et al. 2011) but the reported range is very large, especially for N_2O. More data from a variety of WWTP types

(i.e. primary through tertiary treatment; non-nitrifying, nitrifying and denitrifying capabilities) is needed to understand if stable isotopic ratios of N_2O and CH_4 are predictable by WWTP type, and if they are always different than upstream sources and can be used as tracers.

Chapter 5 showed that N_2O isotopic ratios are highly dependent on net N_2O production rate in laboratory incubations. Two conceptual models were proposed, both of which suggest that N_2O reduction is responsible for the relationship. The stable isotopic effect of N_2O reductase itself has been measured in laboratory experiments, as summarized by Snider et al. (2009). However, the stable isotopic effect of the other enzymes used in denitrification has not been measured. Quantifying $\varepsilon^{15}N$ and $\varepsilon^{18}O$ for each enzyme (nitrate reductase, nitrite reductase, nitric oxide reductase) could help our understanding of N_2O isotope dynamics and indicate which, if any, reaction is limiting, as the isotopic fractionation of the limiting step is likely to influence the net fractionation observed for NO_3^- reduction to N_2. Additionally, it is unclear why N_2O reductase (Nos) activity changes between incubations. Further research is needed to determine if Nos is inhibited by high NO_3^- or high NO_2^- in these incubations and/or if the N_2O reductase lag time is related to NO_3^- concentration. NO_3^- inhibition seems unlikely to influence only high-NO_3^- incubations, as the lower NO_3^- additions were still very high (775 mg N/L). NO_2^- limitation is much more plausible and NO_2^- should be quantified in future incubations of this type. Future incubations could also measure N_2O and/or Nos activity throughout incubations to quantify lag time and use a long runtime (> 5 hours), as shifts in Nos activity were not captured in this experiment. This could provide valuable insight into how N_2O pulses occur at the onset of anoxia (Codispoti 2010).

Chapter 6 provides some insight into NO_3^- sources and sinks on a watershed scale. Much has been published on various N cycling processes in watersheds but there is very little published work on watershed-scale budgets. This is probably because of the difficulty of estimating N sources and process rates on a watershed scale. In Canada and other developed countries, NH_4^+ and NO_3^- export from WWTPs is typically easy to quantify using WWTP reports. However, N loading from agriculture is spatially heterogeneous (depending on crop type, fertilizer application and soil properties) and temporally heterogeneous (depending in rain events, crop rotation, season, etc.). The IPCC provides equations to estimate the amount of agricultural N loading (see Chapter 6). However, there is very little data to support these values. Three studies report lower N loading values than IPCC estimates from a variety of agricultural environments (Brown et al. 2001, Delgado et al. 2010,

Silgram et al. 2001). Additionally, denitrification rates in soil and in streams and rivers are extremely variable spatially and temporally, which has greatly hindered global denitrification estimates (Davidson and Seitzinger 2006). Watershed-scale mechanistic N models such as RiverStrahler (Billen and Garnier 1997) or SWAT (Krysanova et al. 1998) may provide insight into N cycling, but care must be taken to calibrate the models with real data and to acknowledge that mechanistic models can match real data with incorrect inputs (Oreskes et al. 1994). To fully understand the role of rivers and streams in denitrifying N inputs from catchments, more measurements of in-river denitrification rates and watershed-scale N transport are needed.

Chapter 6 also indicates than several other N cycling processes in rivers require further research. Denitrification rates in rivers are very difficult to quantify (Seitzinger et al. 2006); this study takes a novel approach by using N_2O emissions as a proxy for denitrification rate. N_2O appears to be produced almost entirely from denitrification in the Grand River (Thuss 2008). However, it is likely that the $N_2O:(N_2O+N_2)$ ratio produced is highly variable with temperature and concentration of DO, NO_2^- and NO_3^-, as has been shown in other river systems (Silvennoinen et al. 2008, Silvennoinen et al. 2008). Silvennoinen et al. (2008a, 2008b) report a $N_2O:(N_2O+N_2)$ range of 0.001 to 0.038 for boreal river sediments. Ratios decreased with increased temperature and DO concentration. This could indicate that denitrification rates were overestimated in winter in this study and were overestimated during hypoxia events. Further research is needed to fully understand controls on the $N_2O:(N_2O+N_2)$ ratio in denitrification. Lastly, N assimilation was not measured in this study but it may be a significant portion of the river's N budget. ^{15}N labeling experiments on estuary sediments indicated that 83% to 150% of NO_3^- loss was due to N assimilation (Porubsky et al. 2008). NH_4^+ and NO_3^- uptake rates were measured in 11 American streams in the LINX experiment, and were always an order of magnitude higher than nitrification rates (denitrification was not measured) (Webster et al. 2003). The NO_3^- uptake rate was ~10 times greater than denitrification rates in a forested stream in Tennessee at ambient NO_3^- concentration (not stated) (Mulholland et al. 2004). N assimilation rates are a large part of the N cycle in streams and rivers; more measurements are needed in the Grand River and in other rivers worldwide. More research is also needed into understanding why N uptake and removal rates appear to be much higher in small streams than in large rivers. This could be because smaller streams have higher N reaction rates due to more benthic area, as postulated for watersheds in the Gulf of Mexico (Alexander et al. 2000).

Chapter 7 examined nonparametric relationships between N_2O emission, temperature and concentration of DO and NO_3^- in 24 streams and rivers in Southern Ontario, as well as the global published dataset. Highest NO_3^- concentrations occurred in streams with the lowest proportion of wetlands in their watershed, and highest N_2O emissions occurred when percentage agricultural land was highest. The opposite trend – positive relationships between NO_3^- export and percentage wetland in the catchment was reported in non-agricultural boreal forest streams, perhaps because wetlands, not agriculture, are the primary source of NO_3^- in these systems (Sarkkola et al. 2012). No studies have reported trends in NO_3^- or N_2O and agricultural land use. However, a negative relationship between dissolved organic matter concentration and percentage agriculture in watersheds in Europe has been shown (Mattsson et al. 2008). Further research is needed to determine if land use is a useful predictor of stream NO_3^- and/or N_2O concentration. This observation should be refined to include only land upstream of the study sites (instead of land-use from the whole river catchment). If a strong relationship exists between land use and NO_3^- or N_2O, estimates of N leaching and/or N_2O emission from agricultural streams and rivers can be improved.

Chapter 7 also highlighted the paucity of N_2O emission and NO_3^- concentration data from rivers and streams worldwide. Of the 1450 data points used in the study, 1133 were collected by this study in Southern Ontario. Few studies reporting NO_3^- and N_2O emissions also reported temperature or DO concentration, which are useful in predicting N_2O emissions (Chapter 3). In addition, most research has focused on relatively low-NO_3^- systems (< 4 mg N/L). The paucity of N_2O emission data from streams with higher NO_3^- (> 4 mg/L) makes it difficult to interpret the data in terms of the conceptual model Presented in this chapter. It is possible that N_2O emission variability decreases at high NO_3^-, where oxic conditions persist. Alternatively, it is also possible that high-NO_3^- systems with sufficient hypoxia to produce high N_2O may exist but have not been studied. Further research should focus on high NO_3^- systems, as well as on low-DO systems, where N_2O can be high but the controls on N_2O are still not fully understood.

8.3 Recommendations for River Management

River managers (e.g. conservation authorities, water authorities, government environmental ministries) typically focus on geochemical parameters relating to ecosystem health and drinking water regulations, such as pH, conductivity, temperature, biological oxygen demand, DO, NO_3^- and NH_4^+. They also typically sample occasionally (e.g. the Ontario Provincial Water Quality Monitoring

Network, 10 samples/yr). The link between agricultural land use and NO_3^- loading and export for rivers is known (Hong et al. 2013, Tesoriero et al. 2013) but site-specific variation is high (Davidson and Seitzinger 2006). In the heavily agricultural Grand River watershed, annual watershed N loads from WWTP effluent (1.5 Tg N/year) are much smaller than N loads from agriculture (41.2 Tg N/year) (Chapter 6). This suggests that upgrading WWTPs to reduce N in effluent is less useful than reducing N loading from agriculture. Several beneficial management practices (BMPs) have been suggested to reduce agricultural N loading (e.g. conservation tillage, proper N fertilizer application rates and timing, and erosion control (Lemke et al. 2011)). However, it is still unclear if BMPs consistently reduce nutrients to the landscape, and on what timescale (Lemke et al. 2011). BMP implementation requires will and funding from farmers, politicians and other stakeholders. Because highest NO_3^- concentrations occur in watersheds with lowest percentage wetland (Chapter 7), focus on wetland creation and restoration may reduce river NO_3^- concentrations. This may reduce NO_3^- toxicity in aquatic ecosystems, help achieve drinking water quality targets, and reduce export of NO_3^- to N-limited systems such as marine coasts. However, managing the river for NO_3^- may not be useful for reducing eutrophication in non-N limited systems. Management for phosphorus could help reduce eutrophication; further research is needed to address major sources of labile P to the watershed.

Chapter 6 also shows that the Grand River receives only 17% to 32% of total annual N loading from the watershed (agricultural, sewage and septic beds). The remaining 68% to 83% of watershed NO_3^- is lost before entering the river, presumably in smaller streams, groundwater, wetlands, riparian zones, etc. or stored in soil or groundwater. Of the NO_3^- entering the Grand River, 26% to 59% is lost via denitrification, assimilation or storage. Because the river denitrifies a small portion of total watershed NO_3^- loading (0.5% to 19%), NO_3^- management should focus on the watershed scale. Watershed managers can likely increase NO_3^- removal by investing in riparian zone restoration and wetland protection and creation. Removing large amounts of NO_3^- before water enters the main branch of the river also helps reduce river eutrophication. Additionally, areas that remove NO_3^- by assimilation and denitrification, such as constructed wetlands, also remove P by assimilation and sedimentation (Mietto and Borin 2013), which is more useful than NO_3^- removal in P-limited ecosystems. N assimilation is a temporary N sink (i.e. some or all N will later be released during N mineralization); organic and mineralized N can also be flushed downstream when vegetation senesces in autumn. This essentially exports N pollution rather than removing it. In contrast, denitrification and anammox produce non-biologically reactive N (N_2) and should be encouraged. This requires hypoxia

or anoxia, either in microsites in otherwise oxic environments, or in larger environments, such as anoxic sediments. While anoxic sediments may promote denitrification and anammox, anoxic water columns are harmful to aerobic life forms (benthic invertebrates, fish, etc.) and should be prevented. This can be achieved by promoting decreases in water velocity to increase sedimentation of fine material (e.g. wetlands, river pools) and by removing nutrients on the landscape, so river ecosystems are nutrient-limited and community respiration in the water column is low. The relationship between N_2O:(N_2O+N_2) ratios and oxygen level is not clear, but full anoxia and low NO_3^- should promote low N_2O production as N_2O reduction occurs when DO is very low and NO_3^- and NO_2^- are low (Firestone et al. 1980).

8.4 Recommendations for Greenhouse Gas Inventories

The most dramatic finding of this thesis is the poor to non-existent relationship between N_2O and NO_3^- on the instantaneous and annual scale, contrary to the IPCC estimates of N_2O emissions from rivers. Accurate greenhouse gas (GHG) inventories are necessary for (a) a complete understanding of GHG budgets, (b) practical and realistic mitigation strategies, and (c) any future GHG cap-and-trade, credits or taxation system on the local, regional, national or international scale. Based on the regression tree analysis performed in Chapter 7 and in the Grand River (Venkiteswaran et al., in submission), the following decision scheme is recommended for greenhouse gas inventories including emissions from rivers and streams:

(1) Identify and quantify hypoxia in rivers and streams, as these conditions produce very high N_2O emissions relative to their area (Chapter 3). A method for anoxia quantification has not been published for rivers, but one has been published for lakes (Nurnberg 1995) and could be adapted. The anoxic factor is quantified as:

$$AF = (duration\ of\ anoxia\ \times anoxic\ sediment\ area)/A_O \qquad \text{Equation 8.1}$$

where AF is the anoxia factor in days per year, and A_O is the total lake (or river) surface area (Nurnberg 1995). Hypoxia and anoxia in river water columns appears to be relatively rare and related to releases of WWTP effluent or high-DOC water from forest flooding (Kerr et al. 2013). However, very little data exists on river surface sediment anoxia and the condition may be more widespread than currently understood. Good collection of DO data is the first step to quantifying N_2O emissions from rivers.

(2) Devise an N_2O sampling plan taking diel N_2O variability (Chapter 2) and seasonal, annual and spatial variability (Chapter 3) into account. Highest N_2O emissions from the Grand River occur during summer at night, downstream of a large WWTP where hypoxia occurs. N_2O emissions were higher in a drier, warmer year than in a cooler and wetter one. During N_2O sampling, temperature, DO, NO_3^- and NH_4^+ should also be measured so that predictive factors (if any) of N_2O emissions can be determined. Gas exchange coefficients can have a large impact on N_2O emission estimation, especially when N_2O concentrations are near saturation. Gas exchange coefficients can be estimated based on water depth and velocity (Jha et al. 2004) or modeled, e.g. with PoRGy (Venkiteswaran et al. 2007). Note that not all gas exchange measurement methods provide identical results (Beaulieu et al. 2012, Raymond and Cole 2001); this may bear further investigation on a local level. Local relationships between water depth, velocity, and/or discharge and the gas exchange coefficient can be determined. River sampling of N_2O could be combined with river monitoring programs (e.g. Ontario's Provincial Water Quality Monitoring Network), which routinely sample parameters of interest such as pH, temperature, DO, NO_3^- and NH_4^+.

(3) Determine any relationships, parametric or nonparametric, between N_2O emissions and predictive factors (DO, temperature, NO_3^-, NH_4^+). If hypoxic sites exist, splitting data into hypoxic and non-hypoxic groups may help sort them. Regression tree analysis does this automatically with any input parameter if provides the best fit. Acknowledge that any relationships found may not be stable over time due to changes in microbial community; quantity and lability of organic carbon; concentration of atrazine and other pesticides (Laursen and Carlton 1999) may change these relationships.

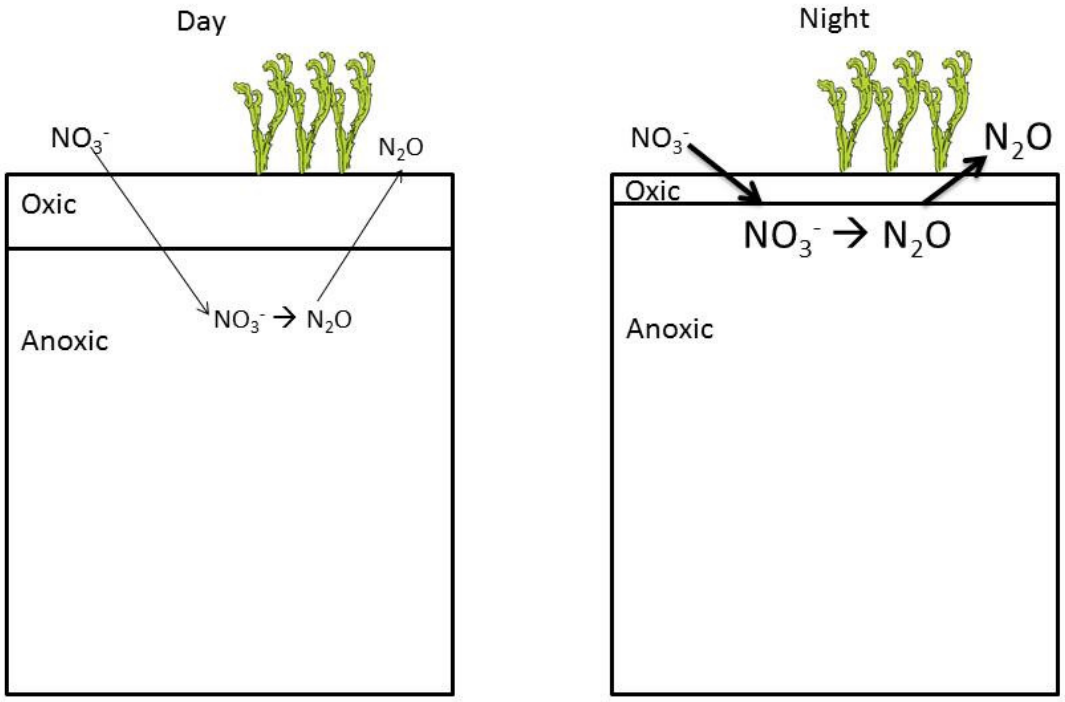

Figure 8.1: Conceptual diagram of diel changes in N_2O production in river sediment in summer. Font sizes correspond to concentrations, and arrow thicknesses correspond to rates. During the day, primary producers increase DO concentrations in the water column, resulting in a relatively deep sediment oxic layer (left panel). NO_3^- from the water column must diffuse across this layer, limiting N_2O production via denitrification. At night, DO concentration decreases, the sediment oxic layer thins, and NO_3^- diffusion into the sediment anoxic layer is rapid.

Appendix A: N_2O Isotopomers in the Grand River

A.1 Introduction

N_2O is an asymmetrical molecule (Figure A.1). The $\delta^{15}N$ ratio of the central N atom (termed the α atom) and the terminal N atom (β atom) can now be measured with good precision. The difference between the $\delta^{15}N$ values is termed "site preference" (SP):

$$\boldsymbol{SP = \delta^{15}N_{\alpha} - \delta^{15}N_{\beta}} \qquad \textbf{Equation A.0.1}$$

Previous work using pure cultures has shown that N_2O SP is very different for N_2O produced by bacterial nitrification via the hydroxylamine pathway (SP ~ 33‰) than by bacterial denitrification (SP ~ 0‰) (Sutka et al. 2006) (Table A.1). This is presumably because of the different enzymes used in the two pathways. Nitrifier denitrification (i.e. NO_2^- reduction to N_2O and N_2 by nitrifying bacteria) produces SP values like denitrification (Sutka et al. 2006). SP ratios were consistent even when $\delta^{15}N$-N_2O (bulk) and $\delta^{18}O$-N_2O values changed (e.g. when different substrates were used) (Sutka et al. 2006). Though only a few laboratories worldwide have the capability to measure N_2O SP, it has gained favour as a method of distinguishing N_2O production processes because it is supposedly independent of substrate $\delta^{15}N$ values (e.g. (Kato et al. 2013, Well et al. 2006)).

However, there are several factors that can complicate the interpretation of SP values. First, several processes do not fit squarely into the paradigm (Table A.1): *Nitrosomonas europaea* cultures can have SP values ~14‰ during hydroxylamine oxidation (Sutka et al. 2003). Fungal denitrifiers have SP values ~30‰, similar to ammonia oxidizers (Sutka et al. 2008), as do pure cultures of the denitrifying bacteria *Pseudomonas fluorescens* (Toyoda et al. 2005). Only one study has examined soil denitrifier communities, which yielded a range of SP values intermediate between bacterial denitrification and nitrification (Table A.1). Lastly, N_2O reduction to N_2 increases SP with an isotopic fractionation of about 5‰ to 6‰ in soil bacterial cultures (Ostrom et al. 2007). A recent review has highlighted some of these problems and recommended caution when using SP for N_2O source apportionment (Decock and Six 2013).

The purpose of this study is to determine if changes in N_2O production pathway are observable in N_2O SP values over a 24-hour cycle at Blair (Site 11) in the Grand River, and if this helps determine processes responsible for the diel cycling of N_2O seen at this site. N_2O concentration is typically very

high at Site 11 in summer at night (Chapter 2) and moderate during the day. It is possible that (a) N_2O production is dominated by denitrification pathways at all times of day and rate increases at night, or (b) some daytime N_2O is produced by nitrification (Thuss 2008).

A.2 Methods

N_2O, dissolved oxygen (DO), nitrate (NO_3^-) and ammonium (NH_4^+) were collected at Site 11 in the Grand River (see Chapter 1, Table 1.2) on July 7 and 8, 2010 using methods described in Chapter 2. Samples were collected approximately every 1.5 hours. Additionally, effluent was collected from the Kitchener Wastewater Treatment Plant (WWTP) (as described in Chapter 4) three times over the course of the sampling. All chemical analyses except N_2O SP measurements were completed as in Chapter 2 and Chapter 4 (N_2O isotope collection and measurement).

N_2O was cryogenically trapped in vials for N_2O isotope analysis. After bulk N_2O isotope analysis at the University of Waterloo, samples were shipped to the Yoshida laboratory at the Tokyo Institute of Technology, Yokohama, Japan, where they were analysed using a MAT252 isotope-ratio monitoring mass spectrometer with an on-line cryogenic N_2O concentration system and gas chromatograph. For N_2O SP analysis, an electron impact ion source was used to fragment N_2O to NO^+, containing the central (α) N of the N_2O; the $\delta^{15}N\text{-}NO^+$ ratio was then measured.

A.3 Results

DO, NO_3^-, NH_4^+ and N_2O concentration; bulk $\delta^{15}N\text{-}N_2O$, N_2O SP, and $\delta^{18}O\text{-}N_2O$ are shown in Table A1. DO and N_2O concentrations are shown in Figure A.2 and N_2O isotopic ratios and SP are shown in Figure A.3

A.4 Discussion

Surprisingly, N_2O SP values are very high with the exception of one point (range: -7.4‰ to 36.7‰). It is unlikely that all N_2O over the diel cycle at Site 11 is produced by hydroxylamine oxidation, which requires oxygen and NH_4^+. Additionally, $\delta^{15}N\text{-}N_2O$ (bulk) values are higher than expected for hydroxylamine oxidation. It is more likely that the high N_2O SP values represent N_2O reduction, which is likely high in the Grand River (see Chapter 5). Figure A3 shows $\delta^{15}N\text{-}N_2O$ (bulk) vs. N_2O SP, and shows expected areas for N_2O produced by hydroxylamine oxidation, denitrification, and N_2O reduction. Based on pure culture studies, N_2O reduction should result in an SP:$\delta^{15}N$ ratio of 1.1

and an SP:δ^{18}O-N_2O ratio of 0.45 (Ostrom et al. 2007) but data from this study do not follow these ratios (Figure A.4). This could indicated that the δ^{15}N ratio of source NO_3^- changes over the diel cycle (as observed by (Thuss 2008)) and/or that mixed microbial populations in Grand River sediment have different ε^{15}N and SP values than pure cultured bacteria. Given that multiple processes can increase N_2O SP (nitrification, fungal denitrification, some bacterial denitrification, N_2O reduction), a relatively high N_2O SP in the Grand River is not unexpected. Unfortunately, the multiple processes resulting in high SP values make source apportionment impossible in this environment.

N_2O from the Kitchener WWTP appeared in or near the expected range of isotopic ratios and SP for nitrifier-denitrification, which is consistent with findings in Chapter 4.

Table A.1: N_2O site preference (SP) values for microbial metabolic processes from the literature.

Reaction	Organism(s)	N_2O SP	Reference	Notes
Hydroxylamine Oxidation	*Methylococcus capsulatus Bath*	30.8 ± 5.9‰	(Sutka et al. 2003)	
	Nitrosomonas europaea	14.9 ± 3.7‰		
	Nitrosomonas europaea	33.5 ± 1.2‰	(Sutka et al. 2006)	
	Nitrosospira multiformis	32.5 ± 0.6‰		
	Methylosinus trichosporium	35.6 ± 1.4‰		
Archaeal NH_4^+ oxidation	Archaeal enrichment culture CN25	30.3 ±1.2‰	(Santoro et al. 2011)	
Nitrifier denitrification	*Nitrosomonas europaea*	-0.8 ± 5.8‰	(Sutka et al. 2003)	
	Nitrosospira multiformis	0.1 ± 1.7‰	(Sutka et al. 2006)	
Bacterial denitrification	*Pseudomonas fluorescens*	23.3 ±4.2‰	(Toyoda et al. 2005)	
	Paracoccus denitrificans	5.1 ± 1.8‰		
	Pseudomonas chlororaphis	–0.6 ± 1.9‰	(Sutka et al. 2006)	
	Pseudomonas aureofaciens	–0.5 ± 1.9‰		
Fungal denitrification	*Fusarium oxysporum*	37.1 ± 2.5‰	(Sutka et al. 2008)	
Fungal denitrification	*Cylindrocarpon tonkinense*	36.9 ± 2.8‰		
Community denitrification	Sand and silt loam soils	3.1‰ to 8.9‰	(Well and Flessa 2009)	N_2O reduction inhibited with C_2H_2
N_2O Reduction	*Pseudomonas stutzeri*	-5.0‰	(Ostrom et al. 2007)	
	Pseudomonas denitrificans	-6.8‰		

Table A.2: DO, NO_3^-, NH_4^+, N_2O, $\delta^{15}N$-N_2O, N_2O SP and $\delta^{18}O$-N_2O at Site 11, July 7-8, 2010.

Sample	Date and Time	DO (mg/L)	NO_3^- (mg N/L)	NH_4^+ (mg N/L)	N_2O (nmol/L)	$\delta^{15}N$-N_2O (‰)	N_2O SP (‰)	$\delta^{18}O$-N_2O (‰)
BL 20-1	07/07/2010 19:20	8.8	3.31	0.078	65			
BL 20-2	07/07/2010 21:40	5.5	3.29	0.100	130	-4.7	19.5	38.3
BL 20-3	07/07/2010 23:45	2.9	3.25	0.128	158	-6.6	21.6	38.0
BL 20-4	08/07/2010 1:50	1.9	3.02	0.193	135	-11.7	18.4	35.4
BL 20-5	08/07/2010 3:45	1.5	2.90	0.211	93	-12.8	34.7	15.5
BL 20-6	08/07/2010 5:50	1.6	2.66	0.362	58			
BL 20-7	08/07/2010 7:45	2.4	2.77	0.210	39	-7.8	21.9	41.9
BL 20-8	08/07/2010 9:45	5.5	2.98	0.088	32	-5.9	20.2	42.8
BL 20-9	08/07/2010 11:45	9.1	3.01	0.073	42	-4.6	19.4	41.4
BL 20-10	08/07/2010 13:10	10.7	3.10	0.040	34	-2.8	17.8	40.8
BL 20-11	08/07/2010 15:50	11.5	3.16	0.142	32	-3.6		36.7
BL 20-12	08/07/2010 17:45	11.5	3.10	0.132	32	-2.5	-7.4	37.9
BL 20-13	08/07/2010 19:45	8.7	3.29	0.126	31	-3.3		37.5
BL 20-14	08/07/2010 21:50	5.0	3.28	0.196	38	-3.0	20.6	38.4
BL 20-15	08/07/2010 23:45	3.0	2.76	0.233	71	-5.4	21.8	39.7
KTP 20-1	07/07/10 12:30	4.5	BD	24.48	274	-10.2	-5.9	18.5
KTP 20-2	07/07/10 12:30	1.6	BD	24.40	18	-11.5	-0.9	17.8
KTP 20-3	07/0710 12:25	4.7	BD	23.72	17	-10.4	14.6	13.8
KTP 20-3	07/0710 12:25	4.7	BD	23.72	17	-8.7	3.3	24.5

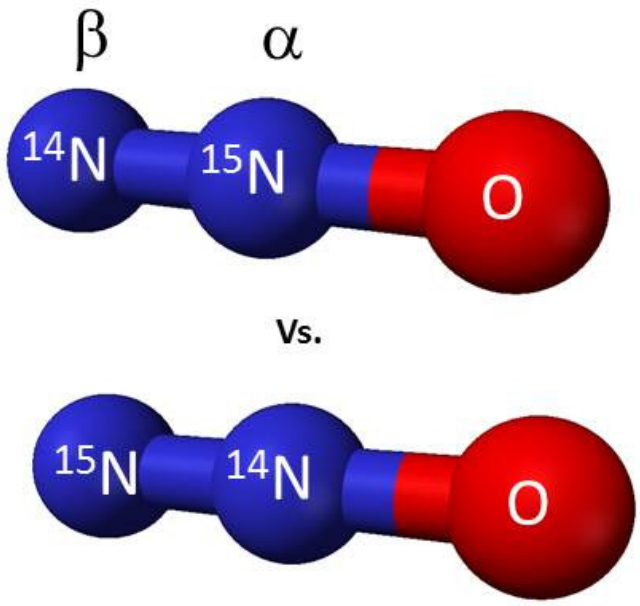

Figure A.0.1: The N_2O molecule with central (α) and terminal (β) N atoms labeled.

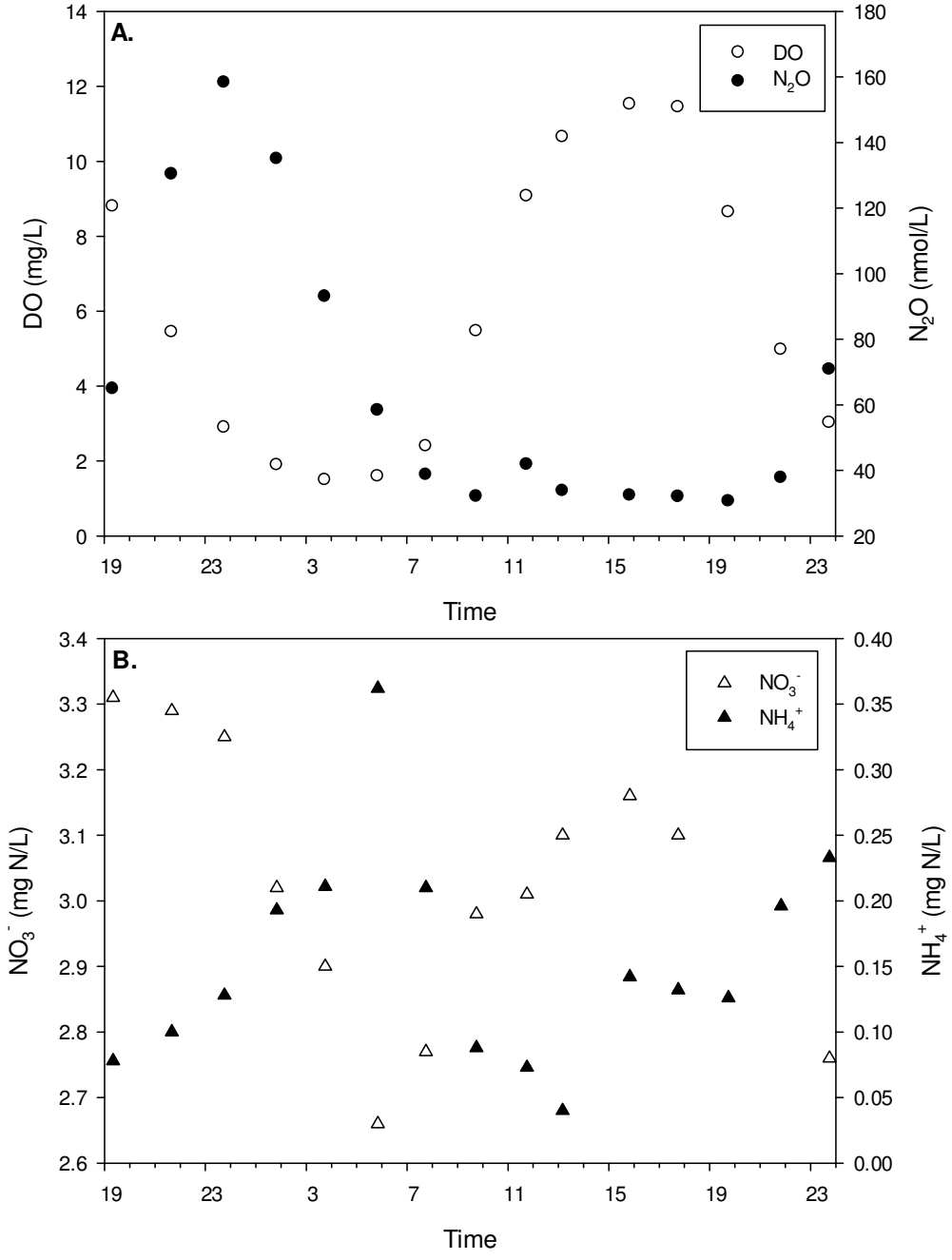

Figure A.2: DO and N_2O concentrations at Site 11 (Panel A) and NO_3^- and NH_4^+ (Panel B) over the diel sampling event.

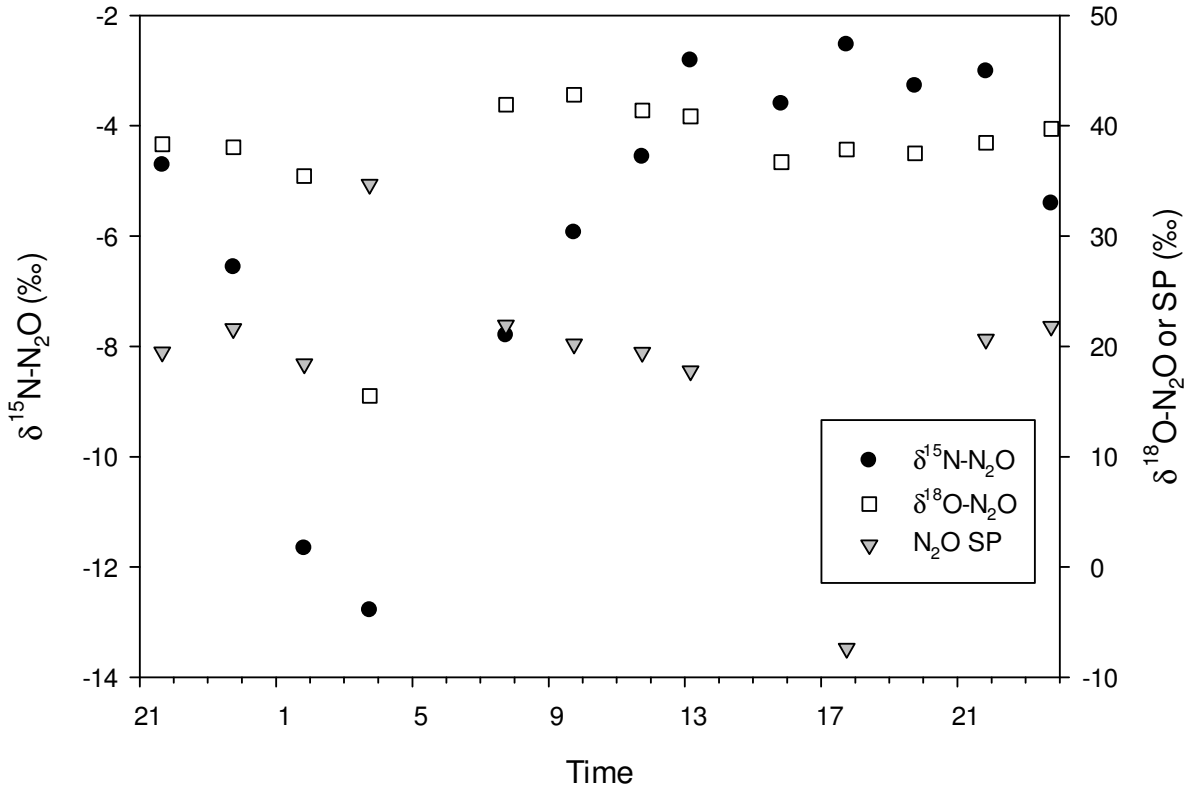

Figure A.3: $\delta^{15}N\text{-}N_2O$, N_2O SP and $\delta^{18}O\text{-}N_2O$ at Site 11 over the diel sampling event.

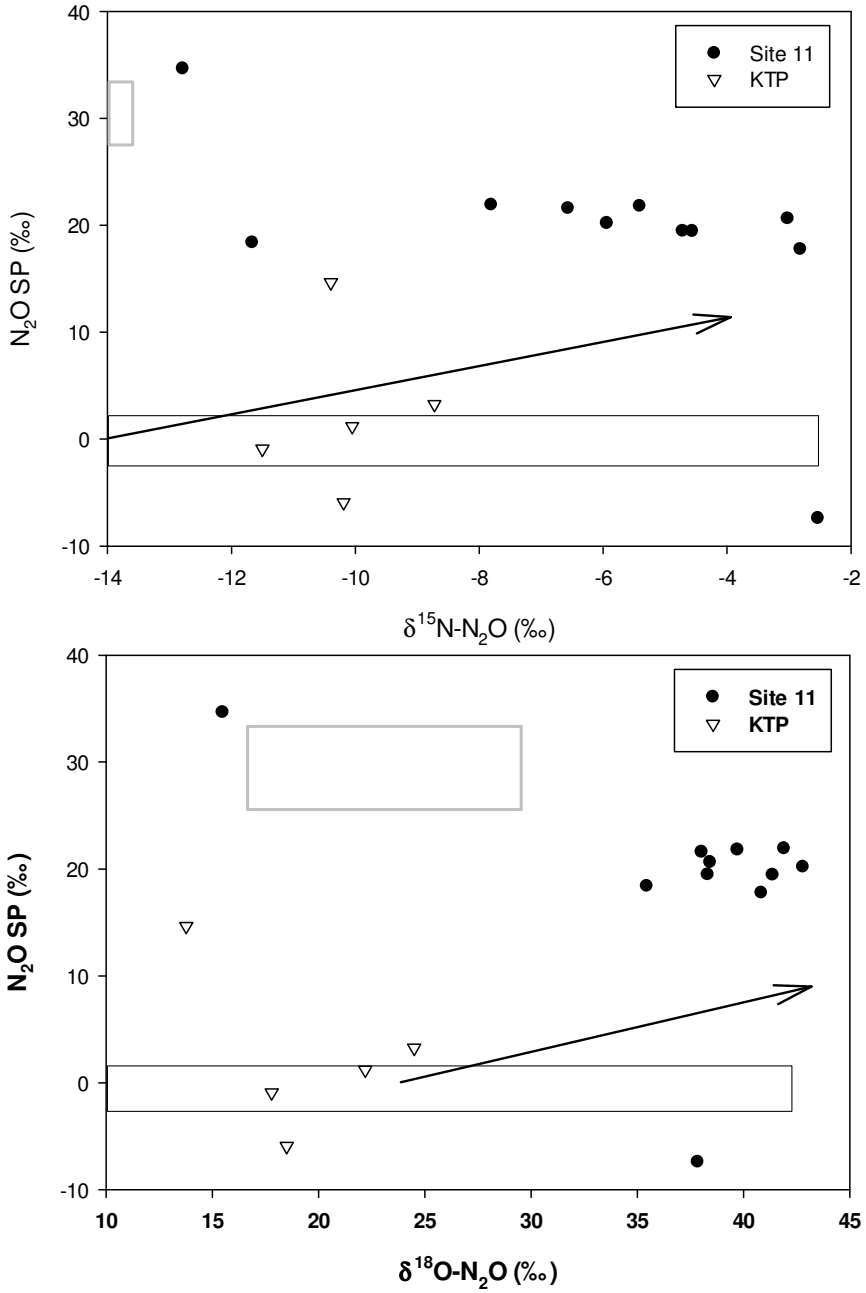

Figure A.4: $\delta^{15}N$-N_2O and $\delta^{18}O$-N_2O cross-plotted with N_2O SP for Site 11 diel samples and samples from Kitchener WWTP (KTP) effluent. Black boxes indicate expected ranges for SP and isotope ratios for denitrification based on the literature (Snider 2011) and $\varepsilon^{15}N$ and $\varepsilon^{18}O$

values from Grand River sediment (Chapter 5). Arrows show the expected slope for N_2O reduction (Ostrom et al. 2007). Grey boxes represent expected ranges for SP and isotope ratios for nitrification based on the literature.

References

Ahn JH, Kim S, Park H, Rahm B, Pagilla K, Chandran K (2010) N_2O emissions from activated sludge processes, 2008-2009: Results from a national monitoring survey in the United States. Environmental Science & Technology 44:4504-4511

Alexander RB, Smith RA, Schwarz GE (2000) Effect of stream channel size on the delivery of nitrogen to the Gulf of Mexico. Nature 403:758-761

Alsterberg C, Sundbäck K, Hulth S (2012) Functioning of a Shallow-Water Sediment System during Experimental Warming and Nutrient Enrichment. PLoS ONE 7:e51503

American Public Health Association (1995) Standard methods for the examination of water and wastewater. APHA, Washington, DC

An S, Joye SB (2001) Enhancement of coupled nitrification-denitrification by benthic photosynthesis in shallow estuarine sediments. Limnology and Oceanography 46:62-74

Anderson M (2012) Assessment of Future Water Quality Conditions in the Grand and Speed Rivers. I Grand River Water Management Plan Steering Committee. http://www.grandriver.ca/waterplan/TechBrief_AssimilativeCapacity_2012.pdf. Accessed 09/25 2013

Andrade SLA, Dickmanns A, Ficner R, Einsle O (2005) Crystal structure of the archaeal ammonium transporter Amt-1 from *Archaeoglobus fulgidus*. Proceedings of the National Academy of Sciences 102:14994-14999

Anisfeld SC, Barnes RT, Altabet MA, Wu T (2007) Isotopic apportionment of atmospheric and sewage nitrogen sources in two Connecticut rivers. Environmental Science & Technology 41:6363-6369

Aquaresource I (2009) Integrated water budget report: Grand River watershed. Grand River Conservation Authority. http://www.sourcewater.ca/swp_watersheds_grand/Grand_2009WaterBudget_final.pdf. Accessed 06/19 2011

Arai H (2011) Regulation and Function of Versatile Aerobic and Anaerobic Respiratory Metabolism in*Pseudomonas aeruginosa*. Frontiers in Microbiology 2:103-105

Arnold JG, Kiniry JR, Srinivasan R, Williams JR, Haney EB, Neitsch SL (2011) Soil and Water Assessment Tool: Input/output file documentation Version 2009. Texas Water Resource Institute. http://swat.tamu.edu/media/19754/swat-io-2009.pdf. Accessed 08/16 2013

Averill BA (1996) Dissimilatory nitrite and nitric oxide reductases. Chemical Reviews 96:2951-2965

Barlow-Busch L, Baulch HM, Taylor WD (2006) Phosphate uptake by seston and epilithon in the Grand River, southern Ontario. Aquatic Sciences 68:181-192

Barnett PJ (1992) Quaternary geology of Ontario. In: Geology of Ontario Special Volume 4, Part 2. Ontario Geological Survey, Toronto, pp 1011-1088

Batson JA, Mander U, Mitsch WJ (2012) Denitrification and a Nitrogen Budget of Created Riparian Wetlands. Journal of Environmental Quality 41:2024-2032

Baulch HM, Schiff SL, Maranger RJ, Dillon PJ (2011) Nitrogen enrichment and the emission of nitrous oxide from streams. Global Biogeochemical Cycles 25:GB4013-15

Baulch HM, Venkiteswaran JJ, Dillon PJ, Maranger RJ (2010) Revisiting the application of open-channel estimates of denitrification. Limnology and Oceanography: Methods 8:202-215

Beaulieu JJ, Shuster WD, Rebholz JA (2012) Controls on gas transfer velocities in a large river. Journal of Geophysical Research: Biogeosciences 117

Beaulieu JJ, Tank JL, Hamilton SK, Wollheim WM, Hall Jr RO, Mulholland PJ, Peterson B, Ashkenas LR, Cooper LW, Dahm CN, Dodds WK, Grimm NB, Johnson SL, McDowell WH, Poole GC, Valett HM, Arango CP, Bernot MJ, Burgin AJ, Crenshaw CL, Helton AM, Johnson LT, O'Brien JM, Potter JD, Sheibley RW, Sobota DJ, Thomas SM (2011) Nitrous oxide emission from denitrification in stream and river networks. Proceedings of the National Academy of Sciences USA 108:214-219

Beaulieu JJ, Shuster WD, Rebholz JA (2010) Nitrous oxide emissions from a large, impounded river: The Ohio River. Environmental Science & Technology 44:7527-7533

Beaulieu JJ, Arango CP, Hamilton SK, Tank JL (2008) The production and emission of nitrous oxide from headwater streams in the Midwestern United States. Global Change Biology 14:878-894

Bedard C, Knowles R (1989) Physiology, biochemistry, and specific inhibitors of CH_4, NH_4^+ and CO oxidation by methanotrophs and nitrifiers. Microbiological Reviews 53:68-84

Betlach MR, Tiedje TM (1981) Kinetic explanation for accumulation of nitrous oxide, nitric oxide, and nitrous oxide during bacterial denitrification. Applied and Environmental Microbiology 42:1074-1084

Bettez ND, Groffman PM (2012) Denitrification Potential in Stormwater Control Structures and Natural Riparian Zones in an Urban Landscape. Environmental Science & Technology 46:10909-10917

Billen G, Garnier J (1997) The Phison River plume: coastal eutrophication in response to changes in land use and water management in the watershed. Aquatic Microbial Ecology 13:3-17

Böhlke JK, Harvey JW, Voytek MA (2004) Reach-scale isotope tracer experiment to quantify denitrification and related processes in a nitrate-rich stream, midcontinent United States. Limnology and Oceanography 49:821-838

Böhlke JK, Denver JM (1995) Combined use of groundwater dating, chemical, and isotopic analyses to resolve the history and fate of nitrate contamination in two agricultural watersheds, Atlantic coastal plain, Maryland. Water Resources Research 31:2319-2339

Bollman A, Conrad R (1997) Acetylene blockage technique leads to underestimation of denitrification rates in oxic soils due to scavenging of intermediate nitric oxide. Soil Biology and Biochemistry 29:1067-1077

Boontanon N, Ueda S, Kanatharana P, Wada E (2000) Intramolecular stable isotope ratios of N_2O in the tropical swamp forest in Thailand. Naturwissenschaften 87:188-192

Boyer EW, Howarth RW (2008) Nitrogen fluxes from rivers to the coastal oceans. In: Capone D, Bronk DA, Mulholland MR, Carpenter EJ (eds) Nitrogen in the Marine Enviornment, 2nd edn. Elsevier, Oxford, pp 1565-1578

Brady NE, Weil RR (2002) The Nature and Properties of Soils. Prentice Hall, Upper Saddle River, NJ

Breiman L, Friedman JH, Olshen RA, Stone CJ (1984) Classification and regression trees. Chapman and Hall, New York

Brooks PD, Starks JM, McInteer BB, Preston T (1989) Diffusion method to prepare soil extracts for automated nitrogen-15 analysis. Soil Science Society of America Journal 53:1707-1711

Brown L, Armstrong Brown S, Jarvis SC, Syed B, Goulding KWT, Phillips VR, Sneath RW, Pain BF (2001) An inventory of nitrous oxide emissions from agriculture in the UK using the IPCC methodology: emission estimate, uncertainty and sensitivity analysis. Atmospheric Environment 35:1439-1449

Bryan BA, Shearer G, Skeeters JL, Kohl DH (1983) Variable expression of the nitrogen isotope effect associated with denitrification of nitrite. Journal of Biological Chemistry 258:8613-8617

Burgin AJ, Hamilton SK (2007) Have we overemphasized the role of denitrification in aquatic ecosystems? A review of nitrate removal pathways. Frontiers in Ecology 5:89-96

Burns DA, Boyer EW, Elliott E,M., Kendall C (2009) Sources and Transformations of Nitrate from Streams Draining Varying Land Uses: Evidence from Dual Isotope Analysis. Journal of Environmental Quality 38:1149-1159

Cabello P, Roldan MD, Moreno-Vivián C (2004) Nitrate reduction and the nitrogen cycle in archaea. Microbiology 150:3527-3546

Cameron KC, Di HJ, Moir JL (2013) Nitrogen losses from the soil/plant system: a review. Annals of Applied Biology 162:145-173

Campos JL, Arrojo B, Vasquez-Padin JR, Mosquera-Corral A, Mendez R (2009) N_2O production by nitrifying biomass under anoxic and aerobic conditions. Applied Biochemistry and Biotechnology 152:198

Casciotti KL (2009) Inverse kinetic isotope fractionation during bacterial nitrite oxidation. Geochimica et Cosmochimica Acta 73:2061-2076

Casciotti KL, Böhlke J,K., McIlvin MR, Mroczkowski SJ, Hannon JE (2007) Oxygen Isotopes in Nitrite: Analysis, Calibration, and Equilibration. Analytical Chemistry 79:2427-2436

Casciotti KL, Sigman DM, Galanter Hastings M, Bolke JK, Hilkert A (2002) Measurement of the oxygen isotopic composition of nitrate in seawater and freshwater using the denitrifier method. Analytical Chemistry 74:4905-4912

Chang CCY, Kendall C, Silva SR, Battaglin WA, Campbell DH (2002) Nitrate stable isotopes: tools for determining nitrate sources among different land uses in the Mississippi River Basin. Canadian Journal of Fisheries and Aquatic Science 59:1874-1885

Chapra SC, Di Toro DM (1991) Delta method for estimating primary production, respiration, and reaeration in streams. Journal of Environmental Engineering 117:640-655

Chen F, Jia G, Chen J (2009) Nitrate sources and watershed denitrification inferred from nitrate dual isotopes in the Beijiang River, south China. Biogeochemistry 94:163-174

Chen G (2013) Ecosystem oxygen metabolism in an impacted temperate river network. Dissertation or Thesis, University of Waterloo

Chesterikoff A, Garban B, Billen G, Poulin M (1992) Inorganic nitrogen dynamics in the River Seine downstream from Paris (France). Biogeochemistry 17:147-164

Clough TJ, Buckthought LE, Casciotti KL, Kelliher FM, Jones PK (2011) Nitrous oxide dynamics in a braided river system, New Zealand. Journal of Environmental Quality 40:1532-1541

Clough TJ, Buckthought LE, Kelliher FM, Sherlock RR (2007) Diurnal fluctuations of dissolved nitrous oxide (N_2O) concentrations and estimates of N_2O emissions from a spring-fed river: implications for IPCC methodology. Global Change Biol 13:1016-1027

Clough TJ, Bertram JE, Sherlock RR, Leonard RL, Nowicki BL (2006) Comparison of measured and $EF_{5\text{-}r}$-derived N_2O fluxes from a spring-fed river. Global Change Biology 12:477-488

Codispoti L (2010) Interesting times for marine N_2O. Science 327:1339-1340

Cohen MJ, Heffernan JB, Albertin A, Martin JB (2012) Inference of riverine nitrogen processing from longitudinal and diel variation in dual nitrate isotopes 117:1-17

Cohen RA, Bradham A,M. (2010) Uptake of stable N isotopes by *Myriophyllum spicatum* is not selective. Aquatic Botany 92:22-232

Cole JJ, Caraco NF (2001) Emissions of nitrous oxide (N_2O) from a tidal, freshwater river, the Hudson River, New York. Environmental Science & Technology 35:991-996

Cole JJ, Caraco N (1998) Atmospheric exchange of carbon dioxide in a low-wind oligotrophic lake measured by the addition of SF_6. Limnology and Oceanography 43:647-656

Conley DJ, Paerl HW, Howarth RW, Boesch DF, Seitzinger SP, Havens KE, Lancelot C, Likens GE (2009) Controlling eutrophication: Nitrogen and phosphorus. Science 323:1014-1015

Conley DJ, Carstensen J, Vaquer-Sunyer R, Duarte CM (2009) Ecosystem thresholds with hypoxia. Hydrobiologia 629:21-29

Cooke S (2006) Water Quality in the Grand River: A Summary of Current Conditions (2000-2004) and Long Term Trends. Grand River Conservation Authority. http://www.grandriver.ca/water/2006_waterquality_1.pdf. Accessed 03/20 2011

Coplen TB, Böhlke JK, DeBièvre P, Ding T, Holden NE, Hopple JA, Krouse HR, Lamberty A, Peiser HS, Revesz K, Rieder SE, Rosman KJR, Roth E, Taylor PDP, Vocke J,R.D., Xiao YK (2002) Isotope-abundance variations of selected elements (IUPAC Technical Report). Pure and Applied Chemistry 74:1987-2017

Council of Canadian Academies (2013) Water and agriculture in Canada: towards sustainable Management of Water resources. http://www.scienceadvice.ca/uploads/eng/assessments%20and%20publications%20and%20news%20releases/Water_Agri/WAG_fullreportEN.pdf. Accessed 6/13 2013

Crusius J, Wanninkhof R (2003) Gas transfer velocities measured at low wind speed over a lake. Limnology and Oceanography 48:1010-1017

Curie F, Ducharne A, Sebilo M, Bendjoudi H (2009) Denitrification in a hyporheic riparian zone controlled by river regulation in the Seine river basin (France). Hydrological Processes 23:655-664

Czepiel PC, Crill P, Harriss R (1995) Nitrous oxide emissions from municipal wastewater treatment. Environmental Science & Technology 29:2352-2356

Czepiel PC, Crill P, Harriss R (1993) Methane emissions from municipal wastewater treatment processes. Environmental Science & Technology 27:2472-2477

Dairy Farmers of Ontario (2013) Ontario Dairy Facts and Figures. Dairy Farmers of Ontario. https://www.milk.org/Corporate/pdf/DairyEducation-FactsAndFiguresEN.pdf. Accessed 08/16 2013

Davidson EA, Seitzinger SP (2006) The enigma of progess in denitrification research. Ecological Applications 16:2057-2063

de Boer W, Kowalchuk GA (2001) Nitrification in acid soils: Micro-organisms and mechanisms. Soil Biology and Biochemistry 33:866

De'ath G, Fabricius KE (2000) Classification and Regresstion Trees: A Powerful Yet Simple Technique for Ecological Data Analysis. Ecology 81:3178-3192

Decock C, Six J (2013) How reliable is the intramolecular distribution of ^{15}N in N_2O to source partition N_2O emitted from soil? Soil Biology and Biochemistry 65:114-127

Delgado J, Del Grosso SJ, Ogle S (2010) ^{15}N isotopic crop residue cycling studies and modeling suggest that IPCC methodologies to assess residue contributions to N_2O -N emissions should be reevaluated. Nutrient Cycling in Agroecosystems 86:383-390

Derse E, Knee KL, Wankel SD, Kendall C, Berg CJJ, Paytan A (2007) Identifying sources of nitrogen to Hanalei Bay, Kauai, utilizing the nitrogen isotope signature of macroalgae. Environmental Science & Technology 41:5223

Desloover J, Vlaeminck SE, Clauwaert P, Verstraete W, Boon N (2012) Strategies to mitigate N_2O emissions from biological nitrogen removal systems. Current Opinion in Biotechnology 23:474-482

Diez Ercilla M, Lopez Pamo E, Sanchez Espana J (2009) Photoreduction of Fe(III) in the acidic mine pit lake of San Telmo (Iberian Pyrite Belt): Field and experimental work. Aquatic Geochemistry 15:391-419

Dodds WK, Jones JR, Welch EB (1998) Suggested classification of stream trophic state: distributions of temperate stream types by chlorophyll, total nitrogen, and phosphorus. Water Research 32:1455-1462

Dong LF, Naqasima Sobey M, Smith CJ, Rusmana I, Phillips W, Stott A, Osborn AM, Nedwell DB (2011) Dissimilatory reduction of nitrate to ammonium, not denitrification or anammox, dominates benthic nitrate reduction in tropical estuaries. Limnology and Oceanography 56:279-291

Dong LF, Nedwell DB, Colbeck I, Finch J (2004) Nitrous oxide emission from some English and Welsh rivers and estuaries. Water, Air, and Soil Pollution: Focus 4:127-134

Dougherty E, Young K (2005) USDA Reports an Increase in the Average Weight of a Turkey. United States Department of Agriculture. http://www.nass.usda.gov/Newsroom/2005/11_15_2005.asp. Accessed 08/16 2013

Duff JH, Triska FJ, Oremland RS (1984) Denitrification associated with stream periphyton: chamber estimates from undisrupted communities. Journal of Environmental Quality 13:514-517

Dumont E, Harrison JA, Kroeze C, Bakker EJ, Seitzinger SP (2005) Global distribution and sources of dissolved inorganic nitrogen export to the coastal zone: Results from a spatially explicit, global model. Global Biogeochemical Cycles 16:1-13

Elsaholi M, Kelly-Quinn M (2013) The effect of nutrient concentrations and ratios on periphyton biomass in low conductivity streams: implications for determination of nutrient limitation. Inland Waters 3:451-458

Encalada Romero ML (2008) Inputs of DO into the Grand River in the Glen Morris Area: The role of groundwater and riparian zones. Dissertation or Thesis, Univeristy of Waterloo

Ensign SH, Doyle MW (2006) Nutrient spiralling in streams and river networks. Journal of Geophysical Research 111:G04009

Environment Canada (2010) National Pollutant Release Inventory: Tracking Pollution in Canada. Environment Canada. http://www.ec.gc.ca/inrp-npri/Default.asp?lang=En&n=4A577BB9-1. Accessed 04/20 2011

Environment Canada (2003) CCME guidelines for the protection of aquatic life. Environment Canada. http://www.waterquality.ec.gc.ca/waterqualityweb/guidelines.aspx?catId=1. Accessed 07/26 2013

European Environment Agency (2013) Atmospheric concentration of Nitrous Oxide (ppb). http://www.eea.europa.eu/data-and-maps/figures/atmospheric-concentration-of-n2o-ppb-1. Accessed 07/12 2013

Evans CD, Monteith DT, Cooper DM (2005) Long-term increases in surface water dissolved organic carbon: Observations, possible causes and environmental impacts. Environmental Pollution 137:55-71

Falkowski PG, Raven JA (2007) Aquatic Photosynthesis. Princeton University Press, Princeton, NJ

Farías L, Faúndez J, Fernández C, Cornejo M, Sanhueza S, Carrasco C (2013) Biological N_2O Fixation in the Eastern South Pacific Ocean and Marine Cyanobacterial Cultures. PLoS ONE 8:e63956

Farm Animal Shelters (2013) Rabbit Care. Farm Animal Shelters. http://www.farmanimalshelters.org/care_rabbit.htm. Accessed 08/16 2013

Farrelly DJ, Everard CD, Fagan CC, McDonnell KP (2013) Carbon sequestration and the role of biological carbon mitigation: A review. Renewable & Sustainable Energy Reviews 21

Firestone MK, Firestone RB, Tiedje JM (1980) Nitrous oxide from soil denitrification: Factors controlling its biological production. Science 208:749-751

Firestone MK, Smith MS, Firestone RB, Tiedje JM (1979) The influence of nitrate, nitrite, and oxygen on the composition of the gaseous products of denitrification in soil. Soil Science Society of America Journal 43:1140-1144

Firestone MK, Tiedje JM (1979) Temporal change in nitrous oxide and dinitrogen from denitrification following onset of anaerobiosis. Applied and Environmental Microbiology 38:673-679

Forster P, Ramaswamy V, Artaxo P, Berntsen T, Betts R, Fahey DW, Haywood J, Lean J, Lowe DC, Myhre G, Nganga J, Prinn R, Raga G, Schulz M, Van Dorland R (2007) Changes in Atmospheric Constituents and in Radiative Forcing. In: Solomon S, Qin D, Manning M, Chen Z, Marquis M, Avery KB, Tignor M, Miller HL (eds) Climate Change 2007: The Physical Science Basis. Contribution of Working Group I to the Fourth Assessment Report of the Intergovernmental Panel on Climate Change. Cambridge University Press, Cambridge, UK, pp 129-234

Galloway J, Dentener F, Capone DG, Boyer EW, Howarth RW, Seitzinger SP, Asner GP, Cleveland CC, Green PA, Holland EA, Karl DM, Michaels AF, Porter JH, Townsend AR, Voosmarty CJ (2004) Nitrogen Cycles: Past, Present, and Future. Biogeochemistry 70:153-226

Galloway J (2003) 8.12: The global nitrogen cycle. In: Holland HD, Turekian KK (eds) Treatise in Geochemistry. Elsevier Science & Technology Books, pp 557-583

Gammons CH, Babcock JN, Parker SR, Poulson SR (2009) Diel cycles in stable-isotope composition of nitrate, ammonia, dissolved oxygen, and dissolved inorganic carbon in a hypereutrophic stream. Portland GSA Annual Meeting

Gammons CH, Wood SA, Nimick DA (2005) Diel behavior of rare earth elements in a mountain stream with acidic to neutral pH. Geochimica et Cosmochimica Acta 69:3747-3758

Garcia-Ruiz R, Pattinson SN, Whitton BA (1999) Nitrous oxide production in the River Swale-Ouse, North-East England. Water Research 33:1231-1237

Garnier J, Cebron A, Tallec G, Gilles B, Sebilo M, Martinez A (2006) Nitrogen behaviour and nitrous oxide emission in the tidal Seine River estuary (France) as influenced by human activities in the upstream watershed. Biogeochemistry 77:305-326

Geywitzhetz S, Bussmann M, Schon G (1993) Influence of some environmental conditions on N2O release by activated sludge under anoxic conditions. Acta Hydrochimica et Hydrobiologica 21:258-266

Gold AJ, Deragon WR, Sullivan WM, Lemunyon JL (1990) Nitrate-nitrogen losses to groundwater from rural and suburban land uses. Journal of Soil and Water Conservation 45:305-310

González-Ballester D, Camargo A, Fernández E (2004) Ammonium transporter genes in*Chlamydomonas*: the nitrate-specific regulatory gene Nit2 is involved in Amt1;1 expression. Plant Molecular Biology 56:863-78

Goreau TJ, Kaplan WA, Wofsky SC, McElroy MB, Valois FW, Watson SW (1980) Production of NO_2-and N_2O by nitrifying bacteria at reduced concentrations of oxygen. Applied and Environmental Microbiology 40:526-532

Grand River Conservation Authority (2008) Grand River Chacterization Report. Grand River Conservation Authority. http://www.sourcewater.ca/swp_watersheds_grand/Characterization_summary_Grand.pdf.

Grand River Conservation Authority (2008) Grand River Information Network. Grand River Conservation Authority. http://www.grandriver.ca/index/document.cfm?Sec=63&Sub1=0&sub2=0. Accessed 6/12 2013

Grimm NB, Petrone KC (1997) Nitrogen fixation in a desert stream ecosystem. Biogeochemistry 37:33-61

Groffman PM, Altabet MA, Böhlke JK, Butterbach-Bahl K, David MB, Firestone MK, Giblin AE, Kana TM, Voytek MA (2006) Methods for measuring denitrification: Diverse approaches to a difficult problem. Ecological Applications 16:2091-2122

GSP Group I (2010) Grand River, Long Point Region, Catfish Creek and Kettle Creek Watershed Areas: Population Forecasts. In: . Ontario Ministry of the Environment. http://www.sourcewater.ca/swp_watersheds_Grand/PopReport_Jan2010.pdf. Accessed 08/26/2013 2013

Gutschick VP (1978) Energy and Nitrogen Fixation. BioScience 28:571-575

Harrison JA, Matson PA, Fendorf SE (2005) Effects of a diel oxygen cycle on nitrogen transformations and greenhouse gas emissions in a eutrophied subtropical stream. Aquatic Science 67:308-315

Harrison JA, Matson PA (2003) Patterns and controls of nitrous oxide emissions from waters draining a subtropical agricultural valley. Global Biogeochemical Cycles 17:1080-1093

Hasegawa K, Hanaki K, Matsuo T, Hidaka S (2000) Nitrous oxide from the agricultural water system contaminated with high nitrogen. Chemosphere - Global Change Science 2:335-345

Hatzenpichler R (2012) Diversity, Physiology, and Niche Differentiation of Ammonia-Oxidizing Archaea. Applied and Environmental Microbiology 78:7501-7510

Hayatsu M, Tago K, Saito M (2008) Various players in the nitrogen cycle: Diversity and functions of the microorganisms involved in nitrification and denitrification. Soil Science and Plant Nutrition 54:33-45

Health Canada (2012) Nitrate and nitrite in drinking water. Government of Canada. http://www.hc-sc.gc.ca/ewh-semt/alt_formats/pdf/consult/_2012/nitrite-nitrite/nitrite-nitrite-eng.pdf. Accessed 6/11 2013

Herrero A, Muro-Pastor AM, Flores E (2001) Nitrogen control in cyanobacteria. Journal of Bacteriology 183:425

Hillebrand E (2011) Poverty, growth and inequality over the next 50 years. In: Looking Ahead in World Food and Agriculture: Perspectives to 2050. Food and Agriculture Organization of the United Nations, Rome, pp 159-190

Hinshaw SE, Dahlgren RA (2013) Dissolved Nitrous Oxide Concentrations and Fluxes from the Eutrophic San Joaquin River, California. Environmental Science & Technology 47:1313-1322

Hlavacova E, Rulik M, Cap L, Mach V (2006) Greenhouse gas (CO_2, CH_4, N_2O) emissions to the atmosphere from a small lowland stream in Czech Republic. Archiv für Hydrobiologie 165:339-353

Hoch MP, Fogel ML, Kirchman DL (1994) Isotope fractionation during ammonium uptake by marine microbial assemblages. Geomicrobiology Journal 12:113-127

Hoffman JL, Canace RJ (2004) A Recharge-Based Nitrogen Dilution Model for New Jersey. New Jersey Department of Environmental Protection.
http://www.state.nj.us/dep/njgs/pricelst/ofreport/ofr04-1.pdf. Accessed 08/26/2013 2013

Holysh S, Pitcher J, Boyd D (2001) Grand River Regional Groundwater Study: Technical report

Hong B, Swaney DP, Howarth RW (2013) Estimating Net Anthropogenic Nitrogen Inputs to U.S. Watersheds: Comparison of Methodologies. Environmental Science & Technology 47:5199-5207

Hood JLA (2012) The role of submersed macrophytes in river eutrophication and biogeochemical nutrient cycling. Dissertation or Thesis, University of Waterloo

Howarth R, Swaney D, Billen G, Garnier J, Hong B, Humborg C, Johnes P, Morth C-, Marino R (2012) Nitrogen fluxes from the landscape are controlled by net anthropogenic nitrogen inputs and by climate. Frontiers of Ecology and the Environment 10:37-43

Howarth RW, Hayn M, Marino RM, Ganju N., Foreman K, McGlathery K, Giblin AE, Berg P, Walker. J.D. (2013) Metabolism of a nitrogen-enriched coastal marine lagoon during the summer. Biogeochemistry

Howarth RW, Schneider R, Swaney D (1996) Metabolism and organic carbon fluxes in the tidal freshwater Hudson River. Estuaries 19:848-865

Huffman T, Yang JY, Drury CF, De Jong R, Yang XM, Liu YC (2008) Estimation of Canadian manure and fertilizer nitrogen application rates at the crop and soil-landscape polygon level. Canadian Journal of Soil Science 88:619-627

Humphrey C, O'Driscoll MA, Armstrong MC (2012) Onsite Wastewater System Nitrogen Loading to Groundwater in the Newport River Watershed, North Carolina. Environment and Natural Resources Research 2:70-79

Intergovernmental Panel on Climate Change (1996) Revised 1996 IPCC Guidelines for National Greenhouse Gas Inventories: Reference Manuel

IPCC (2007) Climate Change 2007: The Physical Science Basis. Contribution of Working Group I to the Forth Assessment Report of the Intergovernmental Panel on Climate Change. Cambridge University Press, Cambridge, UK

IPCC (2007) Climate Change 2007: Mitigation of Climate Change. Cambridge University Press, Cambridge, UK

IPCC (2006) Waste. In: Eggleston HS, Buendia L, Miwa K, Ngara T, Tanabe K (eds) 2006 IPCC Guidelines for National Greenhouse Gas Inventories, Prepared by the National Greenhouse Gas Inventories Programme. IGES, Hayama, Japan

Iribar A, Sanchez-Perez JM, Lyautey E, Garabetian F (2008) Differentiated free-living and sediment-attached bacterial community structure inside and outside denitrification hotspots in the river-groundwater interface. Hydrobiologia 598:109-121

Itokawa H, Hanaki K, Matsuo T (1996) Nitrous oxide emission during nitrification and denitrification in a full-scale night soil treatment plant. Water Science and Technology 34:277-284

Ivens WPMF, Tysmans DJJ, Kroeze C, Lohr AJ, van Wignen J (2011) Modeling global N_2O emissions from aquatic systems. Current Opinion in Environmental Sustainability 3:350-358

Jackson AL, Inger R, Parnell AC, Bearhop S (2011) Comparing isotopic niche widths among and within communities: SIBER - Stable Isotope Bayesian Ellipses in R. Journal of Animal Ecology 80:595-602

James CS, Eaton JW, Hardwick K (2006) Responses of three invasive aquatic macrophytes to nutrient enrichment do not explain their observed field displacements. Aquatic Botany 84:347-353

Jamieson T (2010) Quantification of Oxygen Dynamics in the Grand River Using a Stable Isotope Approach. Dissertation or Thesis, University of Waterloo

Jepson BJN, Marietou A, Mohan S, Cole JA, Butler CS, Richardson DJ (2006) Evolution of the soluble nitrate reductase: defining the monomeric periplasmic nitrate reductase subgroup. Biochemical Society Transacations 34:122-126

Jha R, Ojha CSP, Bhatia KKS (2004) A supplimentary approach for estimating reaeraton rate coefficients. Hydrological Processes 18:65-79

Jha R, Ojha CSP, Bhatia KKS (2001) Refinement of predictive reaeration equations for a typical Indian river. Hydrological Processes 15:1047-1060

Johannsen A, Dahnke K, Emeis K (2008) Isotopic composition of nitrate in five German rivers discharging into the North Sea. Organic Geochemistry 39:1679-1689

Jones RI, King L, Dent MM, Maberly SC, Gibson CE (2004) Nitrogen stable isotope ratios in surface sediments, epilithon and macrophytes from upland lakes with differing nutrient status. Freshwater Biology 49:382-391

Kaberia B, Mutia P, Ahuya C (2003) Farmers Dairy Goat Production Handbook. Food and Agriculture Organization of the United Nations. http://teca.fao.org/sites/default/files/technology_files/Farmers%20Dairy%20Goat%20Production%20Handbook_0.pdf. Accessed 08/16 2013

Kaiser J, Rockman T, Brenninkmeijer CAM (2003) Complete and accurate mass spectrometric isotope analysis of tropospheric nitrous oxide. Journal of Geophysical Research - Atmosphere 103

Kampschreur MJ, van der Star WRL, Wielders HA, Mulder JW, Jetten MSM, van Loosdrecht MCM (2008) Dynamics of nitric oxide and nitrous oxide emission during full-scale reject wate treatment. Water Research 42:812-826

Karrow PF, Morgan AV (2004) Glaciation and recent events in the Grand River basin. In: Nelson JG (ed) Towards a Grand Sense of Place. University of Waterloo Press, Waterloo, ON, pp 21-34

Kartal B, Kuypers MMM, Lavik G, Schalk J, Op den Camp HJM, Jetten MSM, Strous M (2007) Anammox bacteria disguised as denitrifiers: nitrate reduction to dinitrogen gas via nitrite and ammonium. Environmental Microbiology 9:635-642

Kartal MB (2008) Ecophysiology of the anammox bacteria. Dissertation or Thesis, Radboud University Nijmegen

Kato T, Toyoda S, Yoshida N, Tang Y, Wada E (2013) Isotopomer and isotopologue signatures of N_2O produced in alpine ecosystems on the Qinghai–Tibetan Plateau. Rapid Communications in Mass Spectrometry 27:1517-1526

Kellman L, Hillaire-Marcel C (1998) Nitrate cycling in streams: using natural abundances of NO_3-$\delta^{15}N$ to measure in-situ denitrification. Biogeochemistry 43:273-292

Kendall C, Caldwell EA (1998) Fundamentals of Isotope Geochemistry. In: Kendall C, Caldwell EA (eds) Isotope Tracers in Catchment Hydrology. Elsevier Science B.V, Amsterdam, pp 51-86

Kerr JL, Baldwin DS, Whitworth KL (2013) Options for managing hypoxic blackwater events in river systems: A review. Journal of Environmental Management 114:139-147

Kimochi Y, Inamori Y, Mizuochi M, Zu K-, Matsumura M (1998) Nitrogen removal and N_2O emission in a full-scale domestic wastewater treatment plant with intermittent aeration. Journal of Fermentation and Bioengineering 86:202-206

Klemedtsson L, Svensson BH, Rosswell T (1988) Relationships between soil moisture content and nitrous oxide production during nitrification and denitrification. Biology & Fertility of Soils 6:106-111

Kool DM, Wrage N, Oenema O, Harris D, Van Groenigen JW (2009) The ^{18}O signature of biogenic nitrous oxide is determined by O exchange with water. Rapid Communications in Mass Spectrometry 23:104-108

Kool DM, Wrage N, Oenema O, Dolfing J, Van Groenigen JW (2007) Oxygen exchange between (de)nitrification intermediates and H_2O and its implications for source determination of NO_3^- and N_2O: a review. Rapid Communications in Mass Spectrometry 21:3569-3578

Koppelman LE (1978) The Long Island comprehensive waste treatment management plan, vol. 2: Summary documentation report. 2

Körner H, Zumft WG (1989) Expression of denitrification enzymes in response to the dissolved oxygen level and respiratory substrate in continuous culture of *Pseudomonas stutzeri*. Applied Environmental Microbiology 55:1610-1676

Kraiser T, Gras DE, Gutierrez AG, Gonzales B, Gutierrez RA (2011) A holistic view of nitrogen acquisition in plants. Journal of Experimental Botany 62:1455-1466

Kroeze C, Dumont E, Seitzinger SP (2005) New estimates of global emissions of N_2O from rivers and estuaries. Environmental Science 2:159-165

Krysanova V, Muller-Wohlfeil DI, Becker A (1998) Development and test of a spatially distributed hydrological water quality model for mesoscale watersheds. Ecological Modelling 106:261-289

Kuuppo P, Tamminen T, Voss M, Schulte U (2006) Nitrogenous discharges to the eastern Gulf of Finland, the Baltic Sea: Elemental flows, stable isotope signatures, and their estuarine modification. Journal of Marine Systems 63:191-208

Laursen A, Seitzinger SP (2004) Diurnal patterns of denitrification, oxygen consumption and nitrous oxide production in rivers measured at the whole-reach scale. Freshwater Biology 49:1448-1458

Laursen A, Seitzinger SP (2002) Measurement of denitrification in rivers: an integrated, whole reach approach. Hydrobiologia 485:67-81

Laursen AE, Carlton RG (1999) Responses to atrazine of respiration, nitrification, and denitrification in stream sediments measured with oxygen and nitrate microelectrodes. FEMS Microbiology Ecology 29:229-240

Law CS, Rees AP, Owens NJP (1992) Nitrous oxide: Estuarine sources and atmospheric flux. Estuarine, Coastal and Shelf Science 35:301-314

Lemke AM, Kirkham KG, Lindenbaum TT, Herbert ME, Tear TH, Perry WL, Herkert JR (2011) Evaluating Agricultural Best Management Practices in Tile-Drained Subwatersheds of the Mackinaw River, Illinois. Journal of Environmental Quality 40:1215-1228

Lide DR, Frederikse HPR (1995) CRC Handbook of Chemistry and Physics

Limmer AW, Steele KW (1982) Denitrification potentials: Measurement of seasonal variation using a short-term anaerobic incubation technique. Soil Biology and Biochemistry 14:179-184

Lin JT, Stewart V (1998) Nitrate assimilation by bacteria. Advanced Microbial Physiology 39:1-30

Loomer HA (2009) The Dynamics of Carbon and Nitrogen Stable Isotope Analysis of Aquatic Organisms within the Grand River Watershed. Dissertation or Thesis, University of Waterloo

Lorenzen J, Larsen LH, Kjaer T, Revsbech NP (1998) Biosensor determination of the microscale distribution of nitrate, nitrate assimilation, nitrification, and denitrification in a diatom-inhabited freshwater sediment. Applied and Environmental Microbiology 64:3264-3269

Loscher CR, Kock A, Konneke M, LaRoche J, Bange HW, Schmitz RA (2012) Production of oceanic nitrous oxide by ammonia-oxidizing archaea. Biogeosciences 9:2419-2429

Luna E (2013) Error Propagation. De Anza University. http://facultyfiles.deanza.edu/gems/lunaeduardo/ErrorPropagation2A.pdf. Accessed 6/18 2013

Maizel MS, Muehlbach G, Baynham P, Zoerkler J, Monds D, Iivari T, Welle P, Robbin J, Wiles J (1997) The potential for nutrient loadings from septic systems to ground and surface water resources and the Chesapeake Bay. In: . US Environmental Protection Agency. http://nepis.epa.gov/Exe/ZyNET.exe/P1001WW6.txt?ZyActionD=ZyDocument&Client=EPA&Index=1995%20Thru%201999&Docs=&Query=&Time=&EndTime=&SearchMethod=1&TocRestrict=n&Toc=&TocEntry=&QField=&QFieldYear=&QFieldMonth=&QFieldDay=&UseQField=&IntQFieldOp=0&ExtQFieldOp=0&XmlQuery=&File=D%3A\ZYFILES\INDEX%20DATA\95THRU99\TXT\00000021\P1001WW6.txt&User=ANONYMOUS&Password=anonymous&SortMethod=h|-&MaximumDocuments=1&FuzzyDegree=0&ImageQuality=r75g8/r75g8/x150y150g16/i425&Display=p|f&DefSeekPage=x&SearchBack=ZyActionL&Back=ZyActionS&BackDesc=Results%20page&MaximumPages=1&ZyEntry=1. Accessed 08/26/2013 2013

Makarewicz JC, Lewis TW, Bosch I, Noll MR, Herendeen N, Simon RD, Zollweg J (2009) The impact of agricultural best management practices on downstream systems: Soil loss and nutrient chemistry and flux to Conesus Lake, New York, USA. Journal of Great Lakes Research 35:23-36

Manconi I, Van der Maas P, Lens P (2006) Effect of copper dosing on sulfide inhibited reduction of nitric and nitrous oxide. Nitric Oxide - Biology and Chemistry 15:400-407

Mariotti A, Mariotti F, Campigny M-, Amarger N, Moyse A (1982) Nitrogen Isotope Fractionation Associated with Nitrate Reductase Activity and Uptake of NO_3^- by Pearl Millet. Plant Physiology 69:880-884

Martin PJ, Frind EO (1998) Modelling a complex multi-aquifer system: The Waterloo Moraine. Ground Water 36:679-690

Mattsson T, Kortelainen P, Laubel A, Evans D, Pujo-Pay M, Räike A, Conan P (2008) Export of dissolved organic matter in relation to land use along a European climatic gradient. Science of the Total Environment 407:1967-1976

Mayer B, Boyer EW, Goodale C, Jaworski NA, van Breemen N, Howarth RW, Seitzinger S, Billen G, Lajtha K, Nadelhoffer K, Van Dam D, Hetling LJ, Nosal M, Paustian K (2002) Sources of nitrate in rivers draining sixteen watersheds in the northeastern U.S.: Isotopic constraints. Biogeochemistry 57/58:171-197

McCutcheon SC (1989) Water Quality Monitoring, Volume 1: Transport and Surface Exchange in Rivers. CRC Press, Boca Raton

McElroy MB, Elkins JW, Wofsy SC, Kolb CE, Duran AP, Kaplan WA (1978) Production and release of N₂O from the Potomac Estuary. Limnology & Oceanogragphy 23:1168-1182

McIlven MR, Altabet MA (2005) Chemical conversion of nitrate and nitrite to nitrous oxide for nitrogen and oxygen isotopic analysis in freshwater and seawater. Analytical Chemistry 77:5589-5595

McKnight DM, Duren SM (2004) Biogeochemical processes controlling midday ferrous iron maxima in stream waters affected by acid rock drainage. Applied Geochemistry 19:1075-1084

McMahon PB, Dennehy KF (1999) N_2O Emissions from a nitrogen-enriched river. Environmental Science & Technology 33:21-25

McMahon PB, Böhlke JK (1996) Denitrification and mixing in a stream-aquifer system: Effects on nitrate loading to surface water. Journal of Hydrology 186:105-128

Mietto A, Borin M (2013) Performance of two small subsurface flow constructed wetlands treating domestic wastewaters in Italy. Environmental Technology 34:1085-1095

Ministry of the Environment of Ontario (2007) Ontario Water Resources Act. http://www.e-laws.gov.on.ca/html/statutes/english/elaws_statutes_90o40_e.htm. Accessed 09/25 2013

Miyajima T, Yoshimizu C, Tsuboi Y, Tanaka Y, Tayasu I, Nagata T, Koike I (2009) Longitudinal distribution of nitrate $\delta^{15}N$ and $\delta^{18}O$ in two contrasting tropical rivers: implications for instream nitrogen cycling. Biogeochemistry 95:243-260

Moir JWB, Wood NJ (2001) Nitrate and nitrite transport in bacteria. Cellular and Molecular Life Sciences 58:215-224

Moog DB, Jirka GH (1998) Analysis of reaeration equations using mean multiplicative error. Journal of Environmental Engineering 124:104-110

Mulholland PJ, Helton AM, Poole GC, Hall Jr RO, Hamilton SK, Peterson BJ, Tank JL, Ashkenas LR, Cooper LW, Dahm CN, Dodds WK, Findlay SEG, Gregory SV, Grimm NB, Johnson SL, McDowell WM, Meyer JL, Valett HM, Webster JR, Arango CP, Beaulieu JJ, Bernot MJ, Burgin AJ, Crenshaw CL, Johnson LT, Niederlehner BR, O'Brien JM, Potter JD, Sheibley RW, Sobota DJ, Thomas SM (2008) Stream denitrification across biomass and its response to anthropogenic nitrate loading. Nature 452:202-206

Mulholland PJ, Valett HM, Webster JR, Thomas SA, Cooper LW, Hamilton SK, Peterson BJ (2004) Stream denitrification and total nitrate uptake rates measured using a field ^{15}N tracter addition approach. Limnology and Oceanography 49:809-820

Muller J, Weise G (1987) Oxygen budget of a river rich in submerged macrophytes (River Zschopau in the South of the GDR). Internationale Revue der gasamten Hydrobiologie 72:653-667

Murray M (2008) Evaluating the isotopic fingerprint of wastewater treatment plant nitrogen and its evolution in the Grand River. Dissertation or Thesis, University of Waterloo

Nakamura Y, Satoh H, Okabe S, Watanabe Y (2004) Photosynthesis in sediments determined at high spatial resolution by the use of microelectrodes. Water Research 38:2440-2448

National Research Council Canada (1982) Nutrient Requirement of Mink and Foxes. National Academy Press. http://www.nap.edu/openbook.php?record_id=1114. Accessed 08/16 2013

Nevison C (2000) Review of the IPCC methodology for estimating nitrous oxide emissions associated with agricultural leaching and runoff. Chemosphere 2:493-500

Nielsen LP, Christensen PB, Revsbech NP, Sorensen J (1990) Denitrification and photosynthesis in stream sediment studied with microsensor and whole-core techniques. Limnology and Oceanography 35:1135-1144

Nielsen LP, Christensen PB, Revsbech NP, Sorensen J (1990) Denitrification and oxygen respiration in biofilms studied with a microsensor for nitrous oxide and oxygen. Microbial Ecology 19:63-72

Nirmal Rajkumar A, Barnes J, Ramesh R, Purvaja R, Upsill-Goddard RC (2008) Methane and nitrous oxide fluxes in the polluted Adyar River and estuary, SE India. Marine Pollution Bulletin 56:2043-2051

Nurnberg GK (1995) Quantifying anoxia in lakes. Limnology and Oceanography 40:1100-1111

O'Connor DJ, Dobbins WE (1958) Mechanism of reaeration in natural streams. ASCE Trans 2934:641-684

Odum HT (1956) Primary production in flowing waters. Limnology and Oceanography 1:102-117

Ontario Cattlemen's Association (2012) Ontario Live Cattle Prices. Ontairo Cattlemen's Association. http://www.cattle.guelph.on.ca/statistics/onliveprices_fed.asp. Accessed 08/16/2013 2013

Ontario Ministry of Agriculture and Food (2011) Agronomy Guide for Field Crops - Publication 811. In: . http://www.omafra.gov.on.ca/english/crops/pub811/p811toc.html. Accessed 06/12 2013

Ontario Ministry of the Environment (1996) Technical Guideline for Individual On-site Sewage Systems: Water Quality Impact Risk Assessment. In: . Ontario Ministry of the Environment. http://www.ene.gov.on.ca/stdprodconsume/groups/lr/@ene/@resources/documents/resource/std01_079313.pdf. Accessed 08/26/2013 2013

Ontario Sheep Marketing Agency (2013) Ontario Sheep Economic Workbook: Annual Lambing Flock. In: . Ontario Sheep Marketing Agency. http://www.ontariosheep.org/LinkClick.aspx?fileticket=qFK3d7lbJKg%3D&tabid=99. Accessed 08/16 2013

Oreskes N, Shrader-Frechette K, Belitz K (1994) Verification, validation, and confirmation of numerical models in the earth sciences. Science 263:641-646

Ostrom NE, Pitt AJ, Sutka RL, Ostrom PH, Grandy AS, Huizinga KM, Robertson GP (2007) Isotopologue effects during N_2O reduction in soils and in pure cultures of denitrifiers. Journal of Geophysical Research: Biogeosciences 112

Otte S, Schalk J, Kuenen JG, Jetten MSM (1999) Hydroxylamine oxidation and subsequent nitrous oxide production by the heterotrophic ammonia oxidizer*Alcaligenes faecalis*. Applied Microbiology and Biotechnology (51:255-261

Ouellet V, Mingelbier M, Saint-Hilaire A, Morin J (2010) Frequency Analysis as a Tool for Assessing Adverse Conditions During a Massive Fish Kill in the St. Lawrence River, Canada. Water Quality Research Journal of Canada 45:47-57

Parker SR, Gammons CH, Poulson SR, DeGrandpre MD, Weyer CL, Smith MG, Babcock JN, Oba Y (2010) Diel behavior of stable isotopes of dissolved oxygen and dissolved inorganic carbon in rivers over a range of trophic conditions, and in a mesocosm experiment. Chemical Geology 269:22-32

Parker SR, Poulson SR, Smith MG, Weyer CL, Bates KM (2009) Temporal variability in the concentration and stable carbon isotope composition of dissolved inorganic and organic carbon in two Montana, USA rivers. Aquatic Geochemistry

Parkhill K, Gulliver JS (1998) Application of photorespiration concepts to whole stream productivity. Hydrobiologia 389:7-19

Passeport E, Vidon P, Forshay K, Harris L, Kaushal S, Kellogg D, Lazar J, Mayer P, Stander E (2013) Ecological Engineering Practices for the Reduction of Excess Nitrogen in Human-Influenced Landscapes: A Guide for Watershed Managers. Environmental Management 51:392-413

Pattinson SN, Garcia-Ruiz R, Whitton BA (1998) Spatial and seasonal variation in denitrification in the Swale-Ouse system, a river continuum. Science of the Total Environment 210/211:289-305

Patureau D, Bernet N, Moletta R (1996) Study of the Denitrifying Enzymatic System of *Comamonas sp*. Strain SGLY2 Under Various Aeration Conditions with a Particular View on Nitrate and Nitrite Reductases. Current Microbiology 32:25-32

Pennock JR, Velinksy DJ, Ludlam JM, Fogel ML (1996) Isotopic fractionation of ammonium and nitrate during uptake by Skeletonema costatum: Implications for $\delta^{15}N$ dynamics under bloom conditions. Limnology and Oceanography 41:451-459

Philippot L, Andert J, Jones CM, Bru D, Hallin S (2011) Importance of denitrifiers lacking the genes encoding the nitrous oxide reductase for N_2O emissions from soil. Global Change Biology 17:1497-1504

Porubsky WP, Velasquez LE, Joye SB (2008) Nutrient-replete benthic microalgae as a source of dissolved organic carbon to coastal waters. Estuaries and Coasts 31:860-876

Poulson SR, Sullivan AB (2010) Assessment of diel chemical and isotopic techniques to investigate biogeochemical cycles in the upper Klamath River, Oregon, USA. Chemical Geology 269:3-11

Pribyl AL, McCutchan JH, Lewis WM, Saunders JF (2005) Whole-system estimation of denitrification in a plains river: a comparision of two methods. Biogeochemistry 73:439-455

Quay P, Stutsman J, Wilbur J, Snover A, Dlugokencky E, Brown T (1999) The isotopic composition of atmospheric methane. Global Biogeochemical Cycles 13:445-461

Ranalli AJ, Macalady DL (2010) The importance of the riparian zone and in-stream processes in nitrate attenuation in undisturbed and agricultural watersheds – A review of the scientific literature. Journal of Hydrology 389:406-415

Ravishankara AR, Daniel JS, Portmann RW (2009) Nitrous oxide (N_2O): The dominant ozone-depleting substance emitted in the 21st century. Science 326:123-125

Raymond PA, Cole JJ (2001) Gas exchange in rivers and estuaries: Choosing a gas transfer velocity. Estuaries 24:312-317

Reay DS, Smith KA, Edwards AC, Hiscock KM, Dong LF, Nedwell DB (2005) Indirect nitrous oxide emissions: Revised emission factors. Environmental Sciences 2:153-158

Reay DS, Smith KA, Edwards AC (2003) Nitrous oxide emission from agricultural drainage waters. Global Change Biol 9:195-203

Reay WG (2004) Septic Tank Impacts on Ground Water Quality and Nearshore Sediment Nutrient Flux. Ground Water 42:1079-1089

Rees RM, Baddeley JA, Bhogal A, Ball BC, Chadwick DR, Macleod M, Lilly A, Pappa VA, Thorman RE, Watson CA, Williams JR (2013) Nitrous oxide mitigation in UK agriculture. Soil Science and Plant Nutrition 59:3-15

Rempel M (2008) NO_3^- and N_2O at the Strawberry Creek Catchment: tracing sources and processes using stable isotopes. Dissertation or Thesis, University of Waterloo

Richards D (2011) Swine Budget. Ontario Ministry of Agriculture and Food. http://www.omafra.gov.on.ca/english/livestock/swine/facts/info-b-mar2011.pdf. Accessed 08/16/2011 2013

Richey JE, Devol AH, Wofsy SC, Victoria R, Riberio MNG (1988) Biogenic gases and the oxidation and reduction of carbon in Amazon River and floodplain waters. Limnology and Oceanography 33:551-561

Risgaard-Petersen N, Rysgaard S, Nielson LP, Revsbech NP (1994) Diurnal variation of denitrification and nitrification in sediments colonized by benthic microphytes. Limnology and Oceanography 39:573-579

Rivett MO, Buss SR, Morgan P, Smith JWN, Bemment CD (2008) Nitrate attenuation in groundwater: A review of biogeochemical controlling processes. Water Research 42:4215-4232

Robertson WD, Moore TA, Spoelstra J, Li L, Elgood RJ, Clark ID, Schiff SL, Aravena R, Neufeld JD (2012) Natural Attenuation of Septic System Nitrogen by Anammox. Ground Water 50:541-553

Robinson AD, Nedwell DB, Harrison RM, Ogilvie BG (1998) Hypernutrified estuaries as sources of N_2O emission to the atmosphere: the estuary of the River Colne, Essex, UK. Marine Ecology Progress Series 164:59-71

Rock L, Mayer B (2004) Isotopic assessment of sources of surface water nitrate within the Oldman River Basin, southern Alberta, Canada. Water, Air, Soil Pollution 4:562

Rodhe H (1990) A comparison of the contribution of various gases to the greenhouse effect. Science 248:1217-1219

Rosamond MS, Thuss SJ, Schiff SL (2012) Dependence of riverine nitrous oxide emissions on dissolved oxygen levels. Nature Geoscience 5:715-718

Rosamond MS, Thuss SJ, Schiff SL, Elgood RJ (2011) Coupled cycles of dissolved oxygen and nitrous oxide in rivers along a trophic gradient in southern Ontario, Canada. Journal of Environmental Quality 40:256-270

Rosegrant MW, Paisner MS, Meijer RS, Witcover J (2001) Global food projections to 2020. International Food Policy Research Institute. http://www.ifpri.org/sites/default/files/publications/gfp.pdf. Accessed 7/7 2013

Rosenzweig BR, Smith JA, Baeck ML, Jaffe PR (2011) Monitoring Nitrogen Loading and Retention in an Urban Stormwater Detention Pond. Journal of Environmental Quality 40:598-609

Rott E, Duthie HC, Pipp E (1998) Monitoring organic pollution and eutrophication in the Grand River, Ontario, by means of diatoms. Canadian Journal of Fisheries and Aquatic Sciences 55:1443-1453

Royer TV, Tank JL, David MB (2004) Transport and Fate of Nitrate in Headwater Agricultural Streams in Illinois. Journal of Environmental Quality 33:1304

Rutting T, Boeckx P, Muller C, Klemedtsson L (2011) Assessment of the importance of dissimilatory nitrate reduction to ammonium for the terrestrial nitrogen cycle. Biogeosciences 8:1779-1791

Ryden JC, Lund LJ, Focht DD (1979) Direct measurements of denitrification loss from soils: I. Laboratory evaluation of acetylene inhibition of nitrous oxide reduction. Soil Science Society of America Journal 43:104-110

Rysgaard S, Glud RN, Risgaard-Petersen N, Dalsgaard T (2004) Denitrification and anammox activity in Arctic marine sediments. Limnology and Oceanography 49:1493-1502

Rysgaard S, Risgaard-Petersen N, Sloth NP, Jensen K, Nielsen LP (1994) Oxygen regulation of nitrification and denitrification in sediments. Limnology and Oceanography 39:1643-1652

Sahely H, MacLean HL, Monteith HD, Bagley DM (2006) Comparison of on-site and upstream greenhouse gas emissions from Canadian municipal wastewater treatment facilities. Journal of Environmental Engineering and Science 5:405-415

Sanford RA, Wagner DD, Wuc Q, Chee-Sanford JC, Thomas SH, Cruz-García C, Rodríguez G, Massol-Deyá A, Krishnani KK, Ritalahti KM, Nissen S, Konstantinidis KT, Löffler FE (2012) Unexpected nondenitrifier nitrous oxide reductase gene diversity and abundance in soils. Proceedings of the National Academy of Sciences 109:19709-19714

Sansone FJ, Holmes ME, Popp BN (1999) Methane stable isotopic ratios and concentrations as indicators of methane dynamics in estuaries. Global Biogeochemical Cycles 13:463-474

Santoro AE, Buchwald C, McIlven MR, Casciotti KL (2011) Isotopic Signature of N_2O Produced by Marine Ammonia-Oxidizing Archaea. Science 333:1282-1285

Sarkkola S, Nieminen M, Koivusalo H, Lauren A, Kortelainen P, Mattsson T, Palviainen M, Piirainen S, Starr M, Finer L (2012) Trends in concentrations and export of nitrogen in boreal forest streams. Boreal Environment Research 17:85-101

Sauder LA, Engel K, Stearns JC, Masella AP, Pawliszyn R, Neufeld JD (2011) Aquarium Nitrification Revisited: Thaumarchaeota Are the Dominant Ammonia Oxidizers in Freshwater Aquarium Biofilters. PLOS ONE 6:e23281

Savage C, Elmgren R (2004) Macroalgal (*Fucus vesiculosus*) $\delta^{15}N$ values trace decrease in sewage influence. Ecological Applications 14:517-526

Schindler DW (2012) The dilemma of controlling cultural eutrophication of lakes. Proceedings of the Royal Society B - Biological Sciences 279:4322-4333

Schreiber F, Loeffler B, Polercky L, Kuypers MMM, de Beer D (2009) Mechanisms of transient nitric oxide and nitrous oxide production in a complex biofilm. The ISME Journal 3:1301-1313

Schultz D (2005) Grappling with growth: How will the population boom in the Grand River watershed affect the environment?. Grand River Conservation Authority. http://www.grandriver.ca/WatershedReportCard/2005_Fall_Grand_Pg1.pdf. Accessed 6/13 2013

Schwarz MT, Oelmann Y, Wilcke W (2011) Stable N isotope composition of nitrate reflects N transformations during the passage of water through a montane rain forest in Ecuador. Biogeochemistry 102:195-208

Sebilo M, Billen G, Mayer B, Billiou D, Grably M, Garnier J, Mariotti A (2006) Assessing nitrification and denitrification in the Seine River and Estuary using chemical and isotopic techniques. Ecosystems 9:564-577

Sebilo M, Billen G, Grably M, Mariotti A (2003) Isotopic composition of nitrate-nitrogen as a marker of riparian and benthic denitrification at the scale of the whole Seine River system. Biogeochemistry 63:16-35

Seglenieks F (2011) University of Waterloo Weather Station Data Archives. In: . University of Waterloo. http://weather.uwaterloo.ca/data.html. Accessed 03/20 2011

Seitzinger S, Harrison JA, Böhlke JK, Bouwman AF, Lowrance R, Peterson B, Tobias C, Van Drecht G (2006) Denitrification across landscapes and waterscapes: A synthesis. Ecological Applications 16:2064-2090

Seitzinger SP, Harrison JA, Dumont E, Beuson AHW, Bouwman AF (2005) Sources and delivery of carbon, nitrogen, and phosphorus to the coastal zone: An overview of Global Nutrient Export from Watersheds (NEWS) models and their applications. Global Biogeochemical Cycles 19:GB4S01-11

Seitzinger SP, Kroeze C, Bouwman AF, Caraco N, Dentener F, Styles RV (2002) Global patterns of dissolved inorganic and particulate nitrogen inputs to coastal systems: Recent conditions and future projections. Estuaries 25:640-655

Seitzinger SP, Kroeze C (1998) Global distribution of nitrous oxide production and N inputs in freshwater and coastal marine ecosystems. Global Biogeochemical Cycles 21:93-113

Senbayram M, Chen R, Budai A, Bakken L, Dittert K (2012) N_2O emission and the N_2O /(N_2O + N_2) product ratio of denitrification as controlled by available carbon substrates and nitrate concentrations. Agriculture, Ecosystems and Environment 147:4-12

Sendel T (2010) Estimating Body Weight for Horses. Ontario Ministry of Agriculture and Food. http://www.omafra.gov.on.ca/english/livestock/horses/facts/10-085.pdf. Accessed August/2013 2013

Sferratore A, Billen G, Garnier J, Théry S (2005) Modeling nutrient (N, P, Si) budget in the Seine watershed: Application of the Riverstrahler model using data from local to global scale resolution. Global Biogeochemical Cycles 19:GB4S07

Shields FD, Knight SS (2012) Significance of riverine hypoxia for fish: The case of the Big Sunflower River, Mississippi. Journal of the American Water Resources Association 2012:170-186

Sigman DM, Casciotti KL, Andreani M, Barford C, Galanter M, Böhlke JK (2001) A bacterial method for the nitrogen isotopic analysis of nitrate in seawater and freshwater. Analytical Chemistry 73:4145-4153

Silgram M, Waring R, Anthony S, Webb J (2001) Intercomparison of national & IPCC methods for estimating N loss from agricultural land. Nutrient Cycling in Agroecosystems 60:189-195

Silva SR, Kendall C, Wilkison DH, Ziegler AC, Chang CCY, Avanzino RJ (2000) A new method for collection of nitrate from fresh water and the analysis of nitrogen and oxygen isotope ratios. Journal of Hydrology 228:22-36

Silvennoinen H, Liikanen A, Rintala J, Martikainen PJ (2008) Greenhouse gas fluxes from the eutrophic Temmesjoki River and its Estuary in the Liminganlahti Bay (the Baltic Sea). Biogeochemistry 90:193-208

Silvennoinen H, Liikanen A, Torssonen J, Stange CF, Martikainen PJ (2008) Denitrification and N_2O effluxes in the Bothnian Bay (northern Baltic Sea) river sediments as affected by temperature under different oxygen concentrations. Biogeochemistry 88:63-72

Silvennoinen H, Liikanen A, Torssonen J, Stange CF, Martikainen PJ (2008) Denitrification and nitrous oxide effluxes in boreal, eutrophic river sediments under increasing nitrate load: a laboratory microcosm study. Biogeochemistry 91:105-116

Simon J (2002) Enzymology and bioenergetics of respiratory nitrite ammonification. FEMS Microbiology Reviews 26:285-309

Sjodin AL, Lewis WM, Saunders JF (1997) Denitrification as a component of the nitrogen budget for a large plains river. Biogeochemistry 39:327-342

Smith TE, Laursen AE, Deacon JR (2008) Nitrogen attenuation in the Connecticut River, northeastern USA; a comparison of mass balance and N_2 production modeling approaches. Biogeochemistry 87:311-323

Snider DM, Venkiteswaran JJ, Schiff SL, Spoelstra J (2013) A new mechanistic model of $\delta^{18}O$- N_2O formation by denitrification. Geochimica et Cosmochimica Acta 112:102-115

Snider DM, Venkiteswaran JJ, Schiff SL, Spoelstra J (2012) Deciphering the oxygen isotope composition of nitrous oxide produced by nitrification. Global Change Biology 18:356-370

Snider DM (2011) A characterization of the controls of the nitrogen and oxygen isotope ratios of biologically-produced nitrous oxide and nitrate in soils. Dissertation or Thesis, University of Waterloo

Snider DM, Spoelstra J, Schiff SL, Venkiteswaran JJ (2010) Stable oxygen isotope ratios of nitrate produced from nitrification: ^{18}O-labelled water incubations on agricultural and temperate forest soils. Environmental Science & Technology

Snider DM, Schiff SL, Spoelstra J (2009) $^{15}N/^{14}N$ and $^{18}O/^{16}O$ stable isotope ratios of nitrous oxide produced during denitrification in temperate forest soils. Geochimica et Cosmochimica Acta 73:877-888

Song H, Niederweis M (2012) Uptake of sulfate but not phosphate by *Mycobacterium tuberculosis* is sower than that for *Mycobacterium smegmatis*. Journal of Bacteriology 194:956-964

Spoelstra J, Murray M, Elgood RJ (2011) A simplified diffusion method for $\delta^{15}N$ analysis of dissolved ammonium. Environment Canada Report 11-038:17

Spoelstra J, Schiff SL, Elgood RJ, Semkin RG, Jeffries DS (2001) Tracing sources of exported nitrate in the Turkey Lakes Watershed using $^{15}N/^{14}N$ and $^{18}O/^{16}O$ isotopic ratios. Ecosystems 4:536-544

Steen A, Ütkür FO, Borrero-de Acuña JM, Bunk B, Roselius L, Bühler B, Jahn D, Schobert M (2013) Construction and characterization of nitrate and nitrite respiring *Pseudomonas putida* KT2440 strains for anoxic biotechnical applications. Journal of Biotechnology 163:155-165

Stein LY, Yung LY (2003) Production, isotopic composition, and atmospheric fate of biologically produced nitrous oxide. Annual Review of Earth and Planetary Sciences 31:329-356

Stevenson P (2007) EU Directive on the Welfare of Meat Chickens. Compassion in World Farming. http://www.ciwf.org.uk/includes/documents/cm_docs/2009/e/eu_legislation_broilers.pdf. Accessed 8/16 2013

Stief P, Schramm A, Altmann D, de Beer D (2003) Temporal variation of nitrification rates in experimental freshwater sediments enriched with ammonia or nitrate. FEMS Microbiology Ecology 46:63-71

Stow C, Walker JT, Cardoch L, Spence P, Geron C (2005) N_2O emissions from streams in the Neuse River watershed, North Carolina. Environmental Science & Technology 39:6999-7004

Strohm TO, Griffin B, Zumft WG, Schink B (2007) Growth yields in bacterial denitrification and nitrate ammonification. Applied Environmental Microbiology 73:1420-1424

Sun H, Yang Q, Peng Y, Shi X, Wang S, ZHANG S (2009) Nitrite accumulation during the denitrification process in SBR for the treatment of pre-treated landfillleachate. Chinese Journal of Chemical Engineering 17:1027-1031

Sundback K, Linares F, Larson F, Wulff A, Engelsen A (2004) Benthic nitrogen fluxes along a depth gradient in a microtidal fjord: The role of denitrification and microphytobenthos. Limnology & Oceanography 49:1095-1107

Sutka RL, Adams GC, Ostrom NE, Ostrom PH (2008) Isotopologue fractionation during N_2O production by fungal denitrification. Rapid Commications in Mass Spectrometry 22:3989-3996

Sutka RL, Ostrom NE, Ostrom PH, Breznak JA, Gandhi H, Pitt AJ, Li F (2006) Distinguishing nitrous oxide production from nitrification and denitrification on the basis of isotopomer abundances. Applied and Environmental Microbiology 72:638-644

Sutka RL, Ostrom NE, Ostrom PH, Gandhi H, Breznak JA (2003) Nitrogen isotopomer site preference of N_2O producted by *Nitrosomonas europaea* and *Methylococcus capsulatus* Bath. Rapid Commications in Mass Spectrometry 17:738-745

Syakila A, Kroeze C (2011) The global nitrous oxide budget revisited. Greenhouse Gas Measurement and Management 1:17-26

Tallec G, Garnier J, Billen G, Gousailles M (2006) Nitrous oxide emissions from secondary activated sludge in nitrifying conditions of urban wastewater treatment plants: Effect of oxygen level. Water Reseach 40:2972-2980

Tesoriero AJ, Duff JH, Saad DA, Spahr NE, Wolock DM (2013) Vulnerability of streams to legacy nitrate sources. Environmental Science & Technology 47:3623-3629

Thamdrup B, Dalsgaard T (2002) Production of N_2 through anaerobic ammonium oxidation coupled to nitrate reduction in marine sediments. Applied and Environmental Microbiology 68:1312-1318

Therneau TM, Atkinson B (2012) rpart: Recursive Partitioning. R package version 3.1-51. R Foundation for Statistical Computing. http://CRAN.R-project.org/package=rpart. Accessed 3/13 2012

Thuss SJ (2008) Nitrous oxide production in the Grand River, Ontario, Canada: New insights from stable isotope analysis of dissolved nitrous oxide

Townsend-Small A, Pataki DE, Tseng LY, Tsai C-, Rosso D (2011) Nitrous oxide emissions from wastewater treatment and water reclamation plants in southern California. Journal of Environmental Quality 40:1542-1550

Toyoda S, Suzuki Y, Hattori S, Yamada K, Fujii A, Yoshida N, Kouno R, Murayama K, Shiomi H (2011) Isotopomer analysis of production and consumption mechanisms of N_2O and CH_4 in an advanced wastewater treatment system. Environmental Science and Technology 45:917-922

Toyoda S, Yano M, Nishimuri S, Akiyama H, Hayakawa A, Koba K, Sudo S, Yagi K, Makabe A, Tobari Y, Ogawa NO, Ohkouchi N, Yamada K, Yoshida N (2011) Characterization and production and consumption processes of Rapid Commications in Mass Spectrometry emitted from temperate agricultural soils determined via isotopomer ratio analysis. Global Biogeochemical Cycles 25

Toyoda S, Iwai H, Koba K, Yoshida N (2009) Isotopomeric analysis of N_2O dissolved in a river in the Tokyo metropolitian area. Rapid Communications in Mass Spectometry 23:809-821

Toyoda S, Mutobe H, Yamagishi H, Yoshida N, Tanji Y (2005) Fractionation of N_2O isotopomers during production by denitrifier. Soil Biology & Biochemistry 37:1545

United Nations Department of Economic and Social Affairs (2013) World Population Prospects: The 2012 Revision: Key Findings and Advance Tables. United Nations. http://esa.un.org/wpp/Documentation/pdf/WPP2012_%20KEY%20FINDINGS.pdf. Accessed 7/24/2013 2013

United Nations Department of Economic and Social Affairs (2004) World Population to 2300. In: . United Nations. http://www.un.org/esa/population/publications/longrange2/WorldPop2300final.pdf. Accessed 7/7 2013

Van der Putten WH, Macel M, Visser ME (2010) Predicting species distribution and abundance responses to climate change: why it is essential to include biotic interactions across trophic levels. Philosophical Transactions of the Royal Society B-Biological Sciences 365:2025-2034

Vanderploeg HA, Ludsin SA, Ruberg SA, Hook TO, Pothoven SA, Brandt SB, Lang GA, Liebig JR, Cavaletto JF (2009) Hypoxia affects spatial distributions and overlap of pelagic fish, zooplankton, and phytoplankton in Lake Erie. Journal of Exploratory Marine Biology and Ecology 381:S92-S107

Venkiteswaran JJ, Schiff SL, Wassenaar LI (2008) Aquatic metabolism and ecosystem health assessment using dissolved O2 stable isotope diel curves. Ecological Applications 18:965-982

Venkiteswaran JJ, Wassenaar LA, Schiff SL (2007) Dynamics of dissolved oxygen isotopic ratios: a transient model to quantify primary production, community respiration, and air-water exchange in aquatic ecosystems. Oecologia 153:385-398

Venkiteswaran JJ, Schiff SL (2005) Methane oxidation: isotopic enrichment factors in freshwater boreal reservoirs. Applied Geochemistry 20:683-690

Veraart AJ, de Klein JJM, Scheffer M (2011) Warming can boost denitrification disproportionately due to altered oxygen dynamics. PLoS ONE 6:1-6

Vesilind PA (2003) Wastewater treatment plant design. Water Environment Federation, Alexandria, VA

Vieten B, Blunier T, Neftel A, Alewell C, Conen F (2007) Fractionation factors for stable isotopes of N and O during N_2O reduction in soil depend on reaction rate constant. Rapid Communications in Mass Spectrometry 21:846-850

Vitousek PM, Cassman K, Cleveland C, Crews T, Field CB, Grimm NB, Howarth RW, Marino R, Martinelli L, Rastetter EB, Sprent JI (2002) Towards an ecological understanding of biological nitrogen fixation. Biogeochemistry 57:1-45

Wanninkhof R (1992) Relationship between wind speed and gas exchange over the ocean. Journal of Geophysical Research: Oceans 97:7373-7282

Warnecke-Eberz U, Friedrich B (1993) Three nitrate reductase activities in *Alcaligenes eutrophus*. Archives of Microbiology 159:405-209

Wassenaar LI, Venkiteswaran JJ, Schiff SL, Koehler G (2010) Aquatic community metabolism response to municipal effluent inputs in rivers quantified using diel d18O values of dissolved oxygen. Canadian Journal of Fisheries and Aquatic Sciences 67:1232-1246

Water Survey of Canada (2010) Grand River Near Doon (02GA048) 2006 Daily Discharge (m^3/s). Environment Canada. http://www.wsc.ec.gc.ca/applications/H2O/report-eng.cfm?yearb=&yeare=&station=02GA048&report=daily&data=flow&year=2006. Accessed 03/27 2011

Webster JR, Mulholland PJ, Tank JL, Valett HM, Dodds WK, Peterson B, Bowden WB, Dahm CN, Findlay SEG, Gregory S, Grimm NB, Hamilton SK, Johnson SL, Marti E, McDowell WH, Meyer JL, Morrall DD, Thomas SA, Wollheim WM (2003) Factors affecting ammonium uptake in streams - an inter-biome perspective. Freshwater Biology 48:1329-1352

Weier KL, Doran JW, Power JF, Walters DT (1993) Denitrification and the dinitrogen/nitrous oxide ratio as affected by soil water, available carbon, and nitrate. Soil Science Society of America Journal 57:66-72

Weiskel PK, Howes BL (1991) Quantifying dissolved nitrogen flux through a coastal watershed. Water Resources Research 27:2929-2939

Weiss RF (1970) The solubility of nitrogen, oxygen and argon in water and seawater. Deep-Sea Research 17:735

Well R, Flessa H (2009) Isotopologue signatures of N_2O produced by denitrification in soils. Journal of Geophysical Research: Biogeosciences 114:G02020

Well R, Kurganova I, Lopes de Gerenyu V, Flessa H (2006) Isotopomer signatures of soil-emitted N_2O under different moisture conditions - A microcosm study with arable loess soil. Soil Biology and Biochemistry 38:2923-2933

Westberg RE (2012) The Use of Temperature and Environmental Isotopes as Tools to Characterize Groundwater Discharge to the Grand River, Ontario, Canada. Dissertation or Thesis, University of Waterloo

Wetzel RG (1975) Limnology. W.B. Saunders Company, Philadelphia

Wexler SK, Hiscock KM, Dennis PF (2012) Microbial and hydrological influences on nitrate isotopic composition in an agricultural lowland catchment. Journal of Hydrology 468:93

Wexler SK, Hiscock KM, Dennis PF (2011) Catchment-scale quantification of hyporheic denitrification using an isotopic and solute flux approach. Environmental Science & Technology 45:3967-3973

Wezyk S, Krawczyk J, Calik J, Poltowicz K (2013) Relationship between hen age, body weight, laying rate, egg weight and rearing system. CAB International. http://www.cabi.org/animalscience/Uploads/File/AnimalScience/additionalFiles/WPSAVerona/10360.pdf. Accessed 08/16 2013

Whitehead PG, Wilby RL, Battarbee RW, Kernan M, Wade AJ (2009) A review of the potential impacts of climate change on surface water quality. Hydrological Sciences Journal 54:101-123

Whiticar MJ (1999) Carbon and hydrogen isotope systematics of bacterial formation and oxidation of methane. Chemical Geology 161:291-314

Wilcock RJ, Sorrell BK (2008) Emissions of greenhouse gases CH_4 and N_2O from low-gradient streams in agriculturally developed catchments. Water, Air, Soil Pollution 188:155-170

Wilcock RJ (1988) Study of river reaeration at different flow rates. Journal of Environmental Engineering - ASCE 114:91-105

Wood NJ, Alizadeh T, Richardson DJ, Ferguson SJ, Moir JWB (2002) Two domains of a dual-function NarK protein are required for nitrate uptake, the first step of denitrification in *Paracoccus pantotrophus*. Molecular Microbiology 44:157-170

Xia Y, Li Y, Li X, Guo M, She D, Yan X (2013) Diurnal pattern in nitrous oxide emissions from a sewage-enriched river. Chemosphere 92:421-428

Xue DM, Botte J, De Baets B, Accoe F, Nestler A, Taylor P, Van Cleemput O, Berglund M, Boeckx P (2009) Present limitations and future prospects of stable isotope methods for nitrate source identification in surface- and groundwater. Water Research 43:1159-1170

Yan W, Yang L, Wang F, Wang J, Pei Ma P (2012) Riverine N_2O concentrations, exports to estuary and emissions to atmosphere from the Changjiang River in response to increasing nitrogen loads. Global Biogeochemical Cycles 26

Yan W, Laursen AE, Wang F, Sun P, Seitzinger SP (2004) Measurement of denitrification in the Changjiang River. Environmental Chemistry 1:95-98

Yang L, Yan W, Ma P, Wang J (2011) Seasonal and diurnal variations in N_2O concentrations and fluxes from three eutrophic rivers in Southeast China. Journal of Geographical Sciences 21:820-832

Yoneyama T, Omata T, Nakata S, Yazaki J (1991) Fractionatioin of nitrogen isotopes during the uptake and assimilation of ammonia by plants. Plant and Cell Physiology 32:1217

Yoon SS, Hennigan RF, Hilliard GM, Ochsner UA, Parvatiyar K, Kamani MC, Allen HL, DeKievit TR, Gardner PR, Schwab U, Rowe JJ, Iglewski BH, McDermott TR, Mason RP, Wozniak DJ, Hancock RE, Parsek MR, Noah TL, Boucher RC, Hassett DJ (2002) *Pseudomonas aeruginosa* anaerobic respiration in biofilms: relationships to cystic fibrosis pathogenesis. Developmental Cell 3:593-603

Zafiriou OC (1990) Laughing gas from leaky pipes. Nature 347:15-16

Zar JH (1996) Biostatistical analysis. Prentice Hall, Upper Saddle River, NJ

Zeebe RE, Wolf-Gladrow D (2001) Stable Isotope Fractionation. In: CO_2 in Seawater: Equilibrium, Kinetics, Isotopes. Elsevier, Amsterdam, pp 141-250

Zhang J, Wu P, Hao B, Yu Z (2011) Heterotrophic nitrification and aerobic denitrification by the bacterium *Pseudomonas stutzeri* YZN-001. Bioresource Technology 102:9866-9869

Zumft WC (1997) Cell biology and molecular basis of denitrification. Microbiology and Molecular Biology Review 61:533-616